The synthesis and decomposition reactions of N-hydroxymethyltriazenes

Thesis

THE SYNTHESIS AND DECOMPOSITION REACTIONS OF N-HYDROXYMETHYLTRIAZENES

A Thesis submitted by

Shee Chau Cheng

in partial fulfilment of the requirements
for the Degree of Doctor of Philosophy
of the Open University

DEPARTMENT OF CHEMISTRY
THE OPEN UNIVERSITY

NOVEMBER 1984

Date of submission: November 1984

Date of award: 19 December 1984

ACKNOWLEDGEMENT

I would like to thank my supervisor, Dr Jim Iley for his advice and encouragement throughout my study and especially for his friendliness.

I would also like to thank the technical staff of the Chemistry department for their support and the Open University for offering me a studentship.

My sincerest thanks are also extended to all my friends and colleagues who have made my study here a happy one and to Mrs Sue Hegarty for speedily typing the manuscript.

Finally, I would like to dedicate this thesis to my parents, brothers and sister. Without their unselfish support my studies in England would not have been realised.

ABSTRACT

Two methods of synthesising 1-aryl-3-hydroxymethyl-3-methyltriazenes have been examined. The method of Vernin's *et.al*. was found to be erroneous yielding bistriazenes instead. A mechanism for the formation of hydroxymethyltriazenes and bistriazenes has been proposed. Furthermore, modification of Steven's procedure enabled the synthesis of 4-chlorophenyl-hydroxymethyltriazene.

Hydroxymethyltriazenes were shown to decompose in the presence of metal ion in non-aqueous solutions to give the corresponding arylamines. This reaction was shown to follow a consecutive pseudo-first-order mechanism with the intermediacy of monomethyltriazene. Moreover, the reaction was found to be metal ion and not proton catalysed. Compared to hydroxymethyl-triazenes, monomethyltriazenes are more reactive towards metal ions. This is believed to be due to the higher nucleophilicity of the triazene group in monomethyltriazenes. A salient feature of this study was the stabilising effect of a heteroaryl ring in the decomposition of hydroxymethyltriazenes. The ability of the heteroaryl ring to interact with metal ion is thought to be responsible for this stabilising effect. This was confirmed by the lanthanide shift reagent study.

Lanthanide induced chemical shifts are reported for hydroxymethyltriazenes and related compounds. The induced shifts for both $Eu(fod)_3$ and $Pr(thd)_3$ reveal that the hydroxy-methyltriazenes bind to the M^{n+} ion *via* the hydroxymethyl oxygen atom and that the binding ability of this atom is lowered when the hydroxyl proton is replaced with a bulky group.

The presence of bases was also found to promote the decomposition of hydroxymethyltriazenes. In this instance,

however, monomethyltriazenes are stable enough to exist as the product. The base requires an X-H bond for catalytic activity.

CONTENTS

ABBREVIATIONS

AIC - 5-aminoimidazole-4-carboxamide

DIC - 5(3,3-dimethyl-1-triazeno)imidazole-4-carboxamide

DMT - 1-aryl-3,3-dimethyltriazene

DZIC - 5-diazoimidazole-4-carboxamide

HMIC - 5(3-hydroxymethyl-3-methyl-1-triazeno)imidazole-4-carboxamide

HMT - 1-aryl-3-hydroxymethyl-3-methyltriazene

MIC - 5(3-methyl-1-triazeno)imidazole-4-carboxamide

MMT - 1-aryl-3-methyltriazene

1.1 The mechanism of action of dimethyltriazenes

The antitumour activity of dimethyltriazenes (1) was

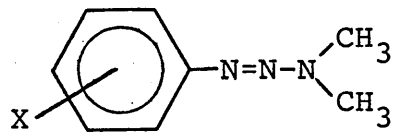

(1)

first reported by Clarke and coworkers nearly fifty years ago.[1] Since this discovery, many attempts have been made to elucidate their mode of action and to find a more effective antitumour agent. Rondestvedt and Davis[2] were the first to make a structure-activity study on dimethyltriazenes. Their major conclusion from this study was that at least one methyl group at the terminal nitrogen of the triazene moiety appeared necessary for antitumour activity. This was later confirmed by other investigators.[3,4] (Table 1.1). Ironically, it was a study aimed at designing antagonists of aminoimidazole carboxamide (AIC) (2), a precursor in purine biosynthesis, that produced the clinically useful triazene—— 5(3,3-dimethyl-1-triazeno)imidazole-4-carboxamide (DIC) (3).[5,6] This triazene is presently used in the clinical treatment of malignant melanoma.[7] Nevertheless, the aryl analogues (1) of this imidazolytriazene were found to be equally effective as antitumour agents.[8,9] This fact indicates that DIC (3) does not act as an antogonist of AIC (2).

(2)

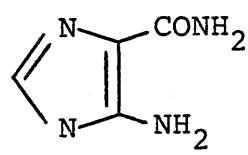

(3)

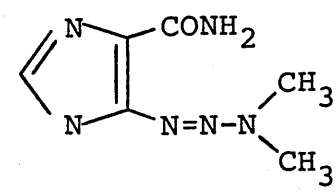

Table 1.1 Effects of various triazenes on the TLX5 lymphoma and their dealkylation by liver microsomes[a]

Compound formula	Optimal dose	%IST	Toxic dose	Substrate %dealkylation
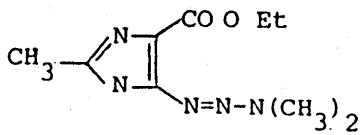	25	67	200	5.3 ± 1.1
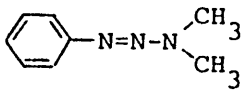	16	53	128	41.6 ± 8.2
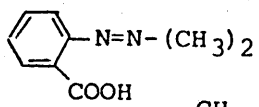	32	68	64	0.8 ± 1.3
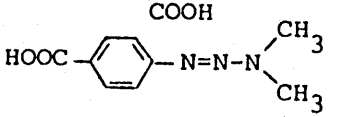	25	72	400	0.4 ± 4.1
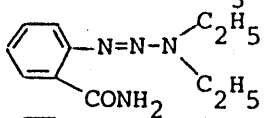	Inactive		200	46 ± 9.0
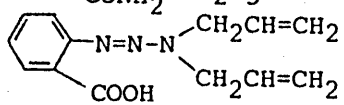	Inactive		400	
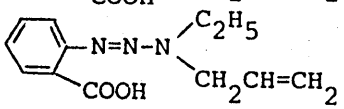	Inactive		400	
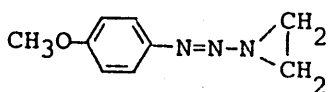	Inactive			
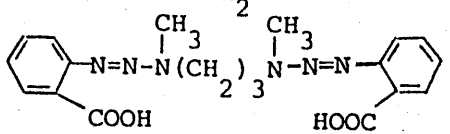	200	18	400	

a from reference 4

A further possible mode of action of DIC (3), which is unstable in light, is that it exhibits its inhibitory action through the formation of a more toxic compound, viz. 5-diazoimidazole-4-carboxamide (DZIC) (4).[10] However, aryltriazenes themselves are stable in light and moreover, within a series of aryldimethyltriazenes shown to have antitumour activity, there is no correlation between such activity and the rate of hydrolysis to the diazonium ion.[11] These results imply that the cytotoxicity and tumour inhibitory activity of triazenes arise from an alternative mode of action.

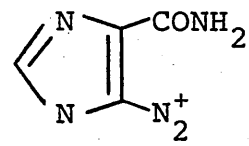

(4)

This alternative mechanism (Scheme 1.1.1) was first proposed by Preussmann and coworkers.[12] They postulated that dimethyltriazenes undergo oxidative N-demethylation by liver microsomes. Such a mechanism involved the intermediacy of a 3-hydroxymethyl-3-methyltriazene (5). This transient species was thought to decompose to yield 3-monomethyltriazene (6) and formaldehyde. They suggested that the monomethyltriazene (6) is the proximate cytotoxic metabolite which could generate a methyl carbonium ion, capable of reacting with nucleic acids. The in vivo mode of action of DMTs, then, was a result of the alkylating ability.

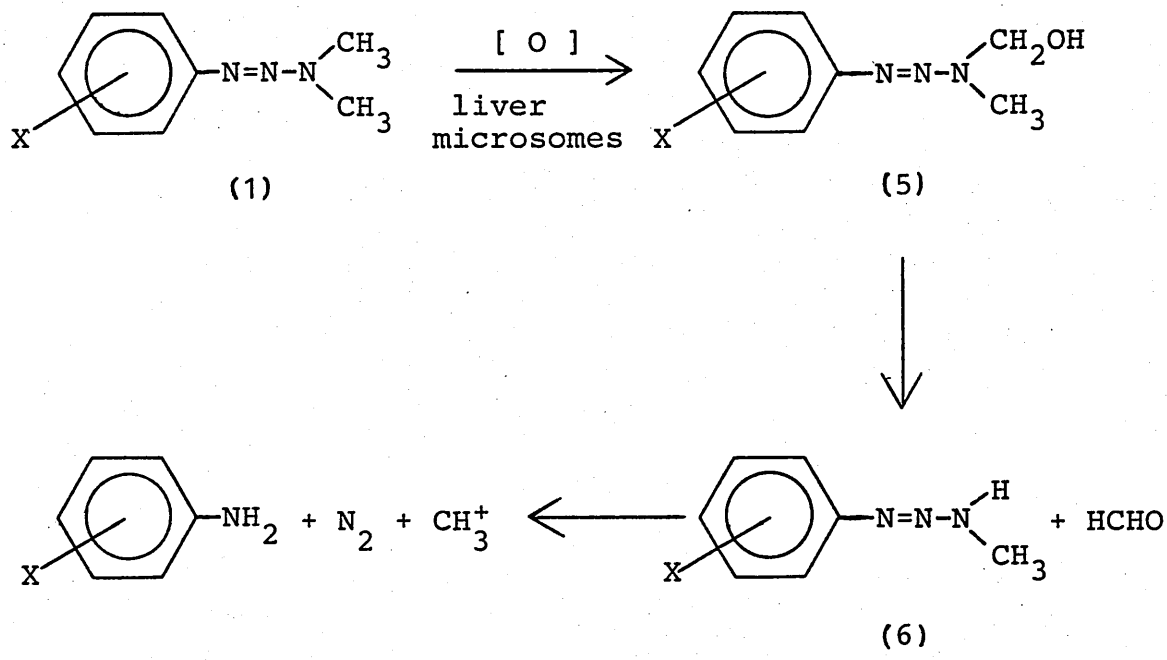

Scheme 1.1.1 Activation of dimethyltriazene to reactive cytotoxic compounds

There is considerable support for this hypothesis. Xenobiotics have long been known to undergo a variety of metabolic transformations in the mammalian body. One such important metabolic pathway common to many N-alkyl containing foreign organic compounds, such as dimethyltriazenes, is oxidative N-dealkylation.[13] The intermediate of this pathway is believed to be an aminocarbinol[14] (commonly known as carbinolamine) (Scheme 1.1.2). This is thought to arise through the enzymic hydroxylation of the carbon atom adjacent to the nitrogen. Such processes usually occur in the liver and involve the cytochrome P450.[13] These aminocarbinols are generally expected to be chemically unstable and to decompose readily to give N-dealkylamine and aldehyde.[15] A number of

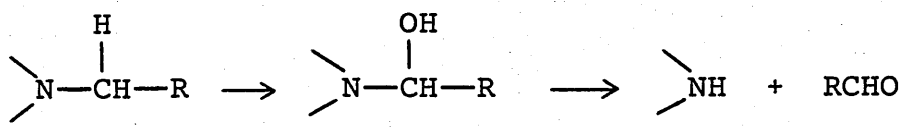

Scheme 1.1.2

clinically active anticancer drugs are thought to undergo this metabolic transformation. These include procarbazine (7), cyclophosphamide (8), streptozotocin (9) and hexamethylmelamine (10).[16]

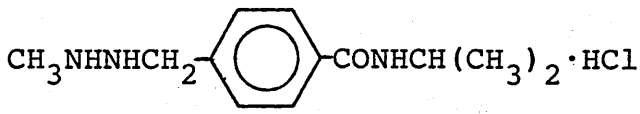

(7)

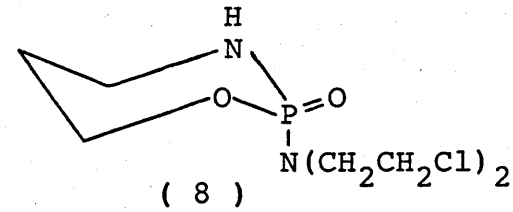

(8)

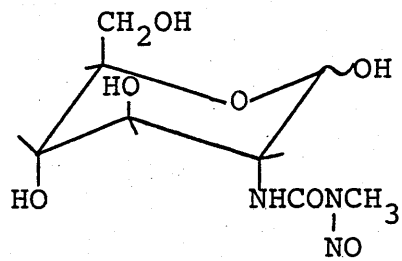

(9)

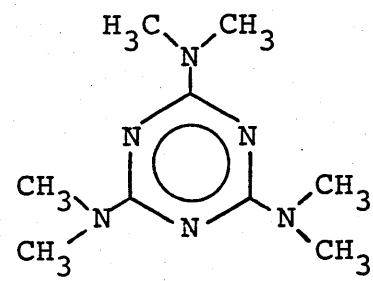

(10)

The hypothesis (Scheme 1.1.1) can be further substantiated with experimental evidence. DIC (3) and 1-phenyl-3,3-dimethyltriazene (1, X=p-H) are N-demethylated *in vitro* by rat liver microsomes to give, along with

formaldehyde, AIC and aniline respectively.[12,17] Under the same system, dimethylamine - a product in the hydrolysis of dimethyltriazenes - is not N-demethylated[12] thus suggesting that formaldehyde is derived solely from the triazenes. Furthermore, in the absence of light, incubation of mammalian cells with DIC labelled with ^{14}C in the side chain methyl groups produces three times as much labelled carbon dioxide as labelled dimethylamine and also results in the labelling of the cellular DNA.[18,19] Indeed, similarly labelled DIC is metabolised by both man and rat to give labelled carbon dioxide[17] together with the methylation of the N-7 position of the guanine group of the nucleic acids.[20] Besides, monomethyltriazenes, the proposed active metabolites, are well known alkylating[21] and carcinogenic,[12] mutagenic[22] and antitumour[23] agents. Isotopically labelled MIC (11) has been shown to methylate DNA <u>in vitro</u>[24] and the methylating agent involved is not a diazomethane but an intact methyl group.[25] Finally, only those triazenes that can be N-dealkylated to the monomethyl derivatives are active antitumour agents. Compound (12) for example does not possess antitumour properties though it undergoes 46% deethylation.

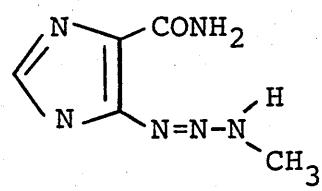

(11)

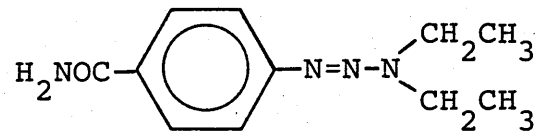

(12)

Despite these observations, there is some controversy regarding monomethyltriazenes as the proximate cytotoxic species. This was highlighted recently by Stevens and Vaughan[21] who pointed out that monomethyltriazenes, though

active *in vitro* are no better antitumour agents than their dimethyl analogues. Whilst this can be assigned to the greater toxicity and shorter biological half-life of monomethyltriazenes [11], the strongest evidence against the argument comes from the study of the selective cytotoxicity of dimethyltriazenes. Dimethyltriazenes are active against TLX lymphoma which has natural resistance to classical alkylating agents. Such selective activity cannot possibly be accomplished by the highly reactive methyl carbonium ions produced from the degradation of monomethyltriazenes as shown in Scheme 1.1.1. Recently, Hickman and coworkers[26] tested the hypothesis that monomethyltriazenes are responsible for the *in vivo* cytotoxicity of dimethyltriazenes by comparing the *in vitro* toxicity of monomethyltriazenes to TLX5S lymphoma which is sensitive to dimethyltriazenes *in vivo* and to TLX5R lymphoma which is resistant *in vivo*. The results showed that monomethyltriazenes are almost equally toxic to both tumours indicating that they are not responsible for the *in vivo* selective cytotoxicity of dimethyltriazenes. In the same study, a dimethyltriazene was activated *in vitro* by liver homogenate and cofactors and was found to produce metabolites which are more toxic to TLX5S lymphoma than to the TLX5R. However, TLX5S lymphoma showed no preferential sensitivity towards the cytotoxic metabolites of a diethyltriazene, which is not an antitumour agent, activated in the same way. Taken together, the results suggest that a mixture of selective and non-selective metabolites are generated during the metabolic activation of dimethyltriazenes *in vitro*. Consequently, the most probable candidate for the selective metabolite is the hydroxymethyltriazene since the metabolism of dimethyltriazene

as shown in Scheme 1.1.1 is believed to involve this compound.

Hydroxymethyltriazenes were first successfully synthesised in 1978 and were found to be surprisingly stable in the crystalline state.[27] They are active against TLX lymphoma both *in vitro* and *in vivo*.[27] By using an *in vitro*/*in vivo* bioassay, Hickman[28] has shown that hydroxymethyl- and not monomethyltriazenes might be responsible for the selective antitumour activity of dimethyltriazenes *in vivo*. Though hydroxymethyltriazenes were once thought to have only transient *in vivo* existence, Kolar and coworkers have managed to isolate a metabolite from the urine of DIC-treated rats which they assigned tentatively as the hydroxymethyl derivatives of DIC (13).[29] The same group of workers have also isolated another hydroxymethyltriazene in the form of its o-glucuronide conjugate (14) from the urine of rats treated with 1-(2,4,6-trichlorophenyl)-3,3-dimethyltriazene (15).[30]

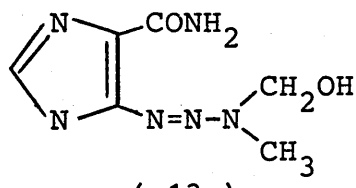

(13)

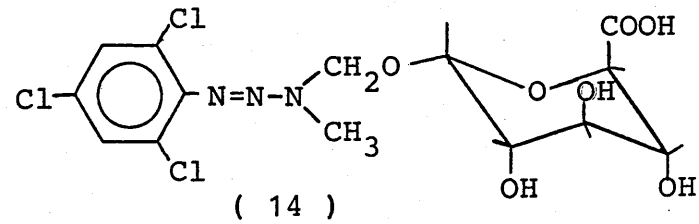

(14)

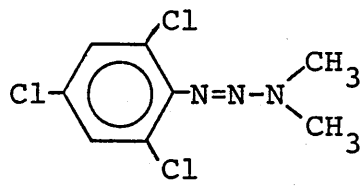

(15)

A new mechanism of action for dimethyltriazenes has to be invoked if hydroxymethyltriazenes are acting as the selective

metabolites of the prodrugs, dimethyltriazenes. Any new hypothesis must account for, apart from other findings, the essential requirement of the presence of at least one terminal N-methyl group for antitumour activity.[2,3,4] It was pointed out[28] that such requirements can be extended to procarbazine (7)[32] and hexamethylmelamine (10)[33] which are believed to undergo the same metabolic activation as dimethyltriazenes. In addition, TLX5 lymphoma is extremely sensitive to procarbazine in vivo and TLX5R lymphoma, which is resistant to dimethyltriazenes, is also resistant to procarbazine. Accordingly, there may be a common mechanism of action for procarbazine and dimethyltriazenes. In fact, aminocarbinols from the metabolism of procarbazine[34] and of hexamethylmelamine[33] have been identified and in the case of hexamethylmelamine, its mode of action was believed to involve the release of formaldehyde. This implication that formaldehyde is possibly involved in the antitumour activity of hexamethylmelamine may be appropriate to other N-methyl containing antitumour compounds such as dimethyltriazenes. If so, the stability of hydroxymethyltriazenes and other aminocarbinols mentioned above can determine the selective activity of dimethyltriazenes and other N-methyl containing anticancer agents.

An alternative mechanism, that involves hydroxymethyltriazenes as the selective cytotoxic species was proposed recently by Soloway and coworkers.[16] In this hypothesis, hydroxymethyltriazenes and other aminocarbinols are believed to be able to react with amines, sulfhydryls and related groups thus allowing them to modify covalently various biopolymers such as nucleic acids and proteins. This

alteration is thought to adversely affect tumour cell replication. A recent report, which gave supportive evidence, implicated the aminocarbinol function as the binding site for the attachment of a number of antibiotics to DNA.[31] However, in the case of cyclophosphamide, the complex formed from the aminocarbinol derivative and thiol-containing proteins are thought to be inactive and require enzymatic activation to release the drug selectivity in the tumour.[39]

Given this growing speculation on the possible participation of hydroxymethyltriazenes in the mode of action of the antitumour dimethyltriazenes it is appropriate to investigate the chemistry of hydroxymethyltriazenes. In particular, such a study should reveal both the stability and the mechanism of decomposition, in the presence of Lewis acids or bases, of this group of compounds. A comparison of the stabilities of hydroxymethyltriazenes with those of monomethyltriazenes may clarify the argument over the possible role of hydroxymethyltriazenes as the metabolic intermediates and selective metabolites in dimethyltriazene metabolism.

1.2 The chemistry of hydroxymethyltriazenes

As was pointed out earlier, hydroxymethyltriazenes are aminocarbinols. Aminocarbinols have frequently been referred to in the literature as intermediates in the metabolism of many N-alkyl containing xenobiotics.[15] However, apart from HMTs, few such aminocarbinols have been synthesised and isolated. A successful example is hydroxymethylmelamine (16).[38] It is, therefore, of particular interest to see what properties, if any, may be introduced to the whole triazene

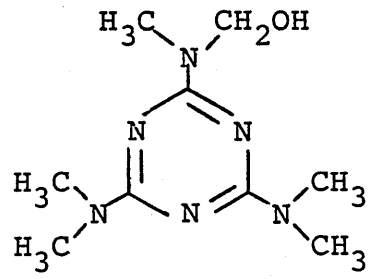

(16)

molecule by the presence of an N-hydroxymethyl group.

Theoretically, the chemical reactivity of hydroxymethyl-triazenes can be broken down into four modes. (Figure).

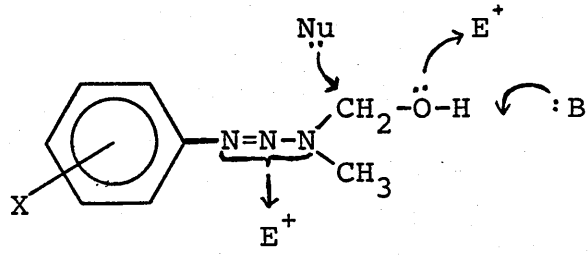

Figure

(i) Firstly, the molecule may react as an electrophile with a nucleophile (Nu:) at the methylene position of the hydroxymethyl group. If the nucleophile is a protein or a nucleic acid, then the molecule may become covalently bonded to protein or DNA thereby functioning as an antimitotic agent as suggested by Soloway and coworkers.[16] Synthetically, this reaction could be used to synthesise other triazene derivatives which can bypass the metabolic activation required by dimethyltriazenes.

(ii) Secondly, in the presence of bases (B:), HMTs might be expected to behave as weak acids due to the alcoholic proton. The acidity of this proton could depend largely on the

electronic effect of the substituents of the aryl group. In this respect, electron withdrawing groups might be expected to have a destabilising effect.

(iii) Thirdly, HMTs, like many alkyl and dialkyltriazenes, should react with either the proton or Lewis acids (E^+), behaving as nitrogen bases. Though the basic site in this type of interaction is the triazene moiety the exact position of reaction could depend on how the molecule behaves. If HMTs react like dimethyltriazenes, the reaction centre should be N-3 of the triazene moiety. Acid catalysed decomposition

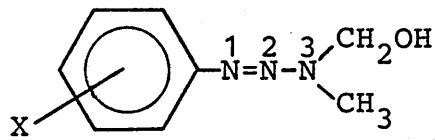

of dimethyltriazenes, for example, involves the initial protonation at the N-3 position followed by the cleavage of the N2—N3 bond (Scheme 1.2.1).[35] Alternatively, HMTs may

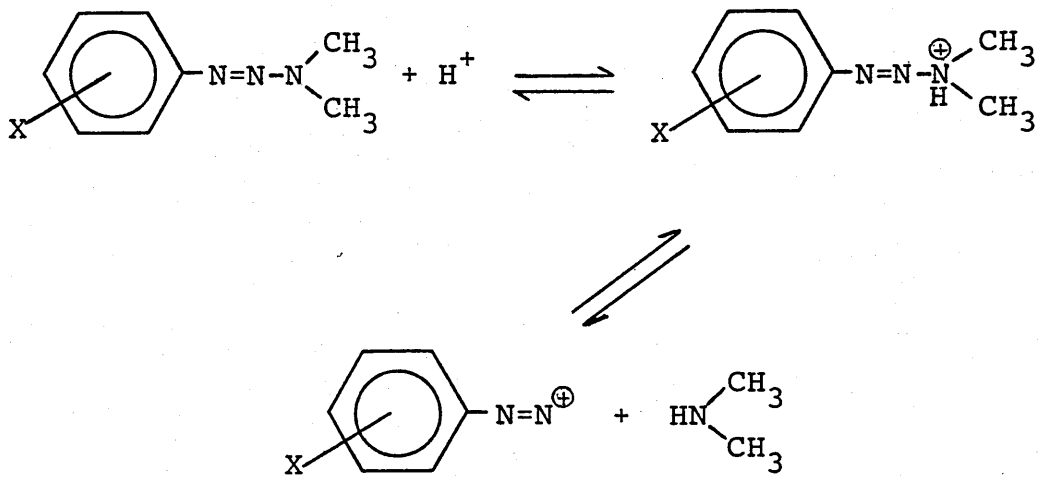

Scheme 1.2.1

behave as "masked" monomethyltriazenes. In this case, N-1 should be the reaction centre. This can be demonstrated by the protolysis of monomethyltriazenes in aqueous solution (Scheme 1.2.2). The products of this reaction are a mixture of anilines and methanol but not phenol[36,37] implying that protonation occurs at the arene bound nitrogen of tautomer II.

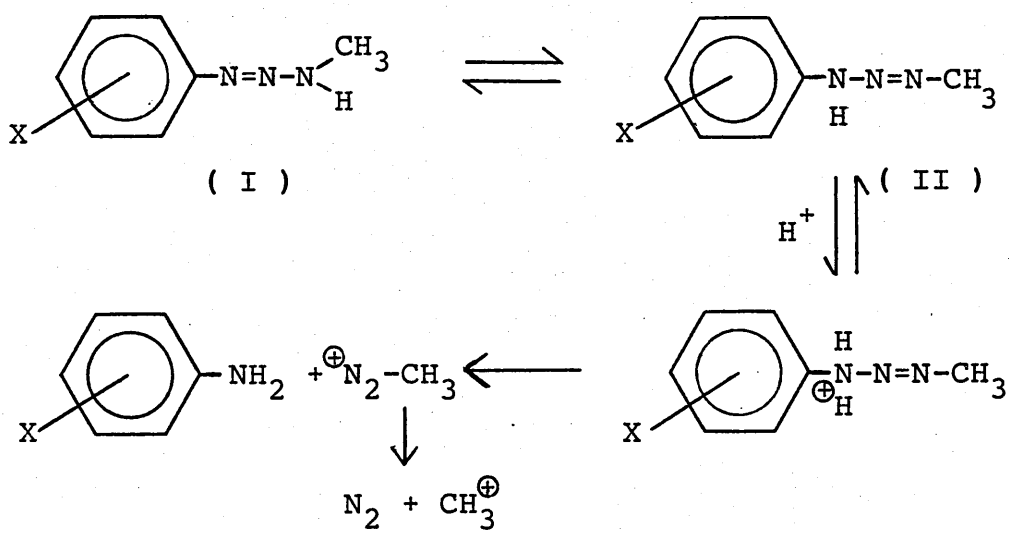

Scheme 1.2.2

(iv) Finally, HMTs may act as oxygen nucleophiles by reacting via the OH oxygen with the proton or Lewis acids. Since oxygen is less nucleophilic than nitrogen this mode is likely to be less important. We shall now consider each mode in turn.

1.2.1 Behaviour as aminomethylating agents

Although aminocarbinols in general are too unstable to form derivatives, the hydroxyl group of some relatively more stable aminocarbinols can be substituted with nucleophiles. For example, aminocarbinols may react with primary or secondary amines to give methylene-bis-amines.[40] An

illustration is the reaction of formaldehydes with dicyclohexylamine and another secondary amine to give unsymmetrical methylene-bis-amines.[41] This is the basis of the well known Mannich reaction,

$$(C_6H_{11})_2NH + HCHO + HNRR' \rightarrow (C_6H_{11})_2NCH_2NRR'$$

Alcohols are the second group of nucleophiles that may displace the hydroxyl group of aminocarbinols. N,N-Diethylaminomethanol - formed from N,N-diethylamine and formaldehyde - can react with ethanol to give N,N-diethyl-aminomethyl ethyl ether.[42]

$$Et_2NH + HCHO \rightarrow Et_2NCH_2OH \overset{EtOH}{\rightarrow} Et_2NCH_2OEt$$

Whilst it is not clear whether the above reactions require acid catalysis, it was observed that protonated N-hydroxymethylmorpholine is about 10-fold more reactive than neutral N-hydroxymethylmorpholine in condensing with another morpholine molecule to give methylene-bis-morpholine.[47] In addition, the aminomethanol derivatives of a number of heterocyclic amines have been shown to react with cysteine and glutathione in aqueous solution at pH7 and 25 ^{o}C.[43]

$$\begin{matrix} R^1 \\ R^2 \end{matrix}\!\!>\!NCH_2OH + HSR^3 \rightleftarrows \begin{matrix} R^1 \\ R^2 \end{matrix}\!\!>\!NCH_2\!-\!SR^3 + H_2O$$

It has also been demonstrated that 4-hydroxycyclophosphamide (17), the aminomethanol derivatives of cyclophosphamide, reacts quantitatively in the presence of acid with thiol compounds such as benzyl mercaptan.[44] However it was not established whether (17) itself, or the ring-open form (18), underwent such substitutions.

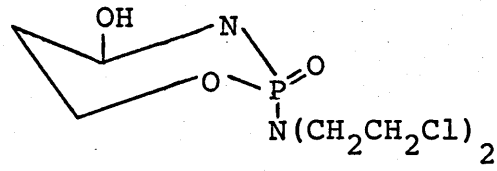

(17)

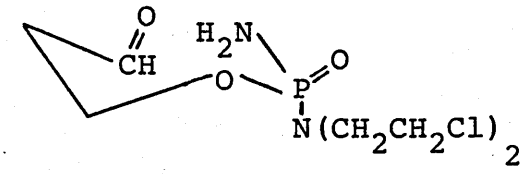

(18)

Interestingly, it appears that aminomethanols that have nitrogen atoms with "available" lone-pair electrons are substituted most easily:

$$R_2\ddot{N}\text{-}CH_2\text{-}\ddot{O}H \rightarrow R_2\overset{+}{N}{=}CH_2 + OH^{\ominus}$$

In HMTs, however, these lone pair electrons are involved in delocalisation over the triazene system and are consequently less available. It is probable that HMTs are among the less reactive aminomethylating compounds.

1.2.2 Behaviour as acids

The pKa values of seven alcohols of the type $R{\cdot}CH_2OH$ have been shown to fit the following Hammett equation at

$$pKa = 15.9 - 1.42\ \sigma^*$$

25 °C.[46] The values, determined by a conductivity method, range from 12.24 ($R = CCl_3$) to 15.5 ($R = H$). Employing another linear free energy relationship, Kallen[47] and coworkers calculated the pKa values of 14.8 for $(CH_3)_2NCH_2OH$. The comparison of this value with those for aliphatic alcohols (Table 1.2.1) suggest that aminocarbinols, in general, may be more acidic than their corresponding aliphatic alcohols.

Table 1.2.1

ROH	pKa
MeOH	15.09
EtOH	15.93
^{n}PrOH	16.1
^{n}BuOH	16.1
^{i}PrOH	17.1
^{t}BuOH	>19
2-BuOH	17.6
2-Me-PrOH	16.1

The acidity of the aminocarbinol moiety can be further illustrated by the studies on the decomposition of the aminocarbinol intermediates in the hydrolysis of Schiff bases and related compounds. One example is the hydrolysis of N-p-chlorobenzylideneaniline.[60] In the pH range where the

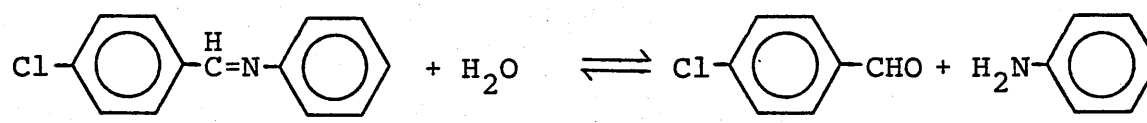

decomposition of the aminocarbinols is rate limiting, the reaction is subjected to general base catalysis.

1.2.3 Behaviour as N-nucleophiles

The presence of a hydroxymethyl group has been shown to lower the basicity of the parent amines by 2-3 pH units.[47,49,50] Since a proton and a hydroxymethyl group have similar polarity[51] - probably due to hyperconjugation, the

decrease in the basicity was attributed to a decrease in solvation energy when a proton is replaced by a hydroxymethyl group.[49] Therefore, monomethyltriazenes are expected to be more nucleophilic than hydroxymethyltriazenes.

1.2.3.1 The hydrolysis of dimethyltriazenes

The stabilities of a series of p-substituted dimethyltriazenes to hydrolysis have been determined in 0.15 M phosphate buffer at pH7 and 37 ^{o}C.[35] This was carried out by withdrawing aliquots of the buffered solution at regular intervals. Any diazonium ion liberated during incubation was first removed by coupling with resorcinol in an alkaline medium. The unreacted triazenes were then cleaved by acid and coupled with N-ethyl-1-naphthylamine to yield a product which absorbs at 525-582 nm. The concentration of this coloured product was determined spectroscopically. From this procedure, the rate constants obtained range from 6 x 10^{-2} min^{-1} (X=4-OCH_3) to 3 x 10^{-6} min^{-1} (X=4-NO_2) giving Hammett ρ value of -4.7. The mechanism of the acid catalysed fission of the triazene molecule was shown earlier in Scheme 1.2.1. However, the report did not suggest whether the reaction was catalysed by specific or general acid.

1.2.3.2 The decomposition of monomethyltriazenes

The decomposition of monomethyltriazenes in aqueous solution at 25 ^{o}C and constant ionic strength was reported to require specific acid catalysis.[52] The mechanism (see Scheme 1.2.2) involves a pre-equilibrium protonation of the triazene

followed by the rate determining decomposition of the protonated species. There is no ionic strength effect and the Hammett ρ value reported is -2.85. Supportive evidence for the involvement of a carbonium ion in the mechanism came from other studies[53] using higher alkyltriazenes in which products resulting from the rearrangement of the alkyl groups were obtained.

In addition to the proton catalysed mechanism, it was reported recently that there might be another route for the decomposition of monoalkyltriazenes in aqueous solution.[54] It involves a unimolecular departure of the $\overset{\ominus}{\text{HN}}\text{Ar}$ group from the $RN_2^{\oplus}$ fragment of the molecule without significant protonation (Scheme 1.2.3). The authors drew their

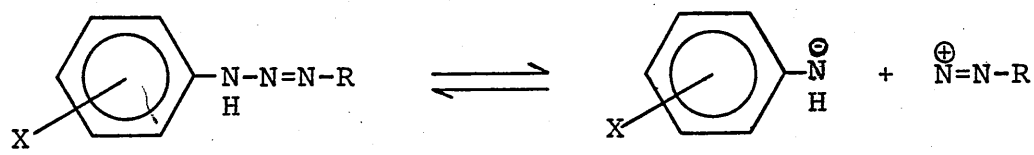

Scheme 1.2.3

conclusion based on the following findings:

i. no solvent isotope effect was observed,
ii. the entropy of activation is near zero,
iii. the pH independent hydrolysis rate constants have been detected and give a β_{lg} value of -1.0.

A third mechanism was invoked to explain the decomposition of monoalkyltriazenes by carboxylic acids in aprotic solvents.[55] In this case, the protonation of triazene is believed to occur at the terminal nitrogen and is thought

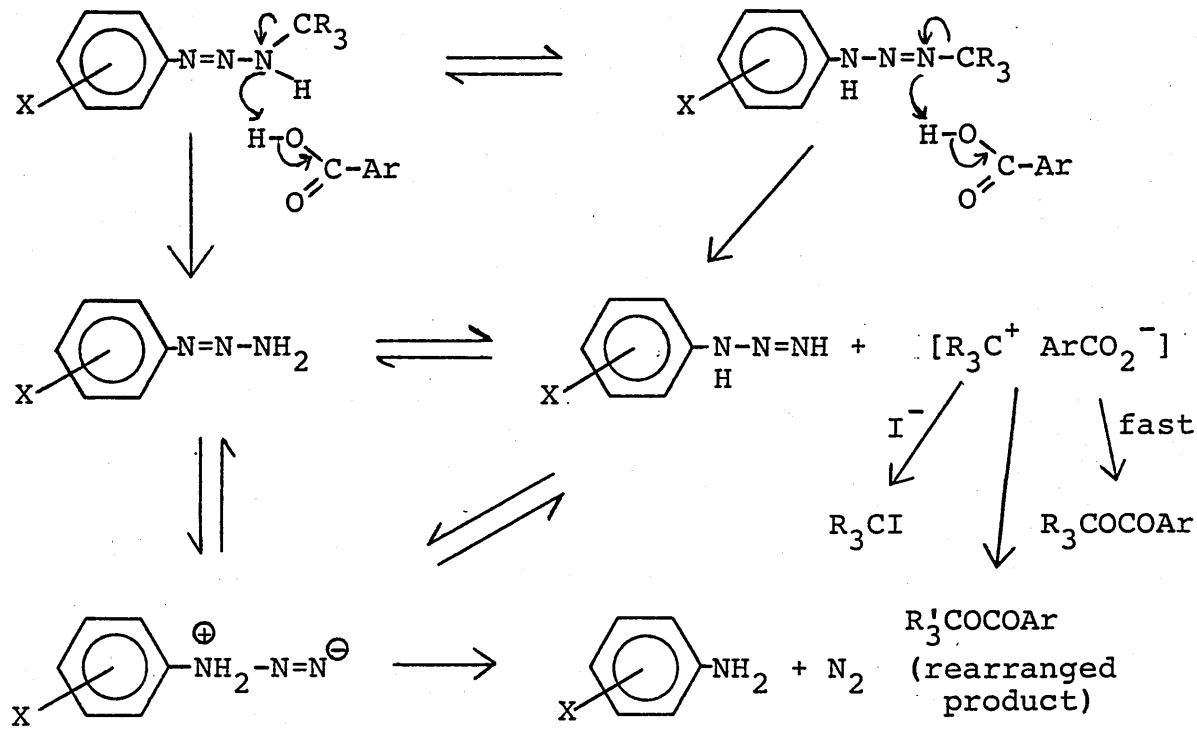

Scheme 1.2.4

to be synchronous with the departure of the alkyl carbonium ion (Scheme 1.2.4). Supportive evidence includes:

i. Primary deuterium isotope effect was observed when benzoic acid was replaced by deuterated derivatives.

ii. Rate constants increase with alkyl groups suggesting that the alkyl groups leave as cations in the rate determining step.

iii. Hammett reaction constant ρ is equal to -0.92.

The decomposition of monoalkyltriazenes in the presence of some Lewis acids had also been studied. Monoalkyltriazenes were reported to decompose over alumina[56] and silica gel[57] and with aluminium trihalides[58] in benzene. In all instances, the deconjugated tautomer (tautomer II in Scheme 1.2.2) is believed to be the reactive tautomer. This was confirmed when, on silica gel,[57] no decomposition was observed with

1,3-diphenyl- and 3,3-dialkyltriazenes under the same condition as monalkyltriazenes. A mechanism (Scheme 1.2.5) was proposed in which an ion-pair was involved because:

i. No cross products were obtained from a mixture of alkyltriazenes implying an intramolecular reaction.

ii. The alkyl groups were found to retain their configuration in the products.

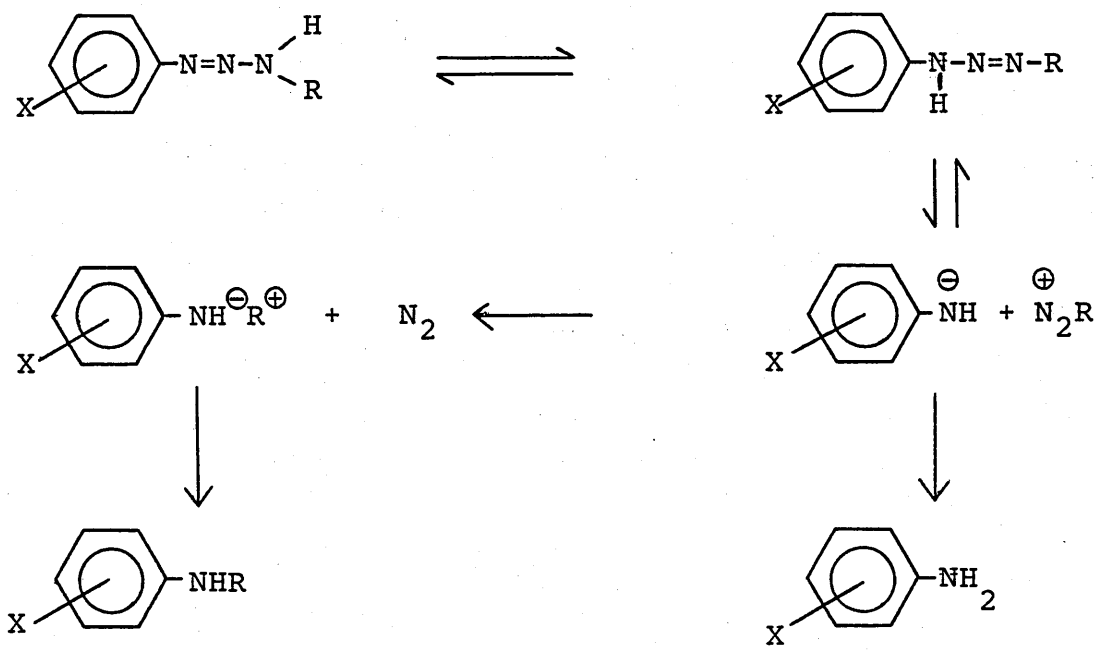

Scheme 1.2.5

1.2.3.3 Triazene-metal complexes

The nucleophilic characters of triazenes can be further illustrated by their ability to form stable complexes with metals.[21] Indeed, 1,3-diaryltriazenes are reported to form stable complexes with platinum, palladium, ruthenium, cobalt and copper. These compounds are synthesised from metal salts and the triazene anion. Several monoalkyltriazenes have also

been reported to form complexes with metals. It appears that only those metals that are classified as 'soft' acids or those that are in the borderline region are capable of forming complexes with triazenes regardless of the substituents on the triazenes. However, no complex of trisubstituted triazenes has so far been reported. Successful attempts were only from the disubstituted ones. Three coordination modes namely, the monodenate (19), the bidenate (20) and the bridging mode (21) have been identified.

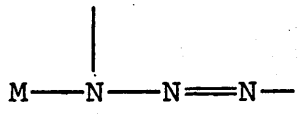

(19)

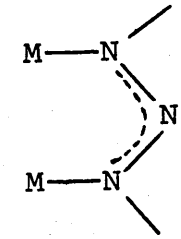

(20)

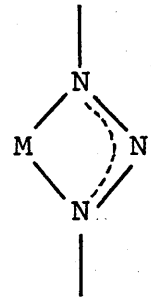

(21)

1.2.4 Behaviour as O-nucleophiles

The ability of hydroxymethyltriazenes to behave as O-nucleophiles can be implicated from the studies on the formation and hydrolysis of Schiff bases and related compounds led by Jencks and other workers.[59-61] In these it was found that the dehydration of the aminocarbinol intermediate derived from amines and aldehydes are subject to both general and specific acid catalysts. This process is promoted by electron donating substituents in either the

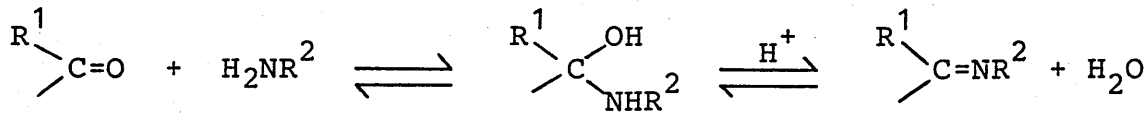

aldehydes, R^1, or the amine, R^2 groups.[62,63] Whilst the dehydration of those aminocarbinols derived from strongly basic amines like phenylhydrazine, hydroxylamine or t-butylamine requires general acid catalysis, those from weekly basic amines like semicarbazide or aniline are catalysed by specific acid.[64] In other words, aminocarbinols derived from strongly basic amines have higher proton affinity than those from weakly basic amines.

As mentioned earlier, aminocarbinols are expected to be more acidic than their aliphatic alcohol counterparts. By corollary, aminocarbinols are believed to be poor o-nucleophiles than aliphatic alcohols. Indeed, the pKa value of $R_2NCH_2\overset{+}{O}H_2$ was estimated to be <-2.3,[47] which, when compared to those calculated values of aliphatic alcohols (Table 1.2.2), lends support to the suggestion.

It has been reported that copper ion promotes the hydrolysis of salicylideneethylamine by trapping the aminocarbinol intermediate[66] (Scheme 1.2.6). This further illustrates the nucleophilicity of the hydroxyl group of aminocarbinols.

Table 1.2.2

$\overset{\oplus}{ROH_2}$	pKa
MeOH	-2.18
EtOH	-1.94
^{n}PrOH	-1.90
^{n}BuOH	-1.87
^{i}PrOH	-1.73
^{t}BuOH	-1.47

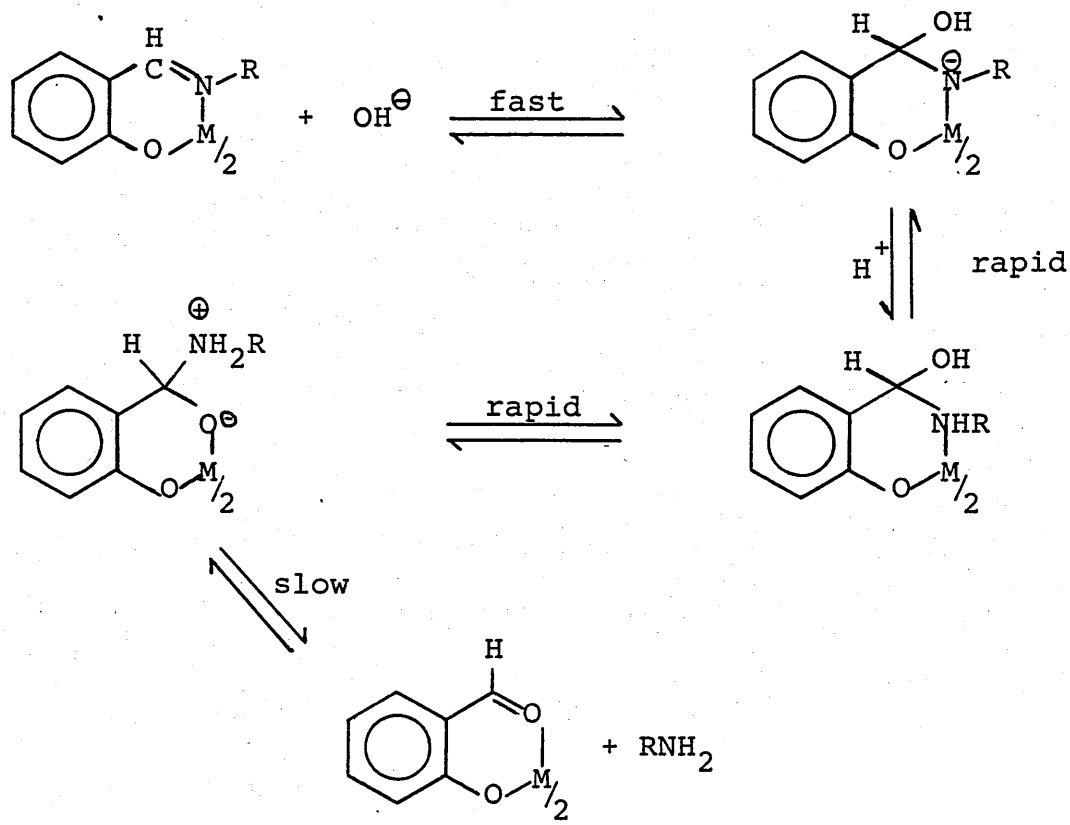

Scheme 1.2.6

1.3 The synthesis of hydroxymethyltriazenes

The chemical synthesis of HMTs was first reported about six years ago by Stevens and coworkers.[27] It involves the coupling of aryldiazonium ions with a premixed solution of methylamine and formaldehyde at -5 to 0 °C. Using this method, the authors managed to synthesise those triazenes from diazonium ions that contain electron withdrawing substituents at the para-position of the benzene ring. Subsequently, a second report claimed to be an improved version was published by Julliard and coworkers.[67] They modified the method by isolating the diazonium ions as fluoroborate salts first before coupling them with a premixed solution of methylamine and formaldehyde. With this modified method, both p-chloro- and p-bromohydroxymethyltriazenes were reported to have been synthesised. The third report was specifically on the synthesis of HMIC[30] (13) which was required for the identification of an isolated metabolite. The synthesis involves the condensation of an anhydrous methanolic solution of formaldehyde with MIC (11).

1.4 Scope of thesis

This thesis looks at the effects of Lewis acids and bases on the decomposition of HMTs. In the case of Lewis acids, it was decided to investigate metal ion rather than proton catalysis because the former is more likely to be biologically significant. This may be illustrated by the natural abundance of metal ions in human blood (pH = 6-7) shown in Table 1.4. Furthermore, lanthanide shift reagents were employed to investigate the metal chelating properties

of HMTs so as to gain a better insight into the mechanism of the decomposition of HMTs by these metal ions. Finally, the synthesis of HMTs has also been investigated.

Table 1.4

M^{n+}	$10^3 \times [M^{n+}]/M$
Fe^{n+}	7
Cu^{2+}	1.5×10^{-2}
Zn^{2+}	0.1
Ca^{2+}	2.5
Pb^{2+}	1×10^{-3}
Cd^{2+}	1×10^{-4}
Mg^{2+}	2
Na^{+}	4
K^{+}	1

CHAPTER 2

SYNTHESIS OF 1-ARYL-3-HYDROXYMETHYL-3-METHYLTRIAZENES AND RELATED COMPOUNDS

2.1 Introduction

The growing speculation on the participation of HMT in the metabolism of the antitumour agent, DMT, has increased the significance of the chemistry of HMT. Our interest in studying the interaction of HMTs with Lewis acids has led us to undertake a synthesis of these compounds. Two reported methods of HMT synthesis were available, *viz* using soluble diazonium chlorides or insoluble diazonium fluoroborates. We reinvestigated both procedures.

The method for the synthesis of HMTs reported by Vernin and coworkers[67] differs from that reported by Stevens' group[27] in two aspects. Firstly, the former group employed a ratio diazonium salt : methylamine : formaldehyde of 1 : 5.3 : 28 compared to that of 1 : 1.8 : 30 used by the latter. Secondly, Stevens' method coupled the diazonium chlorides generated *in situ* directly with a premixed solution of methylamine and formaldehyde whilst Vernin's method involved isolation of the diazonium ions as fluoroborate salts first, thereby avoiding the presence of acid during the coupling process. Given that acid catalyses the decomposition of triazenes (see Section 1.2.3), Vernin's method therefore has an advantage over Stevens'. In the light of this observation, the procedure outlined by Vernin and coworkers was adopted initially.

2.2 The Synthesis of 1-aryl-3-hydroxymethyl-3-methyltriazenes

Vernin's procedure gives satisfactory yields of products whose physical and spectral data are almost identical to

those reported[67] (Table 2.2.1). However, upon closer examination, the spectral data appears to be inconsistent with the expected structure of HMTs.

i. the integration of the four signals in the ^1H nmr spectra give ratios of 1.5 : 2 : 3 : 4 whilst they should be 1 : 2 : 3 : 4.

ii. The signals assigned by Vernin and coworkers as the -OH proton and the $-CH_2$ protons of HMT do not couple with each other even in $(CD_3)_2SO$.

iii. The signal at ca. δ 2.4 ppm assigned to the -OH proton of HMT remains as a sharp singlet even when the sample is shaken with D_2O.

Contrary to the report, the ir spectra do not show the presence of an OH group at 3440 cm^{-1}. This was substantiated with elemental analyses (Table 2.2.2) which revealed either no or a substantially reduced oxygen content present in the products.

Subsequently, on the basis of the following evidence the products were assigned with a new structure viz, N,N-bis-(1-aryl-3-methyltriazen-3-yl)methyl methylamine (22).

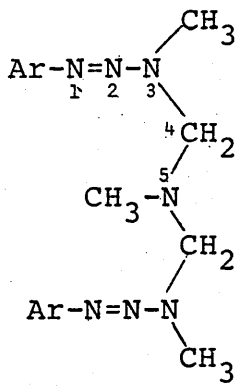

(22)

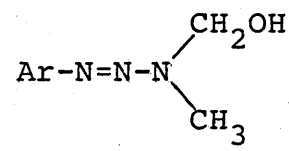

(23)

Table 2.2.1 Melting temperatures and ^{1}Hnmr spectral data for products obtained using Vernin's method

compound	m.t[a]/°C	^{1}Hnmr/ppm	
		observed[b]	reported[c]
Ar=4-ClC_6H_4	110-112 (110)	7.14-7.54(8H,AA'BB');4.56(4H,s); 3.20(6H,s);2.39(3H,s)	7.36(2H,d);7.33(2H,d);4.70(2H,s); 3.32(3H,s);2.52(1H,s)
Ar=4-BrC_6H_4	128 (128)	7.23-7.49(8H,AA'BB');4.59(4H,s); 3.21(6H,s);2.39(3H,s)	7.50(2H,d);7.35(2H,d);4.70(2H,s); 3.30(3H,s);2.52(1H,s)
Ar=4-$COCH_3C_6H_4$	95-96 (115)	7.41-8.12(8H,AA'BB');4.71(4H,s); 3.30(6H,s);2.59(6H,s);2.49(3H,s)	7.99(2H,d);7.55(2H,d);4.75(2H,s); 3.32(3H,s);2.62(3H,s);3.50(aH,s)
Ar=4-CNC_6H_4	107-8 (102)	7.40-7.79(8H,AA'BB');4.70(4H,s); 3.30(6H,s);2.47(3H,s)	7.54(2H,s);7.52(2H,s);4.70(2H,s); 3.32(3H,s);2.49(1H,s)
Ar=4-$NO_2C_6H_4$	141 (108)	7.41-8.24(8H,AA'BB');4.74(4H,s) 3.32(6H,s);2.49(3H,s)	8.22(2H,d);7.57(2H,d);4.76(2H,s); 3.32(3H,s);2.50(1H,s)

a. Values in parentheses are reported by Vernin et. al.[67]

b. Spectra obtained in $(CD_3)_2SO$

c. In $CDCl_3$ ref. 67

Table 2.2.2 Elemental analyses of products

Compound	Elemental analyses									
	Found %					Required %				
	C	H	N	O	X	C	H	N	O	X
Ar=4ClC$_6$H$_4$	51.51	5.25	24.87	0.68	17.75	48.12	5.01	21.05	8.02	17.80
Ar=4-NO$_2$C$_6$H$_4$	49.47	5.05	30.78	14.67		45.71	4.76	26.67	22.86	

The presence of two non-equivalent CH_3 signals in the ^{13}C nmr spectra (Table 2.2.3) confirms that the product contains two different N-CH_3 groups. The -CH_2- signal at 74 ppm can be assigned to an N-CH_2-N functionality. This is good evidence for presuming the compound has structure (22). The microanalytical data are also consistent with the formation of the products as the bis-triazenes (22) (Table 2.2.4). Such observation was also subsequently reported independently by Vaughan and coworkers.[68]

From the structure of (22), it is obvious that the ^1H signal at δ 2.50 ppm which Vernin's group assigned as the OH proton, actually belongs to the N-5 methyl group. Separated by a nitrogen atom, the methyl protons therefore cannot couple with the -CH_2- protons. Furthermore, as the protons are attached to carbon, no proton exchange was observed.

However, reaction of arenediazonium chlorides with a premixed methylamine/formaldehyde solution using the procedure outlined by Stevens and coworkers[27] gives rise to a crude mixture of two products, the ratio of which depends on the diazonium chloride. With the 4-CH_3CO-, 4-CH_3OCO- and 4-H_2NCO- substituted diazonium chloride the minor product (less than 5%) was separated by washing with hexane or chloroform (in which the major product was only slightly soluble) and identified by ^1Hnmr as the bis-triazene compound (22). Based on the following evidence, the major products of the reactions for these substituents were identified as the HMTs:

Table 2.2.3 ^{13}C NMR Chemical shifts (δ/ppm) off resonance multiplicity and $^{1}J_{CH}$ data for bis-triazenes

Compound	Triazene-CH_3	N-CH_3	-CH_2-	Aromatics				Other signals	
Ar=4-ClC_6H_4	34.35(q) (139 hz)	37.57(q) (135 hz)	74.05(t) (146 hz)	121.05(d) (162 hz)	128.85(d) (166 hz)	130.98(s)	149.13(s)		
Ar=4-BrC_6H_4	34.41(q) (139 hz)	37.57(q) (135 hz)	74.05(t) (147 hz)	118.97(s)	122.30(d) (163 hz)	131.70(d) (167 hz)	149.53(s)		
Ar=4-$CH_3COC_6H_4$	34.53(q) (137 hz)	37.68(q) (134 hz)	74.28(t) (150 hz)	120.64(d) (163 hz)	129.43(d) (161 hz)	134.31(s)	154.31(s)	26.48(q) (127 hz)	197.27(s)
Ar=4-$NO_2C_6H_4$	34.70(q) (141 hz)	37.63(q) (127 hz)	74.85(t) (148 hz)	120.93(d) (166 hz)	124.77(d) (169 hz)	145.11(s)	155.51(s)		
Ar=4-CNC_6H_4	34.53(q) (140 hz)	37.51(q) (135 hz)	74.68(t) (137 hz)	119.26(s)	121.27(d) (164 hz)	132.93(d) (166 hz)	153.89(s)	109.29(s)	

Table 2.2.4 Elemental analyses for bis-triazenes

Compound	Found (%)					formula	Required (%)				
	C	H	N	O	X		C	H	N	O	X
Ar=4-ClC_6H_4	51.51	5.25	24.81		17.75	$C_{17}H_{21}N_7Cl_2$	51.78	5.37	24.87		17.98
Ar=4-BrC_6H_4	42.36	4.26	20.55			$C_{17}H_{21}N_7Br_2$	42.26	4.38	20.29		
Ar=4-$CH_3COC_6H_4$	61.64	6.70	23.81			$C_{21}H_{27}N_7O_2$	61.61	6.60	23.96		
Ar=4-$NO_2C_6H_4$	49.47	5.05	30.47	14.67		$C_{17}H_{21}N_9O_4$	49.16	5.06	30.36	15.42	
Ar=4-CNC_6H_4	60.72	5.61	33.77			$C_{19}H_{21}N_9$	60.80	5.60	33.60		

i. the signals in the ^{1}Hnmr spectra (Table 2.2.5) assigned to the -OH and $-CH_2-$ protons exist as a triplet and a doublet respectively in $(CD_3)_2SO$, though in $CDCl_3$ the OH signal was difficult to observe,

ii. when the sample is shaken with D_2O, the triplet signal disappears while the doublet signal collapses to a singlet thus confirming that the $-CH_2-$ and -OH protons are coupling to each other,

iii. the integration of the four signals are in the ratios of 1 : 2 : 3 : 4,

iv. the ^{13}C nmr spectra reveal only one CH_3 signal (Table 2.2.6),

vi. the ir spectra show the presence of an OH group (Table 2.2.7),

v. the elemental analyses of the compounds agree with their formulation as HMTs (Table 2.2.7).

In contrast, reaction of $4-NO_2-$, 4Cl- or 4Br-benzenediazonium chloride gives rise in fairly moderate yield to corresponding bis-triazene (22) as the only isolable products. This marked variation of product ratio on the structure of the diazonium chloride used also depends on several other factors.

On lowering the reaction temperature from -5 ^{o}C to between -10 and -15 ^{o}C the proportion of HMTs increased in all cases except for 4-Cl and 4-Br. The ratio diazonium salt : methylamine : formaldehyde was found to be another factor. It was observed that reducing this ratio from 1 : 1.8 : 30 used in the standard Stevens procedure to 1 : 1 : 30 yielded

Table 2.2.5 ^{1}HNmr chemical shifts (δ/ppm) for the hydroxymethyltriazenes

Compound	Aromatic	CH_2	Triazene CH_3	OH[a]	Other signals
Ar=4-ClC_6H_4	7.09-7.85(4H,AA'BB')	5.13(2H,d,J=7 hz)	3.14(3H,s)	6.26(1H,t,J=7 hz)	
Ar=4-$NO_2C_6H_4$	7.50-8.43(4H,AA'BB)	5.20(2H,d,J=7 hz)	3.23(3H,s)	6.51(1H,t,J=7 hz)	
Ar=4-CNC_6H_4	7.33-7.86(4H,AA'BB')	5.09(2H,d,J=7.5 hz)	3.11(3H,s)	6.33(1H,t,J=7.5 hz)	
Ar=4-$CH_3OCOC_6H_4$	7.49-8.15(4H,AA'BB')	5.16(2H,d,J=7 hz)	3.18(3H,s)	6.34(1H,t,J=7 hz)	3.84(3H,s)
Ar=4-$C_2H_5OCOC_6H_5$	7.40-8.17(4H,AA'BB')	5.19(2H,d,J=7.5 hz)	3.20(3H,s)	6.37(1H,t,J=7.5 hz)	4.32(2H,q,J=7 hz) 1.32(3H,t,J=7 hz)
Ar=4-$CH_3COC_6H_4$	7.37-8.15(4H,AA'BB')	5.17(2H,d,J=7.5 hz)	3.20(3H,s)	6.38(1H,t,J=7.5 hz)	2.56(3H,s)
Ar=4-$NH_2COC_6H_4$	7.30-8.03(4H,AA'BB')	5.13(2H,d,J=7 hz)	3.15(3H,s)	6.24(1H,t,J=7 hz)	7.04-8.03(2H, ex)
Ar=4-$CF_3C_6H_4$	7.55-7.68(4H,AA'BB')	5.17(2H,d,J=7 hz)	3.17(3H,s)	6.36(1H,t,J=7 hz)	
Ar=2-$CF_3C_6H_4$	7.50-7.70(4H,AA'BB')	5.17(2H,d,J=7 hz)	3.77(3H,s)	6.32(1H,t,J=7 hz)	

a All OH proton signals disappear in shaking sample in D_2O

Table 2.2.6 ^{13}CNmr chemical shifts (δ/ppm), off resonance multiplicity and J^{1}C-H data for hydroxymethyltriazenes

Compound	Triazene-CH_3	$-CH_2-$	Aromatics				Other signals		
Ar=4-ClC_6H_4	32.92(q) (141 hz)	77.84(t) (157 hz)	121.90(d) (163 hz)	128.80(d) (166 hz)	129.54(s)	149.02(s)			
Ar=4-$NO_2C_6H_4$	33.37(q) (140 hz)	78.73(t) (158 hz)	121.27(d) (166 hz)	125.40(d) (168 hz)	144.67(s)	155.47(s)			
Ar=4-CNC_6H_4	33.09(q) (140 hz)	78.24(t) (157 hz)	119.03(s)	121.04(d) (166 hz)	122.16(d) (166 hz)	153.61(s)	107.36(s)		
Ar=4-$CH_3OCOC_6H_4$	31.15(q) (139 hz)	73.73(t) (155 hz)	133.55(d) (163 hz)	119.13(s)	122.87(d) (164 hz)	145.19(s)	48.92(q) (147 hz)		156.51(s)
Ar=4-$C_2H_5OCOC_6H_4$	33.09(q) (141 hz)	78.18(t) (155 hz)	120.41(d) (164 hz)	126.61(s)	130.23(d) (163 hz)	153.96(s)	14.19(q) (127 hz)	60.49(t) (148hz)	165.50(s)
Ar=4-$CH_3COC_6H_4$	33.09(q) (140 hz)	78.24(t) (157 hz)	120.41(d) (163 hz)	129.48(d) (161 hz)	133.91(s)	153.84(s)	26.48(q) (127 hz)		196.98(s)
Ar=4-$NH_2COC_6H_4$	32.97(q) (140 hz)	77.90(t) (154 hz)	119.95(d) (163 hz)	129.45(d) (162 hz)	131.09(s)	152.35(s)	167.57(s)		
Ar=4-$CF_3C_6H_4$	33.09(q) (138 hz)	78.3(t) (155 hz)	120.98(d) (164 hz)	126.15(d) (164 hz)	118.60(s)	130.57(s)	153.44(s)		
Ar=2-$CF_3C_6H_4$	32.92(q) (140 hz)	78.12(t) (155 hz)	117.82(d) (171 hz)	126.31(d) (159 hz)	133.05(s) (85 hz)	118.2(s)	125.41(d) (185 hz)	125.98(d) (160 hz)	148.15(s)

Table 2.2.7 Ir spectral data and elemental analyses for hydroxymethyltriazenes (23)

Compound	m.t.[a]/°C	i.r./cm^{-1} (nujol)	Found (%)				formula	Required (%)			
			C	H	N	O		C	H	N	O
Ar=4-ClC_6H_4	58-59	3250	48.11	5.08	20.91	8.15	$C_8H_{10}N_3OCl$	48.12	5.01	21.05	8.02
Ar=4-$NO_2C_6H_4$	103-4	3500,1595	45.85	4.88	26.94	22.89	$C_8H_{10}N_4O_3$	45.71	4.76	26.67	22.86
Ar=4-CNC_6H_4	120-1	3410,2210	56.82	5.25	29.31	8.29	$C_9H_{10}N_4O$	56.84	5.26	29.47	8.42
Ar=4-$CH_3OCOC_6H_4$	126 (126-127)	3340,1696	53.95	5.92	18.72	21.23	$C_{10}H_{13}N_3O_3$	53.81	5.83	18.83	21.53
Ar=4-$C_2H_5OCOC_6H_4$	71-72 (73-75)	3455,1690	55.94	6.44	17.83	20.39	$C_{11}H_{15}N_3O_3$	55.70	6.33	17.72	20.25
Ar=4-$CH_3COC_6H_4$	120-2 (117-120)	3345,1650	58.17	6.34	20.30	15.28	$C_{10}H_{13}N_3O_2$	57.97	6.28	20.29	15.46
Ar=4-$NH_2COC_6H_4$	138-9 (141-142)	3450,3200	52.02	5.91	26.95	15.60	$C_9H_{12}N_4O_2$	51.92	5.77	26.92	15.39
Ar=4$CF_3C_6H_4$	50	3380	46.21	4.40	18.08		$C_9H_{10}N_3OF_3$	46.35	4.32	18.02	
Ar=2$CF_3C_6H_4$	60-60.5	3290	46.18	4.39	17.69		$C_9H_{10}N_3OF_3$	46.35	4.32	18.02	

a Values in parentheses are lit. values for ref.27

some 4-Cl- and 100% pure 4-CN- and 4-NO_2HMTs. The yield of 4-ClHMT can also be improved by neutralising the diazonium chloride solution to pH 7 before addition. Surprisingly, if the methylamine/formaldehyde mixture is added to the pH 7 4-Cl benzenediazonium chloride solution, rather than the other way round, the yield of 4-ClHMT is increased still further. The physical and spectral data of all the HMTs are presented in Tables 2.2.5.-2.2.7.

2.3 The Mechanism of Formation of Hydroxymethyltriazenes and Bis-triazenes

Several possibilities present themselves as to how bis-triazenes may be formed. One is that excess methylamine condenses with HMT to give the bis-triazene. Another is that three molecules of methylamine condense with two of formaldehyde yielding the N,N-bis(methylaminomethyl)methylamine (24) which then couples with two diazonium ions (Scheme 2.1).

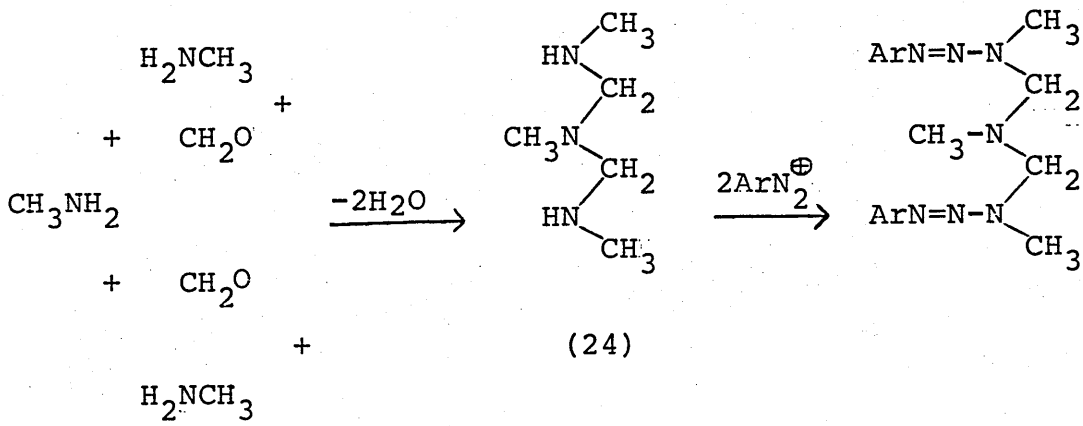

Scheme 2.1

The first hypothesis was tested by stirring the HMT with methylamine in the presence of excess formaldehyde or

with methylamine buffers in the pH range 7-10. No reaction takes place in both cases and HMT was recovered. In contrast, methylamine alone promotes the transformation of HMT to the monomethyltriazene and not the expected bis-triazene (see Chapter 5) (Table 2.3.1).

The second hypothesis seems unlikely since the most likely product from such condensation is the cyclic trimer. There is good evidence for this type of reaction.[45] Formaldehyde is known to condense with aliphatic amines at room temperature in the presence of OH^- to give the corresponding aminomethyl derivatives. Whilst certain aminomethylols are isolable, most of them undergo further reaction, either by condensation with another amine molecule to give the N,N-bis(alkylamino)methane or by dehydration to give the imine. However, the Schiff base from methylamine and formaldehyde is too unstable to exist as a monomer. It cyclises readily to form the cyclic trimer. Given that excess formaldehyde was used in this reaction, the formation of the N,N-bis(methylamino)methane therefore seems unlikely. A further example is the condensation of aldehydes with ammonia.[69] At -10 °C, the product is the 1-amino-1-alkanol hydrates $RCH(OH)NH_2.xH_2O$. This compound can be converted to 2,4,6-trialkyl-1,3,5-hexahydrotriazines (25) on standing in 15M aqueous ammonia at 0-5 °C. This cyclic product loses

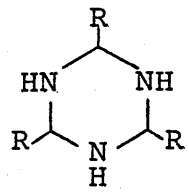

(25)

ammonia upon warming above 25 °C to form N,N-dialkylidene-1,1-diaminoalkanes $RCH(N=CHR)_2$. The aldimines RCH=NH are not

Table 2.3.1 Results of HMT reactions with methylamine

Compound [a]	$[MeNH_2]$/mol	pH	Temp	time/hr	Result
$4\text{-}CNC_6H_4$	4.5×10^{-4}	10.8	0 °C	0.5	HMT
$4\text{-}COCH_3C_6H_4$	4.5×10^{-4}	10.8	0 °C	0.5	HMT
$4\text{-}COCH_3C_6H_4$	1.36×10^{-3}	9.83	0 °C	0.5	HMT
$4\text{-}COCH_3C_6H_4$	1.7×10^{-3} [b]	-	R.T.[c]	15	HMT
$4\text{-}COCH_3C_6H_4$	1.7×10^{-3}	-	R.T.	15	HMT[d]
$4\text{-}COCH_3C_6H_4$	1.7×10^{-3}	8.6	0 °C	0.5	HMT
$4\text{-}NO_2C_6H_4$	1.7×10^{-3}	8.6	0 °C	0.5	HMT
$4\text{-}CNC_6H_4$	1.7×10^{-3}	8.6	0 °C	0.5	HMT

a 0.1g of HMT was used in 40 ml of solution

b with the presence of 1.25×10^{-2} mol of formaldehyde

c R.T. = room temperature

d for complete results, see Chapter 5

obtained. Although the starting materials used in the above study are different from those employed in ours, the pattern of decomposition of such aminocarbinols is likely to be the same.

In addition, no difference in the ratio of HMT : bis-triazene was observed on changing the ratio of methylamine : formaldehyde from 1 : 15 to 1 : 30. One might have anticipated more bis-triazene from the former ratio than the latter.

A mechanism which can account for the formation of both the HMT and the bis-triazene is shown in Scheme 2.2. The

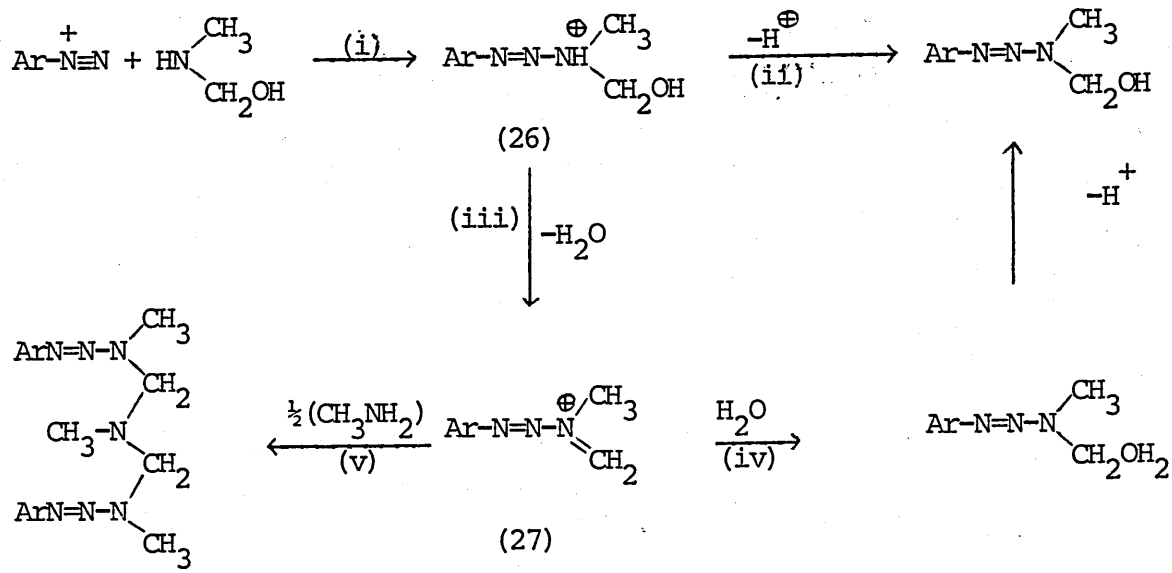

Scheme 2.2

coupling of the diazonium ion with the methylaminomethanol, generated in situ, affords the protonated HMT (26) (Step i). At neutral pH, this compound (26) rapidly deprotonates to give the HMT (Step ii). In a more acidic environment, however, dehydration of (26) to give (27) (Step iii) competes with deprotonation. The intermediate (27) may be trapped either by water to yield the HMT (Step iv) or by unreacted methylamine

to give the bis-triazene (Step v). This reactive "methylenetriazenium" ion (27) has also been proposed as the intermediate in the decomposition of the benzoate ester of 4-$COOCH_3$HMT.[27] Using pKa values as a guide to reactivity, methylamine is some 10^9 times more reactive than water. This difference will far outweigh the difference in concentration of the two species which is roughly $[H_2O]/[MeNH_2] = 10^3$. Consequently, trapping of the intermediate (27) by methylamine will occur preferentially. Other workers[70] have questioned the presence of "free" methylamine in the reaction mixture which is guaranteed by the existence of a equilibrium involving methylamine itself.

Two pieces of experimental evidence lend support to the proposed mechanism (Scheme 2.2). Firstly, as was mentioned earlier (Section 2.2), the dropwise addition of the methylamine/formaldehyde mixture to the neutralised solution of 4-chlorobenzenediazonium chloride affords higher yield than the corresponding inverse addition. Such an observation can be explained by the comparatively higher water : methylamine ratio present in the former procedure than in the latter. As a result, the formation of HMT is more favourable. Secondly, it was found that the synthesis of (4-$COCH_3$)bis-triazene was successful only when the diazonium fluoroborate was used in place of the chloride. The fact that the diazonium fluoroborate is an insoluble solid whereas the diazonium chloride is soluble suggests that fluoroborate ion is a good cation stabiliser. Taken together, it is very likely that the presence of fluoroborate ion stabilises the methylenetriazenium ion thereby making the intermediate become more selective. Consequently,

the triazenium ion prefers to react with the more basic methylamine hence favouring the bis-triazene formation.

2.4 The Synthesis of some Alkyl Homologues of Hydroxymethyltriazenes and Heteroaromatic Hydroxymethyltriazenes

The syntheses of 3-alkyl homologues of hydroxymethyltriazene (28) were carried out with a slightly modified procedure to that described above. Instead of premixing the

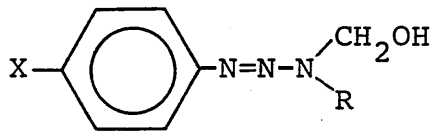

(28)

alkylamine and formaldehyde solutions, aqueous formaldehyde was first poured into the diazonium chloride solution followed by the dropwise addition of alkylamine. In this way, the vigorous reaction of formaldehyde with alkylamines which produces an oil that separates out is avoided. Both 1-(4-acetylphenyl)-3-hydroxymethyl-3-ethyltriazene (28, X=$COCH_3$, R=CH_2CH_3) and the corresponding 3-n-propyl homologue (R=$CH_2CH_2CH_3$) were synthesised using this modified procedure (Table 2.4.1). The n-butyl homologue (28, R=$-(CH_2)_3CH_3$) was obtained as an impure oil which could not be crystallised. Attempts to extend the procedure described above to iso-propyl- and tert-butyl-amines failed to produce the desired compounds. Instead, in the case of the iso-propylamine, the mono-iso-propyl-derivative was obtained. Furthermore, although condensing MMTs with formaldehyde is a established way of HMT synthesis, the synthesis of pACH^{i}PrT from the monoisopropyltriazene did

Table 2.4.1(a) Melting temperature and microanalytical data for

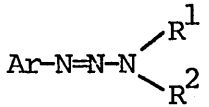

No.	Ar	R^1	R^2	melting tempt./ °C	Found %			Required %		
					C	H	N	C	H	N
I	4-$COCH_3C_6H_4$	$-CH_2OH$	$-CH_2CH_3$	94.5-95.5	59.60	6.86	18.81	59.73	6.79	19.00
II	4-$COCH_3C_6H_4$	$-CH_2OH$	$-CH_2CH_2CH_3$	69-70	61.44	7.54	17.67	61.26	7.28	17.86
III	4-$COCH_3C_6H_4$	$-CH_2OH$	$-CD_3$	123-124	56.66	6.40	19.97	57.13	7.69 [a]	19.99
IV	4-$COCH_3C_6H_4$	-H	$-CH(CH_3)_2$	108-109	63.84	7.42	19.17	64.37	7.37	20.47
V	3-C_5H_4N	$-CH_2OH$	$-CH_3$	118	50.63	5.92	33.55	50.59	6.07	33.71

a Deuterium is considered as H

Table 2.4.1(b) ^{1}HNmr spectral data in $(CD_3)_2SO$ (δ/ppm)

No.	Aromatic	CH_2	OH	R^2	X
I	7.5-8.05(4H, (AA'BB')	5.19 (2H,d,J=7hz)	6.35 (1H,t,J=7hz)	3.82(2H, ,J=7.5hz); 1.22(3H,C,J=7.5hz)	2.59(3H,s)
II	7.45-8.05(4H, (AA'BB')	5.14 (2H,d,J=7hz)	6.28 (1H,t,J=7hz)	3.70(2H,t,J=7.5hz);1.70 (2H,m,J=7.5hz);0.90(3H,d, J=7.5hz)	2.55(3H,s)
III	7.45-8.05(4H, (AA'BB')	5.15 (2H,d,J=7hz)	6.31 (1H,t,J=7hz)	-	2.55(3H,s)
IV	7.25-7.95(4H, (AA'BB')	-	-	3.80(1H,m,J=7hz) 1.23(6H,d,J=7hz)	2.5(3H,s)
V	7.26-8.82 (4H,m)	5.18 (2H,d,J=7hz)	6.36 (1H,t,J=7hz)	3.19(3H,s)	-

Table 2.4.1(c) ^{13}C Nmr spectral data in $(CD_3)_2SO$ (δ/ppm) with off resonance and J^1C-H data

No.	CH_2	R^2	Aromatics	X
I	76.92 (t) (159 hz)	11.37 (q) 40.18(t) (128 hz) (139 hz)	154.01(s) 133.85(s) 129.57(d) 120.29(d) (161 hz) (163 hz)	196.7(s) 26.42(q) (128 hz)
II	77.27 (t) (157 hz)	46.76(t) 19.01(t) 11.55 (q) (135 hz) (126 hz) (124 hz)	158(s) 133.79(s) 129.43(d) 120.29(d) (162 hz) (163 hz)	196.75(s) 26.48(q) (128 hz)
III[a]	78.069(t) (157 hz)		153.78(s) 133.79(s) 129.37(d) 120.29(d) (162 hz) (163 hz)	196.75(s) 26.48(q) (128hz)
IV		60.09(d) 21.66(q) (133 hz) (127 hz)	147(s) 119.83(s) 112.37(d) 130.08(d) (163 hz) (161 hz)	195.89(s) 26.19(d) (127 hz)
V	77.90(t) (157 hz)	32.86(q) (138 hz)	123.80(d) 126.04(d) 143.10(d) 146.49(d) 145.86(s) (164 hz) (169hz) (179 hz) (179 hz)	

a The CD_3 signal was not observed probably due to C-D coupling

not succeed. This may be due to the increase in steric hindrance of the bulky alkyl groups. Jencks and other workers[49,50,51] have demonstrated that the formation of aminocarbinols from formaldehyde and amines is very sensitive to steric effects. An increase in steric hindrance will decrease the equilibrium constant for the aminocarbinol formation.

On the other hand, the method for 4-ClHMT synthesis was successfully applied to that of 3-pyridylHMT (29) (Table 2.4.1). However, some changes were necessary when this procedure was extended to the synthesis of the clinically useful HMIC (13). The most important factor is that diazoimidazole carboxamide is unstable in water, cyclising readily in aqueous solution to form 2-azahypoxanthine (30) over a wide range of pH.[71] Besides, both MIC (11) and DIC (3) are sensitive to light. Consequently methanol was used

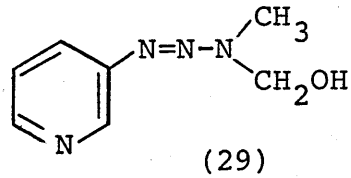

(29)

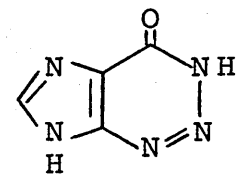

(30)

as solvent while the reaction was protected from light. Aqueous formaldehyde was still employed. Despite all these changes, the product obtained was found to be the MIC (11). The structure was confirmed with a genuine sample prepared by Shealy's method.[72] Kolar's procedure[29] of condensing MIC with a methanolic solution of formaldehyde was subsequently followed and the solid obtained was analysed. The ^{1}Hnmr spectrum revealed two doublets, one at δ5.18 ppm and the other at δ5.63 ppm. In addition, there is also a multiplet at δ6.45 ppm. When the sample was shaken in D_2O, the two doublets

collapsed into two singlets and the multiplet disappeared. The elemental analyses of the product suggests that it was contaminated (Table 2.4.2). It is possible that the two tautomers of MIC can condense with formaldehyde individually giving rise to two isomers of HMIC (Scheme 2.3).

Table 2.4.2 Elemental analyses of products from Kolar's procedure

	Found (%)			Required (%)		
	C	H	N	C	H	N
1st sample	37.36	5.83	34.31	36.36	5.05	42
2nd sample	37.69	5.86	34.45			

Scheme 2.3

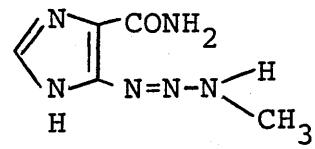

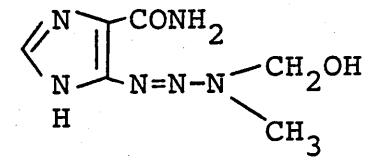

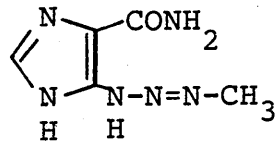

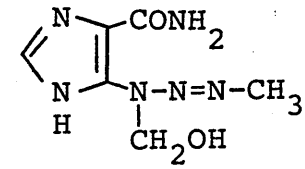

The two isomers of HMIC should however give the required elemental analysis. Finally, it is worth pointing out that Kolar's procedure did not exclude light from the reaction, and it may be possible that, in the event, either HMIC or MIC undergoes photodecomposition thereby contaminating the final product.

CHAPTER 3

LEWIS ACID CATALYSED DECOMPOSITION OF 1-ARYL-3-HYDROXYMETHYL-3-METHYLTRIAZENES

3.1 Introduction

Despite the significance of the chemistry of HMTs to their medicinal efficacy, no detailed study has been conducted so far. The only report is the decomposition of the 4-$COCH_3$HMT to the corresponding aniline at pH7 and no mechanism was given.[27]

Triazenes are known to decompose in the presence of H^+ and monoalkyltriazenes can form metal complexes. Therefore, Lewis acids eg. transition metal ions were anticipated to be capable of bringing about a decomposition of HMTs. Given the physiological ubiquity of metal ions, this reaction should be important in a biological context.

Moreover, in physiological conditions, metal ions are often bound with proteins. Inside these macromolecules, the environment may be very different from a purely aqueous medium. Thus, the effects of ligands and solvents on these metal ion reactions were investigated.

3.2 Metal Ion Promoted Reactions in Water

Water was the first solvent chosen for the metal ion reaction because blood serum consists mainly of water and most metal salts are soluble in water.

3.2.1 Qualitative Studies

These were carried out by stirring a suspension of HMT (0.3 mmol) in an 0.1M solution (40 ml) of the metal ion for

15 hours at room temperature. With Fe^{2+}, Fe^{3+}, Cu^{2+}, Zn^{2+}, Ag^{+}, Cd^{2+} and Pb^{2+}, the products were found to be the N,N-bis(arylamino)-methane(32) (Scheme 3.2.1), whereas with Mg^{2+}, Ca^{2+}, K^{+}, Na^{+} and Mn^{2+}, no reaction was observed (Table 3.2.1). The results for 4CN- and 4-NO_2 HMTs

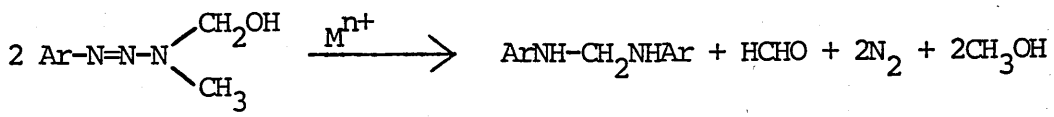

(31) Scheme 3.2.1 (32)

are complicated because of their conversion to MMTs in water (see Chapter 5). Compounds (32) were formed in yields of 75-95% and were characterised by elemental analyses, i.r., ^{1}H and ^{13}C nmr spectroscopies (Table 3.2.2). The formaldehyde coproduct was trapped by treating the filtrate with dimedone, yielding 50% of the theoretical amount.

The former group of metal ions, except Fe^{3+}, can be classified as intermediate/soft acids whilst the latter are hard acids. The fact that all but one of the transition metals used in this study catalysed the reaction and that the triazene moiety of (31) is likely to be a good chelating agent for transition metals[21] suggests that this may be a metal ion coordinated reaction.

It is well established[76] that for a given ligand and divalent ions of the first transition series, the stability constants of the chelate roughly follows the Irving-Williams order of ionic potential, that is:

$$Mn^{2+} < Fe^{2+} < Co^{2+} < Ni^{2+} < Cu^{2+} > Zn^{2+}$$

Table 3.2.1 Products obtained from metal ion catalysed decomposition of HMTs.[a,b]

Compound / Metal Salts	Ar = 4-$COOCH_3C_6H_4$	Ar = 4-$COCH_3C_6H_4$	Ar = 4-CNC_6H_4	Ar = 4-$NO_2C_6H_4$
Na^+Cl^-		HMT		
$(Na^+)_2SO_4^{2-}$	HMT	HMT		
$(K^+)_2SO_4^{2-}$	HMT	HMT		
$Ca^{2+}SO_4^{2-}$	HMT	HMT		
$Ca^{2+}(OAc)_2^-$	HMT			
$Mg^{2+}SO_4^{2-}$	MBA/HMT (10:90)	HMT	MMT/HMT	MMT/HMT
$Mn^{2+}SO_4^{2-}$	HMT	HMT		
$Fe^{2+}SO_4^{2-}$	MBA/aniline (85:15)	MBA [c]	MBA	MBA
$(Fe^{3+})_2(SO_4)_3^{2-}$	MBA/HMT (85:15)	MBA/aniline (20:80)	MBA/MMT (70:30)	MBA/HMT (95:5)
$Cu^{2+}SO_4^{2-}$	MBA/HMT (75:25)	MBA	MBA	MBA/HMT (65:35)
$Ag^+NO_3^-$	MBA	MBA		
$Zn^{2+}SO_4^{2-}$	MBA	MBA	MBA	MBA/MMT/HMT (35:60:5)
$Cd^{2+}SO_4^{2-}$	MBA/HMT (70:30)	MBA		
$Pb^{2+}(NO_3)_2^-$	MBA/HMT (90:10)	MBA		

Note a) numbers within parentheses are ratios of products. b) MBA : N,N-bis(arylamino)methane.

c) 50% of theoretical yield of formaldehyde coproduct was trapped from filtrate with dimedone.

Table 3.2.2 Physical data for N,N-bis(arylamino)methanes (32)

	Substrate	Product	m.p.(°C)/lit.	Found (%)			Calc.(%)		
				C	H	N	C	H	N
(31a)	Ar=4-$MeCOC_6H_4$	(32a)	195-7	72.4	6.4	9.9	72.3	6.4	9.9
(31b)	Ar=4-$MeOCOC_6H_4$	(32b)	210-2	64.4	5.8	8.8	65.0	5.7	8.9
(31c)	Ar=4-$NO_2C_6H_4$	(32c)	240/235-7 [c]	53.8	4.0	19.0	54.2	4.2	19.4
(31d)	Ar=4-CNC_6H_4	(32d)	172-4	72.1	4.7	22.6	72.6	4.9	22.6

Product	^1H n.m.r.[a]				
(32a)	2.42(6H,s),	4.62(2H,t),	6.78(4H,d),	7.30(2H,t,ex),	7.79(4H,d)
(32b)	3.78(6H,s),	4.60(2H,t),	6.78(4H,d),	7.26(2H,t,ex),	7.78(4H,d)
(32c)	4.74(2H,t),	6.85(4H,d),	7.98(2H,t,ex),	8.11(4H,d)	
(32d)	4.58(2H,t),	6.69(4H,d),	7.36(2H,t,ex),	7.51(4H,d)	

Product	^{13}C n.m.r.[b]						
(32a)	25.8(q),	51.1(t),	111.4(d),	125.6(s),	130.2(d),	151.5(s),	195.2(s)
(32b)	51.2(t),	51.2(q),	111.7(d),	116.7(s),	130.8(d),	151.6(s),	166.3(s)
(32c)	50.8(t),	111.6(d),	126.0(d),	136.8(s),	153.1(s)		
(32d)	51.0(t),	97.1(s),	112.6(d),	120.5(s),	133.4(d),	150.9(s)	

a In $(CD_3)_2SO$ using a Perkin-Elmer R12 spectrometer b In $(CD_3)_2SO$ using JEOL FX90Q spectrometer

At lower concentration of M^{n+} (down to 0.0001M), mixture of (32) and (31) were formed. The effectiveness of the metal ion at bringing about the above reaction could thus be judged from the ratio (32):(31) in these mixtures. From the results (Table 3.2.3) the following approximate order is obtained:

$$Fe^{2+} > Cu^{2+} > Fe^{3+} > Zn^{2+} > Pb^{2+} > Cd^{2+}$$

However, this does not correlate well with the Irving-Williams series.

The most likely mode of action of the metal ion is to bring about the decomposition of HMT to MMT and then of MMT to the aniline as MMT was also found to produce (32) with the metal ion and an equimolar amount of formaldehyde. Likewise, treating the corresponding aniline with an equivalent amount of formaldehyde in the presence of the metal ion yields (32).

Table 3.2.3 Percentage conversion (31) → (32) at varying $[M^{n+}]$

Substrate	%(32): %(31) in 0.001M M^{n+} [a]				%(32): %(31) in 0.1M M^{n+} [a]		
	Zn^{2+}	Fe^{2+}	Fe^{3+}	Cu^{2+}	Zn^{2+}	Pb^{2+}	Cd^{2+}
(31a)	25:75	100:0	100:0	95:5	100:0	100:0	100:0
(31b)	60:40	100:0	90:10	100:0	100:0	90:10	70:30

a Determined from the ^1H n.m.r. of the mixture

3.2.2 Kinetic Studies

In order to gain a better insight into the mechanism of these metal ion reactions, kinetic work was undertaken.

3.2.2.1 Unbuffered Solutions

The decomposition of 4-$COCH_3$ and 4-$COOCH_3$HMT in an unbuffered metal ion solution were found to follow first order kinetics (see Experimental). However, the effect of metal ion concentration upon the rate of reaction is less conclusive (Table 3.2.4). Nevertheless, for the reaction of 4-$COCH_3$ with Zn^{2+}, a straight line was drawn using - arbitrarily - half of the experimental data, giving a slope of $2.9405 \times 10^{-2}M^{-1}S^{-1}$ (Fig. 3.2.1a). Likewise, for 4-$COOCH_3$ with Zn^{2+}, a slope of $5.5268 \times 10^{-2}M^{-1}S^{-1}$ was obtained (Fig. 3.2.1b). The results from Cu^{2+} reaction was more scattered.

A major reason for the inconclusive result is the pH of the metal ion solution. Transition metals are known to hydrolyse in water to give acidic solutions. In other words, solutions containing different amount of metal ions will have different pHs. This was confirmed by measuring the pH of $ZnSO_4$ solution at the range of concentrations used in the kinetic studies (Table 3.2.5). Since triazenes are unstable in acid, the hydrolysis of metal ions will inevitably affect the rate of decomposition of HMTs.

Table 3.2.4 Kinetic data for $4\text{-}COCH_3$- and $4\text{-}COOCH_3$HMTs with Zn^{2+} and Cu^{2+} in 10% alc. solution I=0.05M T=25 °C.

Compound \ Metal	$ZnSO_4$		$CuSO_4$	
	$[Zn^{2+}]$/M	kobs $x10^3/s^{-1}$	$[Cu^{2+}]$/M	kobs $x10^3/s^{-1}$
$4\text{-}COCH_3$-HMT	0.01	0.9912	0.0008	1.5525
	0.01	0.6263	0.0008	1.3331
	0.01	0.6209	0.0005	1.6233
	0.01	0.4325	0.0005	0.855
	0.01	0.3753	0.0002	1.382
	0.008	0.5456	0.0002	0.8269
	0.008	0.4674	0.0001	0.248
	0.005	0.5238		
	0.005	0.4614		
	0.002	0.4247		
	0.001	0.3132		
	-	0.1951		
$4\text{-}COOCH_3$-HMT	0.01	1.2575	0.0008	1.5835
	0.008	1.1181	0.0008	1.3337
	0.008	1.1049	0.0005	1.86
	0.005	0.9799	0.0005	1.7365
	0.005	0.9382	0.0002	1.4277
	0.001	0.9271	0.0002	1.1711
	0.001	0.5562		

Fig. 3.2.1a Decomposition of 4-CH_3COHMT in 10% alcohol solution by Zn^{2+} at 25°C I=0.05M

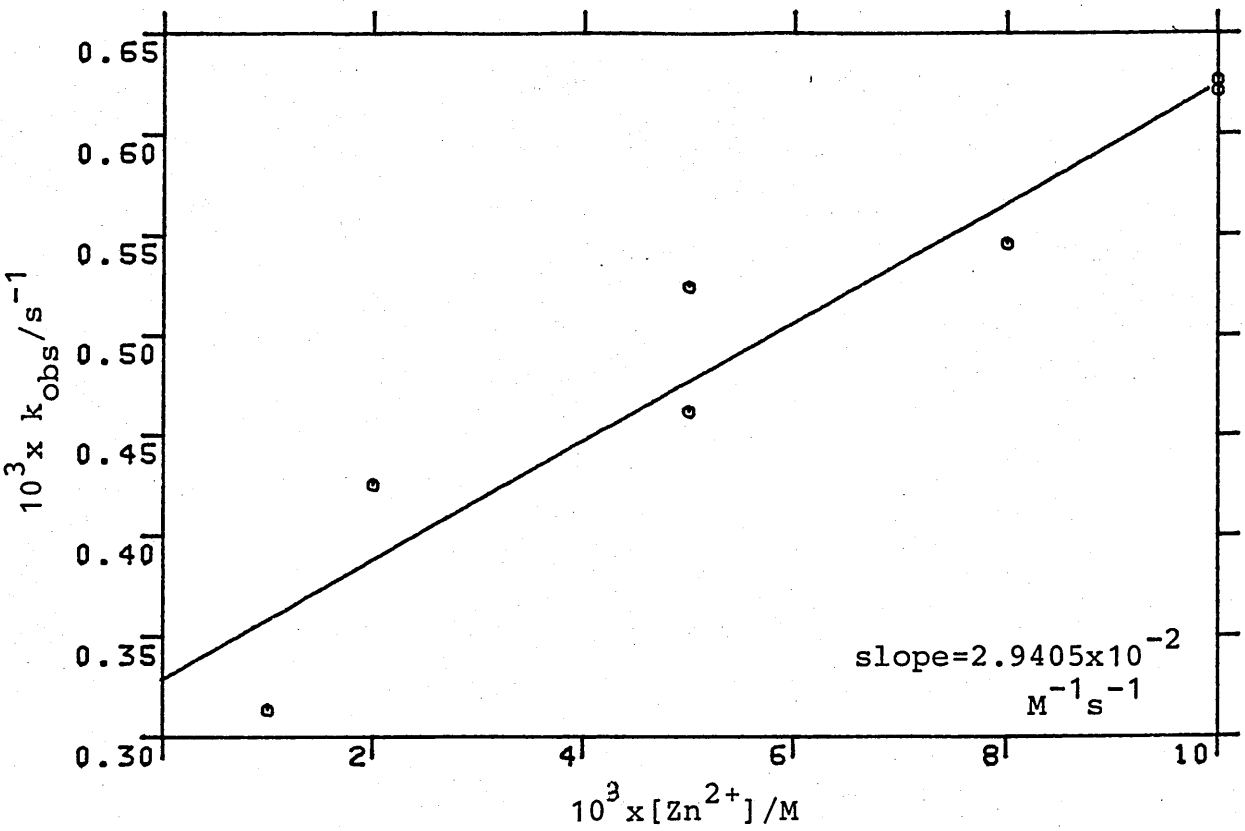

Fig. 3.2.1b Decomposition of 4-CH_3COOHMT in 10% alcohol solution by Zn^{2+} at 25°C I=0.05M

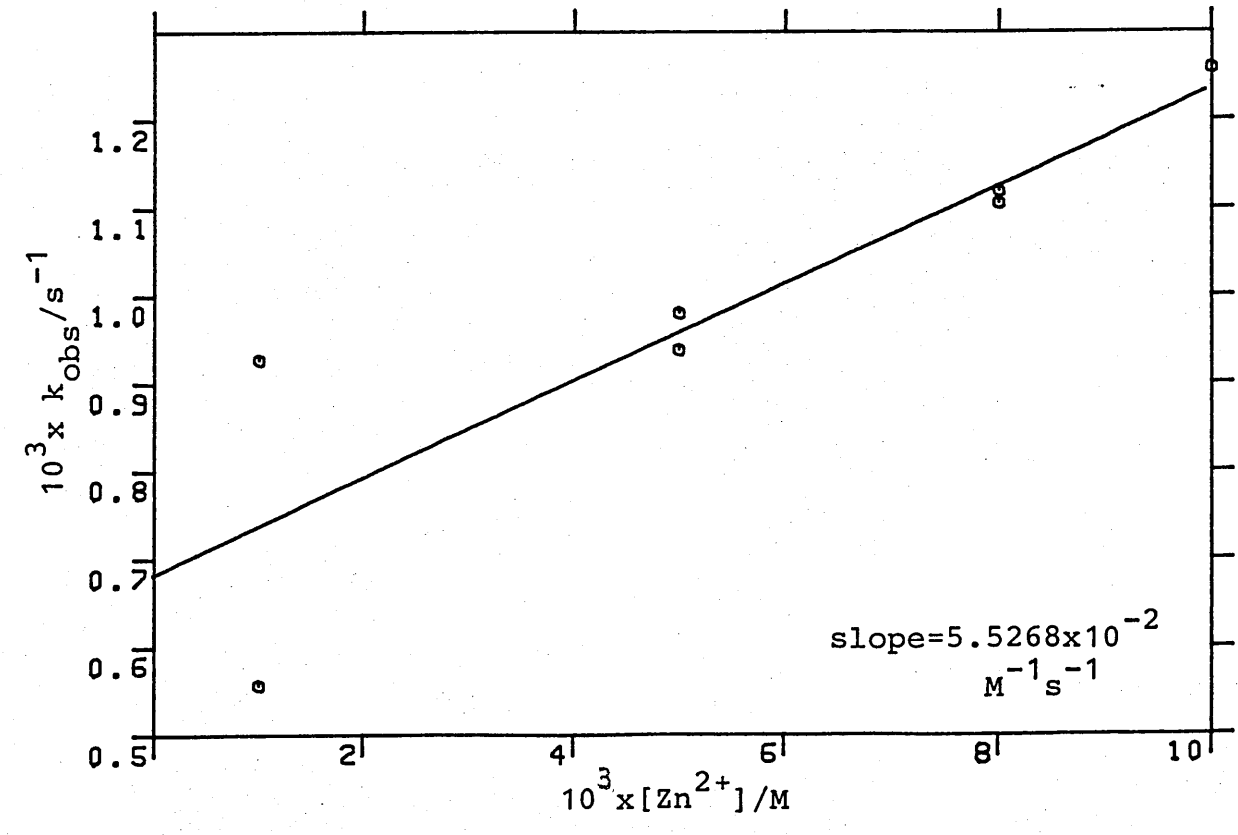

Table 3.2.5 pH of $ZnSO_4$ solution, ionic strength = 0.05M T=25 °C.

$[Zn^{2+}]$/M	pH
0.01	6.22
0.0008	6.278
0.005	6.392
0.001	6.52

3.2.2.2 Buffered Solutions

A buffer is therefore required to maintain the metal ion solution at a constant pH. This is necessary if metal ion effects are to be compared.

Given that HMTs are more stable in a neutral pH and that the physiological pH of blood is about 7.3, it was decided to buffer the metal ion solutions at pH 7. The most commonly used inorganic buffers, namely phosphate and borate, are useless in this case. In both cases precipitation of metal ion salts occurred. The problem of precipitation also arose with organic buffers like N-ethylmorpholine, imidazole and glycine. Acetic acid could not be used because pH 7 is outside its buffering range.

The use of organic buffers in general poses some difficulties when using metal ions. This is because they tend to have high affinities for transition metal ions. Consequently, either the free metal ion concentration may be drastically reduced or the catalytic activity of the bound metal ion may be diminished. The latter could be due to an

increase in steric hindrance by the buffer material - but more likely to the lowering of the effective nuclear charge of the metal ion in the bound state.

These problems are illustrated by triethanolamine (TEA). The Zn^{2+} catalysed decomposition of 4-$COOCH_3$ HMT in 0.05M TEA buffer showed a negative dependence of rate on the total metal ion concentration. On the other hand, the reaction in 0.01M TEA showed no dependence at all (Table 3.2.6, Fig. 3.2.2).

Table 3.2.6 Kinetic results of $ZnSO_4$ and 4-COOMe HMT in 10% alc. solution with TEA buffer T=25 °C pH=7 I=0.1M $[HMT] \simeq 5 \times 10^{-5}$M

[TEA] = 0.05M		[TEA] = 0.01M	
$[Zn^{2+}]$ /M	kobs $x10^4/s^{-1}$	$[Zn^{2+}]$/M	kobs $x10^3/s^{-1}$
0.01	5.755	0.008	6.0917
0.006	6.9433	0.006	6.0065
0.004	7.3632	0.004	5.978
0.002	7.6335	0.002	6.0107
-	7.9843	-	6.0445

Assuming a 1:1 metal buffer complex, the chemical species present in these solutions are Zn^{2+}, Zn:TEA complex and the protonated and unprotonated forms of TEA. The concentrations of each species (Table 3.2.7) were calculated as follows.

Equations (3.2.1) and (3.2.2) represent, respectively, the equilibria of the metal buffer complex and of the buffer material itself.

FIG. 3.2.2 Decomposition of 4-CH_3COOHMT in 10% alcohol soln. by Zn^{2+} at 25°C pH=7 I=0.1M

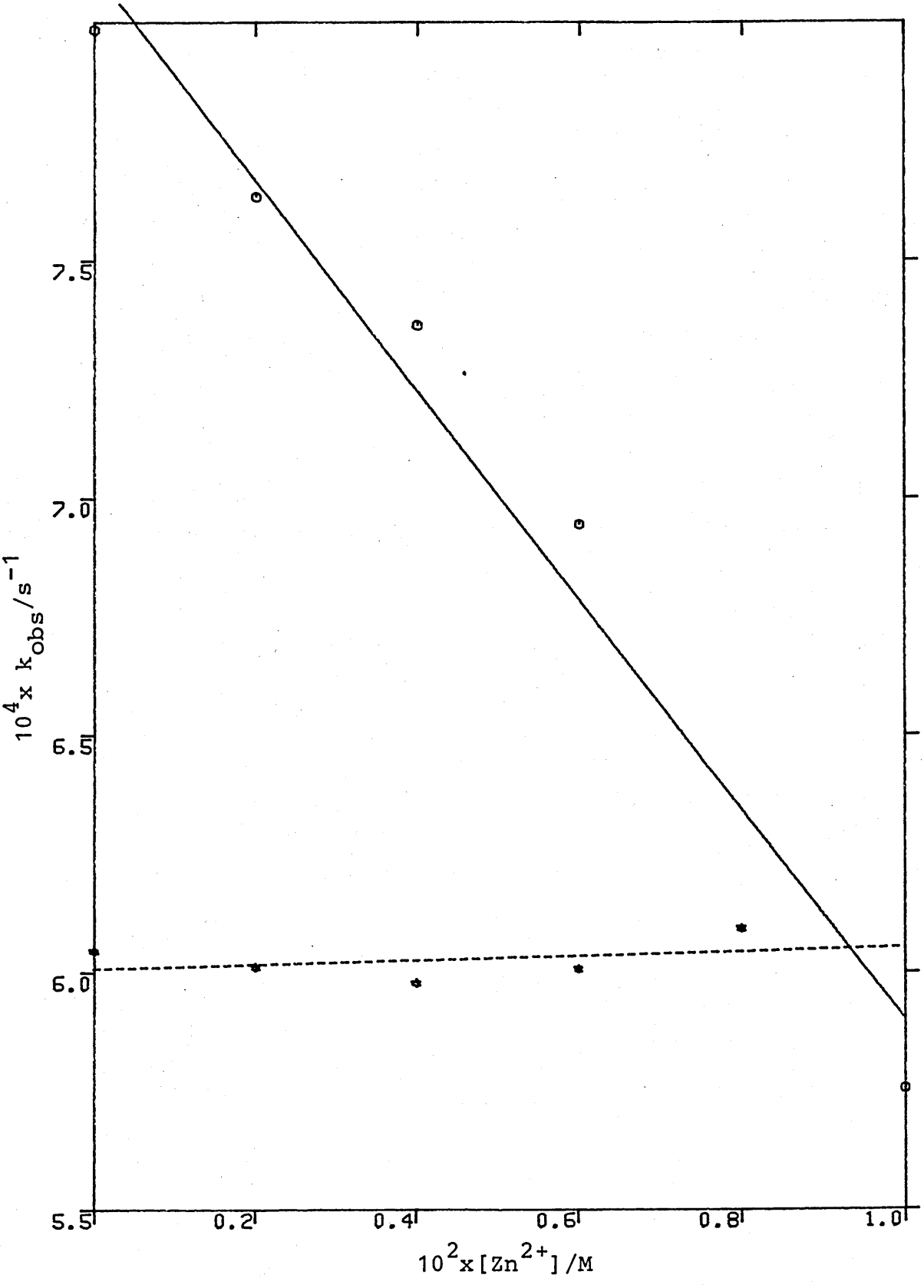

Table 3.2.7 The concentration of each species present in TEA buffered $ZnSO_4$ solution, pH=7

$[TEA]_{total}$ 10^3/M	$[M]_{total}$ 10^3/M	$[M^{n+}] \times 10^3$ /M	$[TEAM]$ 10^3/M	$[TEA]$ 10^3M	$[TEAH^+]$ 10^3M	kobs $\times 10^4$ $/s^{-1}$
50	10	3.0189	6.9811	6.369	36.65	5.755
	6	1.7349	4.2651	6.771	38.964	6.9433
	4	1.132	2.868	6.978	40.154	7.3632
	2	0.5540	1.446	7.188	41.365	7.6335
	0	0	0	7.4026	42.59	7.9843
10	8	5.6655	2.3345	1.1349	6.5306	6.0917
	6	4.1692	1.8308	1.2094	6.9598	6.0065
	4	2.7231	1.2769	1.2915	7.4316	5.978
	2	1.3319	0.6681	1.3815	7.9504	6.0107
	0	0	0	1.4805	8.5195	6.0445

Note: $[TEA]$: total concentration of triethanolamine
$[M]$: total concentration of metal ion
$[M^{n+}]$: concentration of compound metal ion
$[TEAM]$: concentration of bound metal ion
$[TEA]$: concentration of unprotonated triethanolamine
$[TEAH^+]$: concentration of protonated triethanolamine

$$M^{n+} + TEA \underset{}{\overset{K_D}{\rightleftharpoons}} TEAM \qquad TEAH^{+} \overset{K_A}{\rightleftharpoons} TEA + H^{+}$$

$$\therefore K_D = \frac{[TEAM]}{[M^{n+}][TEA]} \quad -(3.2.1) \qquad K_A = \frac{[TEA][H^{+}]}{[TEAH^{+}]} \quad -(3.2.2)$$

$$\Longrightarrow \qquad K_A \times K_D = \frac{[H^{+}][TEAM]}{[M^{n+}][TEAH^{+}]}$$

$$\Longrightarrow \qquad \frac{1}{[M^{n+}]} = \frac{K_A K_D}{[H^{+}]} \times \frac{[TEAH^{+}]}{[TEAM]} \quad -(3.2.3)$$

Now, $[TEA]_{total} = [TEAH^{+}] + [TEAM] + [TEA]$ —(3.2.4)

$$\Longrightarrow \frac{[TEA]_{total}}{[TEAM]} = \frac{[TEAH^{+}]}{[TEAM]} + 1 + \frac{[TEA]}{[TEAM]} \quad -(3.2.5)$$

Now, from (3.2.1) $\dfrac{[TEA]}{[TEAM]} = \dfrac{1}{K_D[M^{n+}]}$

and also $[M]_{total} = [TEAM] + [M^{n+}]$

$$\Longrightarrow \qquad [TEAM] = [M]_{total} - [M^{n+}] \quad -(3.2.6)$$

Therefore (3.2.5) can be rewritten into

$$\frac{[TEA]_{total}}{[M]_{total}-[M^{n+}]} = \frac{[TEAH^{+}]}{[TEAM]} + 1 + \frac{1}{K_D[M^{n+}]}$$

$$\Longrightarrow \qquad \frac{[TEAH^{+}]}{[TEAM]} = \frac{[TEA]_{total}}{[M]_{total}-[M^{n+}]} - 1 - \frac{1}{K_D[M^{n+}]}$$

Substituting this into (3.2.3) gives

$$\frac{1}{[M^{n+}]} = \frac{K_A K_D}{[H^+]} \left\{ \frac{[TEA]_{total}}{[M]_{total}-[M^{n+}]} - 1 - \frac{1}{K_D[M^{n+}]} \right\}$$

$$= \frac{K_A K_D}{[H^+]} \left(\frac{[TEA]_{total}}{[M]_{total}-[M^{n+}]} \right) - \frac{K_A K_D}{[H^+]} - \frac{K_A}{[H^+][M^{n+}]}$$

$$\Longrightarrow \quad \frac{K_A}{[H^+][M^{n+}]} + \frac{1}{[M^{n+}]} = \frac{K_A K_D}{[H^+]} \left\{ \frac{[TEA]_{total}}{[M]_{total}-[M^{n+}]} - 1 \right\}$$

$$\Longrightarrow \quad \left(\frac{K_A+[H^+]}{[H^+]} \right) \left(\frac{1}{[M^{n+}]} \right) = \frac{K_A K_D}{[H^+]} \left\{ \frac{[TEA]_{total}}{[M]_{total}-[M^{n+}]} - 1 \right\}$$

$$\Longrightarrow \quad \left(\frac{K_A+[H^+]}{[H^+]} \right) \left([M]_{total} - [M^{n+}] \right) = \frac{K_A K_D}{[H^+]} \left\{ [TEA]_{total}[M^{n+}] - [M^{n+}]\left([M]_{total} - [M^{n+}] \right) \right\}$$

$$\Longrightarrow \quad \left(\frac{K_A+[H^+]}{[H^+]} \right) \left([M]_{total} - [M^{n+}] \right) = \frac{K_A K_D}{[H^+]} \left\{ [TEA]_{total}[M^{n+}] + [M^{n+}]^2 - [M^{n+}][M]_{total} \right\}$$

$$\Longrightarrow \quad \frac{K_A K_D}{[H^+]} [M^{n+}]^2 + \left\{ \frac{K_A K_D}{[H^+]} [TEA]_{total} - [M]_{total} + \frac{K_A+[H^+]}{[H^+]} \right\} [M^{n+}]$$

$$- \left(\frac{K_A+[H^+]}{[H^+]} \right) [M]_{total} = 0 \quad \text{—— (3.2.7)}$$

Solving this quadratic equation (3.2.7) gives a value for $[M^{n+}]$. Substituting $[M^{n+}]$ into eqn. (3.2.6) will give $[TEAM]$. This in turn will give $[TEA]$ using eqn. (3.2.1). Finally $[TEAH^+]$ can be obtained from eqn. (3.2.4). Values of 1.7378×10^{-8} and 363 for K_A and K_D were obtained from references 74 and 75 respectively.

It is apparent that TEA promotes the decomposition of 4-COOMe HMT since an increase in $[TEA]_{total}$ at $[Zn^{2+}]$ = 0M enhanced the rate of reaction (Table 3.2.7). Furthermore, a positive slope was obtained when kobs was plotted against $[TEAH^+]$ or $[TEA]$ (Fig. 3.2.3). Whilst it is not known whether the protonated or unprotonated form is responsible for the reaction, both concentrations were diminished as the metal ion concentration increased. The ratio $[TEAH^+]$: $[M^{n+}]$ changed from the range of 12-75 in 0.05M TEA solution to that of only 1-6 at $[TEA]_{total}$=0.01M. Also, at $[TEA]_{total}$=0.05M, more than 70% of metal ions existed as the complex whereas more than 60% of metal ions are unbound in 0.01M TEA solution.

These results suggest that at $[TEA]_{total}$=0.05M, the main catalyst is the buffer material itself. As the total metal ion concentration is increased, the concentrations of both the protonated and unprotonated forms of TEA are reduced. The obtained negative slope (Fig. 3.2.2) implies that the increase in total metal ion concentration cannot compensate for the decrease in those of TEA. Since most of the metal ions exist as the complex at this $[TEA]_{total}$. It can therefore be inferred that the metal:buffer complex is inactive as a catalyst in this reaction. On the other hand, at $[TEA]_{total}$=0.01M, more than 60% of metal ions are unbound. These reactive metal ions can make up for the loss in $[TEA]$ and $[TEAH^+]$ thus explaining the horizontal line obtained in $[TEA]_{total}$=0.01M. The relatively higher content of $[M^{n+}]$, as can be illustrated by the $[TEAH^+]$: $[M^{n+}]$ ratio, in 0.01M TEA solution is also believed to have contributed to the observed result.

Fig. 3.2.3 Decomposition of 4-CH_3COOHMT in 10% alcohol soln. by TEA/$TEAH^+$ at 25°C I=0.1M

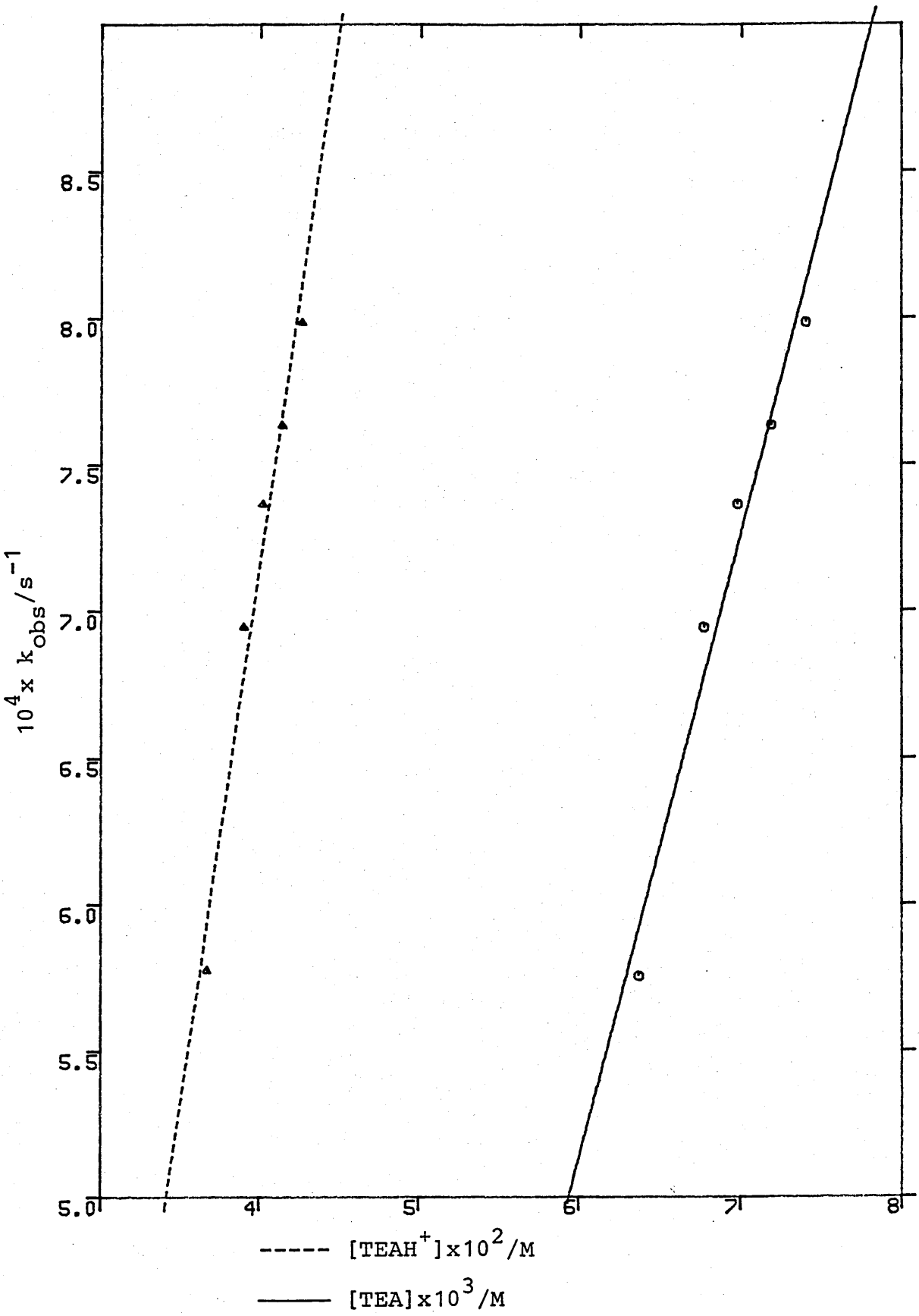

The use of ethylenediaminetetraacetic acid (EDTA) as the buffer for Cu^{2+} or Ag^{+} catalysed reaction produced less than satisfactory results (Table 3.2.8, Fig. 3.2.4). In this instance, due to the complexity of the ionic states of EDTA, it is very difficult to analyse the results. Subsequently, diethylmalonic acid was found to give the best results and was chosen to be the buffer for the metal ions catalysed decomposition of HMTs in water.

Table 3.2.8 Kinetic results of metal ion catalysed decomposition of HMTs in 10% alcohol solution buffered by EDTA at pH 7 T=25 ^{o}C I=1M [EDTA] = 0.05M

4-$COCH_3$HMT + $AgClO_4$		4-COOMeHMT + $CuSO_4$	
$[M^{+}]$ /M	kobsx10^3/S^{-1}	$[M^{2+}]$ /M	kobsx10^3/S^{-1}
0	0.7093	0	0.6968
0	0.7347	0.001	0.4187
0.002	0.8027	0.002	0.4618
0.002	0.8665	0.003	0.4618
0.004	0.8525	0.004	0.5171
0.004	0.9563	0.005	0.9195
0.006	0.8946	0.006	1.2908
0.006	0.9766		

Fig. 3.2.4 Decomposition of 4-$CH_3COOHMT$ by Cu^{2+} at 25°C in 10% alcohol solution [EDTA]=0.05M pH=7 I=1M

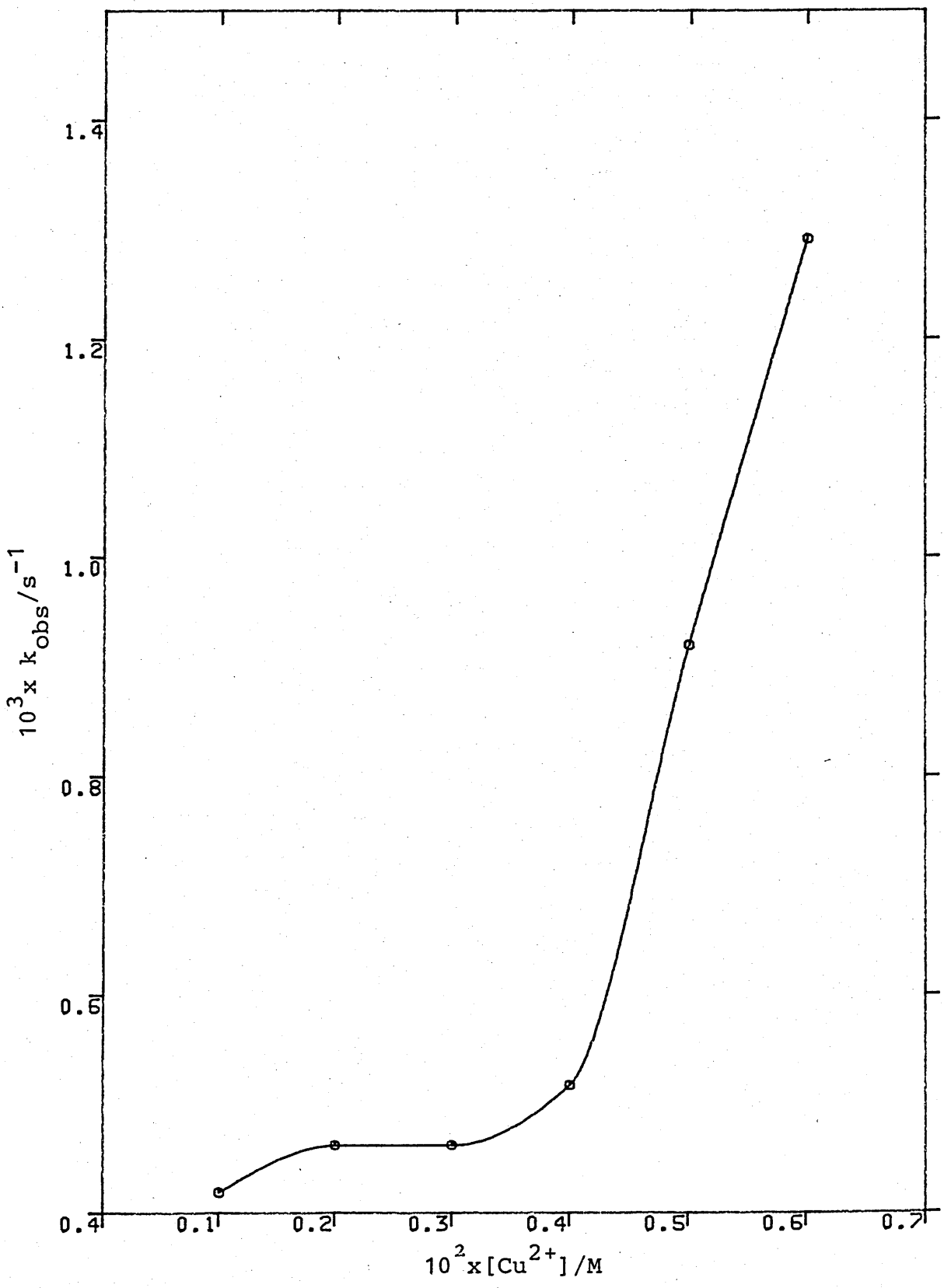

3.2.2.3 Diethylmalonic acid (DEM) buffered solution

Several modifications were made for the study of the decomposition of HMTs catalysed by DEM buffered metal ions.

1. The pKa of DEM is 7.29. Therefore by changing the pH of reaction from 7 to 7.3, the buffering ability of DEM will be at its best while its effects will be reduced.

2. In order to bring the experimental conditions further closer to those physiological ones, the temperature of reaction was raised from 25 ^{o}C to 37 ^{o}C.

3. Throughout this study, ClO_4^- was used as the counterion.

3.2.2.3.1 Zn^{2+} Catalysed Reactions

The decomposition of 4-$COCH_3$HMT with $Zn(ClO_4)_2$ was found (Table 3.2.9, Fig. 3.2.5a) to obey the following rate equation:

$$\text{Rate} = k_o[\text{HMT}] + k_{Zn}[\text{HMT}][Zn^{2+}]$$

where k_o = water rate constant

k_{Zn} = zinc rate constant

The product was the aniline and the rate increased with ionic strength (Table 3.2.10, Fig. 3.2.5b).

Table 3.2.9 Kinetic results of 4-$COCH_3$HMT + $Zn(ClO_4)_2$ in water [DEM] = 0.15M I=1M T=37°C pH=7.3

$[Zn^{2+}]$ /M	kobsx10^3/S^{-1}
0.006	0.9759
0.008	1.0517
0.010	1.1926
0.012	1.3808
0.014	1.3356
0.015	1.3812

Table 3.2.10 Ionic strength effect on 4-$COCH_3$HMT decomposition in water $[Zn^{2+}]$ = 0.015M [DEM] = 0.15M T=37 pH=7.3

I/M	kobsx10^3/S^{-1}
0.5	1.1817
1.0	1.3812
1.3	1.4997
1.5	1.5944
1.7	1.6143
2.0	1.8872

Fig. 3.2.5a Decomposition of 4-CH_3COHMT by Zn^{2+} in water [DEM]=0.15M I=1M T=37°C pH=7.3

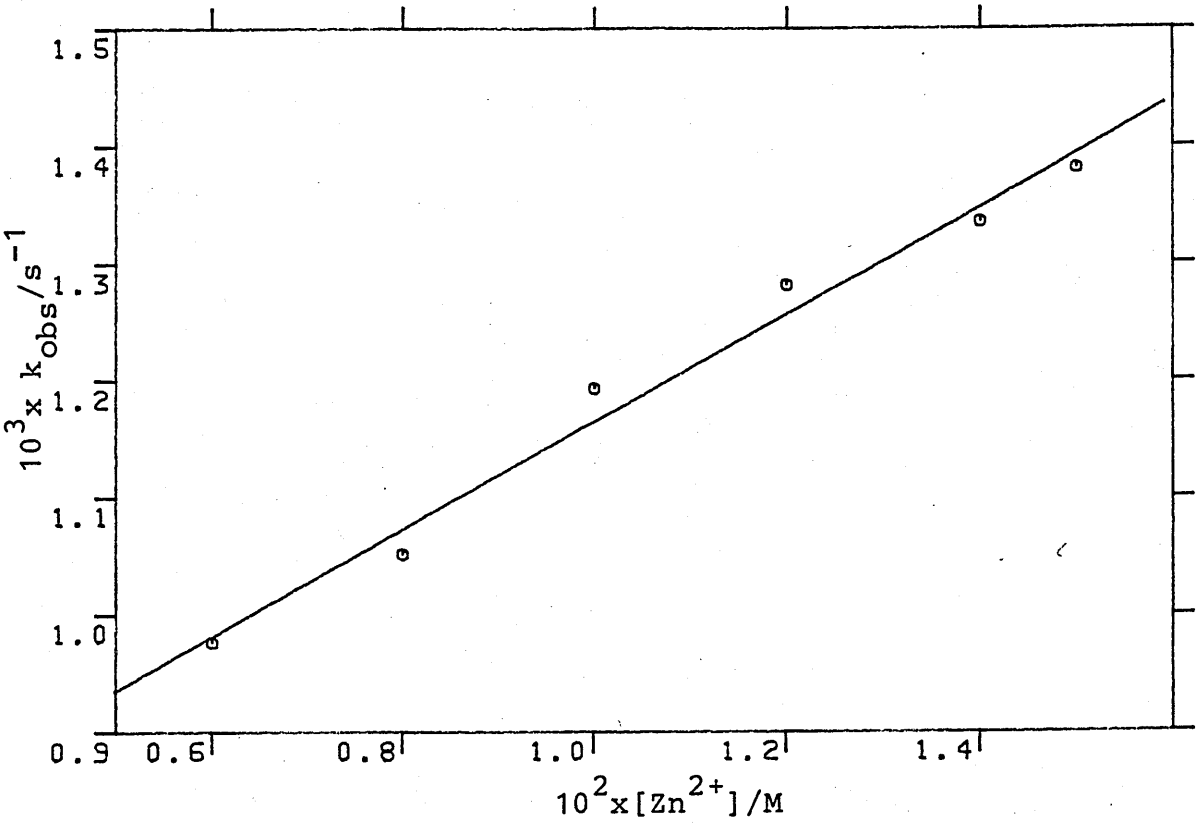

Fig. 3.2.5b Ionic strength effect on the decomposition of 4-CH_3COHMT by Zn^{2+}(0.015M)

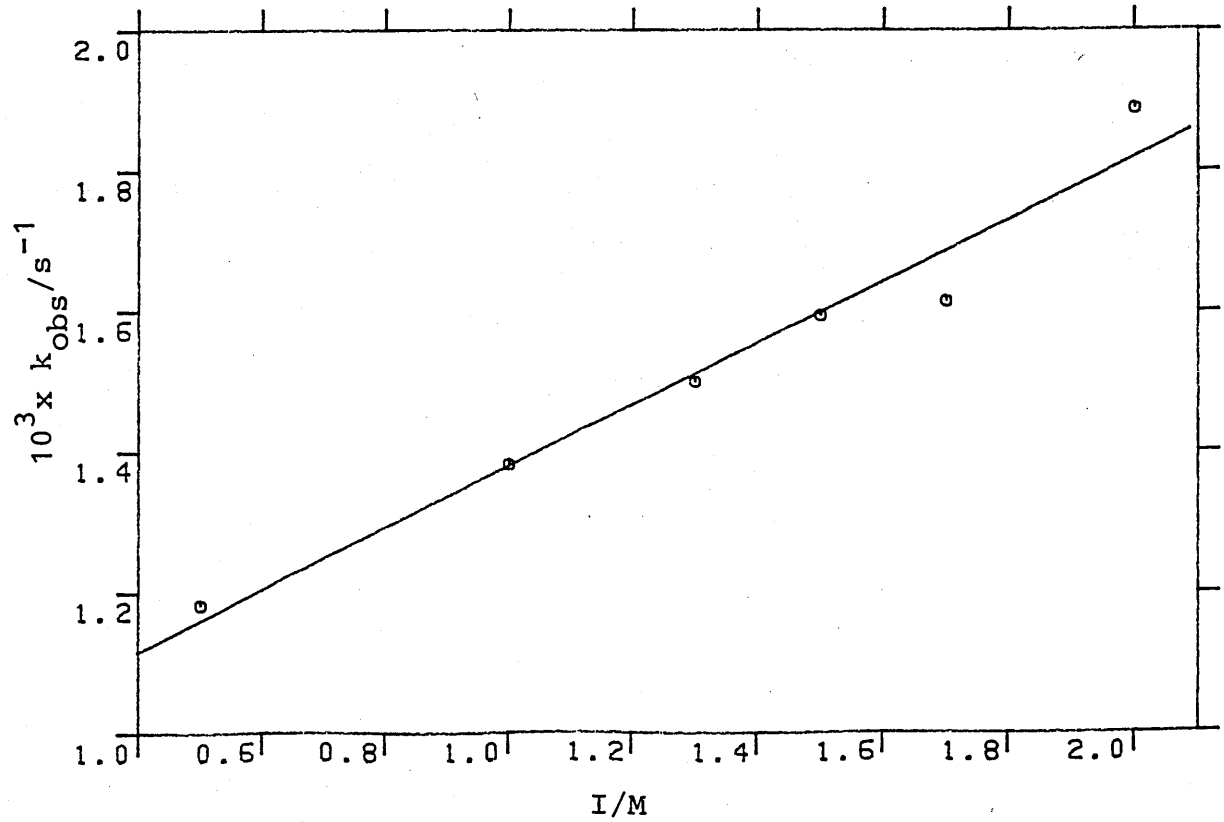

Due to the fact that MMTs have similar uv absorption as their corresponding HMTs (Table 3.2.11) it was necessary to identify the substrate in these studies. The reaction was repeated with MMT.

Table 3.2.11 UV data for 4-$COCH_3$HMT and 4-$COCH_3$MMT

Compound	λ_{max}/nm	$\varepsilon/M^{-1}cm^{-1}$
HMT	322	2.329×10^4
HMT	322	2.423×10^4

The rate constants (Table 3.2.12) so obtained show that the HMT and MMT rate constants are within experimental error. This suggests that the results in Tables 3.2.9 and 3.2.10 are from the decomposition of 4-$COCH_3$MMT and not from the HMT.

Table 3.2.12 Observed rate contstants of 4-$COCH_3$HMT and MMT in water with $Zn(ClO_4)_2$ [DEM]=0.15M T=37 °C pH=7.3 I=1M

$[Zn^{2+}]$ /M	kobs (HMT) $\times 10^3/S^{-1}$	kobs (MMT) $\times 10^3/S^{-1}$
0.015	2.03	1.88
0.10	1.77	1.73
0.0	0.96	0.96

A qualitative experiment was subsequently carried out. 0.05g of 4-$COCH_3$HMT was dissolved in 5ml of EtOH. A solution of $Zn(ClO_4)_2$ (0.015M) buffered by 0.15M DEM at pH7.3 was then added. The reaction was allowed to stand for 8 minutes (first half-life) at 37 ^oC, after which it was extracted into chloroform. The organic layer was washed with water, dried and evacuated off to dryness. The solid obtained was identified using ^{1}Hnmr and found to contain only MMT and aniline in the ratio of 1.1 : 1. This is, within experimental error, precisely that expected after one half life if the HMT decomposes rapidly to the MMT and the decomposition of the latter compound is catalysed by metal ions (Scheme 3.2.2).

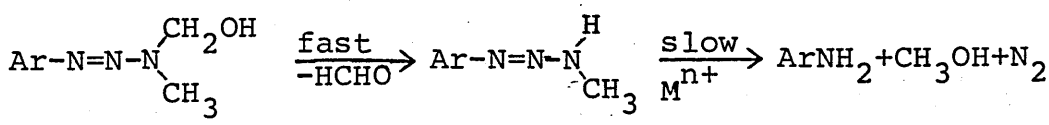

Scheme 3.2.2

In spite of this observation, other HMTs were studied. The results (Table 3.2.13) were rather scattered and showed no correlation with Hammett σ values. For the 4-Cl HMT, the water rate was so fast that no metal ion effect was observed (Fig. 3.2.6).

3.2.2.3.2 Cu^{2+} Catalysed Reaction

In contrast to the Zn^{2+} reaction, the rate of decomposition of 4-$COCH_3$HMT by DEM buffered Cu^{2+} was shown to depend negatively on the total $[Cu^{2+}]$ (Table 3.2.14, Fig. 3.2.7).

Table 3.2.13 Second order rate constants of $Zn(ClO_4)_2$ catalysed decomposition of HMTs in water [DEM]= 0.15M T=37 °C pH=7.3 I=1M

Compound	σ	$k_2/M^{-1}S^{-1}$
$4\text{-}ClC_6H_4$	0.24	0
$4\text{-}COOMeC_6H_4$	0.44	0.039304
$4\text{-}COCH_3C_6H_4$	0.47	0.045838
$3\text{-}C_5H_4N$	0.65	0.032438
$4\text{-}CNC_6H_4$	0.71	0.028443
$4\text{-}NO_2C_6H_4$	0.81	0.056689

Table 3.2.14 Kinetic results of HMT decomposition in water with $Cu(ClO_4)_2$ [DEM] =0.15M T=37 °C pH=7.3 I=1M

$4\text{-}COCH_3HMT$		$4\text{-}COOCH_3HMT$	
$[Cu^{2+}]/M$	$kobsx10^3/S^{-1}$	$[Cu^{2+}]/M$	$kobsx10^3/S^{-1}$
0.004	1.2968	0.006	0.8353
0.005	1.2678	0.008	0.8412
0.006	1.23805	0.009	0.7795
0.008	1.2068	0.012	0.7129
0.009	1.1558	0.014	0.6715
0.010	1.1607	0.015	0.6307
0.012	1.1227		

Fig. 3.2.6 Decomposition of 4-ClHMT in water at 37°C

[DEM]=0.15M I=1M pH=7.3

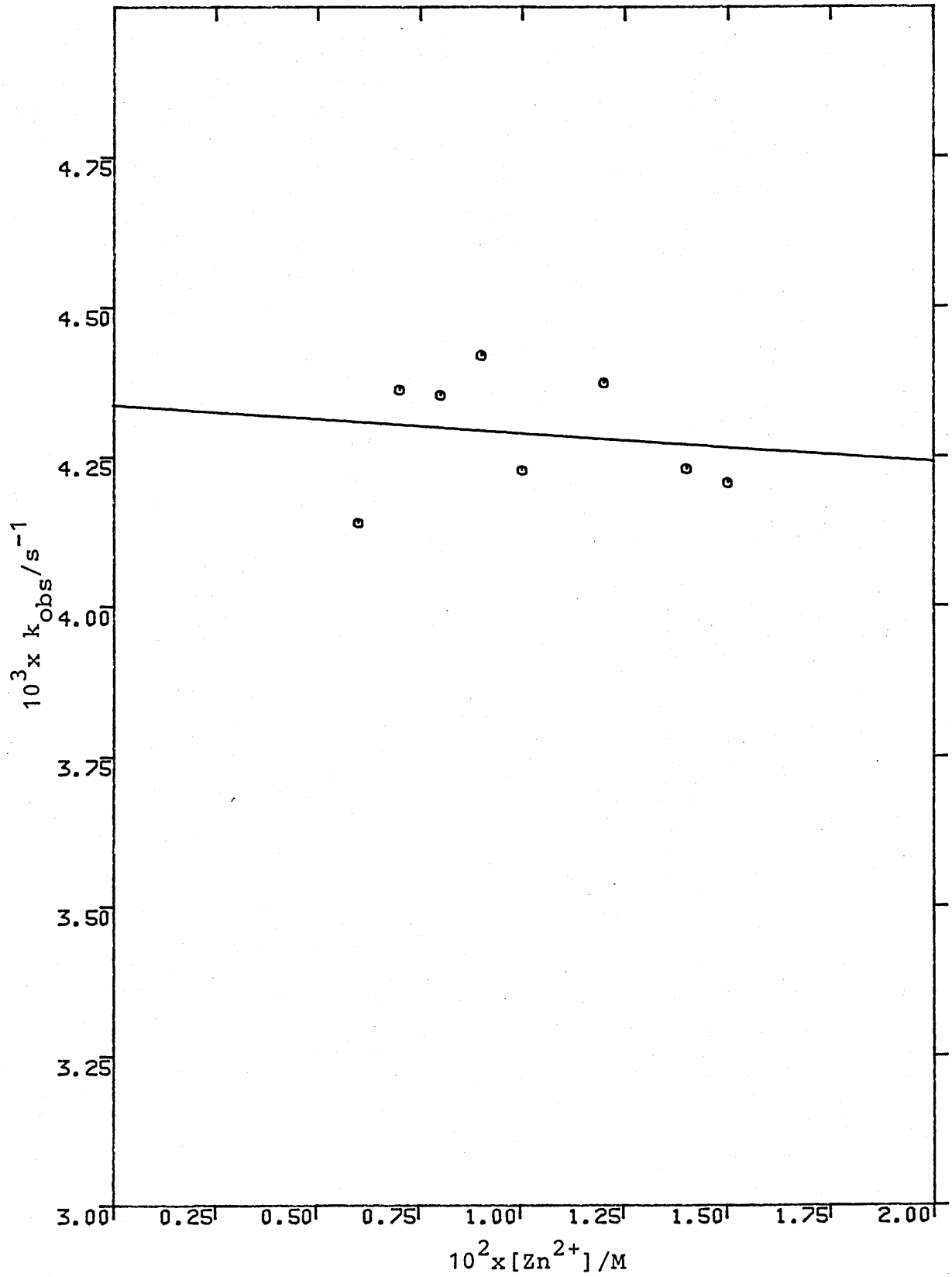

Fig. 3.2.7 Decomposition of HMTs in water

[DEM]=0.15M T=37°C pH=7.3 I=1M

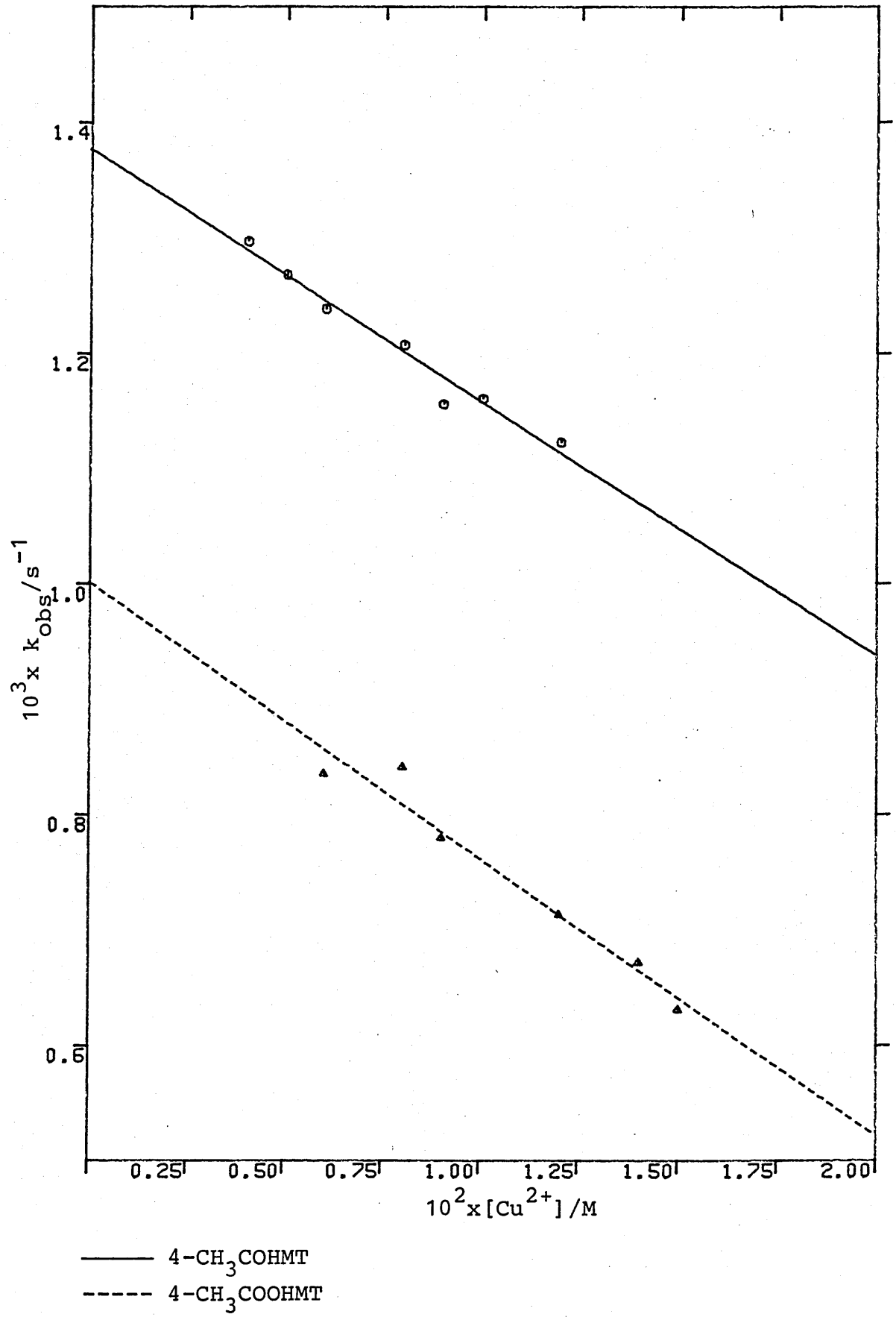

One reason for this difference between the two reactions may be that Cu^{2+} binds more readily with DEM than Zn^{2+}. At 25 ^{o}C and 0.1M ionic strength, the $\log k_1$ for Cu^{2+} and DEM is 4.96 whereas that for Zn^{2+} and DEM is only 2.44.[75] Using equations 3.2.1-3.2.7, the concentration of each species present in this metal ion buffer system can be calculated (Table 3.2.15). From the table it is clear that almost all the Cu^{2+} ion are complexed with DEM. Consequently, the only catalyst present is the buffer material itself. Indeed, a positive slope was obtained when kobs was plotted against $[DEM]$ or $[DEM^{\Theta}]$. (Fig. 3.2.8). On the other hand, in the case of the Zn^{2+} reaction, the small amount of unbound Zn^{2+} can compensate for the rate loss due to a decrease in the concentration of the buffer material.

Table 3.2.15 The concentration of each species present in DEM buffered metal ion solution

pH=7.3 DEM =0.15M

M^{n+}	$10^2[M^{n+}]$total/M	$[M^{n+}]x10^3$/M	$[DEM.M]x10^3$/M	$[DEM^{\Theta}]$/M	[DEM]	10^3xkobs/S^{-1}	
Zn^{2+}	0.6	2.84383	15.7156	0.07297	0.07131	0.9759	4-CH_3COHMT
	0.8	3.84	7.616	0.07201	0.07037	1.0517	
	1.0	4.8616	9.5138	0.07105	0.06944	1.1926	
	1.2	5.9098	11.409	0.07009	0.0685	1.2808	
	1.4	6.9855	13.3014	0.06914	0.06756	1.3356	
	1.5	7.5339	14.2466	0.06866	0.0671	1.3812	
Cu^{2+}	0.4	$5.9384x10^{-3}$	3.9994	0.07385	0.07215	1.2968	4-CH_3COHMT
	0.5	$7.4753x10^{-3}$	4.9992	0.07332	0.07168	1.2678	
	0.6	$9.0319x10^{-3}$	5.9991	0.07283	0.07117	1.23805	
	0.8	$1.2210x10^{-2}$	7.9988	0.07183	0.07017	1.2068	
	0.7	$1.3832x10^{-2}$	8.9986	0.07133	0.06967	1.1558	
	1.0	$1.548x10^{-2}$	9.9985	0.07082	0.06918	1.1607	
	1.2	$1.8849x10^{-2}$	11.9981	0.0698	0.0682	1.1227	
Cu^{2+}	0.6	$9.0319x10^{-3}$	5.9991	0.07283	0.07117	0.8383	4-CH_3COOHMT
	0.8	$1.2210x10^{-2}$	7.9988	0.07182	0.07017	0.8412	
	0.9	$1.3832x10^{-2}$	8.9986	0.07133	0.06967	0.7795	
	1.2	$1.8849x10^{-2}$	11.9981	0.0698	0.0682	0.7129	
	1.4	$2.2315x10^{-2}$	13.9978	0.06878	0.06742	0.6715	
	1.5	$2.4081x10^{-2}$	14.9976	0.06828	0.0667	0.6307	

$[DEM.M]$ = concentration of the metal : DEM complex

$[DEM^{\Theta}]$ = concentration of the deprotonated form of DEM

Fig. 3.2.8 Decomposition of HMTs by DEM/DEM^- in water

pH=7.3 I=1M [DEM]=0.15M

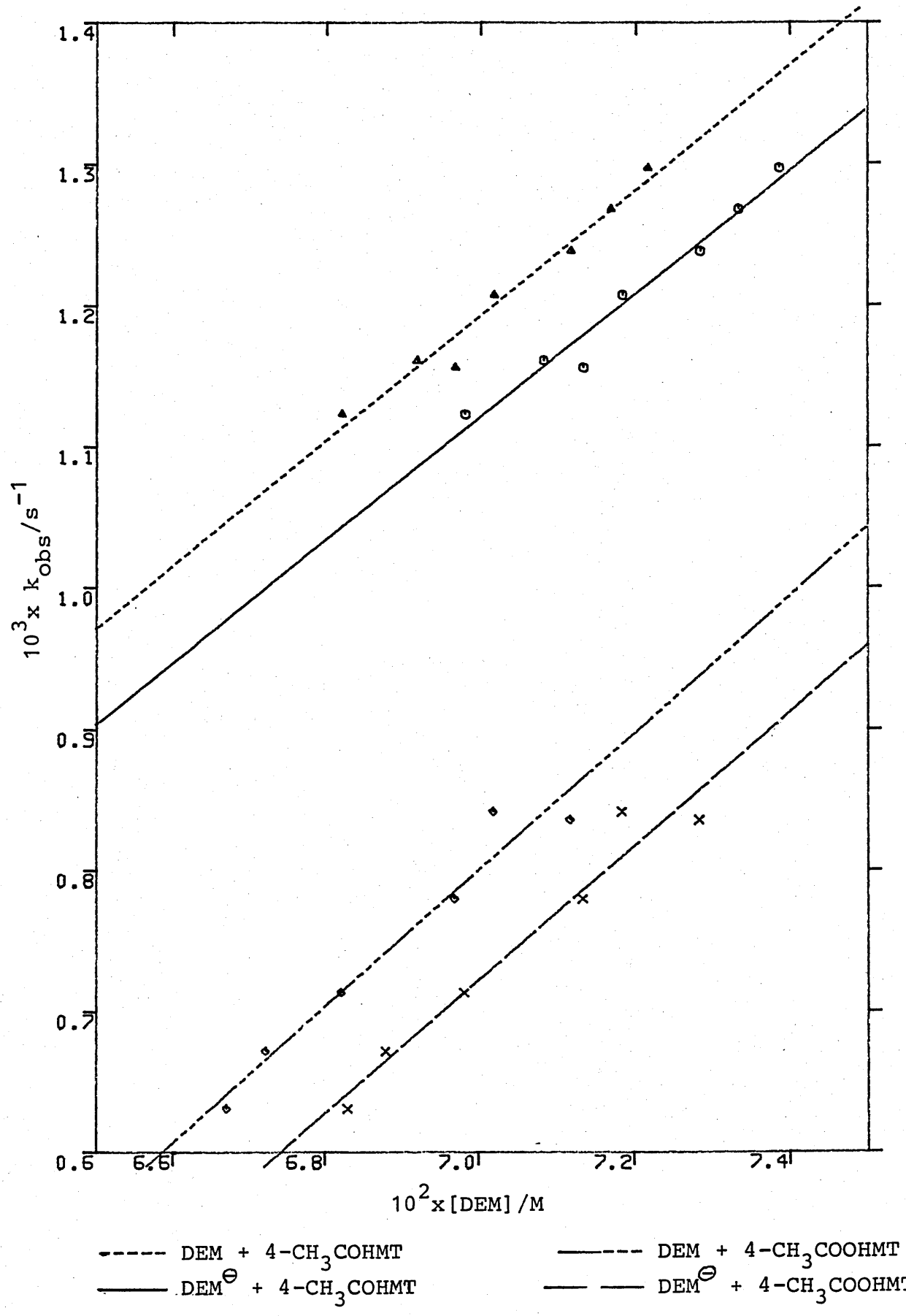

3.2.3 Discussion

The salient finding of this study is the instability of HMTs in aqueous solution. The almost identical rates of decomposition of 4-$COCH_3$ HMT and MMT (Table 3.2.12) in the absence of $Zn(ClO_4)_2$ imply that the decomposition of the HMT to MMT is catalysed by water and not by the metal ion.

The hydrolysis of transition metal ions and the sensitivity of HMTs towards acids together mean that the use of a buffer is necessary if the metal ion effects are to be compared. However, as outlined in Section 3.2.2.2, any change in the metal ion or its concentration will in turn alter the concentration of the buffer material in such a way that a negative dependence of the rate on the total metal ion concentration results. This was observed in the cases of Cu^{2+} with DEM and Zn^{2+} with TEA.

More importantly, from the point of view of studying the chemistry of HMTs, the instability of HMTs in aqueous solution prompts the need to explore other solvents.

3.3 Metal Ion Catalysed Reaction in Ethanol

The smaller dissociation constant of ethanol compared to that of water means that substances dissolved in ethanol are both less basic and acidic than in water. This implies that HMTs should be more stable in ethanol. Indeed, the decomposition of 3-pyridylHMT in ethanol at 37 ^{o}C is very slow (see Section 5.3.3.2). Besides, most metal perchlorates are soluble in ethanol. Taken together, these suggest that ethanol is a good solvent for the study of metal ion catalysed decomposition of HMTs.

Given that no report has been published in the literature on the alcoholysis of transition metal ions, no attempt was made to buffer the metal ion solutions used in this study.

3.3.1 Mechanism of Reaction

3.3.1.1 Identification of Substrate

The decomposition of HMTs in the presence of more than 200-fold excess of various metal perchlorates was found to follow pseudo-first-order kinetics (see Experimental).

Given the results of the previous section it was decided to investigate whether the rate constants observed related to the HMTs or the MMTs. It was found that at $[Zn^{2+}]$=0.0078M, the observed rate of decomposition of 4-CNMMT was nearly 20-fold faster than that of the HMT. (Table 3.3.1.1). These results imply that the substrate in the above reaction is the HMT and

not the MMT. Similar results were obtained for other HMTs (see Section 3.3.3).

Table 3.3.1.1 Observed pseudo first-order rate constants of 4-CNHMT and MMT with $Zn(ClO_4)_2$ in ethanol [Zn]=0.0078M T=37 °C I=0.15M

compound	kobs/ s^{-1}
HMT	3.2×10^{-3}
MMT	62.7×10^{-3}

3.3.1.2 Intermediacy of MMT

Two mechanisms are possible for this reaction (Scheme 3.3.1.1). One involves the stoichiometric conversion of HMT to aniline and other products (routei). The other is through the intermediacy of MMT in a consecutive first order reaction (route ii).

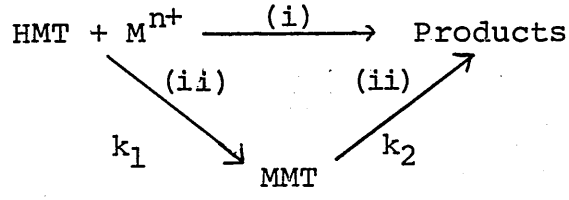

Scheme 3.3.1.1

The results (Table 3.3.1.1), however, do not solve the question. Given that HMT and MMT have identical uv absorption, the following equation can be written for the consecutive mechanism:

$$\frac{A_t - A^\infty}{A_o - A^\infty} = \frac{k_2 e^{-k_1 t} - k_1 e^{-k_2 t}}{k_2 - k_1}$$

Since $k_2 >> k_1$ $\quad k_2 e^{-k_1 t} >> k_1 e^{-k_2 t}$

So, $$\frac{A_t - A^\infty}{A_o - A^\infty} = e^{-k_1 t}$$

$$\ln \frac{A_t - A^\infty}{A_o - A^\infty} = -k_1 t$$

Therefore, if the reaction follows consecutive first order mechanism the observed rate constants are of the decomposition of HMT to MMT.

Furthermore by using the hplc technique (see Section 5.3.3.2), the content of the HMT reaction can be revealed. It was observed that with the presence of 0.01M $Zn(ClO_4)_2$, 3-pyridylHMT decomposed in ethanol to yield first the MMT and then the amine.

A plot of -ln (peak area of HMT/total peak areas of HMT, MMT and aniline) against t for the 3-pyridyl HMT reaction gave a straight line with a slope of $4.74 \times 10^{-4} s^{-1}$. (Fig. 3.3.1.1). Due to the smaller extinction coefficient of the aniline as compared to those of MMT and HMT at the wavelength where the reaction was monitored, adjustments were made for the peak area of aniline in the calculation by multiplying the observed peak area with the ratio ($\varepsilon_{HMT}/\varepsilon_{aniline}$). The obtained value, nevertheless, agrees well with that of $4.89 \times 10^{-4} s^{-1}$ from the 3-pyridylHMT decomposition by 0.01M $Zn(ClO_4)_2$ monitored by the uv method. Thus the decomposition of HMT in ethanol catalysed by metal ion has been proved to be a consecutive first order

Fig. 3.3.1.1. Pseudo-first-order plot for the decomposition of 3-pyridylHMT by Zn^{2+} in EtOH using hplc

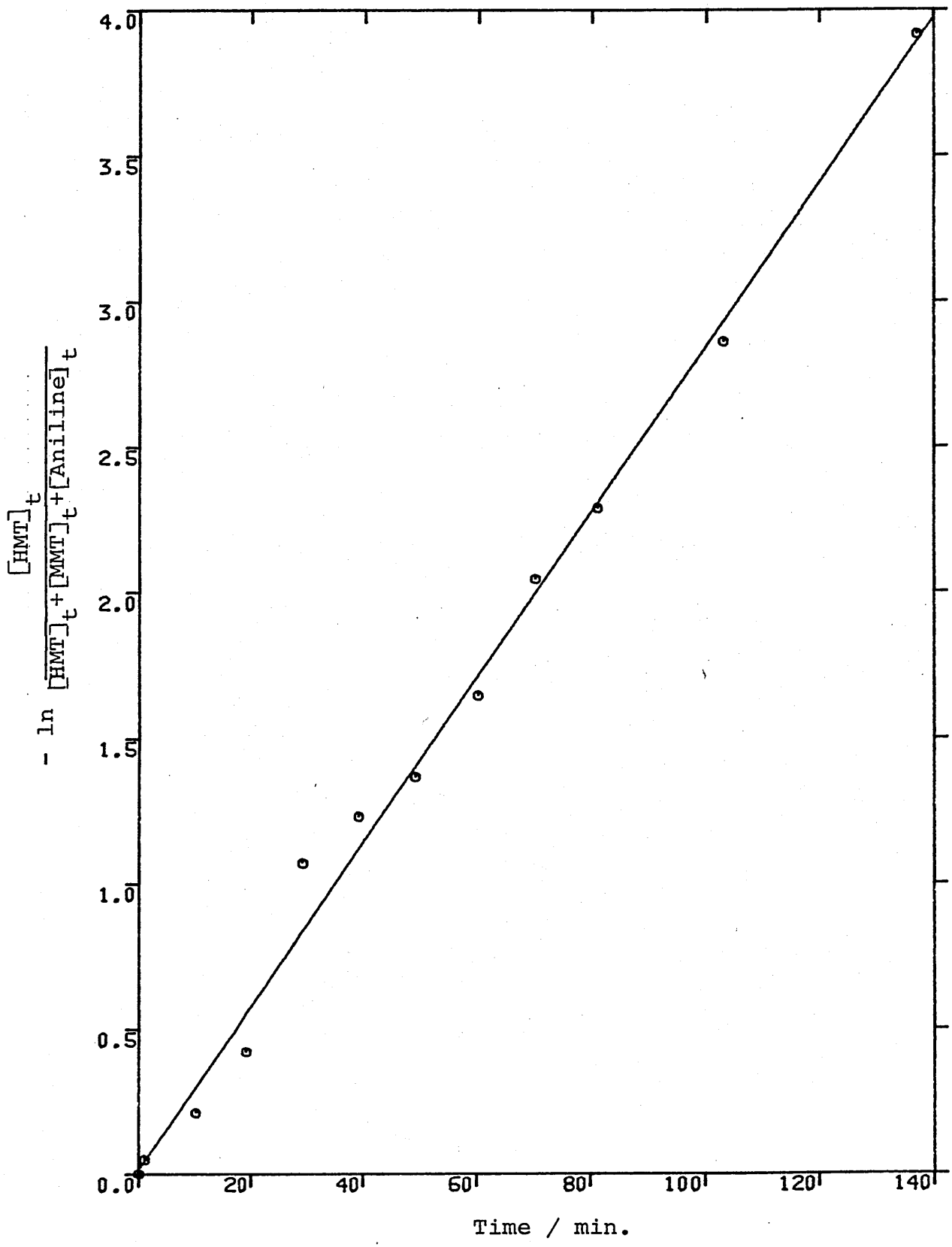

reaction.

Despite the fact that copper complexes of the alkyl-aryltriazenes[77] are quite stable and can be easily synthesised from the corresponding triazenyl anion, attempts aimed at isolating any intermediate of this form failed when copper (II) sulphate pentahydrate ($CuSO_4.5H_{2O}$) on zinc (II) sulphate heptahydrate ($ZnSO_4.7H_2O$) was added with a warm alcoholic solution of 4-CH_3COHMT. Instead, the bis(arylamino)methane was formed.

3.3.1.3 Dependence on Metal Ion Concentration

The observed rate constants for the decomposition of HMTs were found to increase linearly in all cases with the concentration of metal ions e.g. (Fig. 3.3.1.2). The presence of an intercept indicates that there is an uncatalysed pathway which is consistent with the earlier observation that HMT decomposes slowly in ethanol (Section 5.3.3.2) and that the rate constants are of the decomposition of HMT to MMT. Most important of all, these results confirmed the above suggestion that the reaction follows a consecutive first order mechanism.

Because Fe^{3+} absorbs at the uv region where the decomposition of HMT was monitored, the concentration of Fe^{3+} was lowered to *ca*. 10^{-5}M. Despite such low concentrations, the decomposition of HMT still follows first order kinetics (Fig. 3.3.1.3). This implies that Fe^{3+} and other M^{n+} are functioning as catalysts.

Fig. 3.3.1.2 Decomposition of 4-CF_3HMT in ethanol by $Zn(ClO_4)_2$ I=0.15M T=37°C

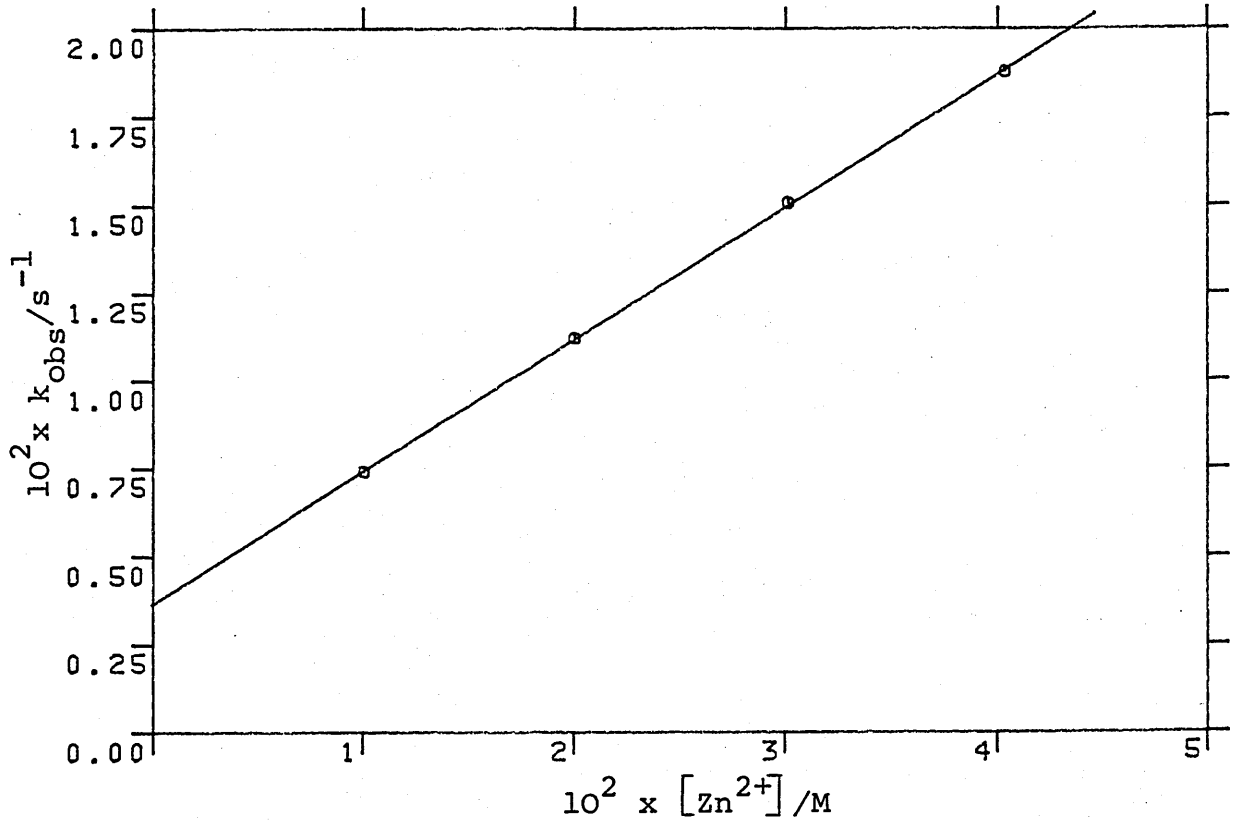

Fig 3.3.1.3 Pseudo-first-order plot for the decomposition of 4-H_2NCOHMT by 5.5365x10-5M Fe^{3+} in EtOH

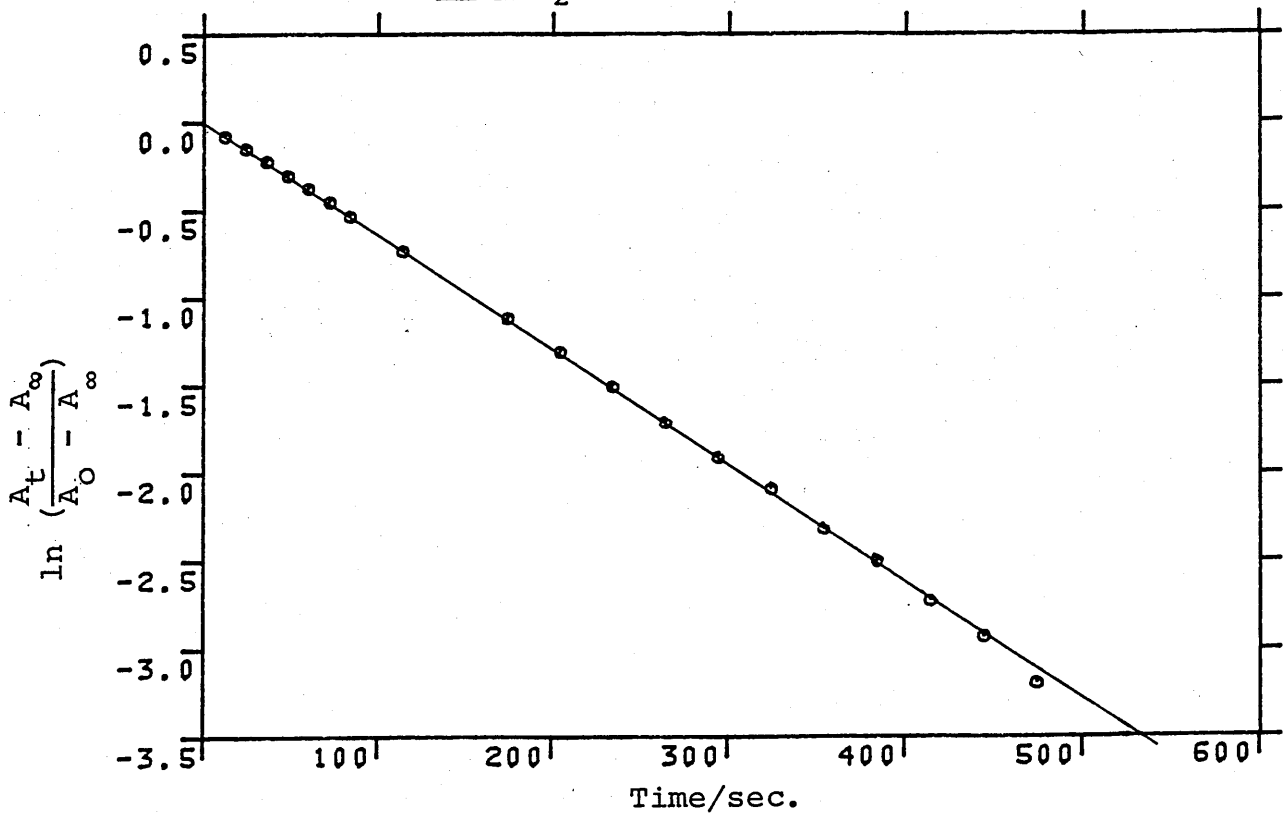

3.3.1.4 Ionic Strength Effects

For the decomposition of 4-CH_3COHMT by $Zn(ClO_4)_2$, no ionic strength effect on rate was observed (Fig. 3.3.1.4). In contrast, both the Zn^{2+} and Fe^{3+} catalysed decomposition of 3-pyridylHMT showed a slight increase of rate with respect to ionic strength (Fig. 3.3.1.5). However, the effect is very small and points against the involvement of two charged species in the reaction(s) before the rate limiting step.

3.3.1.5 Effect of Metal Ion

With 4-CH_3COOHMT as the substrate, there was a significant variation of catalytic effect depending on the metal ion employed (Table 3.3.1.3). The most effective catalyst is Fe^{3+} with a second order rate constant of $41.9 M^{-1}S^{-1}$. In contrast, the rate constant for Mg^{2+} is only $5.7 \times 10^{-3} M^{-1}S^{-1}$ while Na^+ has no effect at all (Section 3.3.1.4).

Table 3.3.1.3 Metal ion effect for decomposition of 4-CH_3COOHMT in ethanol T=37 °C I=0.15M

M^{n+}	$10^3 \times k_2 / M^{-1}S^{-1}$
Fe^{3+}	41908
Fe^{2+}	1183
Zn^{2+}	550
Cu^{2+}	469
Pb^{2+}	325
Mn^{2+}	11.7
Mg^{2+}	5.7
Cr^{3+}	2.978
Na^+	0

Fig. 3.3.1.4 Effect of ionic strength on the decomposition of 4-CH_3COHMT by 0.02M Zn^{2+} T=37°C

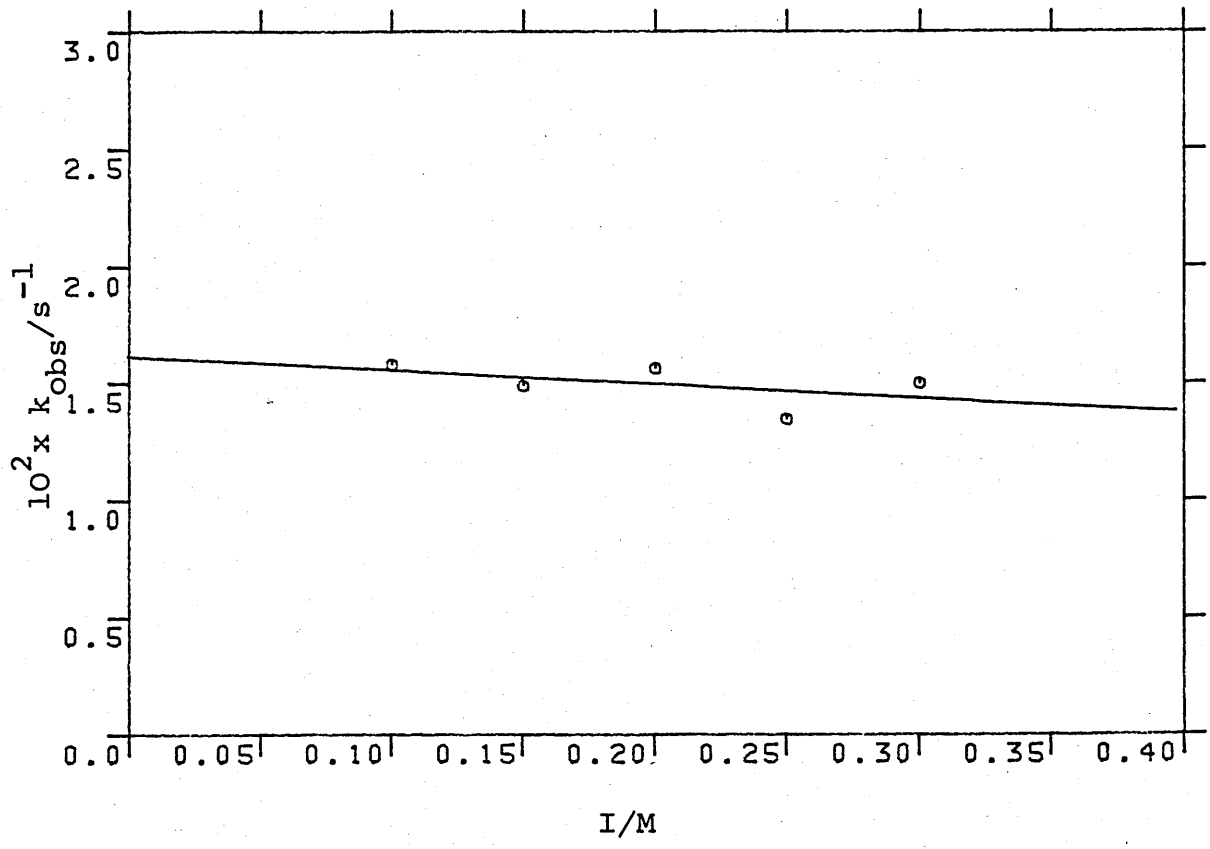

Fig. 3.3.1.5 Effect of ionic strength on the decomposition of 3-pyridylHMT by M^{n+} T=37°C

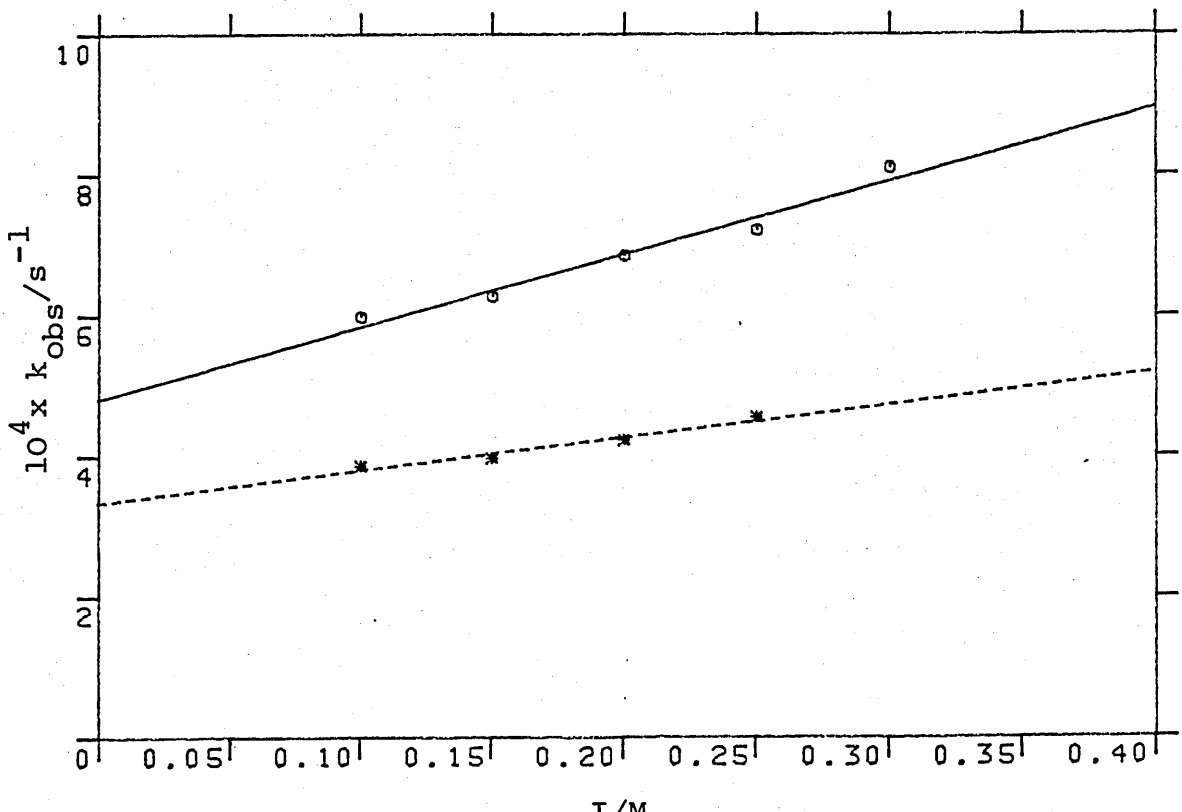

Interestingly, these rate constants showed a remarkable correlation with their aqueous pKa values. (Fig. 3.3.1.6). Since the metal ion solutions were not buffered, the plot can be interpreted as an indication that the reaction is catalysed by protons released from the ethanolysis of the metal ion (Scheme 3.3.1.2).

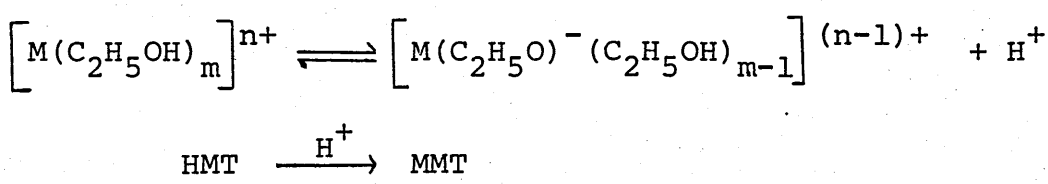

Scheme 3.3.1.2

As the rate constants relate to the decomposition of HMT to MMT, the only possible proton catalysed mechanism is the protonation of the terminal nitrogen of the triazene molecule (Scheme 3.3.1.3). Protonation of the -OH group would not

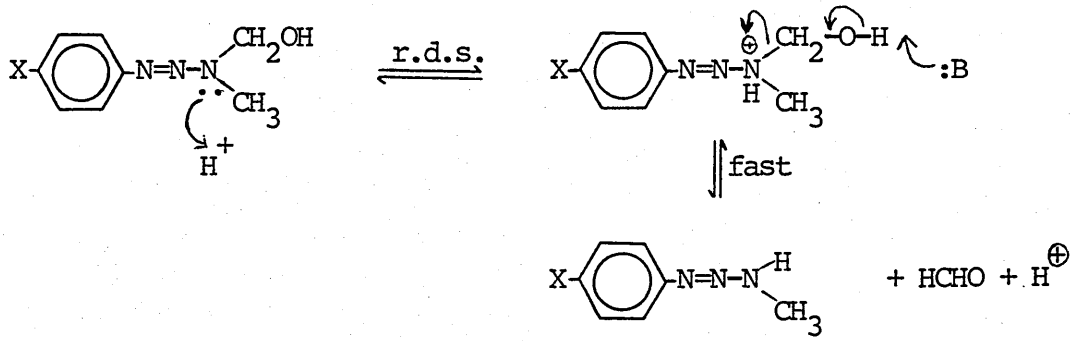

Scheme 3.3.1.3 Proton catalysed decomposition of HMT to MMT

lead to the formation of MMT and will therefore not be involved in the mechanism. According to studies on the decomposition of aminocarbinols[60], the second step in the mechanism would require general base catalysis (Section 1.2.2). If this were true, the first step in the mechanism would have to be rate limiting since the rate increases with the acidity of the metal ions.

Fig. 3.3.1.6 Effect of metal ion on the decomposition of 4-$CH_3COOHMT$ in ethanol I=0.15M T=37°C

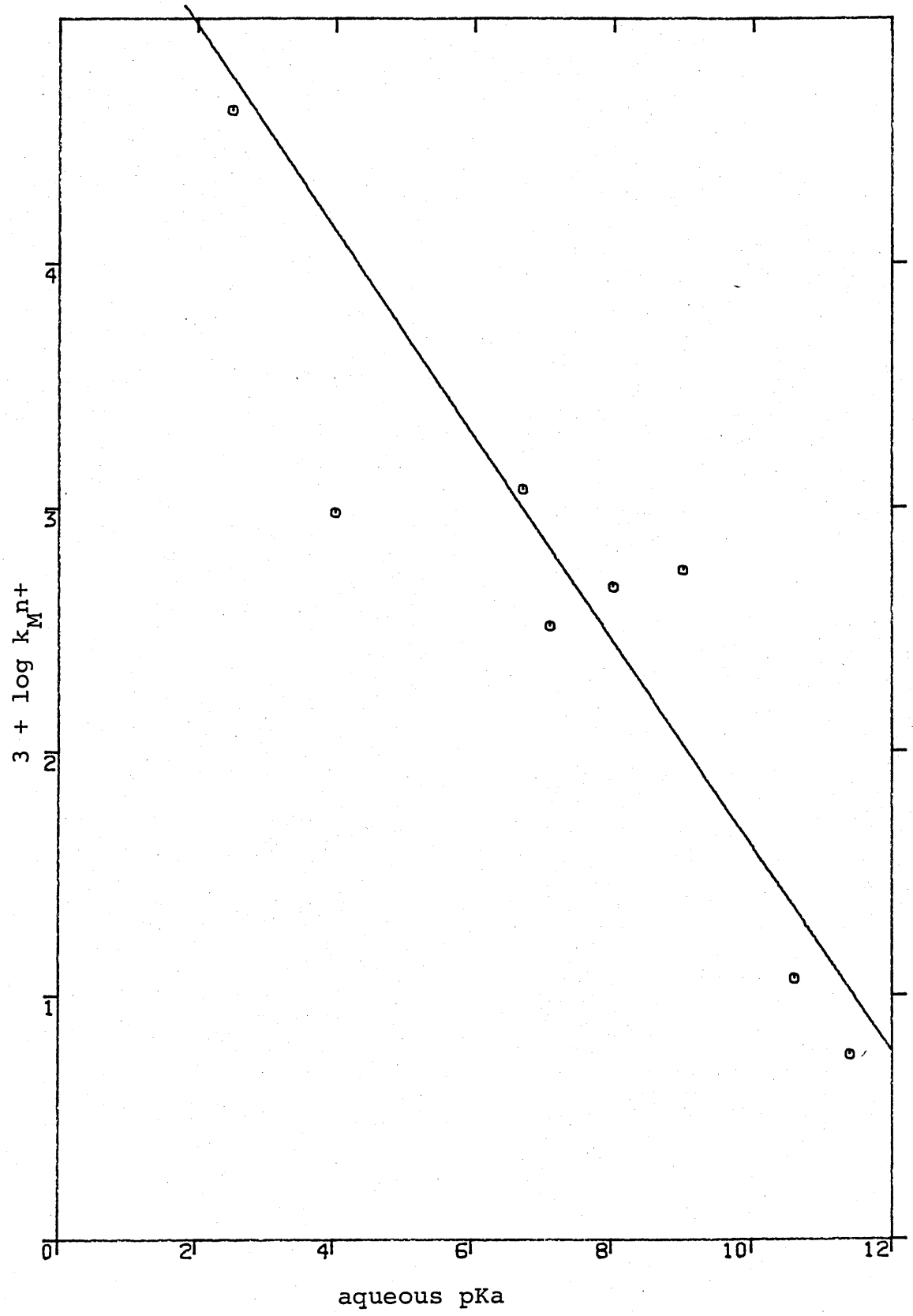

Alternatively, the reaction may involve a coordination of HMT molecule with the metal ion (Scheme 3.3.1.4). By acting as acid catalysts, the metal ions can increase the acidity of the -OH group of HMTs. In other words, the reactivity of HMT towards bases are enhanced in the metal-bound form. Accordingly, the pKa values of metal ions (Fig. 3.3.1.6) can be interpreted as their ability in facilitating the release of proton from their coordinating ligands.

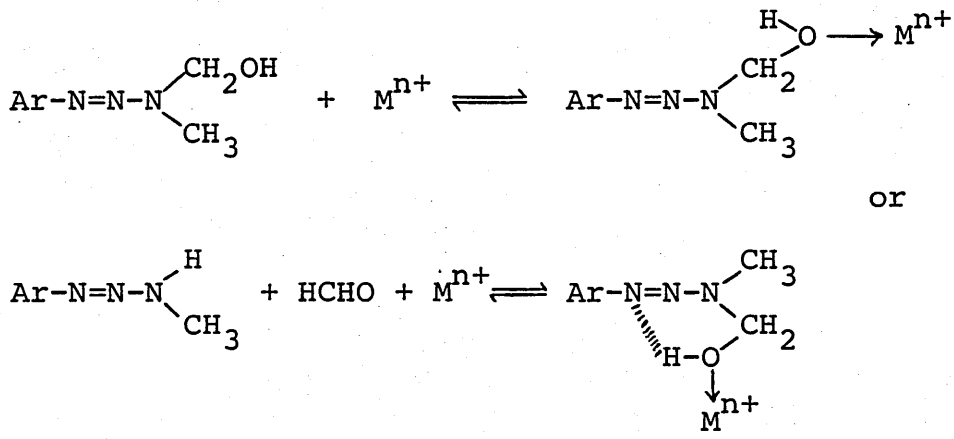

Scheme 3.3.1.4 Metal ion coordinated decomposition of HMT to MMT

Supportive evidence for the latter mechanism comes from the Cr^{3+} catalysed reaction. The observed rate constant for the reaction was 400-fold smaller than that expected from the aqueous pKa of the metal ion (Fig. 3.3.1.6). Given that Cr^{3+} forms inert complexes, this anomaly therefore suggests that a metal:HMT complex is formed during the metal ion catalysed transformation of HMT to MMT.

Having shown that the reaction is more likely M^{n+} and not H^{+} catalysed, it is necessary to confirm if the catalyst in the Fe^{2+} reaction is Fe^{2+} itself or Fe^{3+}. The following experiment was therefore carried out.

A solution of 3.548×10^{-4}M $Fe(ClO_4)_3$ in EtOH and a solution of 0.01M $Fe(ClO_4)_2$ were scanned against EtOH. At 330nm where the decomposition of 4-CH_3COOHMT was monitored

$$A_{Fe^{3+}} = 0.77 \qquad \text{and} \qquad A_{Fe^{2+}} = 0.24$$

$$\text{Extinction coefficient } (Fe^{3+}) = \frac{0.77}{3.548 \times 10^{-4}} \quad M^{-1}cm^{-1}$$

Now, assuming that Fe^{2+} does not absorb at 330nm and that the absorbance of 0.24 for the Fe^{2+} solution is due to Fe^{3+} solely, the observed rate constant for the Fe^{2+} solution should be

$$k_{obs} = k_o + k_M[M^{n+}]$$

since $k_{Fe^{3+}} = 41.91\ M^{-1}S^{-1}$

$$k_{obs} = 0.00387 + 41.91 \times \frac{0.24}{(0.77/3.548 \times 10^{-4})}$$

$$= 0.00387 + 0.00463$$

$$= 8.50 \times 10^{-3} S^{-1}$$

This value compared with the experimental value of $18.05 \times 10^{-3} S^{-1}$ obtained at 0.01M Fe^{2+} solution, can only account for $^1/_3$ of the results. Since it is very unlikely that Fe^{2+} has no absorption at 330nm, it appears reasonable to conclude that the results of Fe^{2+} reaction belong to Fe^{2+}.

3.3.1.6 Effect of Substituent

The Hammett plot for the decomposition of 4-subsituted arylHMTs by $Zn(ClO_4)_2$ reveals a negative slope (Fig. 3.3.1.7), indicating that electron withdrawing substituents have a stabilising effect. It also confirms that the reaction involves an electrophilic attack on the HMT by the metal ion. A significant observation is that the 3-pyridyl-HMT result lies well off the line suggesting that the electron withdrawing effect of the pyridine ring is enhanced. This may be due to the coordination of the pyridyl ring to the metal ion.

The substituents were found to have a greater effect on Fe^{3+} catalysed reaction than the Zn^{2+} reaction (Fig. 3.3.1.8). This observation was based on the slopes obtained and it implies that the transition state in the Fe^{3+} catalysed reaction has a

Fig. 3.3.1.7 Hammett plot for the decomposition of HMTs by $Zn(ClO_4)_2$ in EtOH I=0.15M T=37°C

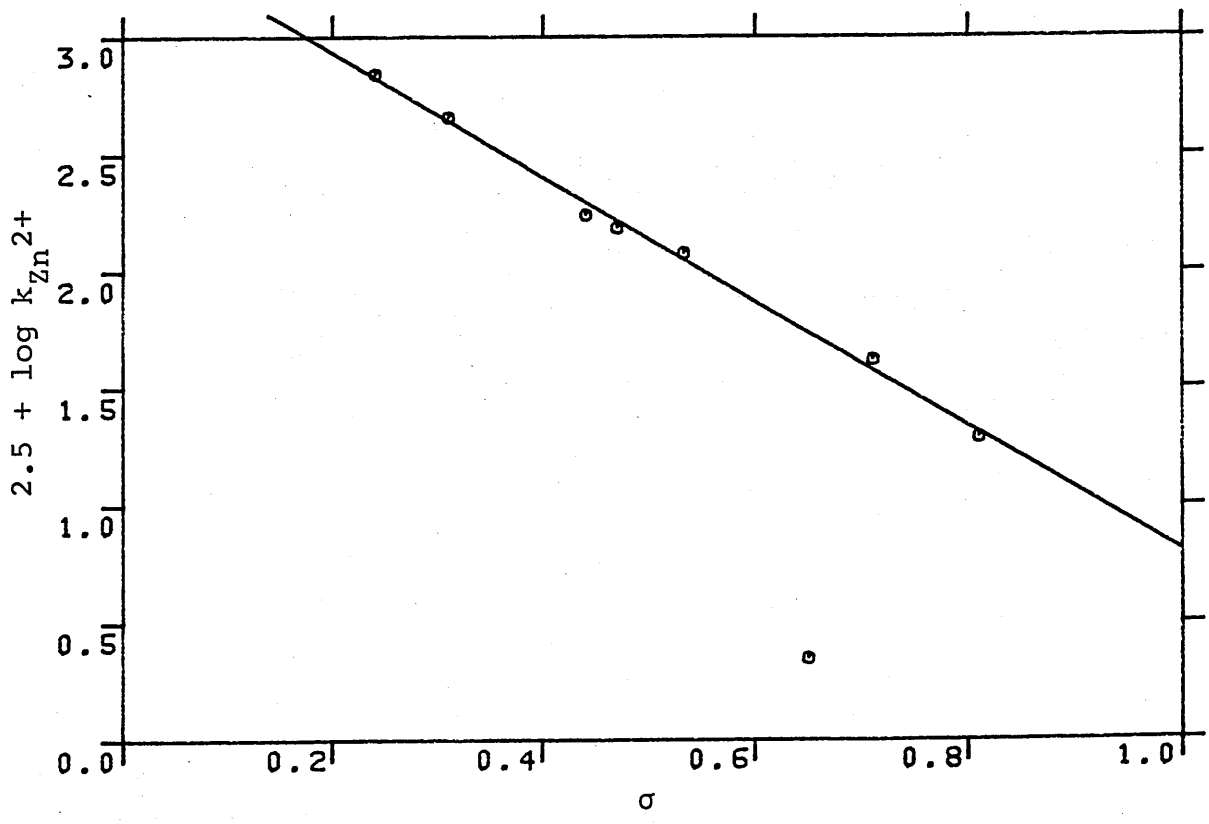

Fig. 3.3.1.8 Hammett plots for the decomposition of HMTs by M^{n+} in ethanol I=0.15M T=37°C

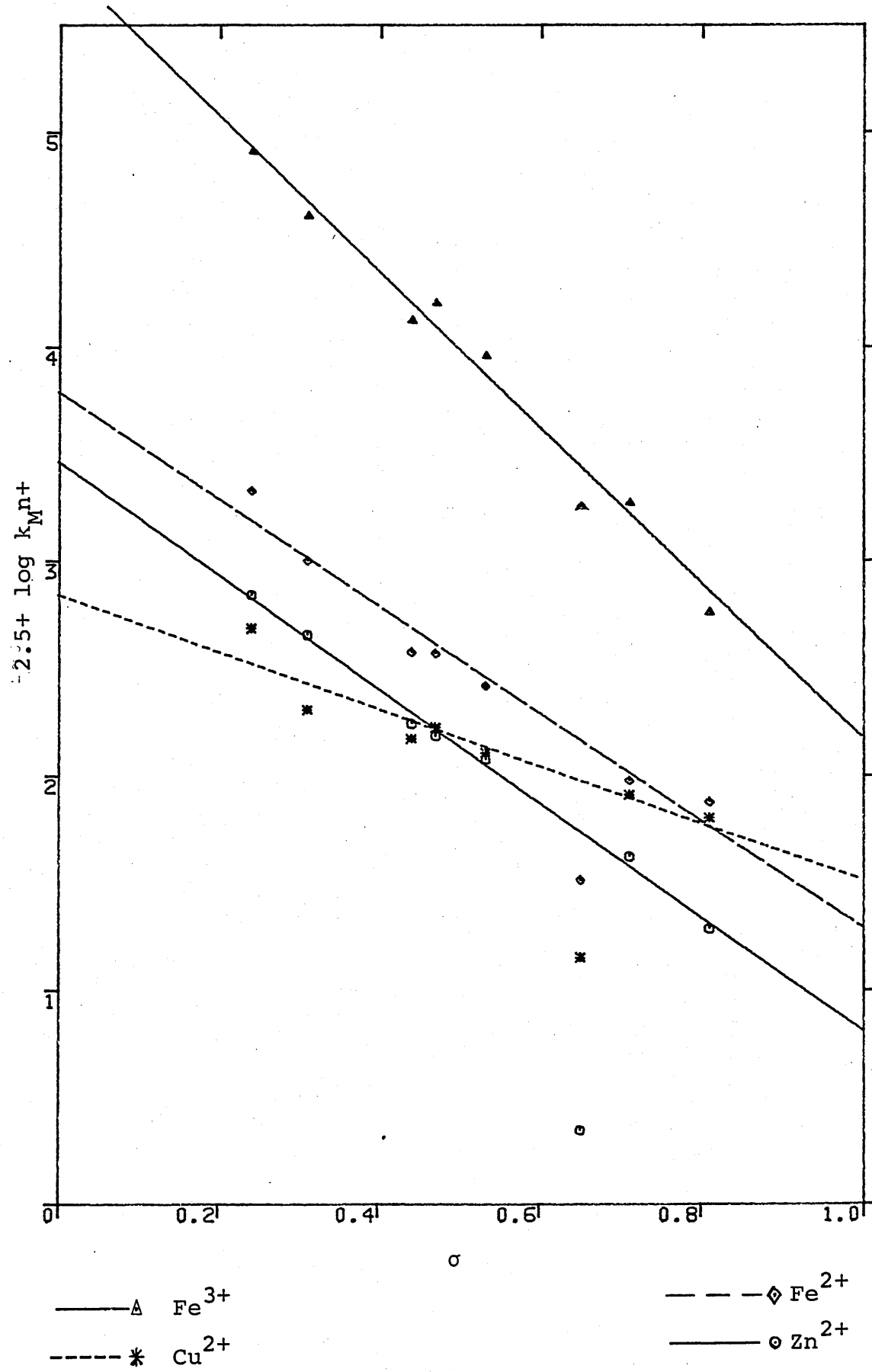

larger positive charge than that in the Zn^{2+} reaction. Such results can only be accomplished by the multivalent M^{n+} and not by H^{+}. Although the difference between these slopes is not large, a rough order of selectivity is

$$Fe^{3+} > Fe^{2+} \simeq Zn^{2+} > Cu^{2+}$$

Interestingly, it was observed that the amount of deviation of the 3-pyridylHMT from the Hammett plot varied according to the M^{n+} used. Indeed deviation followed the order

$$Zn^{2+} > Cu^{2+} > Fe^{2+} > Fe^{3+} \quad \text{(Fig.3.3.1.8)}$$

3.3.1.7 Effect of Temperature

On the basis of the previous section it was decided to study the temperature dependence of the reaction of one homoaryl- and the heteroarylHMT. For this purpose 4-CH_3COHMT was chosen.

3.3.1.7.1 4-CH_3COHMT

Linear Arrhenius plots were observed for all four metal ions used: Fe^{2+}, Fe^{3+}, Cu^{2+} and Zn^{2+} (Fig. 3.3.1.9). The pre-exponential terms and the activation energies derived from these lines are shown in Table 3.3.1.4.

It was interesting to find that Fe^{3+}, despite giving the fastest rate, has the highest activation energy. Whilst the

Fig. 3.3.1.9 Arrhenius plots for the decomposition of 4-CH_3COHMT by M^{n+} in ethanol I=0.15M

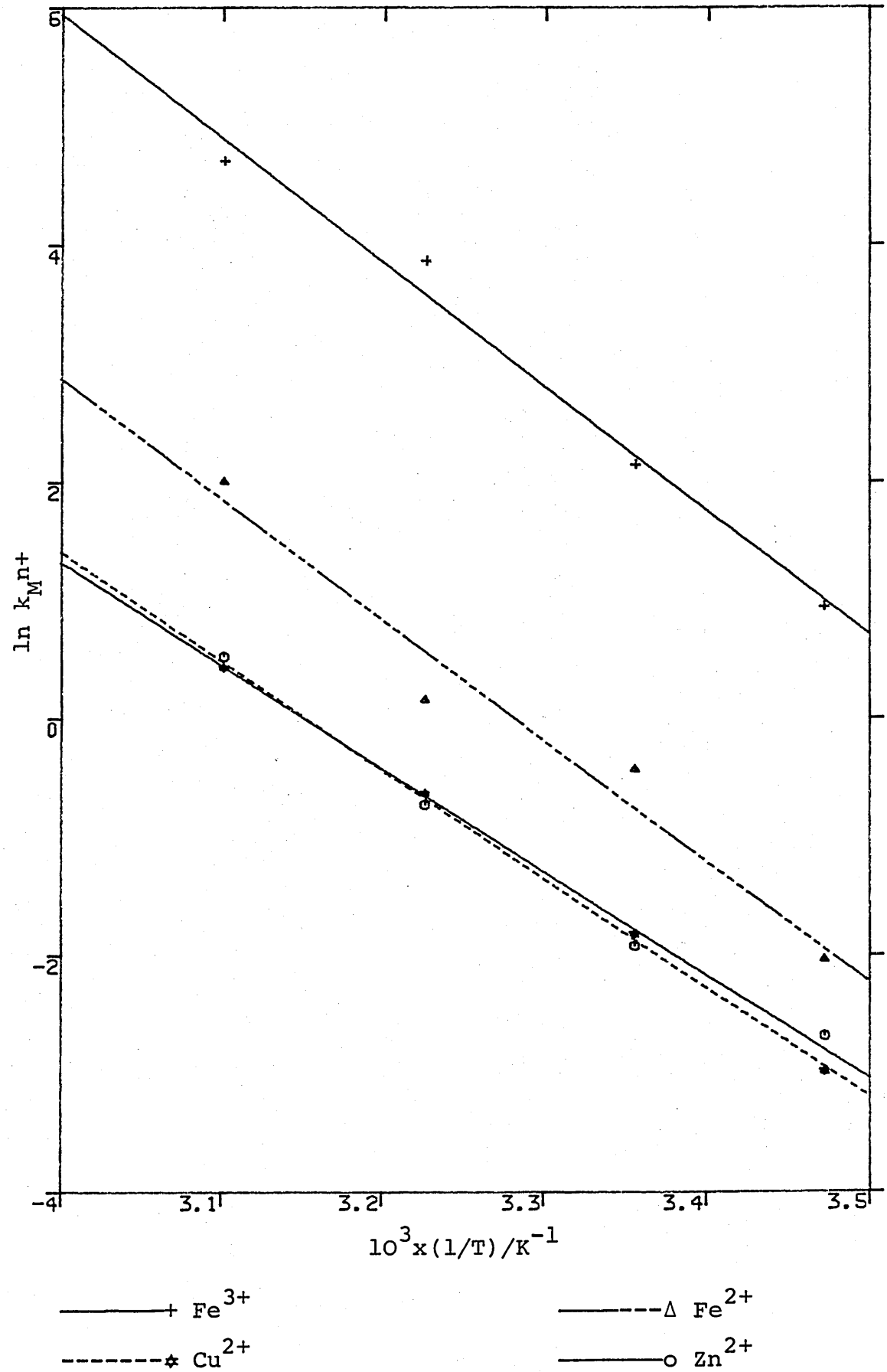

difference was not large, further investigation revealed that $\Delta H^{\ddagger}$ increase with the activation energy (Table 3.3.1.5). However, in the cases of Fe^{2+} and Fe^{3+}, the effect of $\Delta H^{\ddagger}$ was reduced by the positive $\Delta S^{\ddagger}$ to such an extent that $\Delta G^{\ddagger}$ for Fe^{2+} and Fe^{3+} are lower than those for Zn^{2+} and Cu^{2+}. This explains why, despite having relatively higher activation energies, Fe^{2+} and Fe^{3+} are better catalysts than Zn^{2+} and Cu^{2+}. Indeed, the $\Delta G^{\ddagger}$ values are in accord with the rate constants (Table 3.3.1.3).

Table 3.3.1.4 Activation energy and pre-exponential term for the metal ion catalysed decomposition of 4-CH_3COHMT in ethanol I=0.15M

Metal ion	Activation energy/ kJ mol-1	ln A
Zn^{2+}	72.5 ± 4	27.43 ± 1.76
Cu^{2+}	76.5 ± 2	28.93 ± 0.74
Fe^{2+}	85 ± 12	33.44 ± 4.67
Fe^{3+}	87 ± 7	37.32 ± 2.9

A = pre-exponential term

The processes which involve a metal ion catalysed mechanism are:

$$HMT + M \underset{-1}{\overset{1}{\rightleftharpoons}} HMTM$$

$$HMTM \xrightarrow{2} Product$$

Table 3.3.1.5 Thermodynamic parameters for 4-CH_3COHMT decomposition by metal ion in ethanol I=0.15M T=37 °C

M^{n+}	$\Delta H^{\neq}$/kJmol^{-1}	$\Delta S^{\neq}$/Jmol^{-1}K^{-1}	$\Delta G^{\neq}$/kJmol^{-1}
Zn^{2+}	70 ± 4	-26 ± 15	78 ± 6
Cu^{2+}	74 ± 2	-13 ± 6	80 ± 3
Fe^{2+}	82 ± 12	24 ± 39	74.5 ± 17
Fe^{3+}	84.5 ± 7	57 ± 24	67 ± 11

The catalytic rate constant, $k_{M^{n+}}$, can be expressed as

$$k_{M^{n+}} = \frac{k_1 k_2}{k_{-1} + k_2} \qquad 3.3.1.1$$

Two limiting cases are possible:

i. $k_2 >> k_{-1} \Rightarrow k_{M^{n+}} \simeq k_1$

Therefore the overall reaction rate is equal to and determined by the formation of the complex.

ii. $k_{-1} >> k_2 \Rightarrow k_{M^{n+}} \simeq \frac{k_1 k_2}{k_{-1}} = Kk_2$

In this instance, the overall reaction rate will depend on the equilibrium constant for the formation of the complex and the rate of its decomposition. Each of the two steps may be affected independently and to a different extent by temperature.

For a metal ion : HMT complex to be formed, the HMT molecule must first compete with the solvent for the coordination sites at the metal ion. The size of HMT compared to that of ethanol suggests that, during the formation of the complex, more than one solvent molecule will be expelled from the coordination sphere of the metal ion. Thus it appears reasonable to assume that the ΔS reaction for this step is slightly positive. A slightly negative $\Delta S^{\neq}$ value for Zn^{2+}

(even taking into account the standard error) therefore suggests that $k_{Zn^{2+}}$ consists of more than one elementary rate constant.

3.3.1.7.2 3-pyridyl HMT

As in the case of 4-CH_3COHMT, normal Arrhenius behaviour was observed (Fig. 3.3.1.10). Again, Fe^{3+} was found to have the highest activation energy but the lowest $\Delta G^{\neq}$ (Table 3.3.1.6). Though the reason for this transformation was the same, the $\Delta S^{\neq}$ values in this case are all positive.

Furthermore, at 49.5 ^{o}C, k_{obs} was shown to level off at high Zn^{2+} and Cu^{2+} (Fig. 3.3.1.11). Nevertheless, $k_{M^{n+}}$ could still be obtained from the straight part of the plot.

Table 3.3.1.6 Thermodynamic parameters for the decomposition of 3-pyridylHMT by M^{n+} in ethanol I=0.15M

M^{n+}	Ea/kJmol^{-1}	$\Delta H^{\neq}$/kJmol^{-1}	$\Delta S^{\neq}$/Jmol^{-1}K^{-1}	$\Delta G^{\neq}$/kJmol^{-1}
Zn^{2+}	116 ± 8	113 ± 8	81 ± 27	85.5 ± 12
Cu^{2+}	91 ± 22	88.5 ± 2	12 ± 7	85 ± 3
Fe^{3+}	119.5 ± 10	117 ± 10	145 ± 31	72 ± 13

This saturation phenomenon of rate constant with respect to metal ion concentration (Fig. 3.3.1.11) indicates the presence of a metal ion : HMT complex. It also suggests that at 49.5 ^{o}C and high $[M^{n+}]$, there is a change of rate limiting step from k_1 to k_2. Therefore the experimentally obtained $k_{M^{n+}}$ is equal to k_1. This phenomenon was not observed with other HMTs or at other

Fig. 3.3.1.10 Arrhenius plots for the decomposition of 3-pyridylHMT by M^{n+} in ethanol I=0.15M

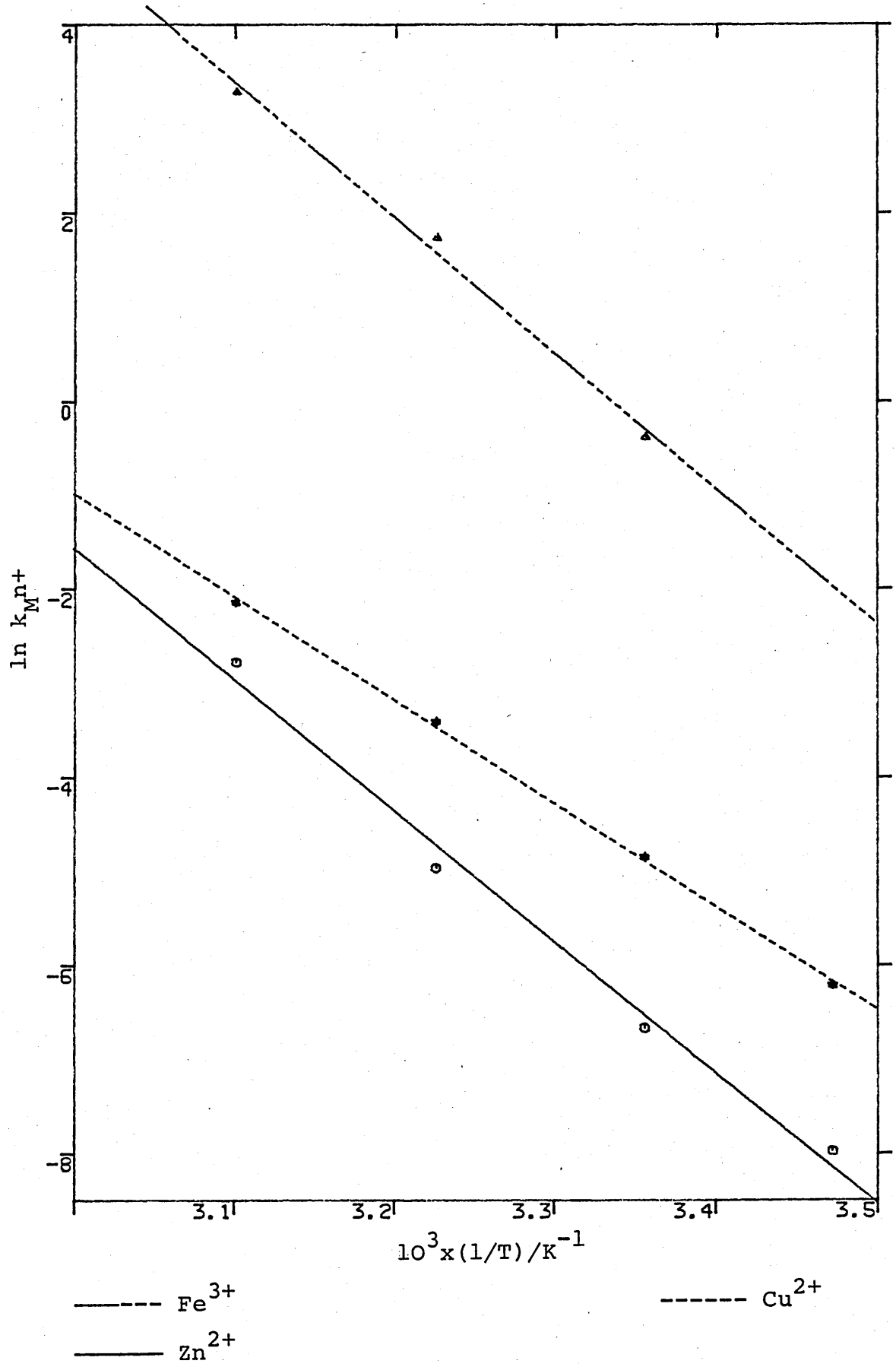

Fig. 3.3.1.11 Decomposition of 3-pyridylHMT in ethanol by M^{n+} I=0.15M T=49.5°C

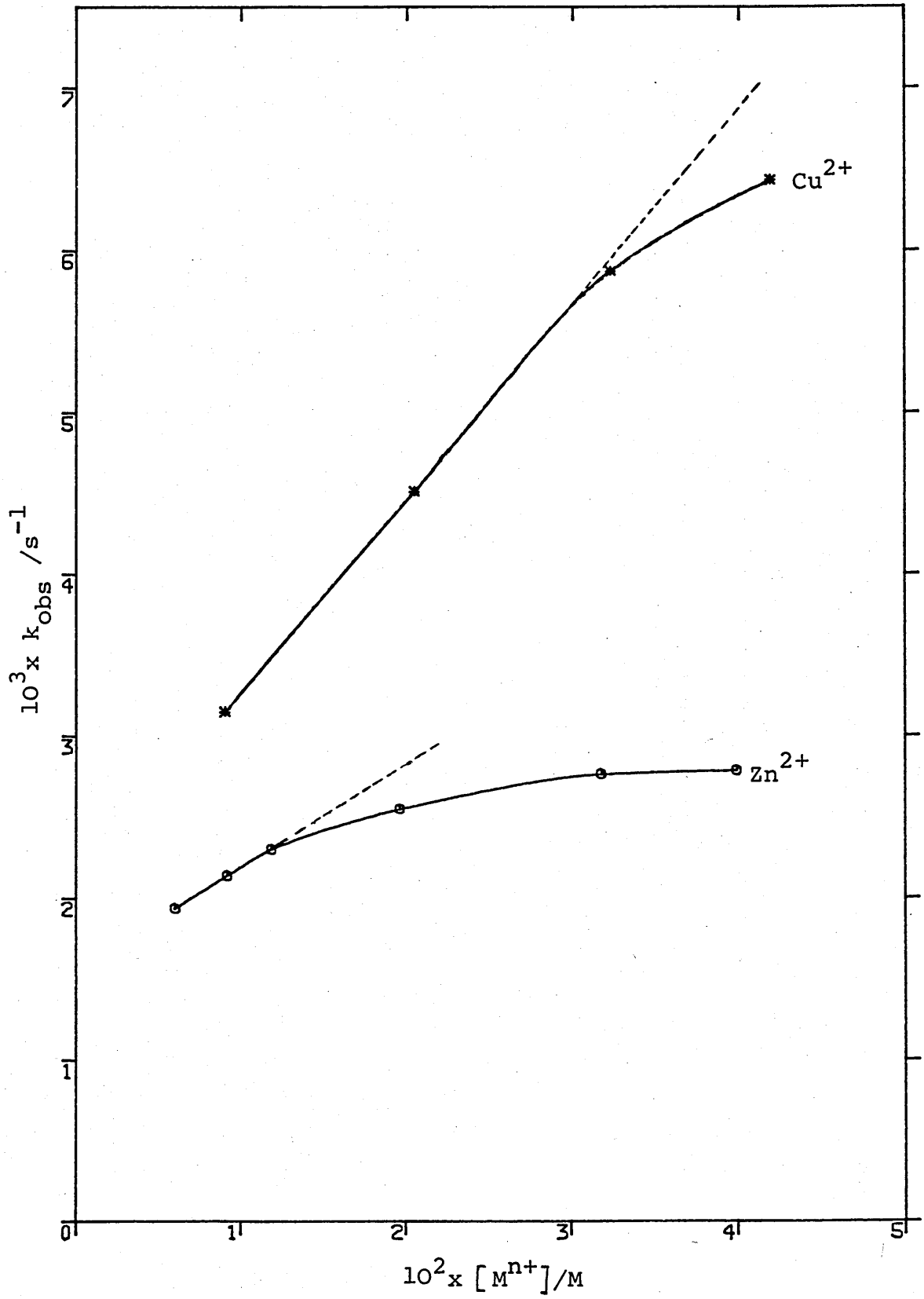

temperatures.

In the light of this result, the interpretation of the thermodynamic parameters (Table 3.3.1.6) becomes less complicated than in the case of 4-CH_3COHMT.

As discussed in the previous section, the formation of a metal ion : HMT complex requires the expulsion of solvent molecules from the coordination sphere of the metal ion. However, the number of solvent molecules expelled not only depends on the size of the ligand but also varies with that of the metal ion. For a given ligand, the number of molecules removed will increase as the metal ion becomes smaller. Thus complexation with a smaller metal ion will usually result in a bigger structural change. Given that the ionic radius of the metal ion increases in the following order:
$Fe^{3+} < Zn^{2+} < Cu^{2+}$, the ΔS value, which increases in the reverse order, is in good accord with the above argument (Table 3.3.1.7).

Table 3.3.1.7 Effect of ionic radius of M^{n+} on the $\Delta H^{\neq}$ and $\Delta S^{\neq}$ for the decomposition of 3-pyridylHMT in ethanol I=0.15M

M^{n+}	ionic radius[a] / nm	$\Delta H^{\neq}$/kJmol^{-1}	$\Delta S^{\neq}$/Jmol^{-1}K^{-1}
Cu^{2+}	0.072	88.5	12
Zn^{2+}	0.069	113	82
Fe^{3+}	0.053	117	145

a) from ref. 78

3.3.1.8 Deuterium Solvent Isotope Effect

As the reaction involves transfer of a proton from O to N and probably involves solvent too, a solvent isotope effect was examined.

The rate of decomposition of 4-$COOCH_3$HMT by Fe^{3+}, Fe^{2+} and Zn^{2+} was shown to be faster in EtOD than in EtOH (Table 3.3.1.8).

Table 3.3.1.8 Deuterium solvent kinetic isotope effect on the decomposition of 4-CH_3COOHMT by M^{n+} T=37 °C I=0.15M

M^{n+}	k_{EtOD}/k_{EtOH}
Fe^{3+}	1.36 ± 0.13
Fe^{2+}	3.17 ± 0.25
Zn^{2+}	2.18 ± 0.12

These results, ironically, are consistent with a H^+ i.e. specific acid catalysis mechanism involving a pre-equilibrium protonation step and a unimolecular rate limiting step (Scheme 3.3.1.4).[79] Nevertheless, this mechanism has been invoked to account for an inverse kinetic solvent isotope effect of a metal ion catalysed reaction in which the metal ion is functioning as a superacid.[98] However, the presence of an exchangeable proton in HMTs which is involved in the reaction means that the observed kinetic isotope effect is probably a combination of solvent, primary and secondary, isotope effects. Thus analysing the results becomes less straightforward. In spite of this,

Scheme 3.3.1.4

$$S + H^+ \rightleftharpoons SH^+ \quad \text{fast}$$

$$SH^+ \longrightarrow \text{Product} \quad \text{slow}$$

the change of solvent from EtOH to EtOD is believed to have little effect on the complexation step. As a result, the decomposition of the complex is thought to be responsible for the rate increase in EtOD.

3.3.1.9 Secondary Deuterium Isotope Effect

The decomposition by Fe^{3+}, Fe^{2+} and Zn^{2+} of (33) was found to be faster than (34) (Table 3.3.1a). These results

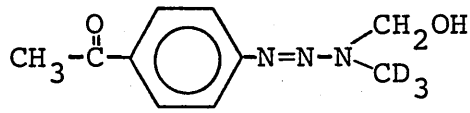

(33)

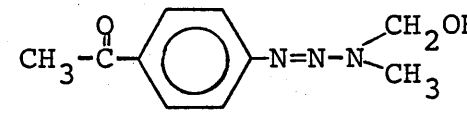

(34)

suggest that the terminal nitrogen of the triazene group has an involvement in the reaction. The CD_3 group is too far to have any effect on the OH group or the arene bound nitrogen atom.

Table 3.3.1.9 Secondary deuterium isotope effects on the decomposition of 4-CH_3COHMT by M^{n+} in EtOH I=0.15M T=37 °C

M^{n+}	kCD_3/kCH_3
Fe^{3+}	1.118 ± 0.2
Fe^{2+}	1.111 ± 0.112
Zn^{2+}	1.26 ± 0.12

3.3.1.10 Steric Effects

3.3.1.10.1 Ortho Effects

In order to test whether the aryl nitrogen was involved in binding to the metal ion, the decomposition of 2-CF_3HMT by $Zn(ClO_4)_2$ was studied and shown to be slower than that of the 4-CF_3HMT by 32% (Table 3.3.1.10). Whilst it could be argued that this is due to the non-coplanarity of the ring, more likely it points to the lack of direct involvement of the aryl nitrogen in metal binding.

Table 3.3.1.10 Ortho effects on the decomposition of HMT by $Zn(ClO_4)_2$ in EtOH I=0.15M T=37 °C

compound	$k_{Zn^{2+}}/M^{-1}s^{-1}$
4-CF_3HMT	0.376
2-CF_3HMT	0.255

3.3.1.10.2 N-Alkyl Group Effect

The rate of decomposition of (35) by $Zn(ClO_4)_2$ was found to increase as R gets larger (Table 3.3.1.11).

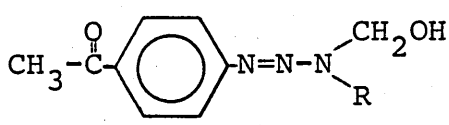

(35)

Table 3.3.1.11 Effect of R on the rate of decomposition of (35) by $Zn(ClO_4)_2$ in EtOH I=0.15M T=37 °C

R	$k_{Zn^{2+}}/M^{-1}S^{-1}$	σ*	E_s
$-CH_3$	0.4825	0	0
$-CH_2CH_3$	2.029	-0.1	-0.07
$-CH_2CH_2CH_3$	3.3818	-0.115	-0.36

Using Pavelich and Taft's equation (3.3.1.2), the effect of the alkyl group (R) can be separated into its polar (σ*) and steric (E_s) effects.

$$\log \frac{k_R}{k_{CH_3}} = \rho^* \sigma^* + \delta E_s \qquad 3.3.1.2$$

In this instance, ρ* and δ were shown to have the values of -5.92 and -0.4594 respectively indicative that the decomposition of HMT by M^{n+} is very sensitive to polar effects (σ*) but only slightly sensitive to steric effects (E_s).

3.3.1.11 Product studies

The major products (ca 90% or more) of this reaction were found to be the arylamine and its N-methyl and N,N-dimethyl derivatives.

For the Fe^{3+}, Fe^{2+} and Zn^{2+} reactions, the minor product is the arene whereas for the Cu^{2+} reaction, azoarene, biaryl and ethoxyarene were also found. These minor products suggest that aryldiazonium ion was formed in this reaction.

3.3.1.12 Discussion on the Metal Ion Catalysed Decomposition Reactions in Ethanol

Sections 3.3.1.1, 3.3.1.2 and 3.3.1.3 indicated that the rate constants obtained from the metal ion catalysed decomposition reactions relate to the conversion of HMT to MMT.

This reaction is thus analogous to the decomposition of the aminocarbinol intermediate of the hydrolysis of imines and related compounds which have been extensively studied by Jencks and coworkers[80] and can be broadly divided into two groups. First, those which involve strongly basic amines whilst the second group includes weakly basic amines. At acidic pH where the rate of decomposition of the aminocarbinol intermediate becomes rate limiting, general base catalysis is required for the expulsion of the weakly basic amines from the protonated aminocarbinol intermediate (Scheme 3.3.1.5).

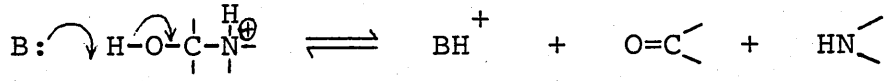

Scheme 3.3.1.5 General base catalysed decomposition of aminocarbinol

In contrast, for the aminocarbinols derived from strongly basic amines, proton transfer from the oxygen to nitrogen is fast and intramolecular. The slow step is the expulsion of the amine from the zwitterion (Scheme 3.3.1.6).

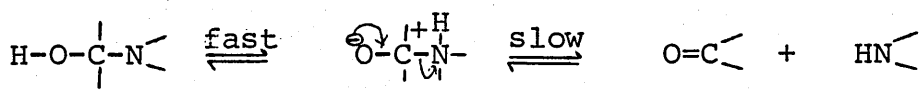

Scheme 3.3.1.6 Unimolecular decomposition of aminocarbinol from strongly basic amines

Since the lone pair electrons of the terminal nitrogen in HMTs are involved in delocalisation over the triazene system, HMTs can be considered as aminocarbinols derived from weakly basic amines.

The result of the Cr^{3+} reaction has categorically proved that the decomposition of HMT to MMT is not catalysed by H^+ but by M^{n+} (Section 3.3.1.5). Nevertheless, this can be further substantiated by the Hammett plots (Section 3.3.1.6). The different slopes of these plots which represent the positive ion character of the transition state, can only be achieved by the polyvalent M^{n+} and not H^+. If the latter were the catalyst identical slopes would be obtained. Similar work on the decomposition of aminocarbinol by M^{n+} has been studied by Martin and coworkers.[66] They found that Cu^{2+} stabilises the aminocarbinol intermediate in the hydrolysis of salicylideneethylamine to such an extent that the rate limiting step shifted from the formation to the decomposition of the intermediate (Scheme 1.2.6). The structure of the Cu^{2+}:aminocarbinol complex (36) has also been proposed.

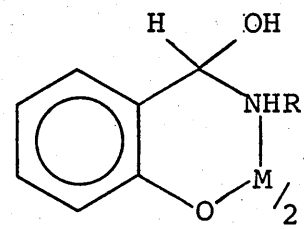

(36)

The presence of the triazene group in HMTs allows the possibilities that M^{n+} can bind to either one of the three nitrogen atoms. Indeed, a stable 6-membered ring can be constructed if M^{n+} binds to the arene bound nitrogen and to the OH group(37).

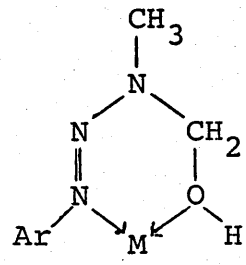

(37)

By chelating to a metal ion, the acidity of the OH proton is increased. Indeed, the acidity of a water molecule coordinated with Cu^{2+} is 10^7 times greater than the acidity of a free water molecule.[81] Likewise, a M^{n+} bound EtOH molecule should be about 10^7 times more acidic than a free EtOH molecule. This means that HMT, when coordinated with M^{n+}, is entering into an acidic environment. Two events can follow (Scheme 3.3.1.7)

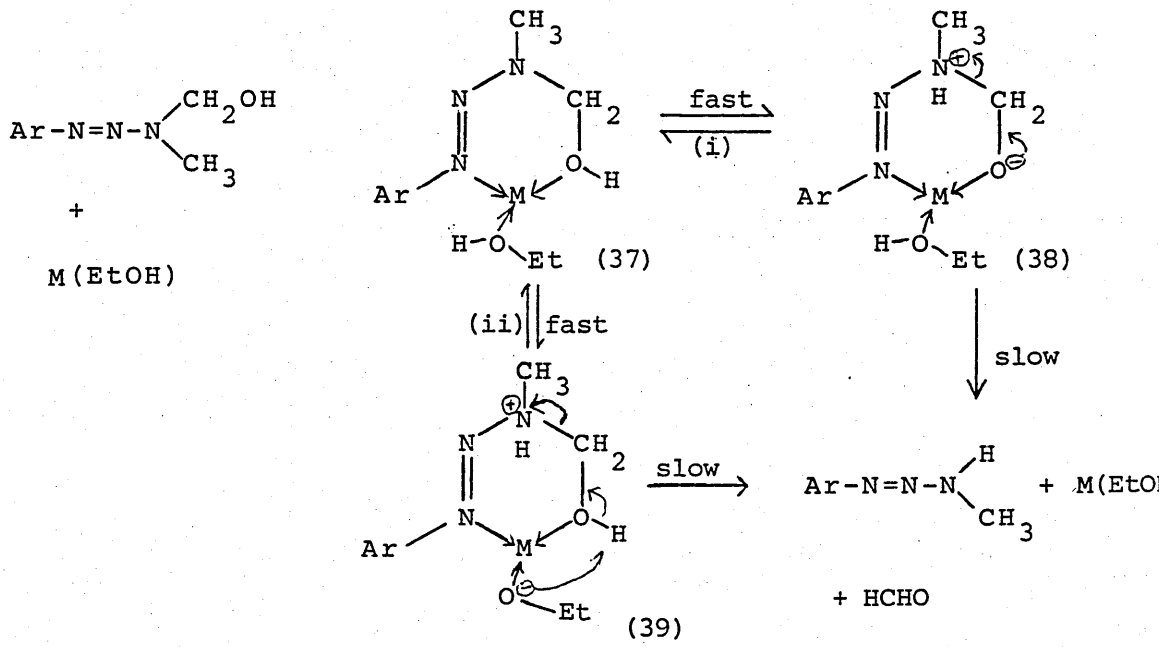

Scheme 3.3.1.7 Mechanism of decomposition of 4-substituted phenylHMT by M^{n+} in EtOH

(i) the OH proton in HMT may migrate from oxygen atom to the terminal nitrogen to give the dipolar form (38) (route i),

(ii) the other possibility is the proton transfer from the metal bound solvent molecule to the triazene group (route ii).

Both (i) and (ii) are believed to be fast and the rate limiting step in both cases is the next one which involves the leaving of the formaldehyde. Like in the hydrolysis of imines, no catalyst is required for the breakdown of the zwitterion intermediate (38) whereas the decomposition of the protonated form (39) would need general base catalysis.

Evidence for the formation of (38) or (39) can be adduced from the inverse secondary deuterium isotope effect (Section 3.3.1.9) which suggests that there is positive change development on the terminal nitrogen atom, N-3, of the triazene group. Further support comes from the effect of N-alkyl substituent (Section 3.3.1.10.2). The results suggest that inductive effects are more significant than steric effects. Thus the formation of (38) or (39) is favoured.

In contrast, as discussed in Section 3.3.1.10.1, the involvement of the arene bound nitrogen atom, N-1, in metal binding is less conclusive. Consequently, (40) cannot be ruled out as an alternative mode of binding.

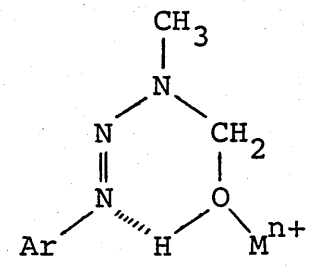

(40)

3.3.2 Ligand Effects on the Decomposition of HMTs in Ethanol

The conversion of HMT to MMT in ethanol have been shown to be facilitated by metal ions. Given that most of the biological reactions are catalysed by enzymes and that the active site of enzymes usually contains a metal ion surrounded by different functional groups, it was decided to investigate the effect of ligand on the metal ion catalysed decomposition of HMTs.

3.3.2.1 Sodium Iodide (NaI)

The effect of (NaI) on the rate of decomposition of 4-CH_3COOHMT by 0.01M $Zn(ClO_4)_2$ in EtOH was shown in Fig. 3.3.2.1.

The rate was found to decrease as the (NaI) increases. The apparent reason is the formation of complexes between Zn^{2+} and I^-, thereby reducing the effective nuclear change of the metal ion and also increasing the steric hindrance on the metal ion. As a result, the catalytic ability of the metal ion is diminished.

Fig. 3.3.2.1 Effect of NaI on the decomposition of 4-CH 4-CH_3COOHMT by 0.01M Zn^{2+} in EtOH I=0.15M T=37°C

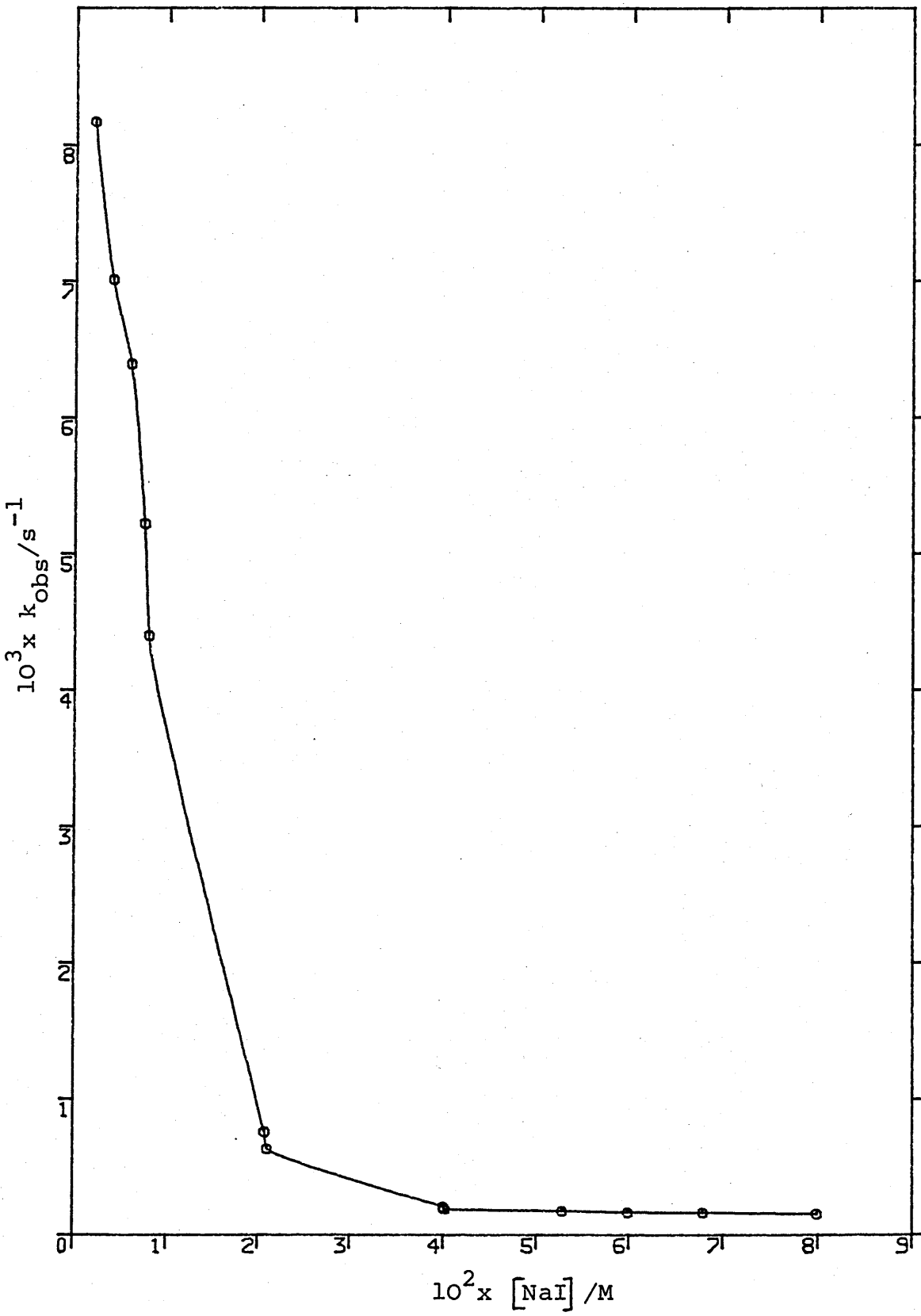

The observed rate constant can therefore be expressed as:

$$k_o = k_{Zn^{2+}}[Zn^{2+}] = k_{(ZnI)}[(ZnI)^+] + k_{ZnI_2}[ZnI_2] + \cdots$$

Since $[Zn^{2+}]$ total is constant

$$\therefore\ k_o = k_{Zn^{2+}}\left([Zn^{2+}]_{total} - [(ZnI)^+] - [(ZnI_2)] - \cdots\right) + k_{(ZnI)}[(ZnI)^+] + k_{ZnI_2}[ZnI_2] + \cdots$$

$$= k_{Zn^{2+}}[Zn^{2+}]_{total} + (k_{(ZnI)^+} - k_{Zn^{2+}})[(ZnI)^+] + (k_{(ZnI_2)} - k_{Zn^{2+}})[ZnI_2] + \cdots$$

$$(k_c - k_o) = (k_{Zn^{2+}} - k_{(ZnI)^+})[(ZnI)^+] + (k_{Zn^{2+}} - k_{ZnI_2})[ZnI_2] + \cdots$$

where $k_c = k_{Zn^{2+}}[Zn^{2+}]_{total}$ — 3.3.2.1

This equation (3.3.2.1) is of identical form to the one used in the determination of metal ligand complex stability constant by the mole ratio method.[82]

In this method, a series of solutions is prepared in which the total concentration of one of the reactants is kept constant while that of the other is varied. The absorbance of these solutions is then measured and plotted against the mole ratio of the reactants. Depending on the composition of the complex and its stability, different plots can be obtained. Two examples are shown in Fig. 3.3.2.2

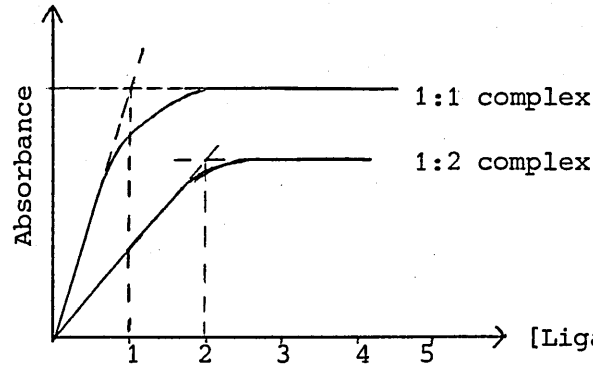

Fig. 3.3.2.2 Typical mole ratio plots for the determination of metal:ligand complex composition

Assume that only 1 complex is formed between metal and ligand and that both metal and ligand do not absorb at the wavelength chosen.

$$\therefore [\text{metal}]_{\text{total}} = [M^{n+}] + [ML_n]$$

$$\text{and } [\text{ligand}]_{\text{total}} = n[ML_n] + [L]$$

$$\text{Absorbance (A)} = \varepsilon_{ML}[ML_n] \quad \text{——— 3.3.2.2}$$

At $[\text{ligand}]_{\text{total}(t)} \ll [\text{metal}]_{\text{total}(t)}$, the absorbance increases as the mole ratio increases suggesting that [complex] is increasing. The determining factor in [complex] in this situation is therefore the $[\text{ligand}]_t$. Thus [complex] $\approx [\text{ligand}]_t/n$.

On the other hand, when $[\text{ligand}]_t \gg [\text{metal}]_t$, all the metal ions are converted into the complex. Because $[\text{metal}]_t$ is constant, a horizontal line is therefore obtained. Hence in this situation: $[\text{metal}]_t = [\text{complex}]$.

The intersecting mole ratio of these two lines thus represent the combining ratio of the complex. Note that the plot for the 1:1 complex curves off more than the 1:2 complex at the mole ratio corresponding to the composition of the complex. This is due to the incomplete combination of metal and ligand i.e. dissociation of the complex occur. In other words, the 1:1 complex in the example is a weaker complex than the 1:2 complex.

Nevertheless, ε_{ML_n} for both complexes can be obtained easily,

$$A \quad [\text{metal}]_t \ll [\text{ligand}]_t \ , \ [\text{metal}]_t \simeq [ML_n]$$

$$\therefore A = \varepsilon_{ML_n}[\text{metal}]_t$$

$$\varepsilon_{ML_n} = A/[\text{metal}]_t$$

For the case of successful complex formation, however, this method will only hold if the stability constants of the various complex species are very different from each other so that several linear sections occur on the plot.

Since Equation (3.3.2.1) is of identical form to Equation (3.3.2.2), the same argument can be applied to the HMT reactions. A plot of (k_c-k_o) vs. $([NaI]_{total}/[Zn^{2+}]_{total})$ was constructed (Fig. 3.3.2.3).

The intersecting point occurs at the ratio of ca 1.75 suggesting that both $(ZnI)^+$ and ZnI_2 are present.

The rate constant for the ZnI_2 species (k_{ZnI_2}), nevertheless can be estimated at $[NaI]_{total} >> [Zn^{2+}]_{total}$. The average pseudo first order rate constant from $[NaI]_{total}$ = 0.04 to 0.08M is $1.708\times10^{-4} \pm 2\times10^{-5} S^{-1}$. Since $[Zn^{2+}]_{total}$ = 0.01M therefore

$$k_{ZnI_2} = \frac{1.708\times10^{-4}}{0.01}$$

$$= 1.708\times10^{-2} \pm 2\times10^{-3} M^{-1}S^{-1}$$

$k_{(ZnI)^+}$ can also be estimated from the other straight line where $[Zn^{2+}]_{total} > [NaI]_{total}$ with the assumption that the concentration of ZnI_2 and the dissociation of $(ZnI)^+$ are negligible in this concentration range. Consequently, $[(ZnI)^+] \simeq [I^-]_{total}$ and the decrease in (k_o-k_c) is due to $[(ZnI)^+]$ alone. Equation 3.3.2.1 can therefore be rewritten as:

Fig. 3.3.2.3 Mole ratio plot for the decomposition of 4-CH_3COOHMT by Zn^{2+} with NaI

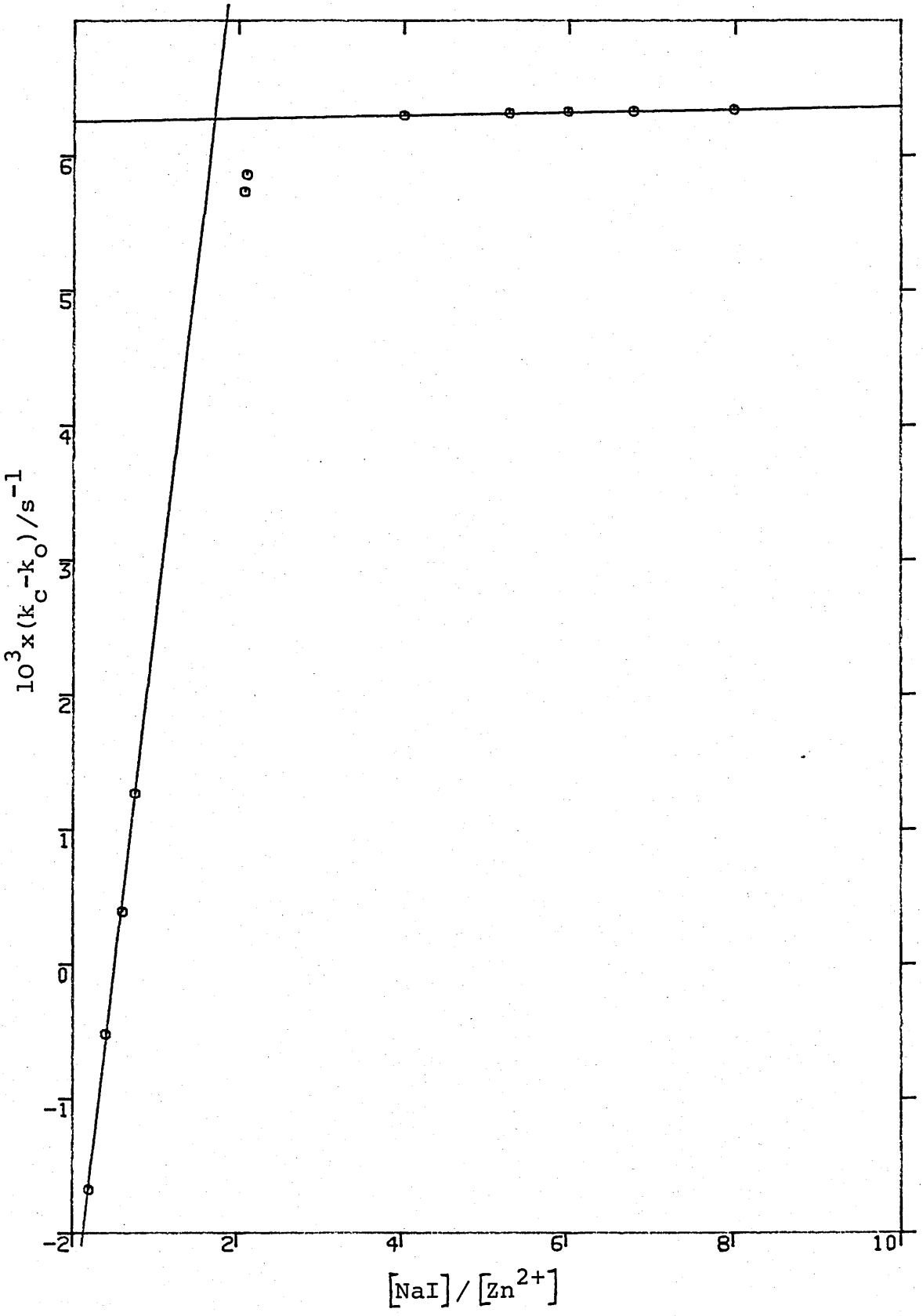

$$(k_o - k_c) = (k_{(ZnI)^+} - k_{Zn^{2+}}) \left[(ZnI)^+\right]$$

$$= (k_{(ZnI)+} - k_{Zn^{2+}}) \left[I^-\right]_{total}$$

Indeed, the plot of $(k_c - k_o)$ vs. $\left[I^-\right]_{total}$ gave a good straight line with a slope of 0.526 (Fig. 3.3.2.4). Therefore,

$$k_{Zn^{2+}} - k_{(ZnI)+} = 0.526$$

since $k_{Zn^{2+}} = 0.55$

$$k_{(ZnI)+} = 0.024 \pm 0.018 \ M^{-1}s^{-1}$$

It has to be emphasised that the value of $k_{(ZnI)+}$ and k_{ZnI_2} given above are estimated values. Accurate calculation of these rate constants has to be performed with the knowledge of their stability constants in ethanol which currently is not available in the literature. However, these estimated values are substantially lower than that for Zn^{2+} i.e.

$$k_{Zn^{2+}} \underset{20}{>} k_{(ZnI)^+} \underset{1.5}{>} k_{ZnI_2}$$

3.3.2.2 Imidazole (Im)

Using the same method as in the case of NaI, $(Zn(Im)_4)^{2+}$ was identified to be one of the complexes formed between Zn^{2+} and imidazole as shown in Fig. 3.3.2.5. Its rate constant was estimated to be $1.385 \times 10^{-3} \pm 2.37 \times 10^{-4}$ $M^{-1}s^{-1}$. For other Zn^{2+} : Im complexes, however, it is more difficult to estimate their rate constants. This is due partly to the presence of various equilibria in the solution and partly to the rather scattered results at low $[\text{imidazole}]_{total}/[Zn^{2+}]_{total}$.

Fig. 3.3.2.4 Mole ratio plot for the decomposition of 4-CH_3COOHMT by Zn^{2+} with NaI

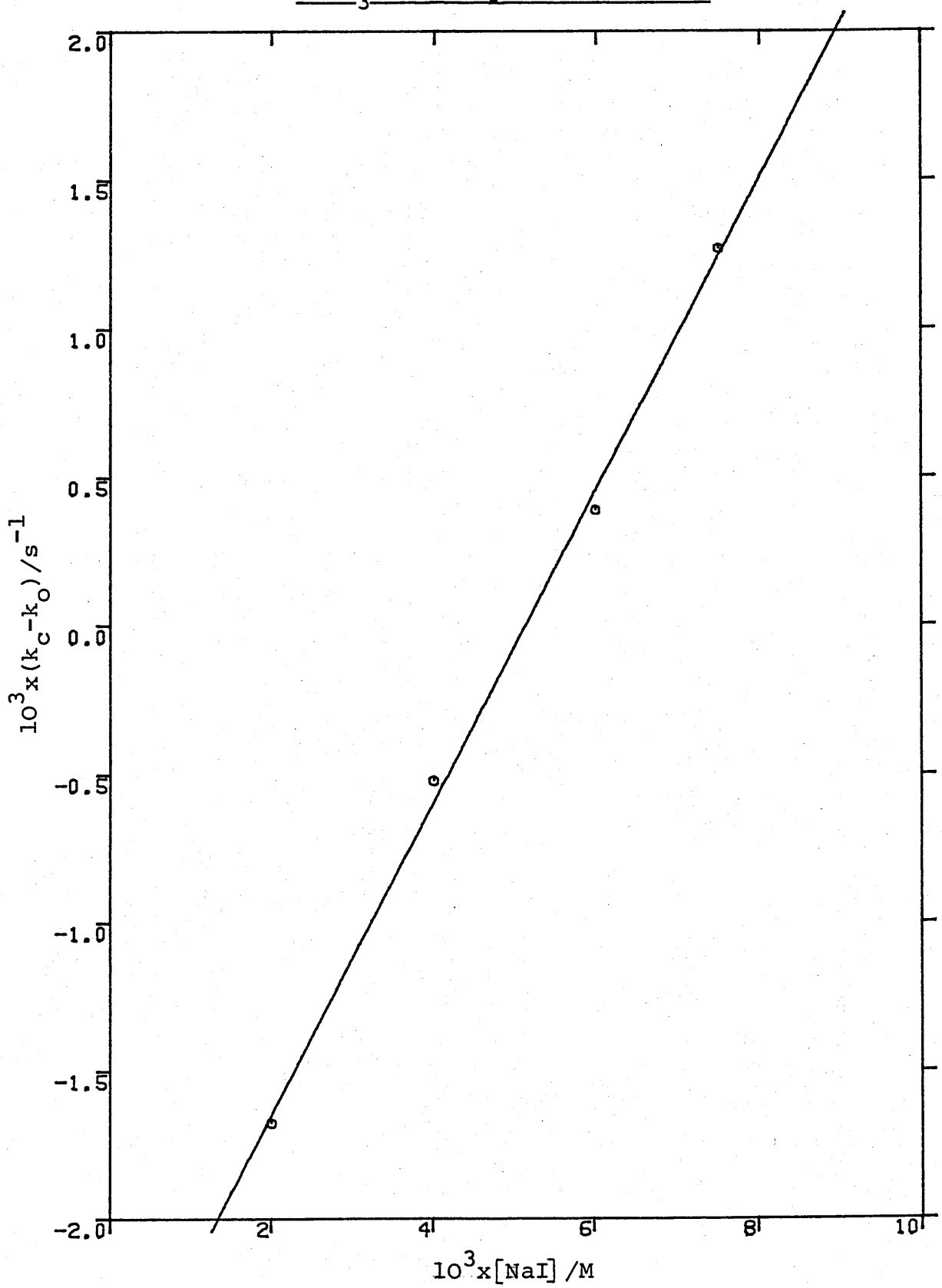

Fig. 3.3.2.5 Mole ratio plot for the decomposition of 4-CH_3COOHMT by 0.01M Zn^{2+} with Imidazole

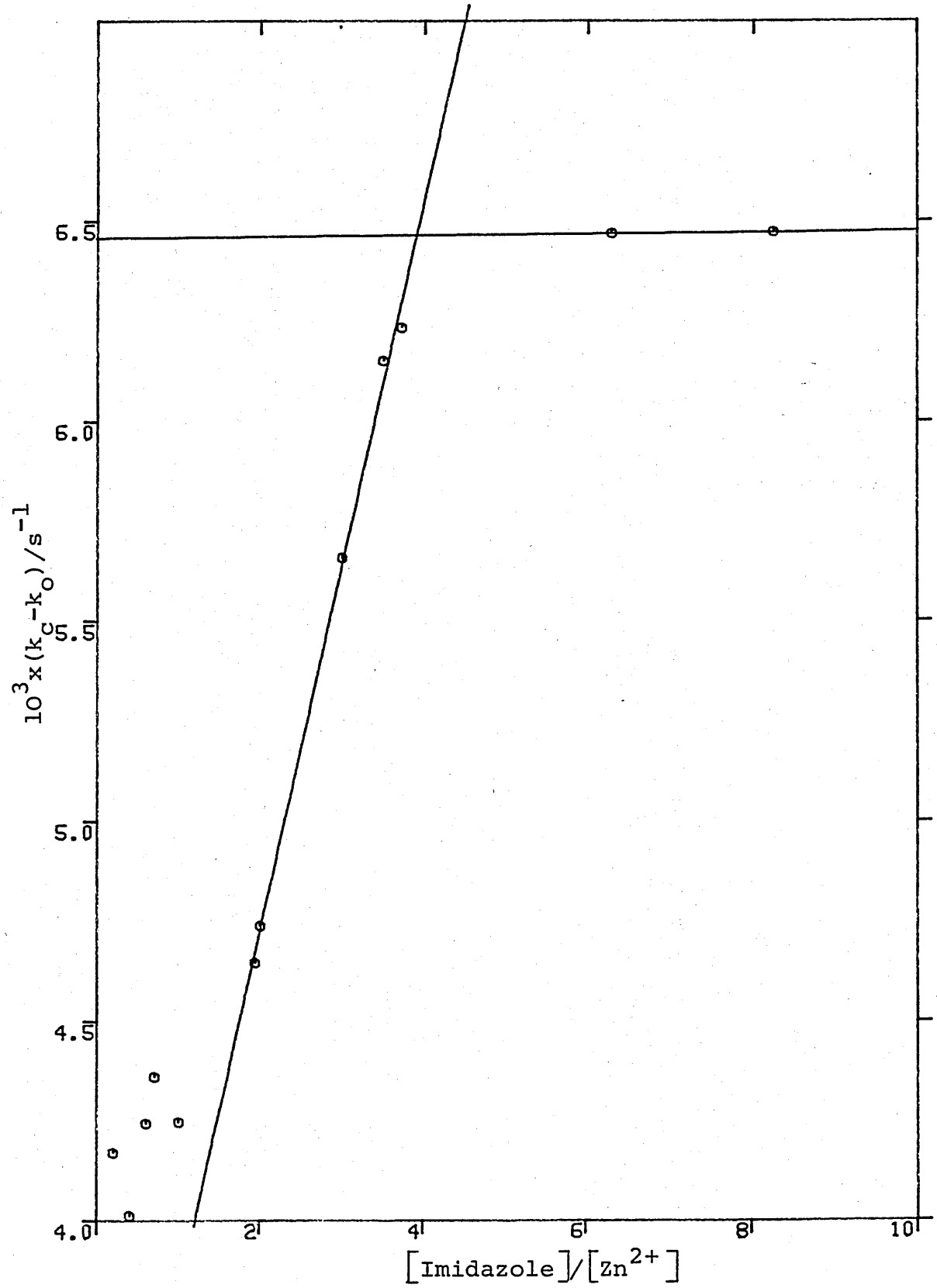

3.3.2.3 Sodium Acetate (NaAc)

The rate of decompositon of 4-CH_3COOHMT by 0.01M $Zn(ClO_4)_2$ with the presence of NaAc is shown in Fig. 3.3.2.6. As in the case of sodium iodide, the rate of reaction decreases as the ligand concentration increases. The plot of (k_c-k_o) vs. $([NaAc]_{total}/[Zn^{2+}]_{total})$ showed that the rate begins to level off at $[NaAc]_{total}$ = 0.04 to 0.05M (Fig. 3.3.2.7). Although these results could be used to estimate the rate constant of the last complex, its composition will not be known due to the limited amount of data obtained.

3.3.2.4 Sodium Bromide (NaBr)

Unlike the three ligands shown earlier, NaBr has no apparent effect on the Zn^{2+} catalysed decomposition of 4-CH_3COOHMT (Fig. 3.3.2.8). This was observed at two $[Zn^{2+}]$.

In order to confirm the above results, the method of continuous variation (Job's method) was followed. The results showed a linear decrease in rate with respect to the mole fraction of $Zn(ClO_4)_2$ (Fig. 3.3.2.9). Thus suggesting no cooperative effect between Zn^{2+} and Br^- in catalysing the decomposition of HMT.

3.3.2.5 Pyridine

The presence of pyridine was also found to decrease the rate of decomposition of 4-CH_3COOHMT catalysed by 0.01M Zn^{2+}. (Fig. 3.3.2.10). Indeed, a good straight line can be drawn through all 4 points which are in the region where [pyridine]

Fig. 3.3.2.6 Effect of NaAc on the decomposition of 4-CH_3COOHMT by 0.01M Zn^{2+} in EtOH I=0.15M

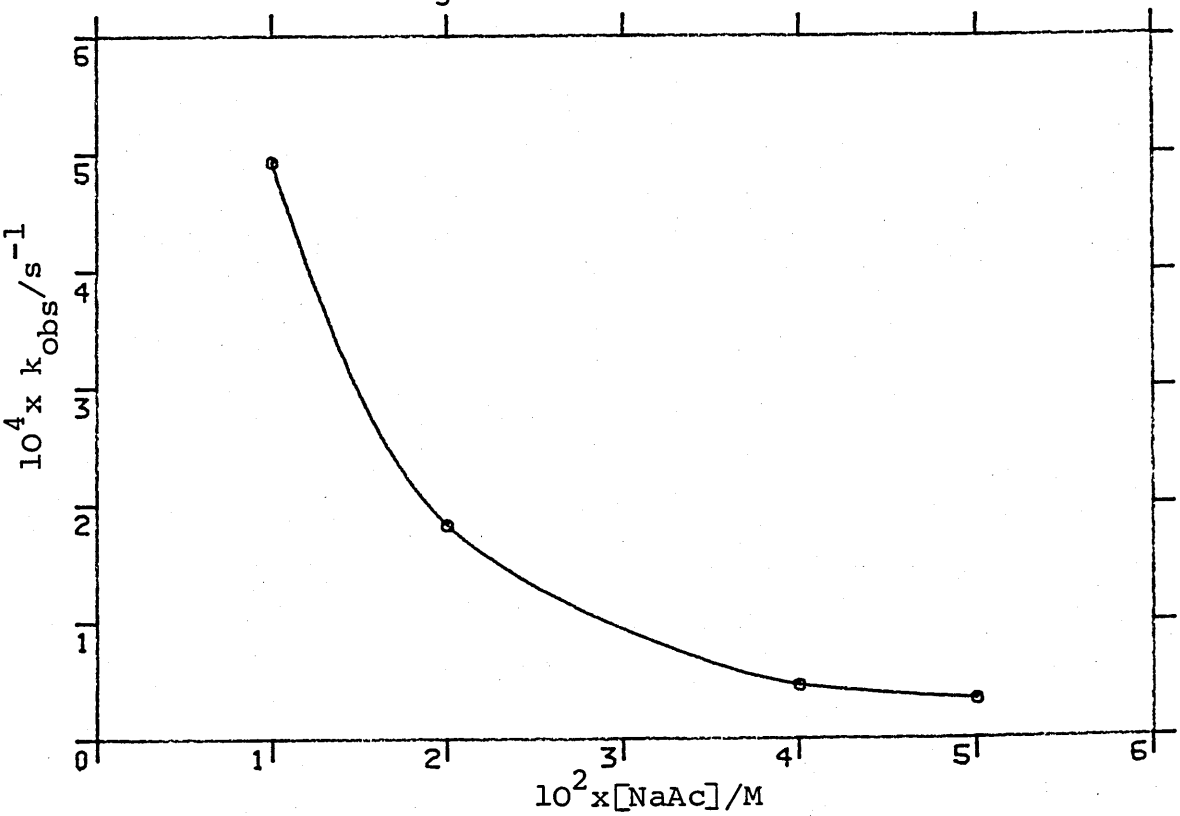

Fig. 3.3.2.7 Mole ratio plot for the decomposition of 4-CH_3COOHMT by 0.01M Zn^{2+} with NaAc

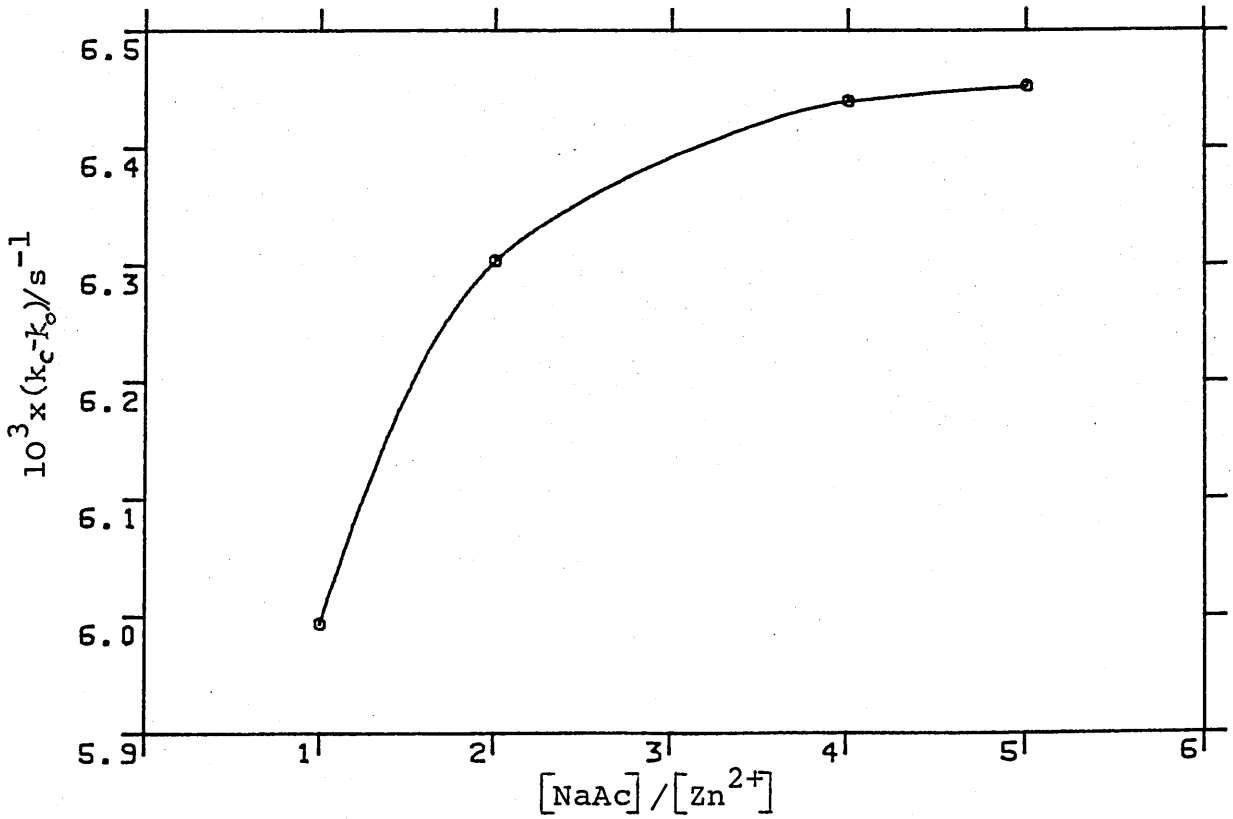

Fig. 3.3.2.8 Effect of NaBr on the decomposition of 4-CH_3-COOHMT by 0.01M Zn^{2+} I=0.15M T=37°C

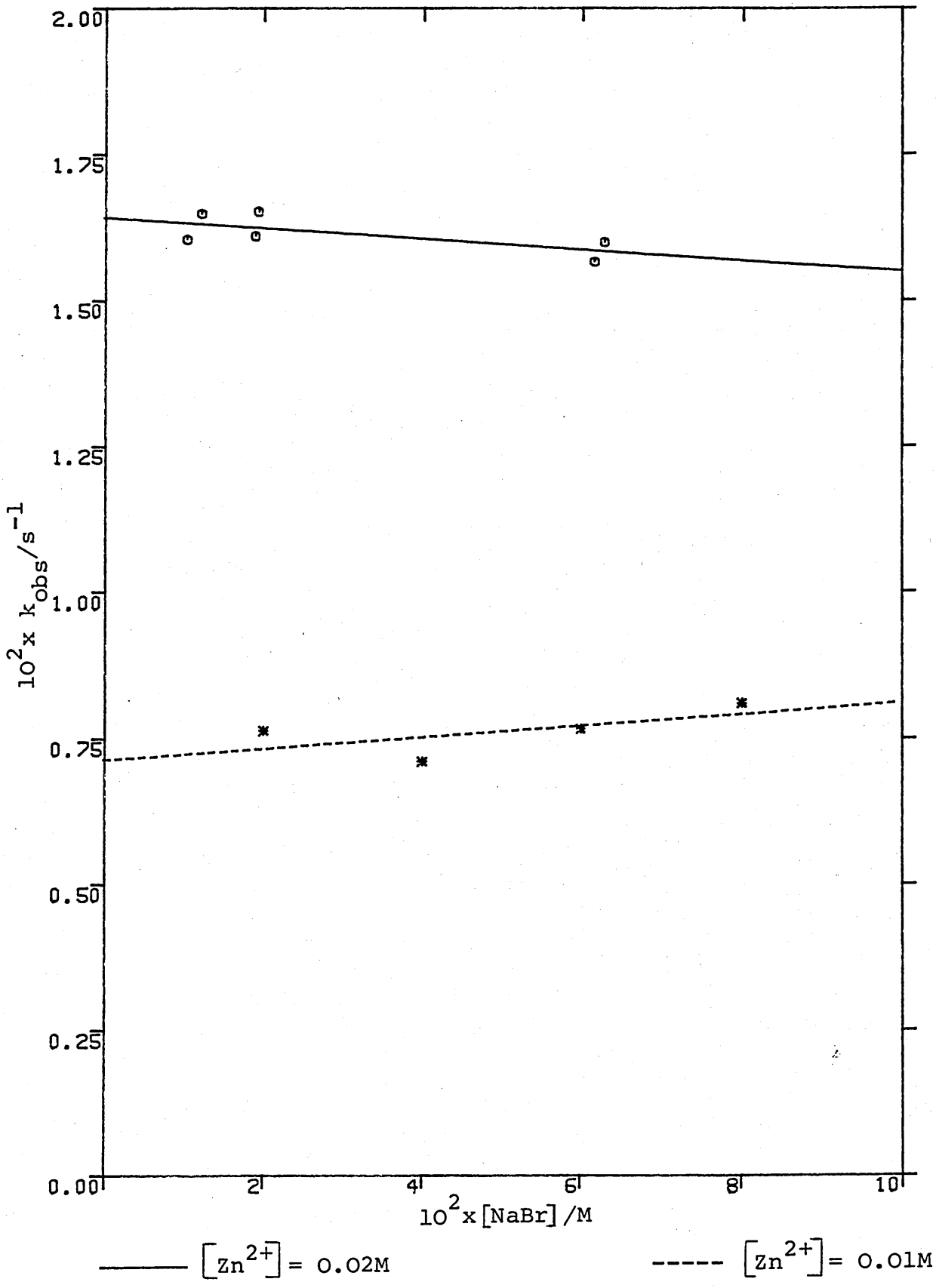

Fig. 3.3.2.9 Job's plot for the decomposition of 4-CH_3COO-HMT by Zn^{2+} with NaBr

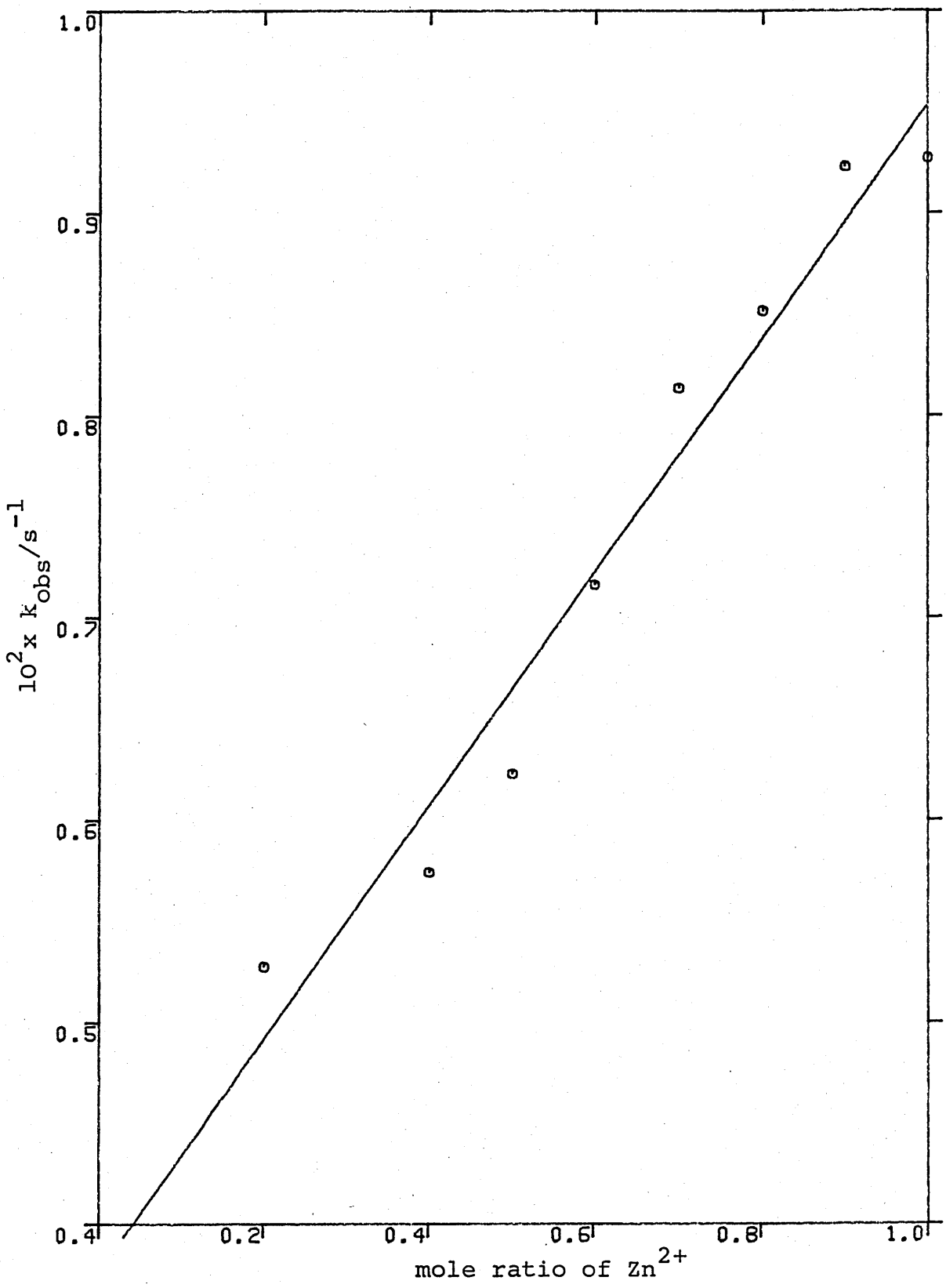

Fig. 3.3.2.9 Job's plot for the decomposition of 4-CH_3COO-HMT by Zn^{2+} with NaBr

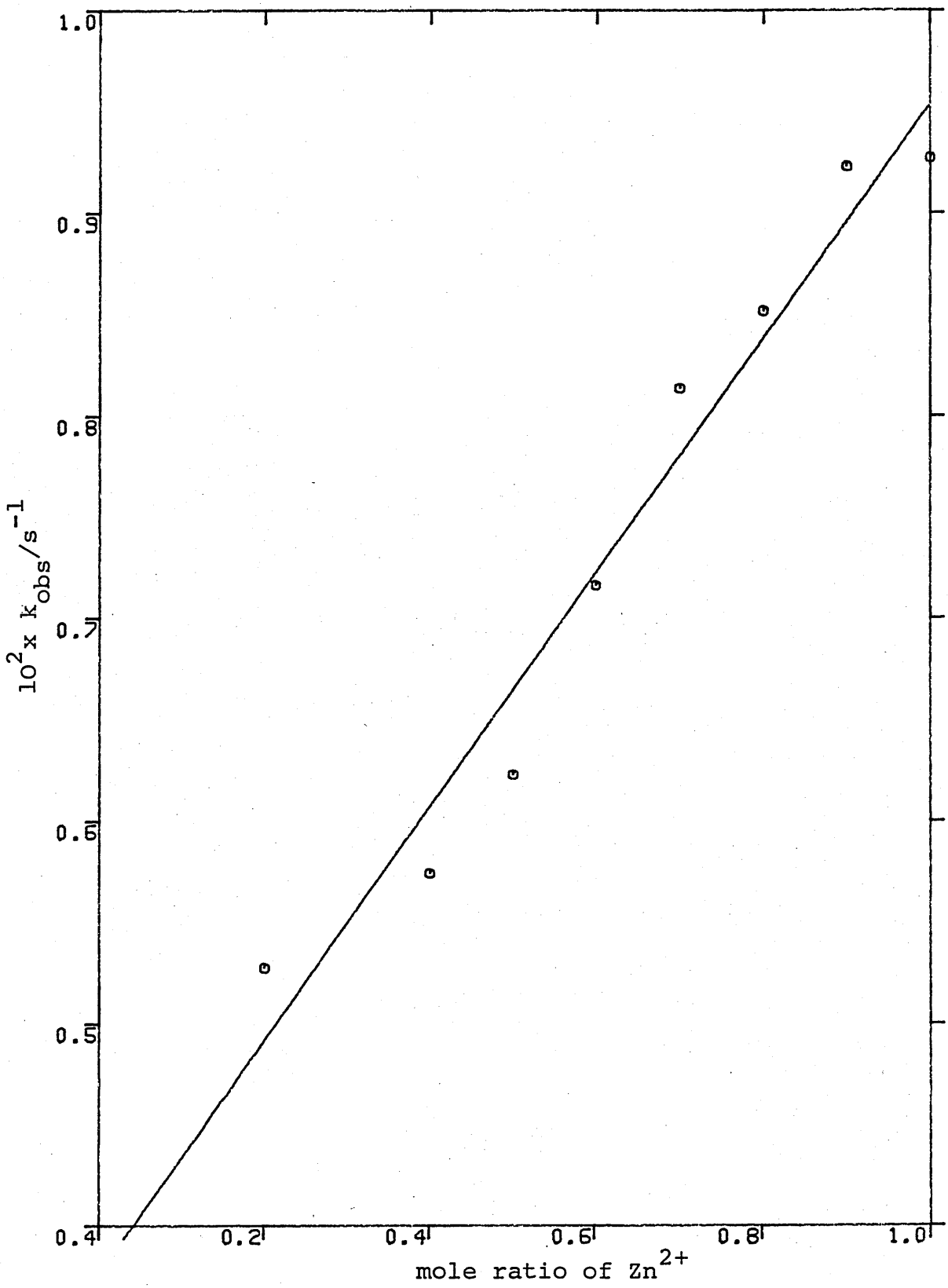

Fig. 3.3.2.10 Effect of pyridine on the decomposition of 4-CH_3COOHMT by 0.01M Zn^{2+} I=0.15M T=37°C

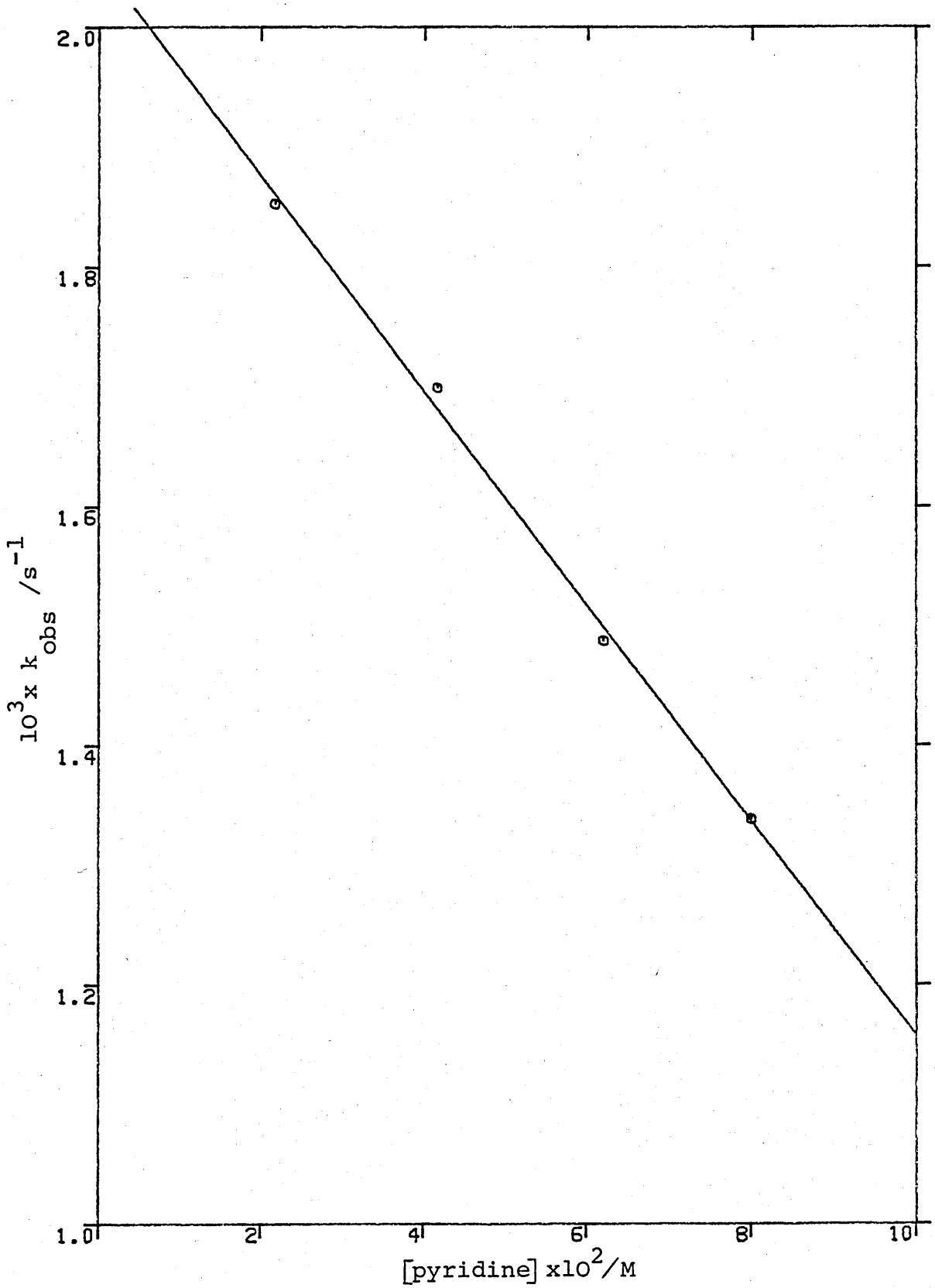

is from 0.0215M to 0.08M. This suggests that the complex formed between Zn^{2+} and pyridine dissociates extensively.

However, without knowing the formation constant of this complex, it is not possible to determine the concentration of the complex and hence its rate constant.

3.3.2.6 Discussion

The application of techniques used in determining the formation constants of metal ligand complexes into kinetic studies have been reported before. Prince and Woolley have successfully showed the cooperative catalysis of hydroxide ion, acetate and pyridine in the zinc catalysed hydration of aldehydes by using Job's method of continuous variation.[83,84,85] With pyridine-2-carboxylate however, the rate of acetaldehyde hydration catalysed by zinc was reported to decrease as the concentration of the ligand increases. This was attributed to a loss of coordination sites in zinc blocked by the ligand though a loss in the effective nuclear change may also be responsible.

The decrease in rate of HMT decomposition caused by the presence of ligands suggests that there is no cooperation between the metal ion and the ligands in catalysing the decomposition of HMTs. Furthermore, without knowing the formation constant for the complexes formed between the metal ions and the ligands used in this study, it is not possible to interpret the results completely.

3.3.3 MMT Decomposition in Ethanol

Although the protolysis of MMTs has been fairly well studied[21] the Lewis acid catalysed decomposition of MMTs has received much less attention. So far, only three reports[56,57,58] have been published on the Lewis acid reaction and a mechanism involving a ion-pair was invoked for the silica gel catalysed reaction[57] (Scheme 1.2.5). This reaction, surprisingly, was reported to be inhibited in ethanol.

Despite the fact that 4-CNMMT decomposes about 20 times as fast as 4-CNHMT in the presence of 0.0078M Zn^{2+} (Section 3.3.1.1), it was decided that more studies on the decomposition of MMTs by M^{n+} were necessary in order to have a better understanding on the degradation kinetics and mechanism.

3.3.3.1 Order of Reaction

The decomposition of MMTs by Zn^{2+} was found to follow pseudo first order kinetics (Fig. 3.3.3.1). This behaviour was still observed even at $[Zn^{2+}] = 10^{-4}M$ — $[HMT] \simeq 5\times10^{-5}M$ — implying that the reaction is catalysed and not promoted by Zn^{2+}.

3.3.3.2 Dependence on the Concentration of Zn^{2+}

The observed pseudo-first-order rate constant was shown to depend on $[Zn^{2+}]^2$ (Fig. 3.3.3.2). This was confirmed by plotting log k_{obs} vs. log $[Zn^{2+}]$ which, indeed, gave a slope of ~ 2 (Fig. 3.3.3.3). Thus the complete rate expression is:

$$\text{Rate} = k_{Zn2+}[MMT][Zn^{2+}]^2$$

Fig. 3.3.3.1 Pseudo first order plot for the decomposition of 4-ClMMT by $1x10^{-4}$M Zn^{2+} in EtOH I=0.15M T=

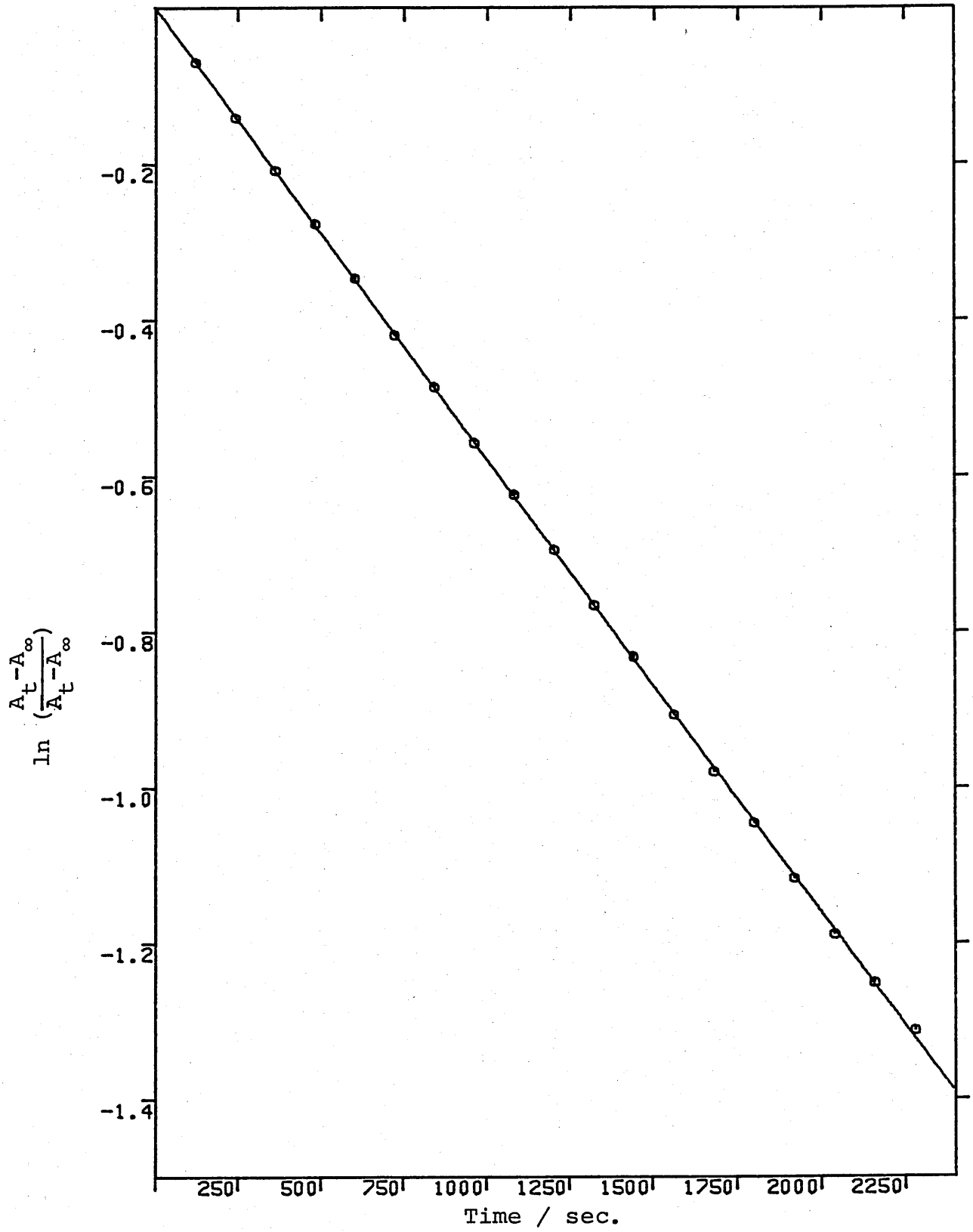

Fig. 3.3.3.2 Decomposition of 4-CNMMT in ethanol by Zn^{2+} I=0.15M T=37°C

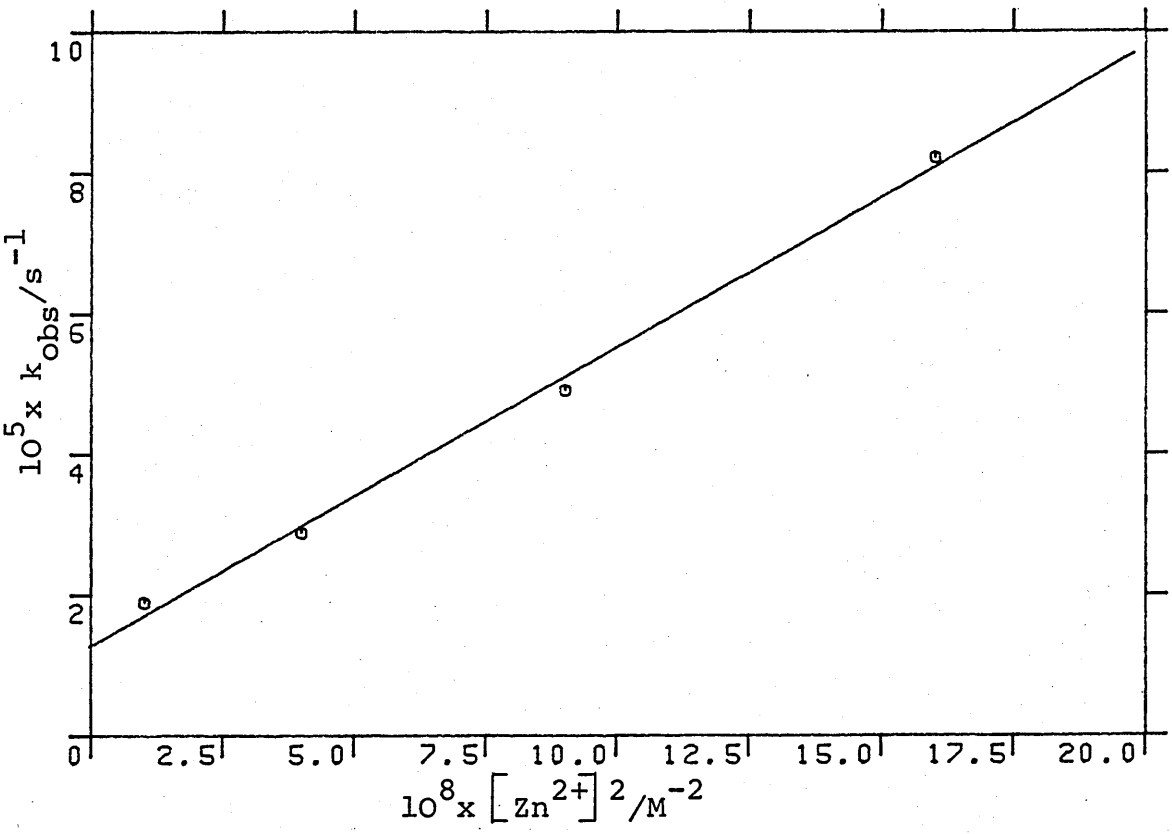

Fig. 3.3.3.3 Log:log plot for the decomposition of 4-CNMMT by Zn^{2+} I=0.15M T=37°C

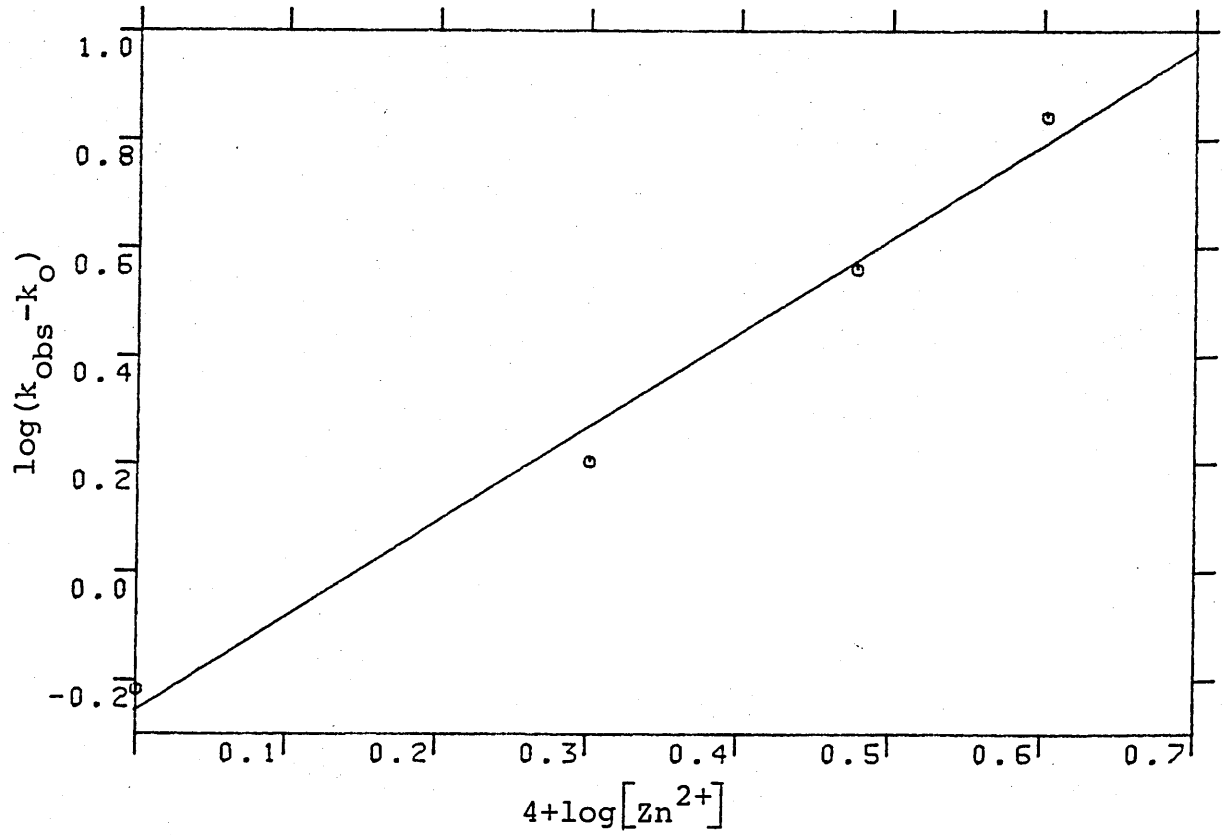

3.3.3.3 Effect of Substituents

A negative ρ-value of 3.385 was obtained from the Hammett plot (Fig. 3.3.3.4). Like in the decomposition of HMTs by M^{n+}, this datum is consistent with a mechanism involving electrphilic attack by Zn^{2+} on the MMTs. Interestingly, the result of 3-pyridylMMT reaction does not deviate from the plot. This implies that the triazene group is of comparable, it not better, coordination power as the pyridyl ring for Zn^{2+}.

3.3.3.4 Ionic Strength Effect

The rate of decomposition of 4-CNMMT at a constant $[Zn^{2+}]$ was found to decrease as the ionic strength increases (Fig. 3.3.3.5) which suggests that two charged species are involved in this reaction.

3.3.3.5 Product Studies

The major products (ca 90% or more) of MMT decomposition by Zn^{2+} was found to be the arylamine and its N-methyl- and N,N-dimethyl- derivatives. The minor product was shown to be the arene ,

3.3.3.6 Discussion

The rate of 3-pyridylMMT reaction with Zn^{2+} correlates well with the Hammett plot for MMT decomposition by Zn^{2+}

Fig. 3.3.3.4 Hammett plot for the decomposition of MMTs in EtOH by $Zn(ClO_4)_2$ I=0.15M T=37°C

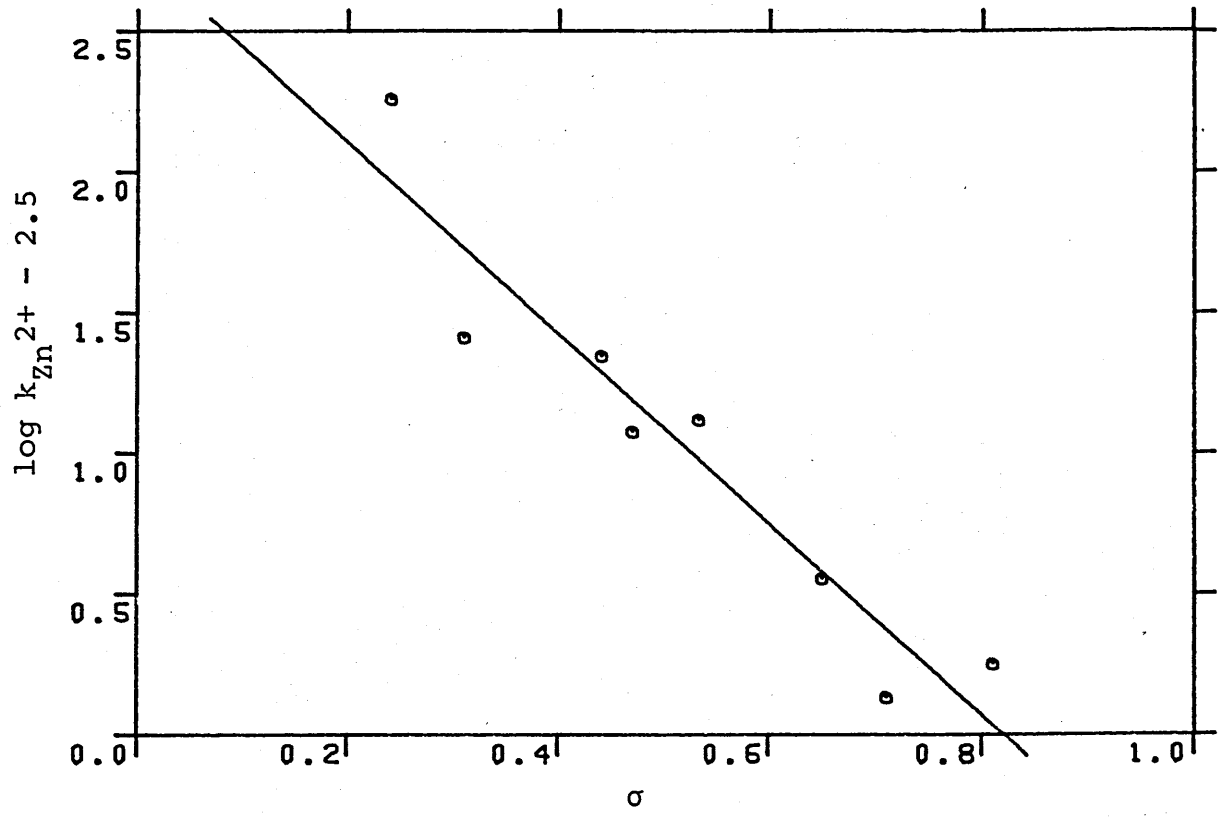

Fig. 3.3.3.5 Ionic strength effect on the decomposition of 4-CNMMT in ethanol I=0.15M T=37°C

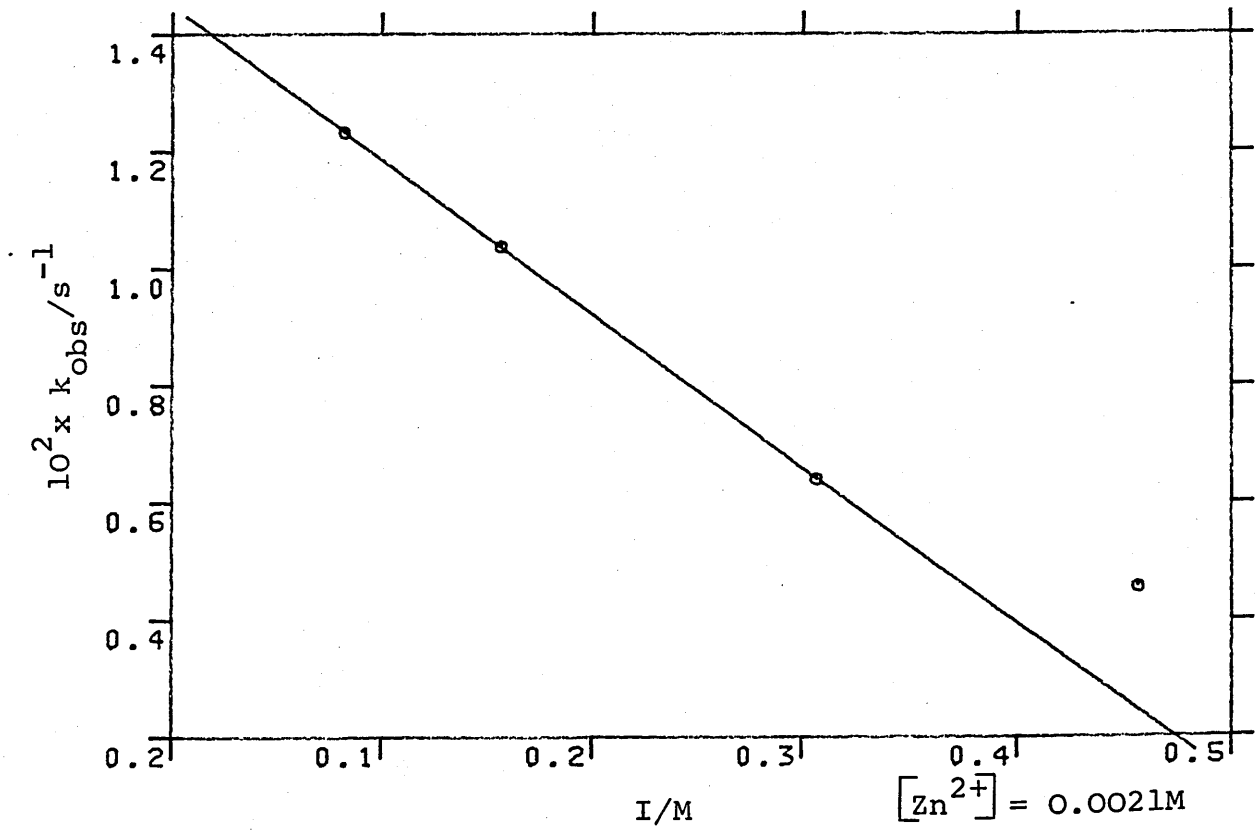

(Fig. 3.3.3.4) and is interpreted as an indication that the triazene group in this MMT is, in line with other MMTs, solely responsible for the coordination of MMT to Zn^{2+}. In contrast, the rate for 3-pyridylHMT reaction deviates significantly from its Hammett plot. Coordination through the pyridyl ring is believed to be responsible for this deviation. Implicit in this argument is that the pyridyl ring is a stronger M^{n+} coordinator than the -OH or triazene group in HMT.

Two explanations are possible for the lowering of M^{n+} coordination ability of the triazene group in HMT. Firstly, the presence of the hydroxymethyl group may sterically hinder the coordination of the triazene group with M^{n+}. Secondly, and more importantly, the pKa of the amino group in an aminocarbinol has been shown to be lower than that of the parent amine by 2-3 units.[49] By analogy, the pKa of the triazene group in HMTs should be 2-3 units lower than that of MMTs. It is very likely that this drop in the pKa of the triazene group in HMT is sufficient enough to upset the situation such that the coordination through the pyridyl ring is preferred.

Apart from the 3-pyridylMMT result, there are other differences between the MMT and HMT reactions. The major one is the dependence on $[Zn^{2+}]^2$ for the MMT decomposition which implies that two metal ions are involved in the reaction. Disubstituted triazenes are known to form a bridging ligand between two metal ions (20, Section 1.2.3.3). Indeed, the results of the ionic strength effect implies that the reaction

involves two charged species. The formation of a zinc: triazenato complex (41) is thus favoured. However, this seems unlikely according to a study on the preparation of

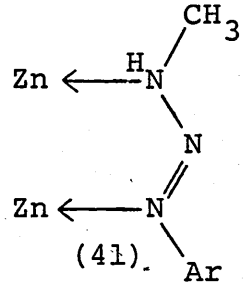

(41)

Cu^{2+}, Ag^{+}, Hg^{+} and Hg^{2+} complexes of alkylaryltriazenes including methylaryltriazenes.[77] Whilst the alkylaryltriazenes of Hg^{+} and Hg^{2+} can be synthesised by reacting an aqueous-alcoholic solution of the triazenes with an alcoholic solution of the metal salts, those of Ag^{+} and Cu^{2+} require an ammoniacal solution of the metal salts. Unfortunately the authors did not account for the use of an ammoniacal solution for Cu^{2+} and Ag^{+}. Nevertheless, it is apparent that the presence of ammonia can, firstly, neutralise the acidic environment around the metal ions and, secondly, promote the formation of the complex by facilitating the loss of proton from the triazenes.

Without the presence of any base, on the other hand, the most possible step is thought to be the breakdown of the triazene group. Despite the fact that the unconjugated tautomer ($Ar\text{-}\overset{H}{N}\text{-}N{=}N\text{-}CH_3$) is generally believed to be the reactive tautomer, there is ample evidence to suggest that the decomposition of the conjugated tautomer ($Ar\text{-}N{=}N\text{-}\overset{H}{N}\text{-}CH_3$), which will subsequently lead to the formation of the aryldiazonium ion, also occurs. The latter view was based on the products obtained from this reaction.

Besides the usual products of the corresponding aniline, N-methyl-and N,N-dimethylanilines formed in the acid catalysed decomposition of MMTs, arene was found to be one of the products in this reaction. The most likely way for the formation of arene is via the dediazoniation of the aryldiazonium ion in ethanol.[86]

Further evidence to support the suggestion that aryldiazonium ions are formed in the MMT decomposition can be adduced from the product studies on the HMT decomposition by M^{n+} where the presence of the corresponding ethoxyarene, biaryl and azoarene were observed.

In the light of these evidence, it is certain that decomposition of the conjugated tautomer of MMT ($Ar-N=N-\overset{H}{\underset{|}{N}}-CH_3$) does occur, though to a small extent. Previous studies on the protolysis of monomethyl- and monobutyltriazenes have also implicated the involvement of this tautomer on the grounds that diaryltriazenes are formed.[87] The latter compound can arise through the coupling of the aryldiazonium ion with the arylamine (Scheme 3.3.3.1).

The mechanism for the degradation of MMTs by M^{n+} is summed up in Scheme 3.3.3.2.

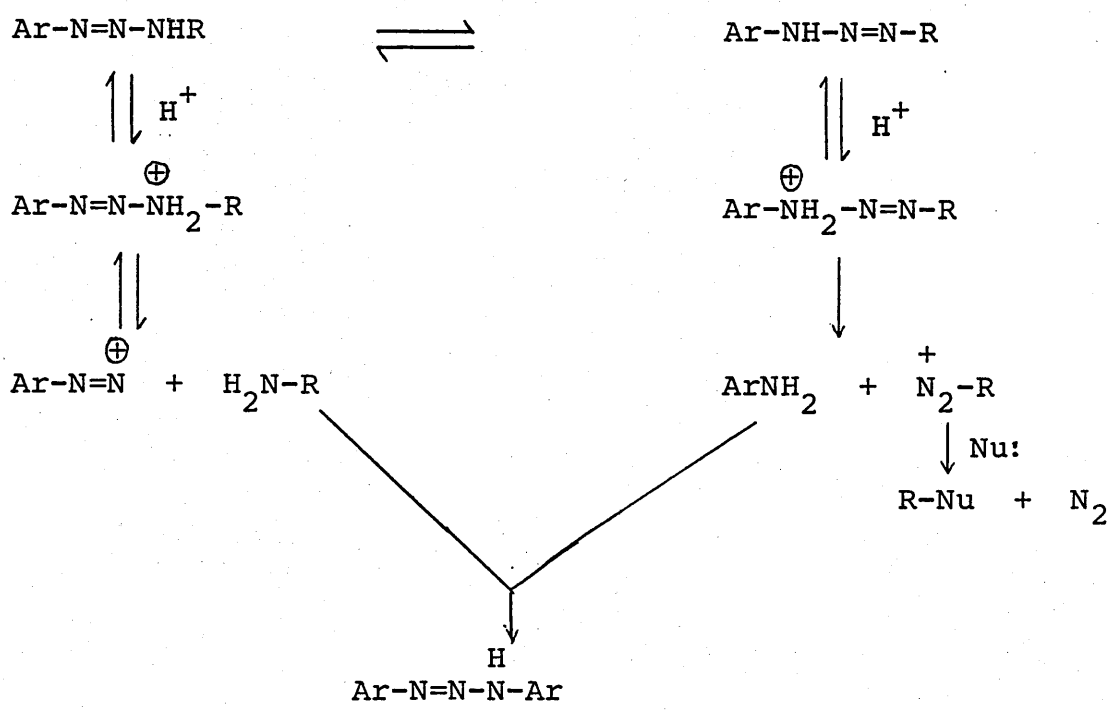

Scheme 3.3.3.1 Mechanism for the formation of diaryltriazene from the protolysis of monoalkyltriazenes

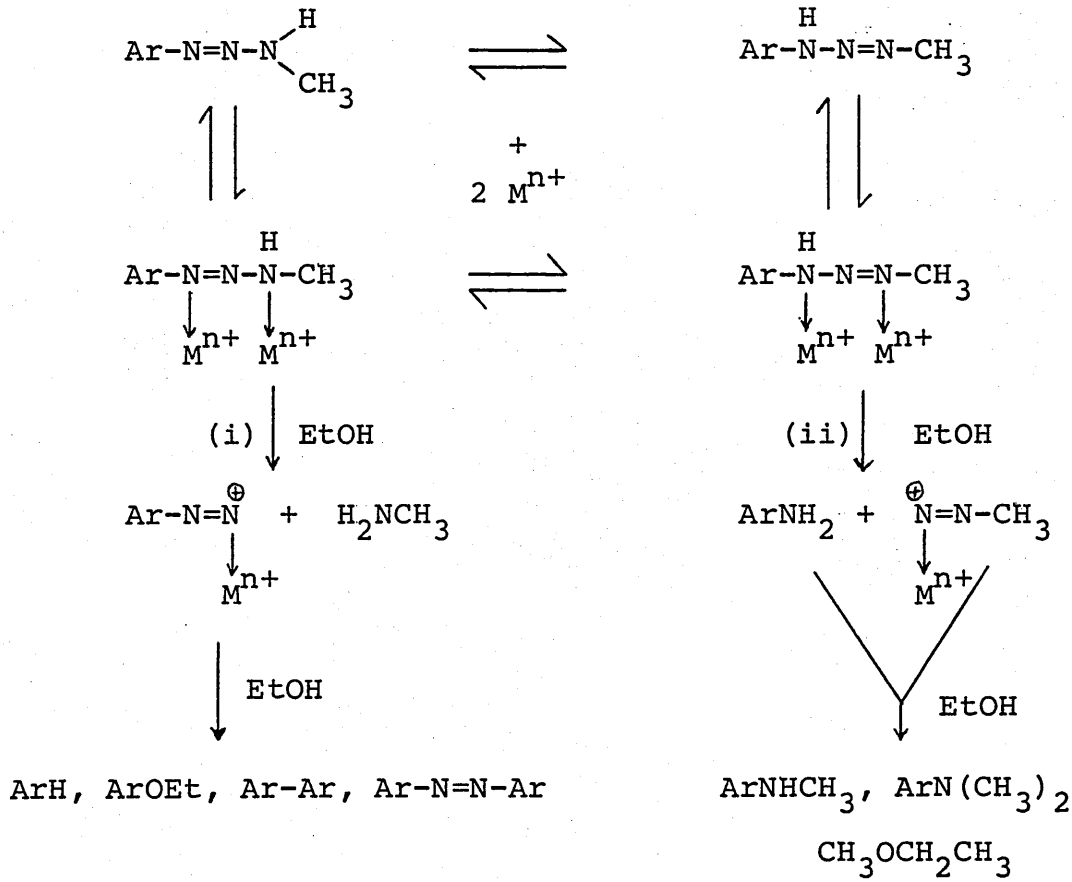

Scheme 3.3.3.2 Mechanism for the metal ion catalysed decomposition of MMTs in ethanol

3.4 Reaction in Dimethylsulphoxide (DMSO)

Having studied the metal ion catalysed decomposition of HMT in water and in ethanol, it was of interest to study the reaction in an aprotic solvent. This change of solvent was anticipated to have substantial effect on a reaction that involves proton transfer in its reaction mechanism.

The high dielectric constant of DMSO means that most metal perchlorates are soluble in it. Thus DMSO was chosen as the aprotic solvent for the metal ion catalysed HMT decomposition.

3.4.1 Mechanism of Reaction

3.4.1.1 Identification of substrate and product

The decomposition of HMT by Zn^{2+} in DMSO was found to follow pseudo-first-order kinetics (see experimental). Furthermore, a difference of $\sim$25 fold in rate between 4-NO_2HMT and 4-NO_2MMT (Table 3.4.1.1) confirms that the observed reaction rate, like that in EtOH, is of the transformation of HMT to MMT.

The products of this reaction are the arylamine, and its N-methyl- and N,N-dimethyl derivatives.

Table 3.4.1.1 Pseudo first order rate constant (k_{obs}) for the decomposition of 4-NO_2HMT and 4-NO_2 MMT by 0.0203M $Zn(ClO_4)_2$ in DMSO I=0.15M T=37 °C

compound	$10^5 x k_{obs}/S^{-1}$
4-NO_2HMT	3.72
4-NO_2MMT	96.2

3.4.1.2 Dependence on Metal Ion Concentration

With the exception of 3-pyridylHMT, the rate of HMT decomposition was shown to depend linearly on the concentration of Zn^{2+} (Fig. 3.4.1.1). Thus

$$\text{Rate} = k_{Zn2+}[HMT][Zn^{2+}] + k_o[HMT]$$

The uncatalysed reaction (k_o) is confirmed by the presence of an intercept in the plot.

The results of 3-pyridylHMT decomposition showed no dependence on $[Zn^{2+}]$ (Table 3.4.1.2). In fact, the rate decreased slightly as the metal ion concentration increased. It is not understood why such phenomenon was observed.

3.4.1.3 Ionic Strength Effect

The rate of decomposition of 4-CH_3COHMT by Zn^{2+} was shown to increase with ionic strength (Fig. 3.4.1.2). This suggests that the transition state is more solvated as the solvent becomes more polar.

Fig. 3.4.1.1 Decomposition of 4-H_2NCOHMT in DMSO by Zn^{2+} I=0.15M T=37°C

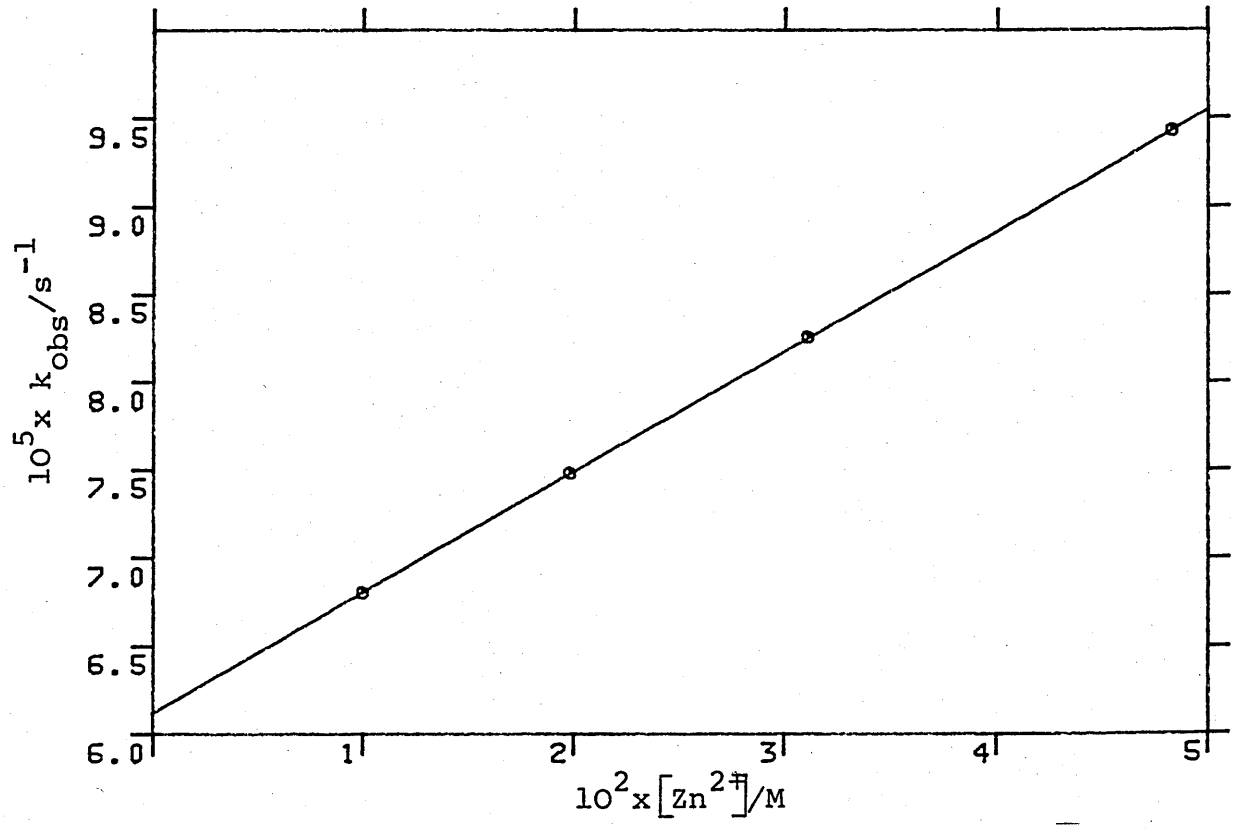

Fig. 3.4.1.2 Ionic strength effect on the decomposition of 4-CH_3COHMT in DMSO by 0.031M Zn^{2+} T=37°C

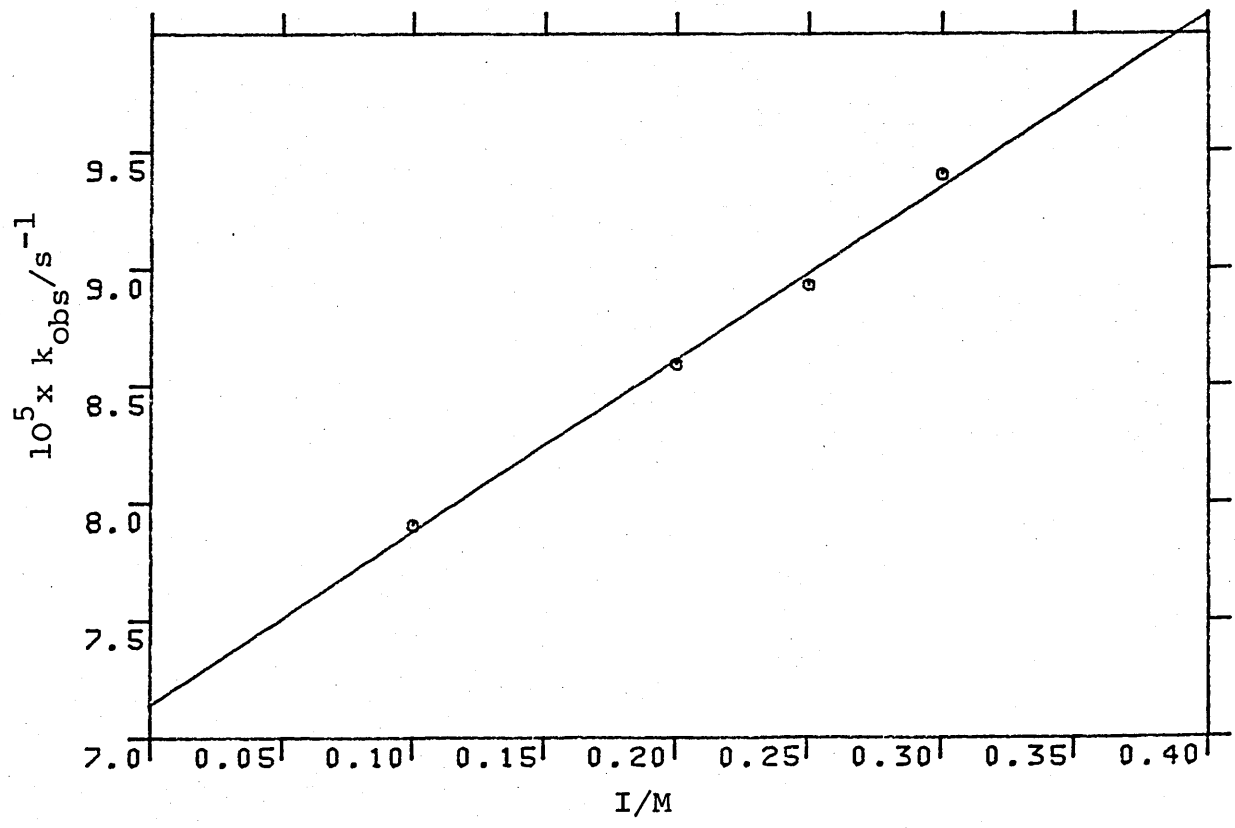

Table 3.4.1.2 Effect of $[Zn^{2+}]$ on the rate of decomposition of 3-pyridylHMT in DMSO I=0.15M T=37 °C

$[Zn^{2+}]$/M	$10^5 x k_{obs}/S^{-1}$
0.01	1.453
0.0188	1.378
0.0324	1.318
0.043	1.318

3.4.1.4 Effect of Substituent

A negative ρ-value of 0.8036 was obtained from the Hammett plot (Fig. 3.4.1.3) which is much smaller than the corresponding value of 2.66 in EtOH. Nevertheless, this value is in accord with an electrophilic attack on HMT by Zn^{2+}.

The rate of 4-ClHMT decomposition was found to deviate from the other results and thus was not included in the construction of the plot. This deviation suggests that there is a change of rate limiting step in the 4-ClHMT decomposition.

3.4.1.5 Deuterium Kinetic Isotope Effect

The rate of decomposition of HMT that contains an O-D instead of O-H group was found to be only slightly faster than the corresponding OH compound (Table 3.4.1.3). This small increase in rate implies that the breaking of the O-H bond is not involved in the rate limiting step.

Fig. 3.4.1.3 Hammett plot for the decomposition of HMTs in DMSO by $Zn(ClO_4)_2$ I=0.15M T=37°C

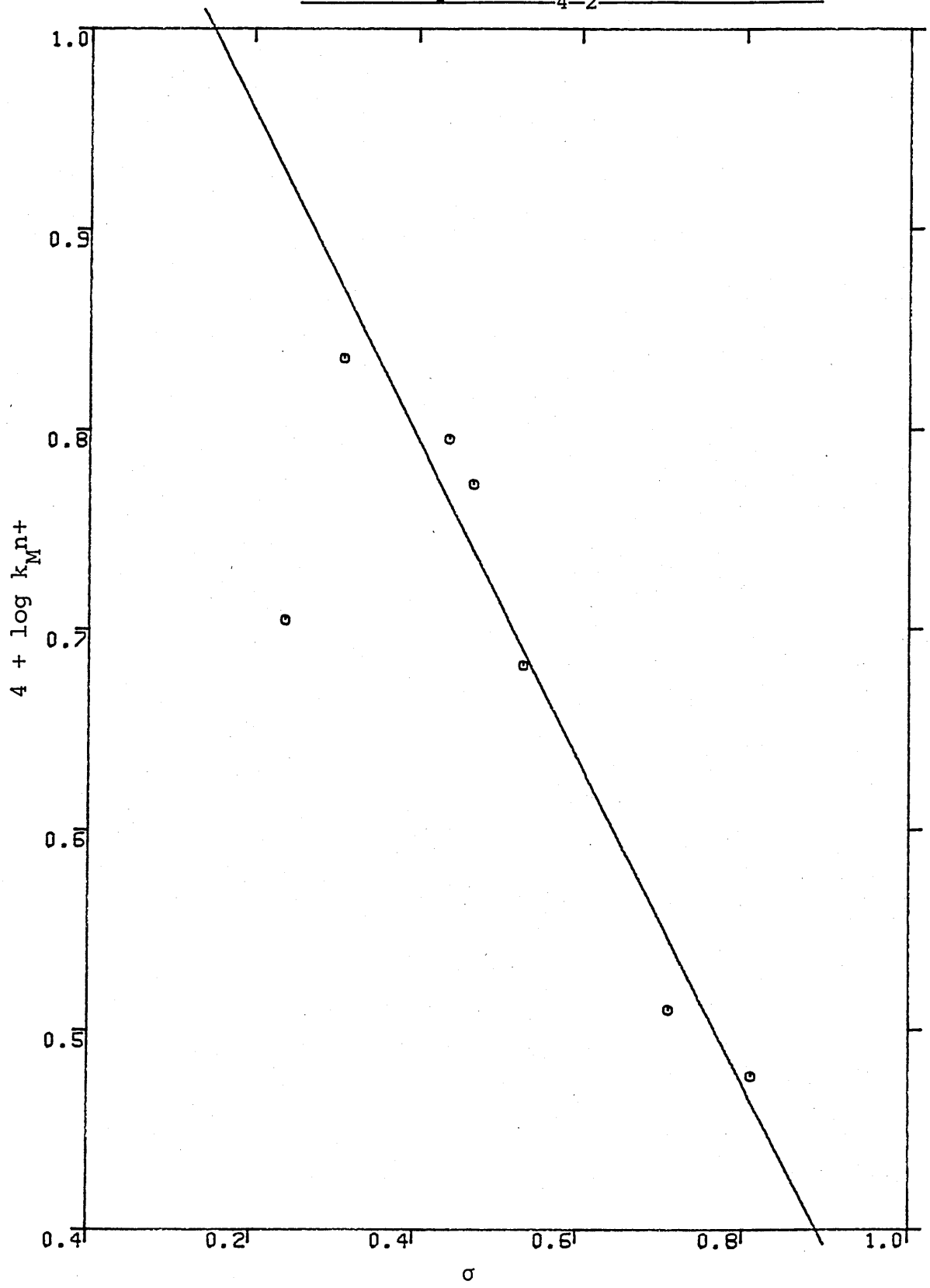

Table 3.4.1.3 Deuterium kinetic isotope effect on the rate of decomposition of HMT in DMSO by Zn^{2+} I=0.15M T=37°C

Compound	k_{OD}/k_{OH}
4-CH_3COHMT	1.0257 ± 0.028
4-CNHMT	1.0263 ± 0.0262

3.4.1.6 Discussion

It was shown earlier that the decomposition of HMT by M^{n+} in EtOH requires the formation of an HMT: metal ion complex (Scheme 3.4.1.1). Furthermore, the metal ion

$$HMT + M^{n+} \underset{1}{\overset{1}{\rightleftharpoons}} (HMT:M)^{n+} \xrightarrow{2} \text{products}$$

Scheme 3.4.1.1 Mechanism for the metal ion catalysed decomposition of HMT

rate constants for the 3-pyridylHMT was shown to be equal to k_1 whilst those for the homoarylHMTs was found to consist of more than one elementary rate constant. With the modest number of results obtained, there is a strong indication from the Hammett plot that in this reaction, both situations are observed with the homoaryl HMTs.

The deviation of the 4-ClHMT result from the plot can only be explained by a change in rate limiting step from k_1 to k_2 i.e. from the case where $k_2 >> k_{-1}$ to the case where $k_2 << k_{-1}$. Thus the second order rate constant (k_{Mn+}) from the 4-ClHMT reaction can be written as:

$$k_{Mn+} = \frac{k_1 k_2}{k_{-1}}$$

whilst for the other HMTs

$$k_{Mn+} = k_1$$

As a result, for 4-ClHMT,

$$\log k_{Mn+} = \log k_1 + \log k_2 - \log k_{-1}$$

Since $k_{-1} >> k_2$ $\quad \log k_{-1} > \log k_2$

$$\Rightarrow \quad \log k_{Mn+} < \log k_1$$

which explains the negative deviation of the 4-ClHMT result.

This breakdown of the linear free energy relationship has also been observed in the acid catalysed hydrolysis of salicylideneanilines which involves a similar mechanism (Scheme 3.4.1.2).[88] Again, there is a switch in rate

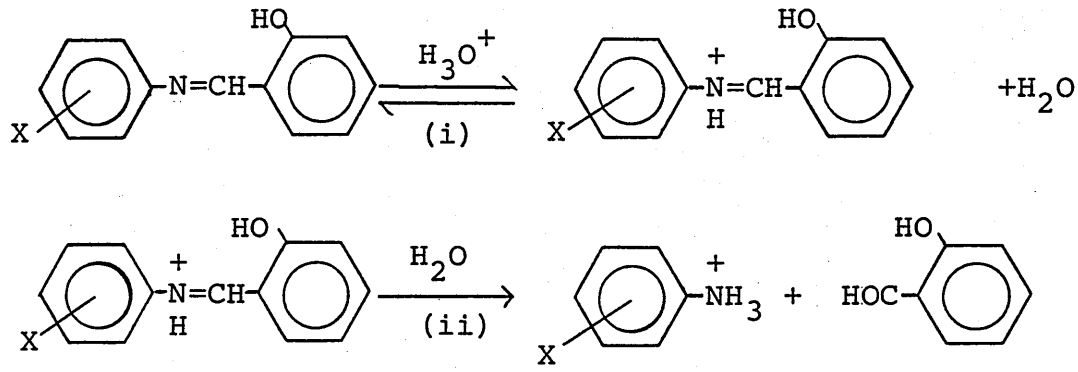

Scheme 3.4.1.2 Mechanism for the acid catalysed hydrolysis of salicylideneanilines

determining step from (i) to (ii) as the substituent becomes less electron withdrawing (Fig. 3.4.1.4).

Fig. 3.4.1.4 Hammett plot for the hydrolysis of salicylideneanilines at pH5.6 [a]

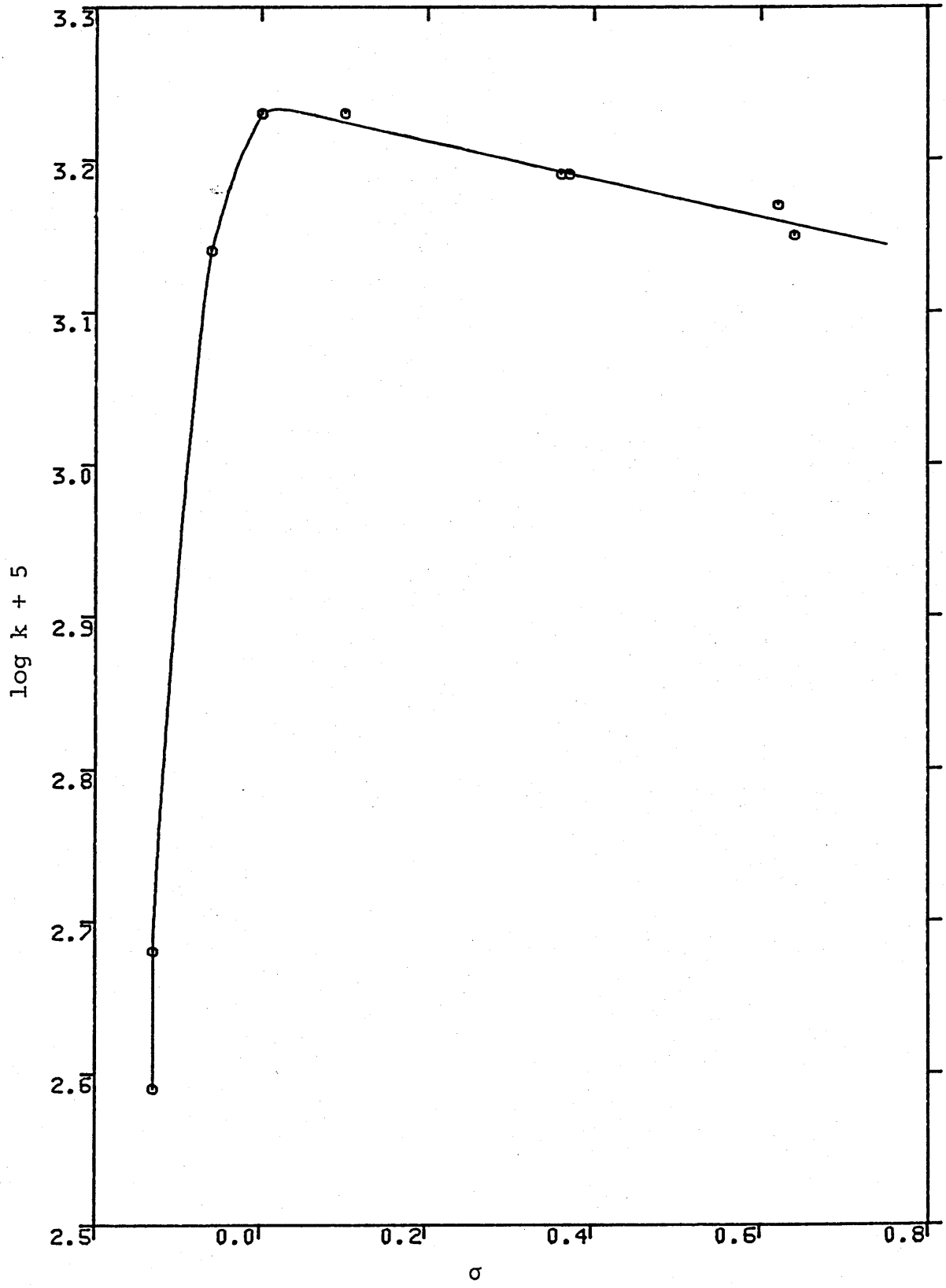

a from reference 88.

In addition, the positive effect of ionic strength upon the rate of reaction is consistent with the earlier observation of the 3-pyridylHMT reaction in EtOH whereby the formation of the complex is also rate limiting.

Having shown that the rate limiting step in this reaction (except that for 4-Cl-) is the formation of the complex, it is not known why such phenomenon occurs since the solvent exchange rate at a divalent metal ion is faster in DMSO than in MeOH.[89] Indeed, the effect of solvent on the rate of metal-ligand formation is currently under discussion.

3.4.2 MMT Decomposition

3.4.2.1 Order and Products of Reaction

The decomposition of MMTs by Zn^{2+} in DMSO was shown to follow pseudo first order kinetics (see Experimental). The products of this reaction were found to contain the arylamine and its N-methyl and N,N-dimethyl derivatives.

3.4.2.2 Dependence on Metal Ion Concentration

Unlike in EtOH, the rate of decomposition of MMTs in DMSO was shown to depend linearly on the concentration of Zn^{2+} (Fig. 3.4.2.1). This was confirmed by plotting $\log k_{obs}$ vs. $\log [Zn^{2+}]$ which gave a slope of ~ 1 (Fig. 3.4.2.2). Furthermore, the small negligible negative intercept in Fig. 3.4.2.1

Fig. 3.4.2.1 Decomposition of 4-CH_3COOMMT in DMSO by Zn^{2+} I=0.15M T=37°C

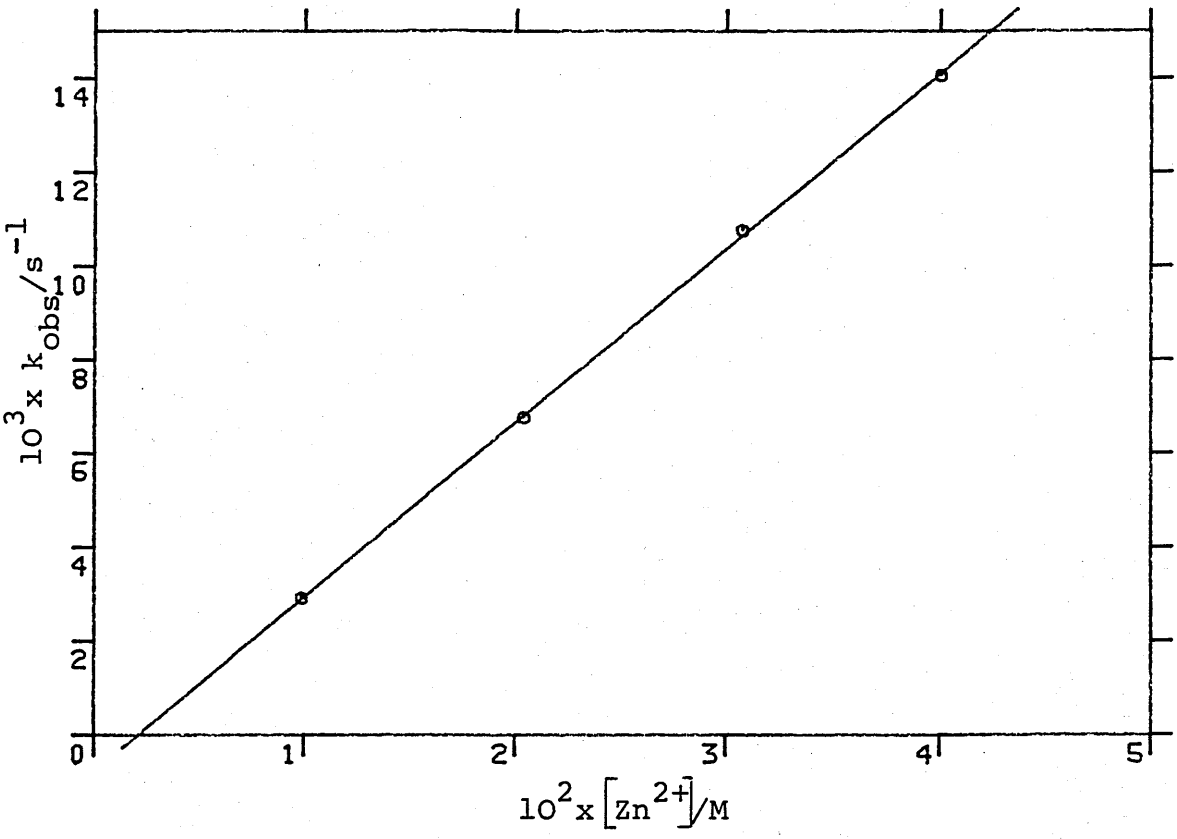

Fig. 3.4.2.2 Log:log plot for the decomposition of 4-CH_3COOHMT in DMSO by Zn^{2+} I=0.15M T=37°C

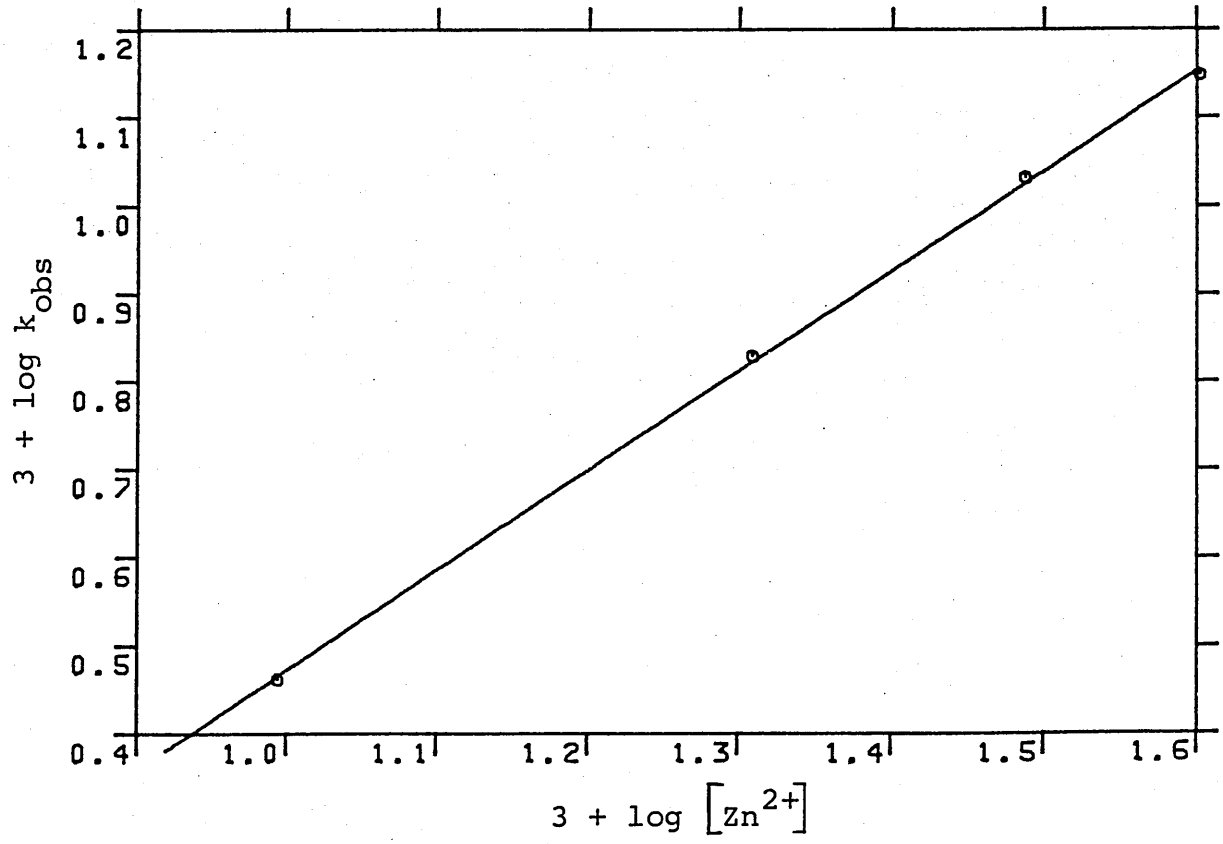

suggests that there is no uncatalysed reaction.

3.4.2.3 Effect of Ionic Strength

Ionic strength was found to have little effect on the decomposition of 4-CNMMT by Zn^{2+} (Fig. 3.4.2.3). Since the formation of metal:HMT complex shows a positive ionic strength effect (Sections 3.3.1.4 for 3-pyridylHMT reaction in EtOH and 3.4.1.3 for HMT reaction in DMSO), this result is inferred as an indication that the formation of MMT:Zn^{2+} complex is not rate limiting. Accordingly, the degradation of the complex is the slow step.

3.4.2.4 Effect of Substituent

The substituents were shown to give a negative Hammett ρ value of 2.56 for the decomposition of MMTs by $Zn(ClO_4)_2$ in DMSO (Fig. 3.4.2.4). This value is substantially greater than that for the HMT reaction in DMSO. In this instance, the 3-pyridylMMT rate deviated positively from the plot and was not included in the calculation of the slope.

3.4.2.5 Discussion

MMTs have been shown to be more nucleophilic than HMTs towards Lewis acids in EtOH. In DMSO, the rate determining step for the decomposition of 4-ClHMT is the decomposition of the Zn:HMT complex. Taken together, it is very likely that for the decomposition of MMT with Zn^{2+} in DMSO, the formation

Fig. 3.4.2.3 Ionic strength effect on the decomposition of 4-CNMMT in DMSO by Zn^{2+} T=37°C

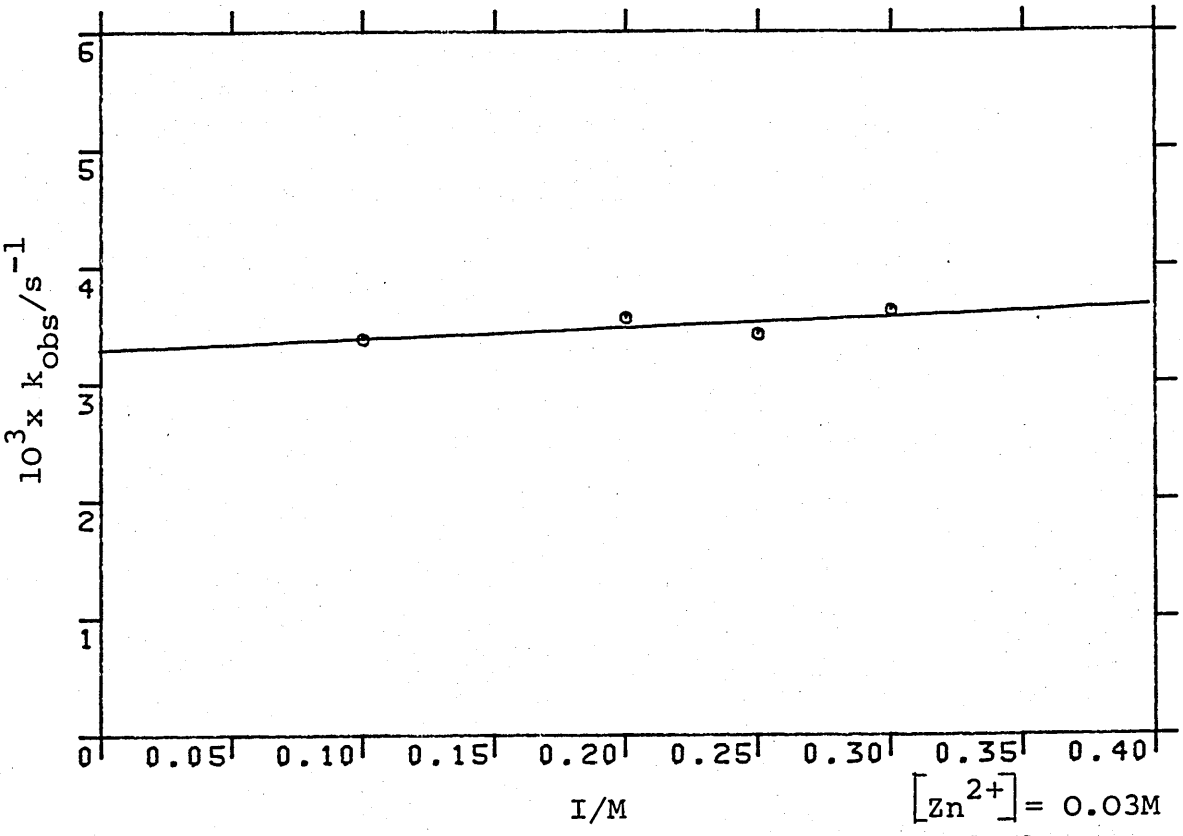

Fig. 3.4.2.4 Hammett plot for the decomposition of MMTs in DMSO by $Zn(ClO_4)_2$ I=0.15M T=37°C

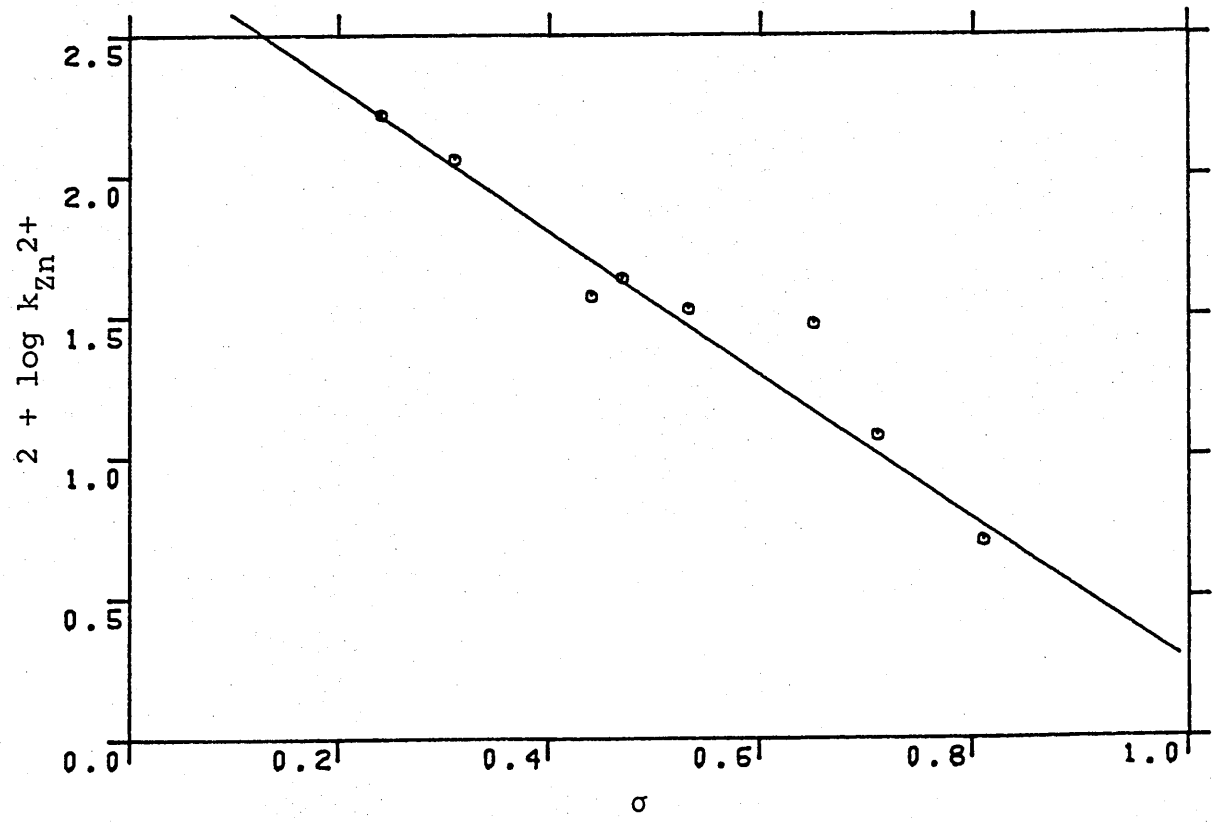

of the Zn:MMT complex is faster than its decomposition. Further support comes from the negligible ionic strength effect on the rate of reaction.

Finally, the absence of arene in the reaction products suggests that the formation of aryldiazonium ion in DMSO is inhibited.

CHAPTER 4

USE OF LANTHANIDE SHIFT REAGENTS IN THE STUDY OF METAL ION CHELATING ABILITY OF 1-ARYL-3-HYDROXYMETHYL-3-METHYLTRIAZENES

4.1 Introduction

The practical application of lanthanide shift reagents (LSRs) for inducing shifts in nmr spectra was first demonstrated by Hinckley some 15 years ago.[90] Since then, LSRs have been successfully applied in areas ranging from structural elucidation to the study of isotope effects. A successful attempt using LSRs in the elucidation of a reaction mechanism was reported for the decarboxylation of oxaloacetic acid.

The decomposition of oxaloacetic acid to pyruvic acid and carbon dioxide is catalysed by transition metal and lanthanide ions (Equation 4.1). Though (42) was believed to

$$HOOCCH_2\text{-}\overset{O}{\overset{\|}{C}}\text{-}COOH \xrightarrow{M^{n+}} CH_3\overset{O}{\overset{\|}{C}}\text{-}COOH + CO_2 \qquad (4.1)$$

be the intermediate in this reaction, (43) and (44) can also be formed. This problem was resolved by Tsai *et al.*[91] who

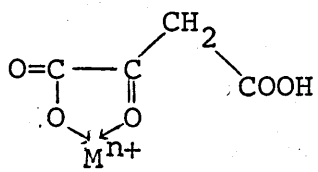

(42)

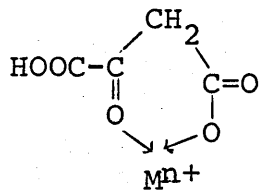

(43)

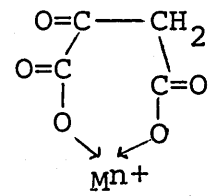

(44)

synthesised (45) and (46). By comparing the induced shift pattern of these two compounds with that of oxaloacetic acid, the authors proved conclusively the presence of (42) in the decarboxylation reaction.

$$HOOC\text{-}CH_2\text{-}\overset{O}{\overset{\|}{C}}\text{-}COOC_2H_5 \qquad (45)$$

$$C_2H_5OOC\text{-}CH_2\text{-}\overset{O}{\overset{\|}{C}}\text{-}COOH \qquad (46)$$

The decomposition of HMTs by M^{n+} in EtOH is believed to involve a cyclic M^{n+} : HMT chelate (Chapter 3). However, the structure of this complex was not resolved. One possibility involves the coordination of both the hydroxyl oxygen atom and N-1 of the HMT with the metal ion (47) whilst another involves the oxygen atom only (48). It was anticipated that the use of lanthanide shift reagents could provide confirmatory evidence for either (47) or (48).

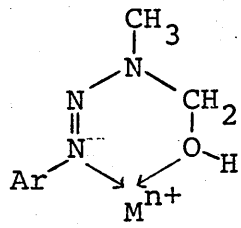

(47)

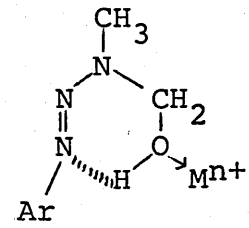

(48)

4.2 Tris(2,2,6,6-tetramethyl-3,5-heptanedionato)-praseodymium(III) ($Pr(thd)_3$)

4.2.1 HMTs

The induced shifts of the protons in HMTs by the presence of ca. 0.2 mole equivalent of $Pr(thd)_3$ in $CDCl_3$ are shown in Table 4.2.1.

In general, the protons exhibiting the biggest shift are those of the hydroxymethyl group, followed by the N-methyl protons. The least shifted are the aromatic protons and those of the substituent. In addition, the difference between the induced shifts of the corresponding protons in the various

Table 4.2.1 The induced shifts ($\Delta\delta$/ppm)[a] of various protons in HMTs by $Pr(thd)_3$ in $CDCl_3$

[HMT] = 0.06 M - 0.2 M

Ar	mole ratio of $Pr(thd)_3$ used	$N-CH_2-O$	$N-CH_3$	Aromatic		Others
				Ar-N=N-N	Ar-X	
$4-ClC_6H_4$	0.2	-2.8	-1.55	-0.4	-0.27	
$4-COOCH_3C_6H_4$	0.2	-2.55	-1.05	-0.4	-0.4	-0.36 ($4-COOCH_3$)
$4-COCH_3C_6H_4$	0.2	-2.5	-1.05	-0.5	-0.47	-0.45 ($4-COCH_3$)
$4CF_3C_6H_4$	0.25	-2.0	-1.2	-0.4	-0.03	
$2CF_3C_6H_4$	0.1313	-1.16	-0.6	-0.15	-0.05	
$4-CNC_6H_4$	0.2	-2.00	-1.00	-0.35	-0.1	
$4-NO_2C_6H_4$	0.2	-2.07	-1.15	-0.47	-0.07	
$3-C_5H_4N$	0.2	-1.97	-1.27	-3 —	-1.3	

a $\Delta\delta = (\delta_{obs} - \delta_{unbound})$, therefore -ve sign for $\Delta\delta$

HMTs is not large. This implies that the substituents have little influence on the mode of binding.

This trend, however, does not apply to the 3-pyridyl HMT, where the largest shifts were observed for the aromatic protons. In all probability, binding of this compound occurs *via* the pyridyl nitrogen atom.

4.2.2 HMT Related Compounds

The structurally related compounds of HMT that were used in this study included the alkyl homologues of 4-$COCH_3$HMT (49), dimethyl- and monomethyl- derivatives of 4-$COCH_3$HMT (50), HMT ether and acetates (51) and 4-$COCH_3$ aniline. These compounds were chosen to gauge the effect of their structural features on the LSR induced chemical shifts.

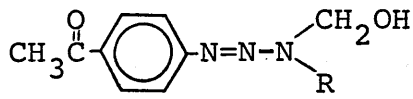

(49)

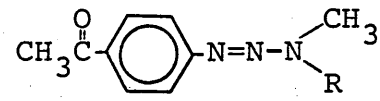

(50)

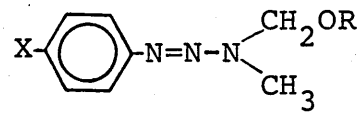

(51)

The induced shifts of the protons in these HMT related compounds brought about by $Pr(thd)_3$ are shown for comparison in Table 4.2.2.

It is apparent that for the alkyl homologues of HMT, i.e. N-ethyl and N-propyl HMT, a similar trend of decrease in the size of the induced shift is observed (entries 1 and 2) i.e.

4.2.2 The induced shifts ($^{\Delta\delta}$/ppm)[a] of various protons in HMT related compounds by $Pr(thd)_3$ in $CDCl_3$

[Substrate] = 0.094M - 0.263M

NO	Compound	mole ratio of $Pr(thd)_3$ used	$N-CH_2-O$	N-R	Aromatic		Others
					Ar-N=N	Ar-X	
1	49, R=CH_2CH_3	0.2	-1.23	-0.5 $N-CH_2-C$ -0.12 $N-C-CH_3$	-0.2	-0.1	-0.1 (4-$COOCH_3$)
2	49, R=$CH_2CH_2CH_3$	0.1974	-2.1	-1.5 $N-CH_2C-C$ -0.73 $N-C-CH_2-C$ -0.12 $N-C-C-CH_3$	-0.4	-0.38	-0.36 (4-$COCH_3$)
3	Ar=4-$COOCH_3$-C_6H_4 51, R=CH_3	0.198	-1.34	-0.8	-0.72	-0.97	-1.1 (4-$COOCH_3$) -1.34 (CH_3-O-)
4	51, Ar=4-$COOCH_3$-C_6H_4 R=CH_3CO	0.2	-0.8	-0.4	-0.45	-0.75	-0.95 (4-$COOCH_3$) -0.73 (CH_3COO-)
5	51, Ar=4-$COCH_3$-C_6H_4 R=CH_3CO	0.27	-1.3	-0.55	-0.97	-0.9	-1.62 (4-$COCH_3$) -1.18 (CH_3COO-)
6	51, Ar=4-$NO_2C_6H_4$ R=CH_3CO	0.144	-0.85	-0.3	-0.06	-0.02	-0.8 (CH_3COO-)
7	50, R=H	0.154		-0.02	-0.18	-0.13	-0.52 (4-$COCH_3$)
8	50, R=CH_3	0.167		0	0	-0.1	-0.34 (4-$COCH_3$)
9	4-amino-acetophenone	0.2			0.37	-0.5	-0.92 (4-$COCH_3$) -1.25 (NH_2)

a) The same sign convention as in Table 4.2.1 was used.

N-hydroxymethyl protons > N-alkyl protons > aromatic and substituent protons

This trend begins to break down for compound (51). (Ar=4-$COOCH_3C_6H_4$, R=CH_3) (entry 3) where the induced shift of the N-CH_2-O protons is smaller than the corresponding one in the 4-$COOCH_3$HMT whilst the 4-$COOCH_3$ protons exhibit a larger induced shift than in the HMT itself. However, the N-$\underline{CH_2}$-O and CH_2-O-$\underline{CH_3}$ protons still display the largest induced shifts, indicating that they are, in all probability, both close to the binding site.

Such a situation is completely reversed in the acetate derivatives (51, R=CH_3CO) (entries 4-6). In these compounds, the substituent protons are the most shifted and the induced shifts are marginally bigger than either the N-CH_2-O protons or the -O-$\overset{O}{\overset{\|}{C}}$-$CH_3$ protons. Similarly, in either 4-$COCH_3$MMT (entry 7) or the DMT homologue (entry 8), the substituent protons are also the most shifted ones. It would appear that $Pr(thd)_3$ preferentially binds oxygen and that the binding ability is reduced when either the steric bulk around the O atom is increased or its nucleophilicity decreased.

4.3 Tris(1,1,1,2,2,3,3-heptafluoro-7,7-dimethyl-4,6-octanedionato)europium(III) ($Eu(fod)_3$)

The induced shifts of HMTs by LSRs was also quantitatively investigated by using $Eu(fod)_3$. One of the main advantages of using $Eu(fod)_3$ over $Pr(thd)_3$ is that Eu^{3+} brings about a downfield shift whilst Pr^{3+} induces an upfield shift. As a result, the interference of the substrate's signals by that of the chelate in the LSR, which ranges from δ 3 to 2 ppm, is lost

by using $Eu(fod)_3$.

Qualitatively, those peaks that exhibit the largest upfield shift with Pr^{3+} should, if they are close to the binding site, also exhibit the largest downfield shift with Eu^{3+}. Quantitatively, the aim of this study was to determine both the chemical shifts of HMTs in the bound state and the binding equilibrium constant. One possible method of determining these two quantities was developed by Armitage and Hall and coworkers.[92] However, part of their derivation was in error, so a full derivation is outlined below.

For a 1 : 1 complex, the binding equilibrium constant (K_B), can be expressed as :

$$K_B = \frac{[LS]}{[L]\ [S]} \qquad \text{——} \qquad 4.3.1$$

where $[LS]$ is the concentration for the substrate in the bound state, and $[L]$ and $[S]$ are the free lanthanide and free substrate concentrations respectively.

Assuming that the exchange rate between the free and bound substrate is fast in the nmr time scale, so that a single resonance will be observed, the observed chemical shift (δ_{obs}) will depend on the concentration of the bound substrate.

Thus $\delta_{obs} = f_{ls}\ \delta_{ls} + f_s\ \delta_s$

where δ_s and δ_{ls} are the chemical shifts for the free and bound substrate respectively, and f_{ls} and f_s are the respective concentration fractions of the two species.

Since $f_s = 1 - f_{ls}$

$$\Rightarrow \quad \delta_{obs} = f_{ls}\ \delta_{ls} + (1-f_{ls})\ \delta_s$$

$$= \delta_s + f_{ls} (\delta_{ls} - \delta_s)$$

$$\Rightarrow \quad (\delta_{obs} - \delta_s) = f_{ls} (\delta_{ls} - \delta_s)$$

This can be rewritten as :

$$\Delta_\delta = f_{ls} \Delta_B$$

where Δ_δ is the induced shift and Δ_B is the chemical shift for the bound substrate relative to that for the free substrate.

Because $f_{ls} = \frac{[LS]}{[S]_o}$ where $[S]_o$ = total substrate concentration

then $\Delta_\delta = \frac{[LS]}{[S]_o} \Delta_B$

$$\Rightarrow \quad [LS] = \frac{\Delta_\delta}{\Delta_B} [S]_o \quad \text{——} \quad 4.3.2$$

Now from Equation 4.3.1

$$K_B = \frac{[LS]}{([L]_o - [LS])([S]_o - [LS])}$$

where $[L]_o$ = total lanthanide concentration

on expanding this will give

$$[LS] = K_B([L]_o[S]_o - ([L]_o + [S]_o)[LS] + [LS]^2) \quad \text{——} \quad 4.3.3$$

By assuming that the term in $[LS]^2$ is neglibible

$$\Rightarrow \quad [LS] = K_B[L]_o[S]_o - K_B[L]_o[LS] - K_B[S]_o[LS]$$

Substituting equation 4.3.2 into this equation gives

$$\left(\frac{\Delta_\delta}{\Delta_B}\right)[S]_o = K_B[L]_o[S]_o - K_B[L]_o \frac{\Delta_\delta}{\Delta_B} [S]_o - K_B[S]_o^2 \left(\frac{\Delta_\delta}{\Delta_B}\right)$$

This can be rearranged into

$$\Delta\delta = \frac{K_B[L]_o \Delta_B}{1 + K_B[L]_o + K_B[S]_o} \qquad \text{——— } 4.3.4$$

On further assuming that $\frac{1}{K_B} \geqslant [S]_o$ and $\Delta\delta << \Delta_B$ equation (4.3.3) can be rewritten as

$$[S]_o = \frac{[L]_o \Delta_B}{\Delta\delta} - \frac{1}{K_B} + [L]_o \qquad \text{——— } 4.3.5$$

Provided that all the assumptions made are true, a plot of $[S]_o$ vs $^1/\Delta\delta$ should give a straight line whose slope is $([L]_o \Delta_B)$ and whose y-intercept is $-(\frac{1}{K_B} + [L]_o)$. Therefore by performing the experiment with a constant $[L]_o$, both Δ_B and K_B can be readily obtained.

Although experiments in this study were carried out in the same manner as suggested above, i.e. $[S]_o$ is varied at a constant $[L]_o$, assumptions of $[LS]^2$, $(\frac{1}{K_B}) \geqslant [S]_o$ and $\Delta\delta << \Delta_B$ were not made in the calculation of Δ_B and K_B. Instead, the full quadratic equation of 4.3.3 was solved in the following manner :

$$[LS] = K_B([L]_o[S]_o - ([L]_o + [S]_o)[LS] + [LS]^2)$$

$$0 = [LS]^2 K_B - (K_B([L]_o + [S]_o) + 1)[LS] + K_B[L]_o[S]_o$$

$$[LS] = \frac{(K_B[L]_o + K_B[S]_o + 1) + \sqrt{(K_B[L]_o + K_B[S]_o + 1)^2 - 4K_B^2[L]_o[S]_o}}{2K_B}$$

Since $\Delta\delta = \frac{[LS]}{[S]_o} \Delta_B$

$$\Rightarrow \quad \Delta_\delta = \Delta_B x \frac{(K_B[L]_o + K_B[S]_o + 1) + \sqrt{(K_B[L]_o + K_B[S]_o + 1)^2 - 4K_B^2[L]_o[S]_o}}{2K_B[S]_o}$$

——— 4.3.6

The error made by the proponants of this method was in the derivation of equation 4.3.6. As the experiment was performed with a constant $[L]_o$, the proponants conveniently changed the equation

$$\Delta\delta = \frac{[LS]}{[S]_o}\Delta_B \quad \text{to} \quad \Delta\delta = \frac{[LS]}{[L]_o}\Delta_B$$

which cannot be justified.

Nevertheless, K_B and Δ_B can be obtained from equation 4.3.6 in the following way. By arbitrarily assigning a value for K_B in the expression, $\Delta\delta$ can be plotted against the roots of one quadratic equation. Using a least squares computer programme, the slope, its correlation coefficient and the standard deviation can all be calculated. This procedure was iterated until the K_B value gave the highest correlation coefficient. In cases where more than one K_B value gave the highest correlation, that value which had the lowest standard deviation was adopted.

The results which were selected according to these criteria, are shown in Tables 4.3.1 and 4.3.2. It was noticed that K_B varies with the functional groups within a HMT. This may be due to the error in measuring the induced shifts or there may be different binding sites within an HMT which compete with each other. Since the protons of the hydroxymethyl group have the biggest Δ_B, except those of the 3-pyridyl HMT, the error in measuring their induced shifts should be the smallest. Thus K_B for the N-CH_2-O protons should be more reliable than the others. Based on this argument, the Δ_B for all the other protons was recalculated using the K_B values derived from the induced shifts of the hydroxymethyl protons.

Table 4.3.1 Bound shifts ($^{\Delta}B$/Hz) [a] [b] for various protons in HMTs by $Eu(fod)_3$ in $CDCl_3$

Ar	$N-CH_2-O$	$N-CH_3$	Ar-N=N	Ar-X	Others
$4-ClC_6H_4$	1585 (1585)	562 (550)	240 (230)	128 (114)	
$4-COOCH_3C_6H_4$	868 (868)	331 (292)	163 (144)	285 (295)	327 (315)
$4-COCH_3C_6H_4$	1598 (1598)	683 (608)	648 (455)	668 (731)	479 (822)
$4-CF_4C_6H_4$	2512 (2512)	913 (931)	250 (250)	250 (250)	
$4-CNC_6H_4$	1419 (1419)	630 (672)	225 (251)	402 (102)	
$4-NO_2C_6H_4$	2030 (2030)	754 (708)	807 (269)	323 (83)	

a Values within parentheses are amended Δ_B using K_B of the $N-CH_2-O$ protons

b These data were calculated using Equation 4.3.6 from the experimental chemical shift values detailed in Chapter 6.

Table 4.3.2 Binding equilibrium constant (K_B/l mol^{-1}) [a] for various protons in HMTs by Eu(fod)$_3$ in $CDCl_3$

Ar	N-CH_2-O	N-CH_3	Ar-N=N	Ar-X	Others
4-ClC_6H_4	65	59	53	33	
4-$COOCH_3C_6H_4$	13	10	10	14	12
4-$COCH_3C_6H_4$	10	8	9	13	15
4-$CF_3C_6H_4$	20	21	20	20	
4-CNC_6H_4	22	26	45	8	
4-$NO_2C_6H_4$	17	15	3	19	

a These data were calculated using Equation 4.3.6 from the experimental chemical shift values detailed in Chapter 6

Comparing the two sets of results (Table 4.3.1), it is evident that Δ_B has altered slightly. In fact, in some HMTs, the amended results are within the experimental limit of their previous ones. Nevertheless, the relative Δ_B values within a HMT molecule remain the same. Indeed, the order of decrease of Δ_B within an HMT molecule, i.e.

N-hydroxymethyl > N-methyl > Aromatic or the substituent

is the same as that of the induced shift ($\Delta\delta$) observed in the case of $Pr(thd)_3$.

A further similarity between the two sets of LSR data is that the 3-pyridyl HMT consistently has larger induced shifts for the aromatic protons than it does for the hydroxymethyl ones. Moreover, amongst the aromatic protons, the most shifted are the two next to the heteroatom in the ring (Table 4.3.3).

Again, the different K_B values suggest that there may be more than one binding site in 3-pyridyl HMT which compete with each other. Alternatively, this may be due to the error in measuring the induced shifts of protons far away from the binding site.

Finally, there is no apparent linear free energy relationship between the K_B values for the hydroxymethyl protons and the Hammett σ values (Table 4.3.4).

Table 4.3.3 Bound shifts (Δ_B/Hz)[a] and K_B (/lmol^{-1}) for various protons in 3-pyridyl HMT by Eu(fod)$_3$ in $CDCl_3$

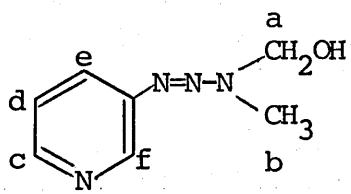

	a	b	c	d	e	f
K_B	86	77	125	1685	480	485
Δ_B	811 (699)	421 (357)	2113 (1924)	571 (585)	724 (723)	1996 (1996)

a $\Delta_B = (\delta_{bound} - \delta_{unbound})$ therefore +ve sign.

b Values within parenthese are amended Δ_B values using K_B = 485 l mol^{-1}

Table 4.3.4 Results of K_B for N-CH_2-O protons in HMTs against Hammett σ values

Compound	log K_B [a]	σ
4-Cl HMT	1.8129	0.24
4-$COOCH_3$HMT	1.1139	0.44
4-$COCH_3$HMT	1.0000	0.47
4-CF_3HMT	1.301	0.532
4-CNHMT	1.3424	0.71
4-NO_2HMT	1.2304	0.81

a K_B are of the N-CH_2-O protons

4.4 Discussion

Sections 4.2 and 4.3 have shown that, in the presence of $Pr(thd)_3$ and $Eu(fod)_3$, the resonance of the ^{1}Hnmr signals of HMTs shifted upfield and downfield respectively. It was also observed that the induced shift ($\Delta\delta$) and indeed the bound shift (Δ_B) varies with the types of protons in HMT. An order of decrease in these two parameters was also established.

Both contact and dipolar interactions are possible for inducing shifts in nmr spectra. Since Gadolinium is known to induce contact shift only, its effect on ^{1}H nmr spectrum of HMT was investigated. However, it was found that, in the presence of $Gd(fod)_3$ the signals were too broad for interpretation. Nevertheless, it has been argued that proton shifts are of dipolar interaction in origin.[92] If this argument is valid, the induced shift and the bound shift for

each group of protons can be explained in terms of their distance away from the paramagnetic metal ion and the angle (θ) between the vector joining the metal ion to the proton and the axis of the lanthanide donor atom bond.

As the hydroxymethyl protons have the highest $\Delta\delta$ and Δ_B it is very likely that the hydroxyl oxygen atom is the principal donor atom in HMT. On the other hand, in the case of 3-pyridyl HMT it was shown that the two aromatic protons next to the heteroatom in the ring have the largest induced and bound shifts. Thus suggesting the main donor atom in this HMT is the pyridyl nitrogen. Whilst these results appear to be in good accord with the proposed model for the metal ion catalysed decomposition of HMT (47 and 48) there is no evidence that the arene bound triazene nitrogen atom is coordinating with the lanthanide ions. This can be demonstrated by the smaller $\Delta\delta$ and Δ_B for the aromatic protons as compared to that of the N-methyl ones. Thus these results favour structure (48).

Interestingly, in the cases of 4-$COOCH_3$- and 4-$COCH_3$HMTs the induced shift for the substituent protons are larger than those of the aromatic ones. Furthermore, the two aromatic protons nearer to the substituent are shifted more than the other two. In contrast, the opposite trend was observed with the aromatic protons in other HMTs. Taken together, these results suggest that in 4-$COOCH_3$HMT and 4-$COCH_3$HMT, there is some interaction between the substituent, presumably through the $\rangle C{=}O$ group, and the lanthanide ion. As a result, either the distance between the metal ion and the functional group gets shorter or the angle (θ) between them becomes more favourable.

It has to be emphasised that in the lanthanide reactions, one is dealing with the ground state of HMTs, whereas in the transition metal ion reactions, the transition state is involved. A further difference between the two reactions is the nature of the two types of metal ions. It was pointed out in a review by Cockerill and coworkers that the 3d electrons in the transition metal ions are more exposed than the 4f electrons in the lanthanide.[93] Consequently, transition metal ions are more ready to react covalently with ligands than the lanthanide ions, resulting in an extensive contact interaction. This difference in the mechanism of interaction between the two types of metal ion is believed to have a strong influence on the chelating behaviour of HMTs towards them.

The concept of hard and soft acids and bases (HSAB) has been applied to the interaction of ligands with LSR.[94] Under the classification of HSAB, europium and lanthanide ions are hard acids. Accordingly, they should react more strongly with hard bases than with soft bases. Indeed, the donor power of monofunctional compounds has been revealed from their induced shifts to decrease in the following order:[93]

NH_2 > OH > ketones > esters > ethers > thioethers > nitriles

Since ketones or esters occupy only one position lower than that for the -OH group, it is not surprising to find that there is some interaction between the substituent in 4-$COOCH_3$HMT and 4-$COCH_3$HMT and the two LSRs used in this study. The results of 4-$COCH_3$ aniline with $Pr(thd)_3$ is also in good accord with the order of donor power. In contrast, the induced shift for the N-CH_3 protons in 4-$COCH_3$MMT is smaller than that for the

substituent protons. This suggests that coordination through the $\backslash C{=}O$ group is stronger. One possible explanation is that the extensive delocalisation of the nitrogen lone pairs over the triazene system lowers the binding ability of the N atoms. This is well illustrated by 4-$COCH_3$DMT in which the 4-$COCH_3$ protons, and not the N-CH_3 protons were shifted by $Pr(thd)_3$.

Finally, substitution at the hydroxyl oxygen atom of HMTs decreases its donating power as is evident from the induced shifts of the N-CH_2-O protons in the HMT ether and acetates. A loss of electron density through substitution is believed to be responsible for this decrease in donating power. Nevertheless, it will be of interest to investigate whether these compounds will behave in a similar manner towards the transition metal ions.

CHAPTER 5

BASE PROMOTED DECOMPOSITION OF 1-ARYL-3-HYDROXYMETHYL-3-METHYLTRIAZENES TO 1-ARYL-3-METHYLTRIAZENES

5.1 Introduction

The transformation of HMTs to MMTs is believed to be a crucial step in the metabolism of DMTs. Despite its significance, however, this reaction has never been observed directly. In aqueous buffer system, pH≤10, HMTs decompose to the corresponding anilines[27,95], and no evidence for the intermediacy of MMT was observed. Moreover, the Lewis acid catalysed decomposition of HMTs in non-aqueous solutions gave only an indirect method for studying this reaction (Chapter 3).

On the other hand, the decomposition of aminocarbinols derived from Schiff bases and related compounds has been reported. This reaction is now known to be general base catalysed[80] (Section 1.2.2). It was anticipated that the reactivity of HMTs towards bases would depend not only on the N-alkyl group, but also the p-substituent in the benzene ring. Given the biological ubiquity of basic materials we undertook to examine how bases interact with HMTs.

5.2 Preliminary Studies on the Mechanism of the Reaction

During the course of establishing a mechanism for the formation of the bis-triazene (22) (Section 2.2), it was discovered that in the presence of three-fold excess of methylamine, HMTs decomposed in aqueous suspension to the corresponding monomethyltriazene (Scheme 5.1). This transformation appears to be promoted by methylamine,

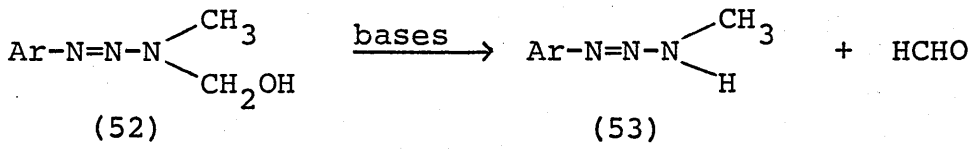

(52) (53)

	Ar
a	$4\text{-}NO_2C_6H_4$
b	$4\text{-}CNC_6H_4$
c	$4\text{-}CH_3COC_6H_4$
d	$4\text{-}CH_3COOC_6H_4$

Scheme 5.1

since both (52c) and (52d) can be recovered unchanged in the absence of the base. Two mechanisms are possible for this transformation (Scheme 5.2). First, methylamine may attack the OH proton of the HMT (route (i)) or second, the base may exchange with the aminocarbinol function by attacking the central nitrogen atom of the triazene (route (ii)) . The two possibilities were tested by looking at the effects by other

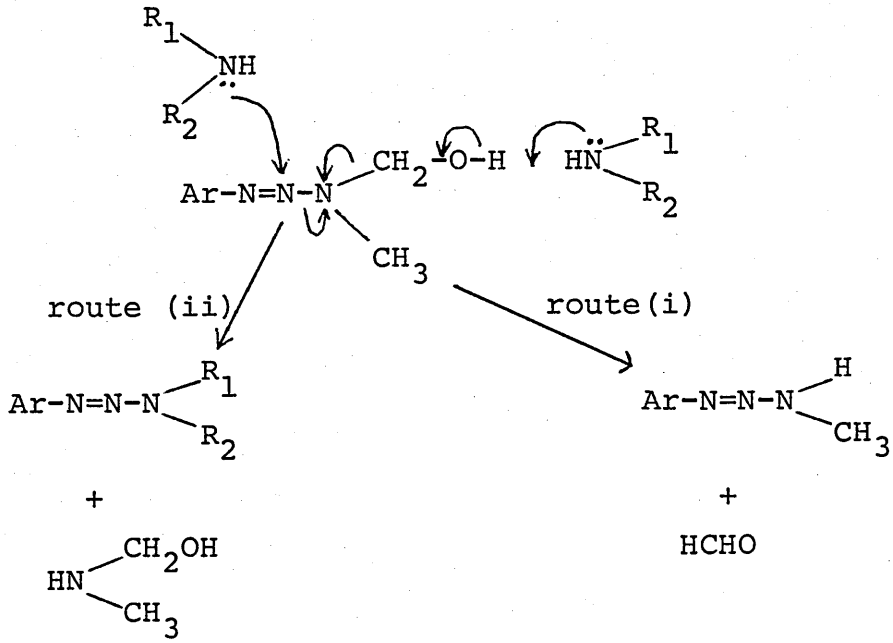

Scheme 5.2

amines. It was found that ethylamine, morpholine and piperidine also effect the complete transformation of HMTs (52, a-d) to the respective MMTs. This confirms that the mechanism proceeds via the abstraction of the OH proton by the amines and not through amine exchange. It also reinforces the earlier speculation that HMTs could behave as acids due to the OH proton.

5.3 Effect of Bases and 4-Substituents

Four different types of bases were employed in this study. They are the simple amines like methyl and ethyl-amines, morpholine and piperidine; heteroaromatics such as pyridine, 4-aminopyridine, adenine and imidazole; amino acids as represented by glycine and lysine and polyfunctional compounds like AMP and poly(lysine). Four HMTs (52, a-d) were also used.

5.3.1 Qualitative Studies

The results are shown in Table 5.1. With simple amines, the reaction goes to completion and the MMTs are the only product formed. Less basic amines, viz, the heteroaromatics are not such good promotors, bringing about the conversion of only (52 a) and (52 b). With hydroxide ion, alone or with the presence of the two amino acids, a strongly coloured solution was formed when the HMTs, except (52d), were stirred into an aqueous solution containing hydroxide ions. Both (52 b) and (52 c) gave a yellow solution whereas (52 a) gave a red solution. The

Table 5.1 The action of bases in converting HMTs in MMTs

Reagents (pKa) \ HMTs	$4\text{-}NO_2C_6H_4$	$4\text{-}CNC_6H_4$	$4\text{-}CH_3COC_6H_4$	$4\text{-}CH_3COOC_6H_4$
methylamine (10.62)	+	+	+	+
ethylamine (10.63)	+	+	+	+
morpholine (8.36)	+	+	+	+
pyridine (5.14)	+	+	-	-
4-aminopyridine (9.11,5.14)	+	+	-	-
adenine (4.15,9.8)	+	+	b -	b -
imidazole (7.05,14.52)	+	+	-	-
glycine at pH 10	+	+	c d +	c d +
lysine at pH 10	+	+	c d +	c +
water at pH 10	+	+	c d +	c +
AMP	b -	b -	b -	b -
acetate ion	+	+	-	-
water	+	+	-	-

a (+) sign indicates some or full conversion; (-) sign indicates no conversion.

b A different product, N,N-bis(arylamino)methane was obtained - see text.

c Products were recovered by evaporating off the water and extracting with chloroform.

d Corresponding anilines (20-30%) were found.

reason for this colour appearance is not clear, though it may be due to the anion of the MMTs.

The amino acids, glycine and lysine, both at pH 10, also bring about the conversion of (52) into (53). Whilst it is clear that it was not the carboxylate group that was responsible for this reaction (since $AcO^{\ominus}$ was ineffective), it is unclear whether the reaction was promoted by the amino acids, since hydroxide ion itself is a promoter.

A new product, viz, N,N-bis(arylamino)methane was produced from the reaction of HMTs with adenosine monophosphate (AMP) (equation 5.1). A similar product was obtained from (52 c) and poly(lysine).

$$Ar\text{-}N{=}N\text{-}N\begin{matrix}CH_2OH\\CH_3\end{matrix} \xrightarrow[\text{polylysine}]{\text{AMP or}} ArNHCH_2NHAr + N_2 + HCHO + CH_3OH$$

Equation 5.1

It is probable that these more acidic compounds decompose the MMTs via acid catalysis to form the corresponding aniline which condenses with the liberated formaldehyde.

5.3.2 Competitive Studies

Since both (52 a) and (52 b) decompose in water overnight in the absence of base, the effectiveness of the bases in promoting the decomposition of these two compounds required closer examination. By stopping the reaction after 1 hour, the effectiveness of bases can therefore be compared by studying the composition of the reaction mixture. ^1H Nmr

proved a suitable method for analysing the reaction mixtures. A ratio of (52) : (53) can be obtained by dividing the integral of the methylene signal of the HMT starting material by that of the total aromatic signals of HMT and MMT.

The results (Table 5.2) confirm that simple amines are better promotors than heteroaromatics. Also, the ratios show that the reactivity of HMTs decreases in the order (52 a) > (52 b) > (52 c,d). In other words, electron withdrawing groups have a destabilising effect in this reaction by making the OH proton more acidic.

Table 5.2 Product ratios over and above water for the base-promoted decomposition of (52 a-d) after 1 hour.[a]

Base (pKa)	Ratio			
	(53a): (52a)	(53b): (52b)	(53c): (52c)	(53d): (52d)
methylamine (10.62)	46 : 54	34 : 66	0 : 100	0 : 100
morpholine (8.36)	14 : 86	10 : 99	0 : 100	0 : 100
pyridine (5.14)	11 : 89	0 : 100	0 : 100	0 : 100

a average of two or more experiments

5.3.3 Kinetic Studies

Efforts to study the kinetics of the transformation of HMT to MMT were initially hampered by the almost identical ultraviolet absorption of the two compounds. (Table 5.3). Using these data, one can estimate the change in absorbance during the course of the reaction. If the initial concentration of 4-$COCH_3$HMT is

Table 5.3 U.V. data for HMTs and MMTs in ethanol

Compound	λ max/nm	$\varepsilon/M^{-1}cm^{-1}$
4-$COCH_3$HMT	322	$2.329x10^4$
4-$COCH_3$MMT	322	$2.433x10^4$
4-$COOCH_3$HMT	307	$2.5884x10^4$
4-$COOCH_3$MMT	307	$2.1886x10^4$

5×10^{-5}M, it will produce an absorbance change of $0.104 \times 10^4 \times 5 \times 10^{-5} = 0.052$. Any measurement of such a small change will inevitably carry a high percentage of error.

5.3.3.1 N.m.r. Method

A possible method of monitoring the reaction was ^{1}H n.m.r. By recording ^{1}H n.m.r spectra at fixed time intervals, the change in the concentration of HMT can be measured as a function of time.

An excess of eight to ten fold of morpholine, piperidine or 1,1-dimethylhydrazine in $(CD_3)_2SO$ brought about a rapid transformation of (52 c) to (53 c). The reaction was completed within 20 minutes thus making it virtually impossible to measure the integration of those nmr signals concerned and to calculate rate constants. By contrast, a seven fold excess of triethylamine in the same solvent or in $CDCl_3$ did not convert (52 c) to (53 c) but only broadened the signals. This difference in reactivity of the bases may be due to the inability of triethylamine to form an adduct with formaldehyde,

the byproduct of the reaction. In this event the monomethyltriazene may condense with the formaldehyde to reform the HMT.

Another possibility is the basicity of the amines. The pKa values of morpholine, piperidine, 1,1-dimethylhydrazine and triethylamine in water are, respectively, 8.36, 11.22, 7.12 and 10.65. Contrary to the reaction results, these data suggest that in water, triethylamine is more basic than morpholine and 1,1-dimethylhydrazine. Although these pKa values sometimes vary drastically on changing the solvent from water to an aprotic organic one, the most likely explanation for the failure of triethylamine is due to the absence of a hydrogen atom next to the nitrogen of the molecule. This means that triethylamine, unlike other compounds such as morpholine or piperidine, cannot self-associate through intermolecular hydrogen bonding in any aprotic solvents. The relationship between self-association and reactivity is discussed below.

The proposed mechanism, which is depicted in scheme 5.3, involves a cyclic transition state. This ring like structure is formed from a number of amines and an HMT molecule linked together by hydrogen bonds. The next step in the mechanism is the simple rearrangement of protons that yields the MMT and formaldehyde. The presence of a cyclic transition state has the advantage of ensuring a concerted proton transfer process. Otherwise, a highly unfavourable and reactive amine anion would be created. Accordingly, only those self-associating amines can form a cyclic structure with HMT and effect the transformation of HMT to MMT.

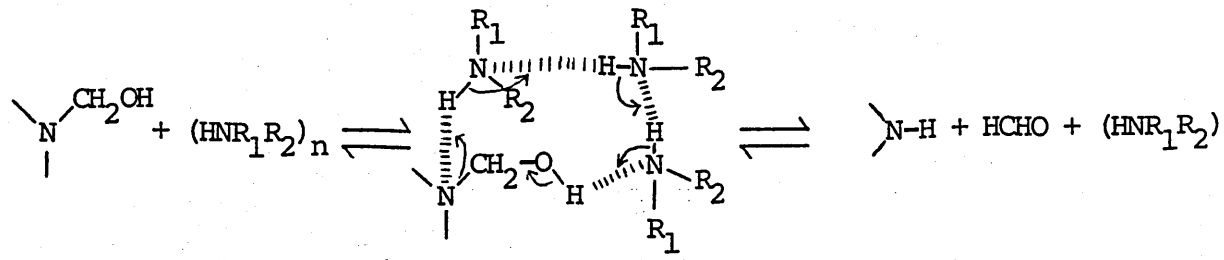

Scheme 5.3

On the other hand, if the reaction is conducted in a protic solvent like water, the problem of generating a reactive and unstable amine anion can be avoided. Behaving as acids, the protic solvents can readily donate a proton to the terminal nitrogen of the triazene moiety thus rendering a complete transfer of protons (Scheme 5.4). The alternative mechanism may account for the observed result of pyridine in water.

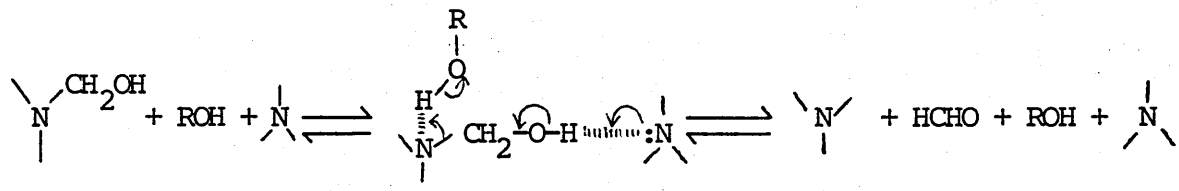

Scheme 5.4

5.3.3.2 HPLC Method

Further methods of studying the kinetics of base promoted decomposition of HMT to MMT is by high performance liquid chromatography (hplc). An eluent has been developed in which one of the HMTs, the 3-pyridyl HMT, is stable enough to be separated from the 3-pyridyl MMT and 3-aminopyridine. The eluent is made up of 20% acetonitrile, 30% of methanol and 50% water buffered at pH 6.3 with 0.5M ammonium acetate. In order to minimise the decomposition of HMT on the column, the temperature of the column was maintained at 4 ^{o}C. A chromatogram which shows the separation of the two pyridyl triazenes is given in Fig. 5.1.

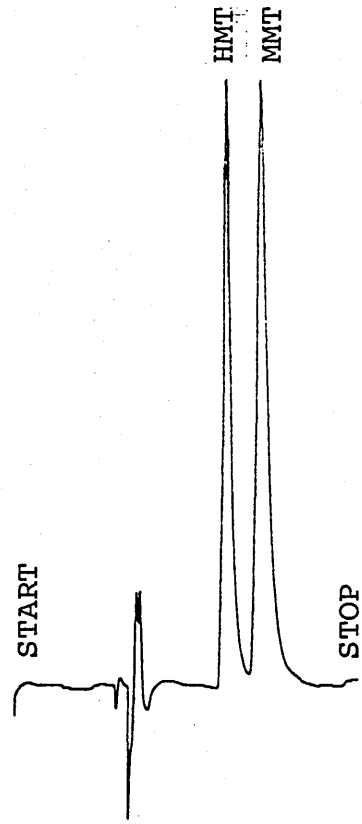

Fig. 5.1 A typical high performance liquid chromatogram for the separation of 3-pyridylHMT and MMT

Assume that the reaction HMT $\xrightarrow{k'}$ MMT is first order in HMT concentration or that the base is present in a sufficient amount to give a pseudo-first-order rate constant (k'), then

$$-\ln \frac{[HMT]_t}{[HMT]_o} = k't \qquad \text{——— (5.2)}$$

Because $[HMT]_o = [HMT]_t + [MMT]_t$

Equation 5.2 can be rewritten into

$$-\ln \frac{[HMT]_t}{[HMT]_t + [MMT]_t} = k't \qquad \text{———(5.3)}$$

The ratio $[HMT]_t/([HMT]_t + [MMT]_t)$ can be easily obtained from the hplc chromatogram by dividing the peak area of HMT by the sum of the peak areas of HMT and MMT because the HMT and MMT have identical ultraviolet absorption. So, a plot of $-\ln [HMT]_t/([MMT]_t + [HMT]_t)$ against time should be a straight line. A typical hplc trace for a reaction run is shown in Figure 5.2.

A typical plot for the decomposition of 3-pyridyl HMT in absolute ethanol, is shown in Fig. 5.3. Water was found to promote this reaction and the rate is proportional to the concentration of water (Table 5.4, Fig. 5.4). The second order rate constant for this reaction is 9.6275×10^{-5} $M^{-1}S^{-1}$.

The results (Table 5.5) of morpholine catalysed reaction also suggest that the rate is proportional to [morpholine]. In contrast, in the presence of an 0.0255M acetate buffer, morpholine appears to have no promotive power (Table 5.6). Since the pH of these buffered solutions were not measured, it is impossible to know if the predominant species in the solution is the morpholinium ion. This could otherwise explain the negative result. Pyridine and acetate buffers also appear to have no effect (Table 5.7). Due to the shortage of time, it was not possible to extend this work into other amines such that a Bronsted plot could be constructed.

Fig.5.2 Typical trace for the decomposition of 3-pyridylHMT in ethanol T=37 °C.

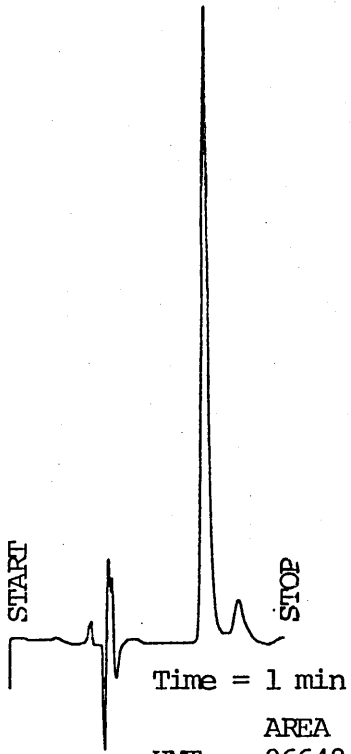

Time = 1 min

	AREA
HMT	96648
MMT	11968
TOTAL	108617

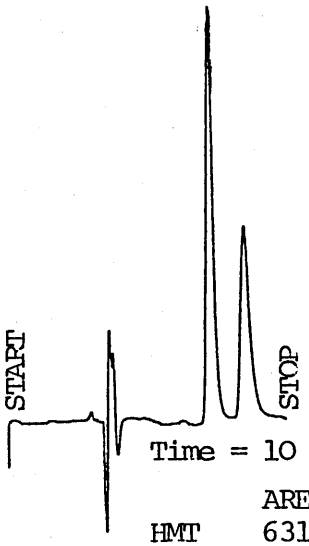

Time = 10 min

	AREA
HMT	63107
MMT	40881
TOTAL	103989

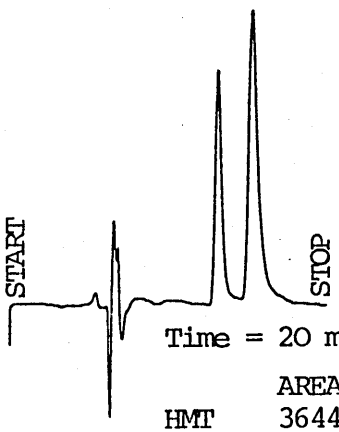

Time = 20 min

	AREA
HMT	36447
MMT	66024
TOTAL	102472

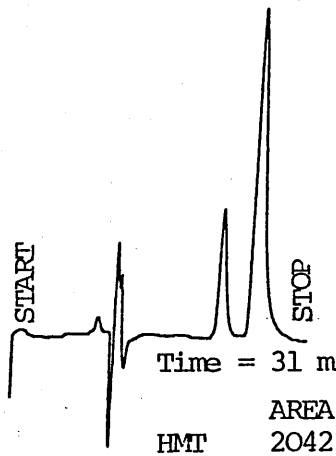

Time = 31 min

	AREA
HMT	20423
MMT	93480
TOTAL	93903

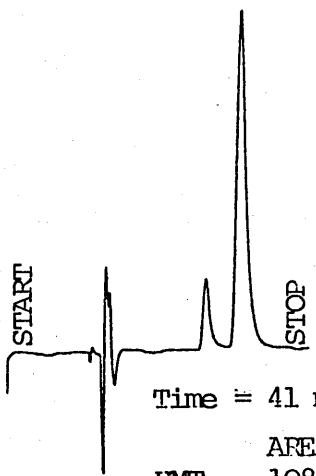

Time = 41 min

	AREA
HMT	10867
MMT	71285
TOTAL	82152

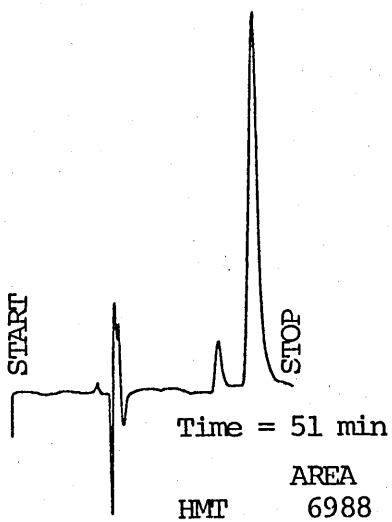

Time = 51 min

	AREA
HMT	6988
MMT	75806
TOTAL	82794

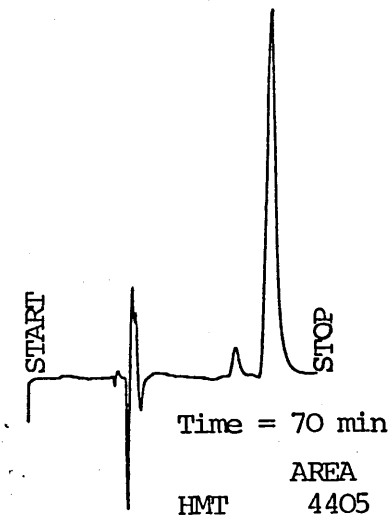

Time = 70 min

	AREA
HMT	4405
MMT	76393
TOTAL	80798

Fig. 5.3 Pseudo first order plot for the decomposition of 3-pyridylHMT in ethanol T=37°C

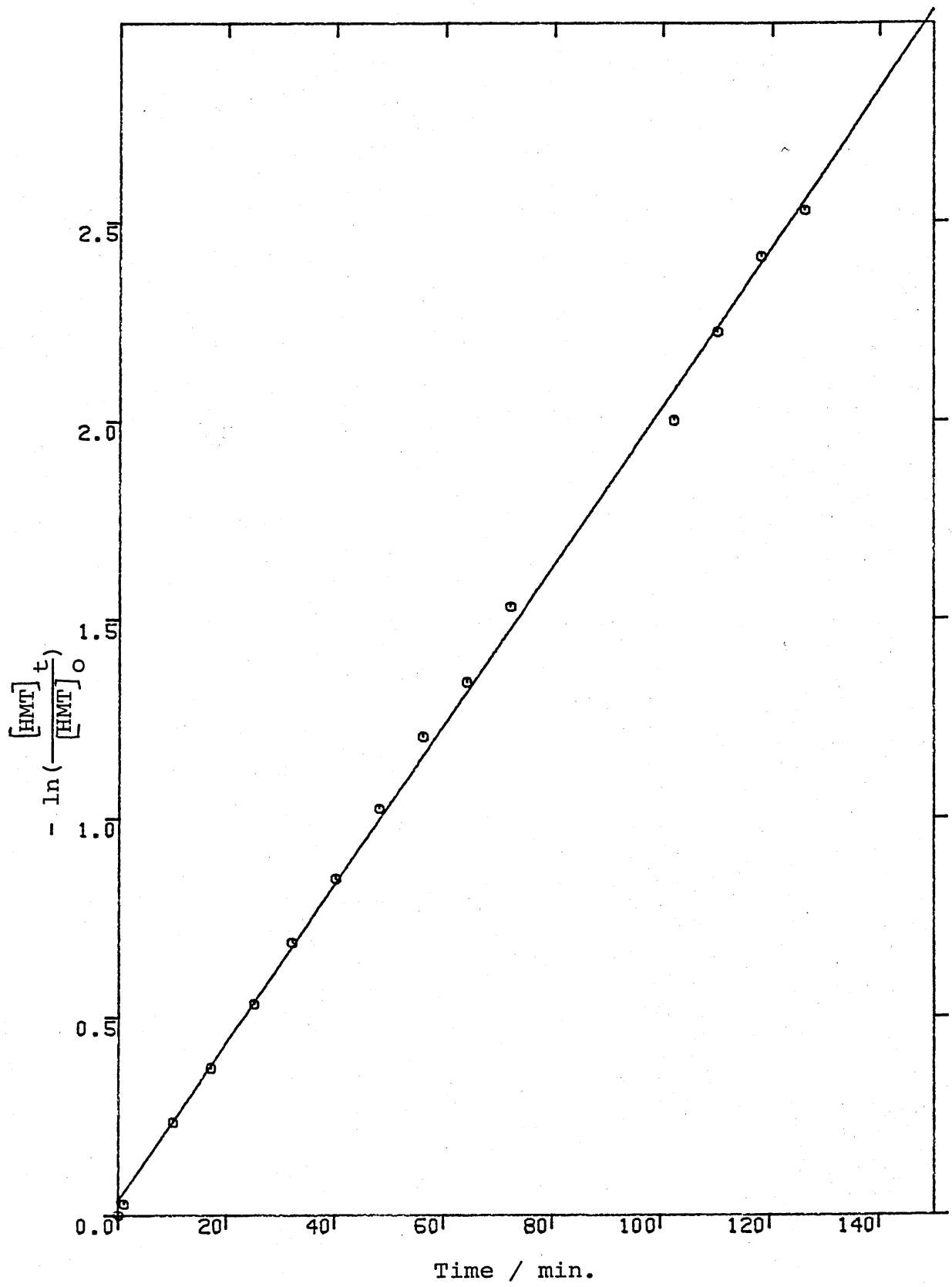

Fig. 5.4 Decomposition of 3-pyridylHMT in ethanol by water T=37°C

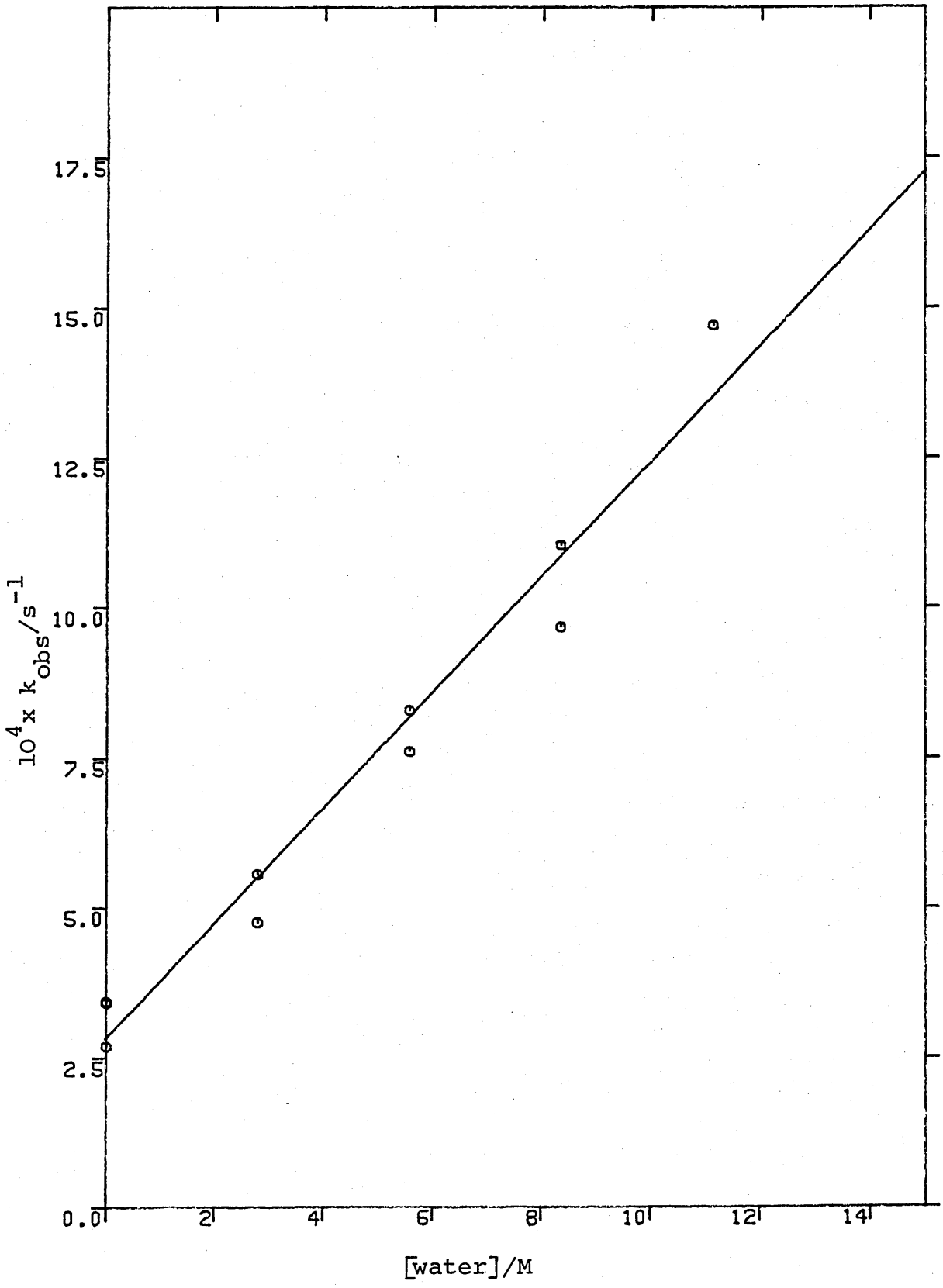

Table 5.4 Results of water promoted decomposition of 3-pyridyl HMT in ethanol T=37 °C.

[water]/M	kobsx10^4/S^{-1}(standard error)
0	3.433 (± 0.167) 3.4 (± 0.033) 2.683 (± 0.05)
2.78	5.55 (± 0.45) 4.75 (± 0.217)
5.56	7.6 (± 0.267) 8.283 (± 0.15)
8.333	9.667 (± 0.383) 11.033 (± 0.285)
11.11	14.7 (± 0.383)

Table 5.5 Results of morpholine promoted decomposition of 3-pyridyl HMT in ethanol T=37 °C.

[morpholine]/M	kobsx10^3/S^{-1}
0.10126	0.2983
0.4272	2.6717
0.5443	2.9783
0.6586	2.735
0.9311	5.33
k_{morph}	5.6311x10^{-3}

Table 5.6 Results of decomposition of 3-pyridyl HMT in an acetate buffered solution with morpholine acetate = 0.0255m

[morpholine]/M	$k_{obs} \times 10^4/S^{-1}$
0.4075	3.25
0.5138	3.12
1.248	3.05

Table 5.7 Decomposition of 3-pyridyl HMT with pyridine and acetate buffer

pyridine		acetate buffer	
[pyridine]/M	$k_{obs} \times 10^4/S^{-1}$	[acetate]/M	$k_{obs} \times 10^4/S^{-1}$
0.5099	2.483	0.03188	3.3
1.4987	2.85	0.0255	3.38

5.4 Discussion

Since pyridine and acetate buffer have no promotive effect on the decomposition of 3-pyridyl HMT in ethanol, the observed rate constants in Table 5.7 must be of the ethanolysis reaction. Likewise, the same argument can be applied to the acetate buffered morpholine reaction (Table 5.6). Averaging these kobs. with the intercept of Fig. 5.4 gives a first order rate constant of $2.983 \times 10^{-4} S^{-1}$. Thus the second order rate constant for the decomposition of 3-pyridyl HMT by ethanol is $1.7385 \times 10^{-5}\ M^{-1}S^{-1}$. Comparing this result with those of morpholine and water (Table 5.8) reveals a decreasing order of morpholine > water ≃ ethanol.

Table 5.8 Rate constants for the decomposition of 3-pyridyl HMT to 3-pyridyl MMT in ethanol T=37 °C.

Base	$kx10^5/M^{-1}S^{-1}$
morpholine	563.11
water	9.6275
ethanol	1.7385

The failure of pyridine in promoting the decomposition of 3-pyridyl HMT in ethanol suggests that the presence of a X-H bond is required for promotive activity. Indeed, this argument is consistent with the result of triethylamine in $(CD_3)_2SO$ discussed earlier. However, the inability to form a cyclic structure is not a valid explanation in this instance since hydrogen bonding with ethanol is possible. The elucidation of this reaction mechanism thus requires further investigation.

Nevertheless, this is the first time that the conversion of HMT to MMT has been observed. It appears that the results are in favour of the general belief that HMT is the intermediate in DMT metabolism and that the compound can be broken down to MMT when triggered appropriately. It also seems to lend support to the alternative mechanism which regards HMT as the progenitor of the toxic formaldehyde and believes that the release of formaldehyde is responsible for the selective cytotoxicity of DMT in vivo. Acting against both arguments, the results, in fact, indicate that HMTs are less stable than their corresponding MMTs, both hetero- and homogenously, in a neutral solution or a base-containing solution. In particular, it shows that bases with X-H bonds are effective promoters for the decomposition of HMTs. Moreover, whilst some N-hydroxymethyl containing compounds are known to aminomethylate, no such reaction was observed with HMTs.

Synthetically, this transformation has provided an alternative route for the synthesis of 1-aryl-3-methyltriazenes. MMTs are generally synthesised by coupling aryl-diazonium ions with methylamine, usually in the presence of bases. However, this method often produces compounds that are contaminated by either penta-azadienes or 1,3-diaryltriazenes.[87] The difficulty of removing these impurities without further decomposing the required products has been described.[96] The synthesis of MMT from HMT therefore has the significant advantage in that it yields analytically pure samples of MMT in reasonably good yields (Table 5.9). Indeed, 1-(3-pyridyl)-3-methyltriazene was obtained only by this method. However, it must be pointed out that this method is limited to those HMTs that can be synthesised, ie. those bearing electron withdrawing substituents in the aryl ring.

Table 5.9 1-aryl-3-alkyltriazenes

Ar	R	Yield(%)	M.p.(lit.)(°C)	Found(calc)(%) C	H	N
$4\text{-}NO_2C_6H_4$	Me	62	110-111(111-113)[87]	46.9 (46.67)	4.3 (4.44)	30.7 (31.11)
$4\text{-}CNC_6H_4$	Me	75	142-143(136)[87]	59.7 (60.00)	4.8 (5.00)	35.4 (35.00)
$4\text{-}MeCOC_6H_4$	Me	50	97(90-92)[87]	61.0 (61.02)	6.2 (6.21)	24.1 (23.73)
$4\text{-}MeOCOC_6H_4$	Me	46	102-103(94-96)[87]	55.6 (55.96)	5.6 (5.70)	21.7 (21.76)
$4\text{-}ClC_6H_4$	Me	72	75-77(82)[97]	50.1 (49.56)	4.7 (4.72)	24.6 (24.78)
$4\text{-}NH_2COC_6H_4$	Me	80	139-140(148-149)[11]	53.6 (53.93)	5.9 (5.62)	30.9 (31.46)
$3\text{-}C_5H_4N$	Me	55	59-61	52.8 (52.94)	6.1 (5.88)	40.9 (41.17)
$4\text{-}MeCOC_6H_4$	Et	60	101-102	62.74 (62.83)	6.91 (6.81)	21.93 (21.99)

CHAPTER 6

EXPERIMENTAL AND REFERENCES

Nmr spectra were recorded using a Perkin Elmer R12B spectrometer (^{1}H) and a Jeol FX90Q spectrometer (^{1}H and ^{13}C). Ultraviolet spectra (for routine scanning and kinetic measurement) were recorded on Pye Unicam SP8-500 and SP8-100 spectrophotometers. Infra-red spectra were recorded using a Unicam SP1050 spectrophotometer. Melting temperatures were measured using a Buchi 510 melting point apparatus. Elemental analyses were performed by Butterworth laboratories, Teddington, Middlesex or by using a Perkin Elmer 240C Elemental Analyser with Model 3400 Data Station. High performance liquid chromatography was performed on a 25cm x 5mm ID spherisorb S5ODS2 analytical column using a Milton Roy/Dosapro single piston pump with a Rheodyne 7125 injector, a Cecil CE 2112 variable wavlength UV detector and a Shimadzu C-RIB integrator. Gas chromatography/mass spectroscopy were performed by courtesy of PCMU Harwell.

6.1 Synthesis of hydroxymethyltriazenes and related compounds

6.1.1 Synthesis of N,N-bis (1-aryl-3-methyltriazene-3-yl) methyl methylamines

The procedure of Vernin et al was followed.[67] Typically, an aqueous solution of the aryldiazonium fluoroborate ($5x10^{-3}$ mol) was added to a premixed solution of aqueous

formaldehyde (37-40% w/v, 11ml) and aqueous methylamine (25-30% w/v, 3ml) at 0 °C. Soon after the addition, a sticky gum was formed. The product was isolated by decanting off the water and was recrystallised from alcohol/water. The yield was ca 20-25%.

6.1.2 Synthesis of 1-aryl-3-hydroxymethyl-3-methyltriazenes

Method A: The method of Stevens et al was followed.[27] Typically, the 4-substituted aniline (2.5×10^{-2} mol) was diazotised in hydrochloric acid (12M, 6.25ml diluted to 60ml), with sodium nitrite (1 mole equivalent) for 1 hour at 0 °C. After which time, the diazotised solution was added over 15-30 minutes to a premixed solution of aqueous formaldehyde (37-40% w/v, 60ml) and aqueous methylamine (25-30% w/v, 6ml) at -5 °C. The precipitate formed was filtered out, washed with cold water and air-dried. Using this method, 4-CH_3CO-, 2-CF_3, 4-CH_3OCO-, 4-CH_3CH_2OCO- and 4-NH_2COHMTs were synthesised with ca 75% yield.

Method B: As method A except that the temperature of the coupling reaction was lowered to -15 °C and the amount of methylamine was reduced to 3ml. In this way, 4-CN- and 4-NO_2HMTs were obtained pure in 43 and 53% yield respectively.

Method C: As method B, except that ice (ca 100g) was added to the diazotised solution which was then carefully neutralised to pH7 with sodium hydroxide solution. A premixed solution of formaldehyde (37-40% w/v, 60ml) and methylamine (25-30% w/v, 3ml) was added slowly over 1-1½ hrs

to the neutralised solution. After the addition has finished, the solution was stirred at 0 ^{o}C until precipitates were formed. In this case, 4-Cl- and 4-CF_3HMTs were obtained in ca 30% yield. 3-PyridylHMT was also synthesised in 80% yield by this method.

6.1.3 Synthesis of 1-(4-acetyl)phenyl-3-hydroxymethyl-3-alkyltriazenes

4-Aminoacetophenone ($2.5x10^{-2}$ mol) was diazotised as in HMT synthesis at 0 ^{o}C. Aqueous formaldehyde (37-40%, 60ml) was then added into the diazotised solution. This was followed by the dropwise addition of the amine (2 mole equivalent). The product was isolated by filtration. The yield for the ethyl and n-propyl homologues are 51 and 30% respectively. The 3-methyl deuterated ($-CD_3$) compound was also synthesised by this method with 25% yield. Both the $-CD_3$ and $-CH_2CH_3$ derivatives were recrystallised from chloroform whilst the $-CH_2CH_2CH_3$ were recrystallised from ether/pet. ether mixture.

6.1.4 Attempted synthesis of 1-(4-acetyl)phenyl-3-hydroxymethyl-3-isopropyltriazene

4-Aminoacetophenone (0.0265 moles) was diazotised as in Section 6.1.2 for 1 hour at 0 ^{o}C. Meanwhile, a solution of iso-propylamine (4.3ml) in water (10ml) was added dropwise into aqueous formaldehyde (37-40% w/v, 4.3g) and

then diluted with water (10ml). This solution was introduced into the diazotised solution dropwise. The solid which precipitated out was collected, air-dried and identified to be the monoisopropyl derivative, $4\text{-}CH_3COC_6H_4N{=}N\text{-}NH^iPr$

^1H nmr: δ/ppm($(CD_3)_2SO$) 7.25-7.95(4H,AA'BB'), 3.80(1H,m,J=7Hz); 1.23(6H,d,J=7Hz)

Analysis: Found: C 63.84; H 7.42; N 19.17%

Required: C 64.37; H 7.37; N 20.47%

6.1.5 Attempted synthesis of 5-(3-hydroxymethyl-3-methyl-1-triazeno)-imidazole-4-carboxamide (HMIC)

Method A - Part I: Shealy's method for the synthesis of DZIC was followed.[71] Typically, a stirred aqueous solution (30ml) of sodium nitrite (1.175g) was cooled to 0-5 °C. A cold solution of AIC (2.5g) in dilute hydrochloric acid (1N, 20ml) was then added in dropwise. After a small portion of the acidic AIC solution had been added, a crystalline precipitate began to form. When the addition was completed, the precipitate was removed by filtration, washed 3 times with 5ml portions of water and dried in vacuo over P_2O_5. The yield for the DZIC was 70%.

melting temperature = 192 °C lit. value = 205-210 °C (dec).[71]

Part II: A suspension of DZIC (0.8g) in methanol (10mol) was cooled by an acetone/cardice bath. The reaction vessel was protected from light and moisture. A premixed solution of aqueous formaldehyde (37-40% w/v, 0.473g) and

methanolic methylamine (7.8% w/w, 2.3g) was added to the suspension in dropwise and the reaction was stirred for 3 hours. The solid product was filtered, washed with methanol and dried *in vacuo*. It was identified to be the MIC:

^{1}Hnmr: δ/ppm($(CD_3)_2SO$) 7.53(1H,s); 7.37(2H,broad); 3.00(3H,s)

Method B Part 1: DZIC was synthesised as in method A. The synthesis of MIC was based on Shealy's method.[72] Typically, methylamine solution in industrial methylated spirit (IMS) (33% w/v, 11.74g) was diluted with IMS (7.125ml) and cooled to 0-5 °C with an ice-bath. DZIC (0.685g) was added in small portions over 45 minutes with the solution. The reaction was protected from light. After the addition was completed, the reaction was stirred for another 2 hours. The solid product was filtered out, air-dried and the yield was *ca* 37%.

^{1}Hnmr: δ/ppm ($(CD_3)_2SO$) 7.53(1H,S); 7.37(2H, broad), 3.00(3H,S)

Analysis: Found: C 35.64; H 4.86; N 49.73%
Required: C 35.71; H 4.76; N 50.00%

Part II: Kolar's method of synthesising HMIC was followed.[29] Typically, MIC(100mg) was added in small portions into a ethanolic solution of formaldehyde (25ml) at room temperature. The suspension was stirred until all the MIC dissolved to give a orangy coloured solution. Equivalent amount of pet.ether (60-80 °C) was then added and the solution was left overnight at -30°C. After which time it was evaporated down to *ca* 5ml and more pet.ether was added. The

precipitates which formed instantly were filtered off and analysed. More precipitates were collected from the filtrate after prolonged cooling. The two samples were found to be contaminated.

Analysis: Found: C 37.69; H 5.86; N 34.45%

Required: C 36.36; H 5.05; N42.00%

The physical and spectral data of all the triazenes synthesised in this study are shown in Tables 2.2.3 to 2.4.1 in Chapter 2.

6.2 Lewis acid catalysed decomposition of 1-aryl-3-hydroxymethyl-3-methyltriazenes

6.2.1 Purification of reagents and solvents

6.2.1.1 Reagents

Sodium perchlorate, sodium acetate, zinc oxide, copper oxide, perchloric acid, ethylenediamineacetic acid and all the metal nitrates and sulphates were AnalaR grade commercial samples and were used without further purification.

All the metal perchlorates were commercial samples and were stored in a desiccator but used without purification.

GPR grade sodium bromide, iodide and ethoxide were used without further purification.

Triethanolamine hydrochloride was recrystallised from ethanol and dried at 80 ^{o}C (m.t. 179 ^{o}C).

Diethylmalonic acid was recrystallised from benzene (m.t. 127 ^{o}C).

Pyridine was distilled over KOH and molecular sieves 4A.

Imidazole was purified by sublimation.

6.2.1.2 Solvents

Deionised water was used for all the aqueous solution and 10% alcohol solution.

Absolute ethanol was refluxed over magnesium and iodine. Gold label deuterated ethanol (CH_3CH_2OD) was used without purification.

Dimethylsulphoxide was distilled under reduced pressure before use.

6.2.2 Qualitative studies in water

In a typical experiment, a suspension of HMT ($3x10^{-3}$ mole) in an aqueous solution of the appropriate metal ion (40ml, 0.1M) was stirred overnight at room temperature. The product formed was filtered,air-dried and identified by ^{1}Hnmr spectroscopy.

The results of this study are summarised in Tables 3.2.1 - 3.2.2 in Chapter 3.

6.2.3 Calculation of rate constants

Based on Equation 6.2.1, the pseudo first order rate constants (k_{obs}) were calculated from the experimental data by means of a least-squares computer program written by Dr P G Taylor of the Department of Chemistry, The Open University.

$$[\text{substrate}]_t = [\text{substrate}]_o \, e^{-k_{obs}t} \quad \text{——} \quad 6.2.1$$

In terms of (A), Equation 6.2.1 becomes

$$(At-A\infty) = (Ao-A\infty) \, e^{-k_{obs}t}$$

Besides calculating k_{obs}, the computer program also calculates the theoretical absorbances and compares the observed absorbances with the calculated ones. Typical runs are shown in Tables 6.2.1 - 6.2.3.

6.2.4 Kinetic method

UV spectrophotometer was used to monitor the decomposition of HMTs by recording the absorbance of the substrate at a fixed wavelength continuously or at regular time intervals.

6.2.4.1 Reaction in water

Method A: For reactions using unbuffered metal ion Solutions.

In a typical experiment, the metal ion solution (ca 20ml) was prepared in a 25ml volumetric flask. The ionic strength of the solution was maintained at 0.05M with $NaClO_4$. Helium gas was passed through the solution for ca 15 minutes in order to degas it, after which it was transferred to a thermostated water bath for 20 minutes. A thermostated ethanolic solution of HMT (2.5ml) was then added to initiate the reaction. The volumetric flask was quickly filled up to the mark with deionised water. After the reaction solution was shaken thoroughly, an aliquot was transferred to a cuvette and the spectrophotometer was started.

Table 6.2.1

4-CNHMT+Zn(0.009M) with [DEM]=0.15M I=1M T=37

14 POINTS

TIME	ABSORBANCE	CALC ABSORBANCE	DIFFERENCE
2.000	1.617	1.620	-0.003
4.000	1.483	1.482	0.001
6.000	1.357	1.356	0.001
10.000	1.138	1.135	0.003
12.000	1.040	1.039	0.001
14.000	0.953	0.951	0.002
16.000	0.870	0.871	-0.001
18.000	0.795	0.798	-0.003
20.000	0.728	0.731	-0.003
22.000	0.670	0.670	0.000
24.000	0.614	0.614	-0.000
26.000	0.563	0.563	-0.000
28.000	0.517	0.516	0.001
30.000	0.476	0.474	0.002

RATE CONSTANT EQUALS 0.45241E-01

INITIAL ABSORBANCE EQUALS 1.771

FINAL ABSORBANCE EQUALS, 0.024

RESIDUAL EQUALS 0.002

PLOT OF ABS(LN(AI-A))AGAINST TIME

CORRELATION COEFFICIENT EQUALS -1.000

STANDARD DEVIATION EQUALS 0.002

FIRST APPROXIMATION OF RATE CONSTANT EQUALS
-0.45185E-01

Table 6.2.2

4-CNHMT+Cu(0.02055M) in EtOH I=0.15 T=37

17 POINTS

TIME	ABSORBANCE	CALC ABSORBANCE	DIFFERENCE
30.000	0.725	0.724	0.001
60.000	0.624	0.626	-0.002
90.000	0.553	0.553	0.000
120.000	0.496	0.497	-0.001
150.000	0.454	0.454	-0.000
180.000	0.423	0.422	0.001
210.000	0.398	0.398	0.000
240.000	0.380	0.379	0.001
270.000	0.365	0.365	-0.000
300.000	0.355	0.354	0.001
330.000	0.347	0.346	0.001
360.000	0.340	0.340	-0.000
390.000	0.335	0.336	-0.001
420.000	0.332	0.332	-0.000
450.000	0.329	0.329	-0.000
480.000	0.327	0.327	-0.000
540.000	0.325	0.325	0.000

RATE CONSTANT EQUALS 0.92204E-02

INITIAL ABSORBANCE EQUALS 0.852

FINAL ABSORBANCE EQUALS, 0.321

RESIDUAL EQUALS 0.001

PLOT OF ABS(LN(AI-A))AGAINST TIME

CORRELATION COEFFICIENT EQUALS -1.000

STANDARD DEVIATION EQUALS 0.031

FIRST APPROXIMATION OF RATE CONSTANT EQUALS
-0.92221E-02

Table 6.2.3

4-COOCH3HMT+Zn(0.02127M) in DMSO I=0.15M T=37

20 POINTS

TIME	ABSORBANCE	CALC ABSORBANCE	DIFFERENCE
30.000	0.840	0.841	-0.001
60.000	0.800	0.800	-0.000
90.000	0.765	0.765	0.000
120.000	0.733	0.733	0.000
150.000	0.708	0.704	0.004
180.000	0.682	0.679	0.003
210.000	0.653	0.657	-0.004
240.000	0.635	0.637	-0.002
270.000	0.621	0.620	0.001
300.000	0.600	0.604	-0.004
330.000	0.592	0.590	0.002
360.000	0.578	0.578	0.000
390.000	0.567	0.567	0.000
420.000	0.556	0.557	-0.001
450.000	0.550	0.549	0.001
480.000	0.540	0.541	-0.001
510.000	0.537	0.534	0.003
540.000	0.530	0.528	0.002
570.000	0.522	0.523	-0.001
600.000	0.517	0.518	-0.001

RATE CONSTANT EQUALS 0.39738E-02

INITIAL ABSORBANCE EQUALS 0.887

FINAL ABSORBANCE EQUALS, 0.481

RESIDUAL EQUALS 0.002

PLOT OF ABS(LN(AI-A))AGAINST TIME

CORRELATION COEFFICIENT EQUALS -1.000

STANDARD DEVIATION EQUALS 0.022

FIRST APPROXIMATION OF RATE CONSTANT EQUALS
-0.23189E-02

Method B: For reactions using TEA or EDTA buffered metal ion solutions.

In a typical experiment, the metal ion solution was mixed with TEA.HCl solution or EDTA solution in appropriate volumes in a 50ml volumetric flask. $NaClO_4$ was used to maintain the ionic strength of 0.1M and 1M respectively. The pH of the solution was then titrated to pH7 with NaOH solution (0.1M). Helium gas was then passed through the solution for 15 minutes in order to degas it, after which it was transferred to a thermostated water bath for 20 minutes. A thermostated ethanolic solution of HMT (5ml) was then added to initiate the reaction. The volumetric flask was quickly filled up to the mark with deionised water. After the reaction solution was shaken thoroughly, an aliquot was transferred to a cuvette and the spectrophotometer was started.

Method C: For reactions using DEM buffered metal ion solutions.

In a typical experiment, the metal perchlorate solution was prepared by dissolving an appropriate amount of the metal oxide in dilute perchloric acid of the same concentration. This was then mixed with DEM solution in appropriate volumes in a 50ml volumetric flask. $NaClO_4$ was used to maintain the ionic strength at 1M. The solution was then titrated to pH7.3 with 0.1M NaOH solution and the flask was filled up to the mark with deionised water. An aliquot was transferred to a cuvette and was then allowed to equilibrate in the spectrophotometer for 20 minutes. The reaction was triggered off by the addition of microlitre quantities of an ethanolic

HMT solution.

The results of HMT decomposition by DEM buffered Zn^{2+} are shown in Table 6.2.4. Other results are summarised in Tables 3.2.4 - 3.2.14 in Chapter 3.

6.2.4.2 Reaction in ethanol and in DMSO

Typically, appropriate amounts of metal perchlorate and sodium perchlorate were weighed directly into a 10ml volumetric flask. Dried and freshly distilled absolute ethanol or freshly distilled DMSO was added to dissolve the solids. An aliquot of this solution was then transferred into a cuvette. This was allowed to stand for 20 minutes in the spectrophotometer before microlitre quantities of the ethanol or DMSO solution of HMT was added to initiate the reaction.

All the kinetic data are summarised in Tables 6.2.5 - 6.2.17.

Table 6.2.4 Pseudo first order rate constants ($k_{obs}x10^3/S^{-1}$) for the decomposition of HMTs in water by Zn^{2+} [DEM] = 0.15M I=1M T=37 °C pH=7.3

Zn^{2+}/M HMTs	4-ClC_6H_4	4-$CH_3COOC_6H_4$	4-$CH_3COC_6H_4$	3-C_5H_4N	4-CNC_6H_4	4-$NO_2C_6H_4$
0.006	4.139		0.976	0.676	0.674	1.874
0.007	4.361	1.194		0.743	0.674	1.913
0.008	4.352	1.27	1.052	0.744	0.733	1.968
0.009	4.419	1.335		0.765	0.754	2.024
0.010	4.227	1.34	1.193		0.782	2.062
0.012	4.373	1.43	1.281	0.863	0.86	2.194
0.014	4.23	1.463	1.336	0.96	0.923	2.2
0.015	4.206	1.553	1.381	0.974	0.93	2.458
$10^2xk_{Zn^{2+}}/M^{-1}s^{-1}$	—	3.93	4.584	3.244	2.844	5.67

Table 6.2.5a Pseudo first order rate constants for the Zn^{2+} catalysed decomposition of HMTs in ethanol

I= 0.15M T=37 ^{o}C

4-ClHMT		$4-H_2NCOHMT$		$4-CH_3COOHMT$		$4-CH_3COHMT$		$4-CF_3HMT$		3-pyridylHMT		4-CNHMT		$4-NO_2HMT$	
$[Zn^{2+}]x$ $10^2/M$	10^2x kobs/ S^{-1}	$[Zn^{2+}]x$ $10^2/M$	10^2x kobs/ S^{-1}	10^2x $[Zn^{2+}]$/ M	10^2x kobs/ S^{-1}	10^2x $[Zn^{2+}]$/ M	10^2x kobs/ S^{-1}	10^2x $[Zn^{2+}]$/ M	10^2x kobs/ S^{-1}	10^2x $[Zn^{2+}]$/ M	10^2x kobs/ S^{-1}	10^2x $[Zn^{2+}]$/ M	10^2x kobs/ S^{-1}	10^2x $[Zn^{2+}]$/ M	10^2x kobs/ S^{-1}
0.233	0.476	0.233	0.45	1	0.648	1.016	0.923	1	0.739	0.75	0.0479	0.75	0.272	0.75	0.516
0.504	1.238	0.504	0.836	2	1.122	2	1.488	2	1.12	1.022	0.0486	3	0.56	3	0.419
0.75	2.377	0.75	1.186	3	1.66	3	1.817	3.01	1.506	2.061	0.584	4.378	0.745	4.378	0.501
1.016	2.219	1.016	0.803	4	2.3	4.378	2.59	4.034	1.877	2.898	0.0628	5	0.835	5	0.841
$Zn^{2+}/M^{-1}S^{-1}$ 2.186		1.424		0.55		0.483		0.376		0.00698		0.132		0.061	

Table 6.2.5b Pseudo first order rate constants for Fe^{2+} catalysed decomposition of HMTs in ethanol

I=0.15M T=37 °C

4-ClHMT		4-H_2NCOHMT		4-CH_3COOHMT		4-CH_3COHMT		4-CF_2HMT		3-pyridylHMT		4-CNHMT		4-NO_2HMT	
$[Fe^{2+}]$ x 10^3/M	k_{obs} x $10^2/S^{-1}$	$[Fe^{2+}]$ x 10^3/M	k_{obs} x $10^2/S^{-1}$	$[Fe^{2+}]$ x 10^3/M	k_{obs} x $10^2/S^{-1}$	$[Fe^{2+}]$ x 10^3/M	k_{obs} x $10^2/S^{-1}$	$[Fe^{2+}]$ x 10^3/M	k_{obs} x $10^2/S^{-1}$	$[Fe^{2+}]$ x 10^3/M	k_{obs} x $10^2/S^{-1}$	$[Fe^{2+}]$ x 10^3/M	k_{obs} x $10^2/S^{-1}$	$[Fe^{2+}]$ x 10^3/M	k_{obs} x $10^2/S^{-1}$
0.461	0.27	0.23	0.33	1.3	0.395	5.115	1.087	9.45	1.269	9.73	1.334	5.115	0.333	5.115	0.227
				5.32	0.948										
0.691	0.424	0.461	0.428	9.97	1.805	1.02	1.679	22.05	2.313	19.73	1	10.2	0.496	10.2	0.312
		0.691	0.406	13.4	1.925										
0.922	0.511	0.922	0.429	2.095	0.49	13.1	2.012	30.23	3.705	30	1.843	13.1	0.539	13.1	0.392
		2.177	0.995	4.08	0.837										
2.177	1.416	5.116	1.829	6.23	1.075	7.72	1.372	8.406	1.195	39	1.633	18.3	0.737	18.3	0.538
				9.01	1.359										
6.73		3.15		1.183		1.169		0.823		0.102		0.299		0.237	

e^{2+}/
$l^{-1}s^{-1}$

Table 6.2.5c Pseudo first order rate constants for Cu^{2+} catalysed decomposition of HMTs in ethanol

I= 0.15M T=37 ^{o}C

4-ClHMT		4-$H_2NCOHMT$		4-$CH_3COOHMT$		4-CH_3COHMT		4-CF_3HMT		3-pyridylHMT		4-CNHMT		4-NO_2HMT	
10^2x $[Cu^{2+}]/M$	10^2x kobs/S^{-1}	10^2x $[Cu^{2+}]/M$	10^2x kobs/S^{-1}	10^2x $[Cu^{2+}]/M$	10^2x kobs/S^{-1}	10^2x $[Cu^{2+}]/M$	10^2x kobs/S^{-1}	10^2x $[Cu^{2+}]/M$	10^2x kobs/S^{-1}	10^2x $[Cu^{2+}]/M$	10^2x kobs/S^{-1}	10^2x $[Cu^{2+}]/M$	10^2x kobs/S^{-1}	10^2x $[Cu^{2+}]/M$	10^2x kobs/S^{-1}
0.297	0.93	0.248	0.723	1.0342	1.0828	1.034	1.1923	1	0.68	0.942	0.088	2.055	0.922	1	0.577
0.48	1.226	0.497	0.956	2.055	1.6096	2.055	1.8	2.194	1.221	1.97	0.136	3.025	1.206	2	0.825
0.62	1.45	0.686	0.995	3.025	2.0893	3.03 3.025	2.176 2.218	3.365	1.662	3.478	0.177	3.03	1.153	3	0.99
1	2.013	1.046	1.234	4.055	2.4935	4.055	2.838	4.097	1.944	4.124	0.196	4.055	1.438	4	1.187
$Cu^{2+}/M^{-1}S^{-1}$ 1.536		0.64		0.47		0.53		0.40		0.033		0.258		0.2	

Table 6.2.5d Pseudo first order rate constants for Fe^{3+} catalysed decomposition of HMTs in ethanol

I=0.15M T=37 ^{o}C

4-ClHMT		4-H_2NCOHMT		4-CH_3COOHMT		4-CH_3COHMT		4-CF_3HMT		3-pyridylHMT		4-CNHMT		4-NO_2HMT	
$[Fe^{3+}]$x 10^5/M	k_{obs} x $10^2/s^{-1}$	$[Fe^{3+}]$x 10^5/M	k_{obs} x $10^2/s^{-1}$	$[Fe^{3+}]$x 10^4/M	k_{obs} x $10^2/s^{-1}$	$[Fe^{3+}]$x 10^5/M	k_{obs} x $10^2/s^{-1}$	$[Fe^{3+}]$x 10^{3+}/M	k_{obs} x $10^2/s^{-1}$	$[Fe^{3+}]$x 10^5/M	k_{obs} x $10^4/s^{-1}$	$[Fe^{3+}]$x 10^4/M	k_{obs} x $10^3/s^{-1}$	$[Fe^{3+}]$x 10^4/M	k_{obs} x $10^3/s^{-1}$
2.353	0.335	4.706	0.610	1	0.644	4.706	0.5	0.96	0.455	0.887	3.053	2.215	3.20	0.266	1.029
4.706	0.861	5.537	0.631	2	1.036	7.06	0.589	1.92	0.743	1.774	3.418	4.43	3.83	0.355	1.219
5.537	0.894	7.06	0.954	3	1.356	8.86	0.734	2.88	1.005	2.661	4	6.64	6.35	2.88	1.498
														3.84	1.993
8.859	2	8.859	1.03	4	1.934	9.413	0.712	3.84	1.273	3.548	4.54	8.86	6.73	4.46	1.92
		9.413	1.242											6.696	2.21
256.68		128.25		41.91		50.38		28.5		5.68		5.917		1.811	

$^{e3+}$/
$^{-1}s^{-1}$

Table 6.2.6a Effect of temperature on the pseudo first order rate constants for the decomposition of 4-CH_3COHMT by M^{n+} in ethanol I = 0.15M

a. T=49.5 °C

$Fe(ClO_4)_3$		$Fe(ClO_4)_2$		$Cu(ClO_4)_2$		$Zn(ClO_4)_2$	
$[Fe^{3+}]x10^4/M$	$kobs/S^{-1}$	$[Fe^{2+}]x10^3/M$	$kobs/S^{-1}$	$[Cu^{2+}]x10^2/M$	$kobs/S^{-1}$	$[Zn^{2+}]x10^2/M$	$kobs/S^{-1}$
1.306	0.028	1.020	0.0194	0.901	0.0397	0.913	0.0284
2.613	0.0394	3.803	0.0388	2.046	0.059	1.958	0.0496
0.653	0.0173	6.918	0.0617	3.23	0.0854	3.483	0.073
0.327	0.0146	8.489	0.075	4.189	0.0868	3.934	0.080
$f^{n+}/M^{-1}S^{-1}$ 110.59		7.41		1.53		1.687	

b. T=25 °C

$Fe(ClO_4)_3$		$Fe(ClO_4)_2$		$Cu(ClO_4)_2$		$Zn(ClO_4)_2$	
$[Fe^{3+}]x10^4/M$	$kobsx10^3/S^{-1}$	$[Fe^{2+}]x10^2/M$	$kobsx10^2/S^{-1}$	$[Cu^{2+}]x10^2/M$	$kobsx10^3/S^{-1}$	$[Zn^{2+}]x10^2/M$	$kobsx10^3/S^{-1}$
1.168	2.01	0.526	0.378	1.014	3.35	1.35	3.81
2.336	2.854	0.81	0.533	2.02	5.13	1.97	4.43
3.504	3.9	1.2 2.02	0.835 1.56	3	6.8	3.68	7.653
4.672	4.986	2.985	1.9	4.4	8.8	4.54	8.214
$M^{n+}/M^{-1}S^{-1}$ 8.546		0.6519		0.1612		0.1466	

c. T=15 °C

$Fe(ClO_4)_3$		$Fe(ClO_4)_2$		$Cu(ClO_4)_2$		$Zn(ClO_4)_2$	
$[Fe^{3+}]x10^4/M$	$kobsx10^3/S^{-1}$	$[Fe^{2+}]x10^2/M$	$kobsx10^3/S^{-1}$	$[Cu^{2+}]x10^3/M$	$kobsx10^3/S^{-1}$	$[Zn^{2+}]x10^2/M$	$kobsx10^3/S^{-1}$
1.54	0.674	1.42	2.483	1.39	1.143	1.19	1.271
3.08	1.074	2.02	3.316	2.645	1.816	2.3	2.087
4.62	1.488	3.55	5.239	3.436	2.228	3.1	2.484
6.16	1.851	4.197	6.136	4.642	2.783	4.74	3.722
2.563		0.13		0.05		0.0682	

$M^{n+}/M^{-1}S^{-1}$

Table 6.2.6b Effect of temperature on the pseudo first order rate constant for the decomposition of 3-pyridylHMT by M^{n+} in ethanol I=0.15M

a. T=49.5 °C

$Fe(ClO_4)_3$		$Fe(ClO_4)_2$		$Cu(ClO_4)_2$		$Zn(ClO_4)_2$	
$[Fe^{3+}]x10^5/M$	$kobsx10^2/S^{-1}$	$[Fe^{2+}]x10^2/M$	$kobsx10^3/S^{-1}$	$[Cu^{2+}]x10^2/M$	$kobsx10^3/S^{-1}$	$[Zn^{2+}]x10^2/M$	$kobsx10^3/S^{-1}$
0.908	1.048	0.587	1.91	0.901	3.215	0.596	1.935
1.817	1.321	1	2.15	2.05	4.51	0.913	2.136
2.1	1.387	2.04	2.463	3.23	5.871	1.956	2.298
4.2	1.95	2.95	2.511	4.189	6.434	3.174	2.765
27.17				0.117		0.06212	

$M^{n+}/M^{-1}S^{-1}$

b. T=25 °C

$Fe(ClO_4)_3$		$Fe(ClO_4)_2$		$Cu(ClO_4)_2$		$Zn(ClO_4)_2$	
$[Fe^{3+}]x10^5/M$	$kobsx10^5/S^{-1}$	$[Fe^{2+}]x10^2/M$	$kobsx10^3/S^{-1}$	$[Cu^{2+}]x10^2/M$	$kobsx10^4/S^{-1}$	$[Zn^{2+}]x10^2/M$	$kobsx10^4/S^{-1}$
2.185	8.225	1.2	4.692	1.136	1.953	1.926	1.272
2.466	8.469	2.02	5.088	2.167	2.982	2.812	1.382
3.699	9.268	2.985	5.278	3.128	3.685	3.97	1.582
4.369	9.740	4	5.822	4	4.196	4.705	1.6
0.6815		0.03812		0.00783		0.00127	

$M^{n+}/M^{-1}S^{-1}$

c. T=15 °C

$Fe(ClO_4)_3$		$Fe(ClO_4)_2$		$Cu(ClO_4)_2$		$Zn(ClO_4)_2$	
$[Fe^{3+}]x10^5/M$	$kobsx10^5/S^{-1}$	$[Fe^{2+}]x10^2/M$	$kobsx10^5/S^{-1}$	$[Cu^{2+}]x10^2/M$	$kobsx10^4/S^{-1}$	$[Zn^{2+}]x10^2/M$	$kobsx10^5/S^{-1}$
0.329	2.349	0.386	2.713	1.854	0.642	1.087	3.784
0.658	2.205	0.781	2.938	2.51	0.744	2.565	4.555
0.986	2.262	1.022	3.15	4.113	1.123	4.093	5
1.315	2.37	1.384	3.233	4.95	1.228	4.823	5.05
$k_M^{n+}/M^{-1}S^{-1}$	0.0257		$5.41x10^{-4}$		$2x10^{-3}$		$3.42x10^{-4}$

Table 6.2.7 Pseudo first order rate constants for the decomposition of 4-$CH_3COOHMT$ by M^{n+} in ethanol I=0.15M T=37 ^oC

$Pb(ClO_4)_2$		$Mn(ClO_4)_2$		$Mg(ClO_4)_2$		$Cr(ClO_4)_3$	
$[Pb^{2+}]$/M	kobs/S^{-1}	$[Mn^{2+}]$/M	kobs/S^{-1}	$[Mg^{2+}]$/M	kobs/S^{-1}	$[Cr^{3+}]$/M	kobs/S^{-1}
0.0106	0.00665	0.00955	$1.874x10^{-4}$	0.0107	$7.454x10^{-5}$	0.0048	$3.66x10^{-5}$
0.0203	0.00972	0.0209	$3.413x10^{-4}$	0.0196	$1.383x10^{-4}$	0.010	$5.3x10^{-5}$
0.031	0.01372	0.0314	$4.308x10^{-4}$	0.0307	$2.232x10^{-4}$	0.01444	$6.68x10^{-5}$
0.0434	0.01719	0.04	$5.543x10^{-4}$	0.0398	$2.327x10^{-4}$	0.02072	$8.55x10^{-5}$
$k^{n+}/M^{-1}S^{-1}$	0.325		0.0117		$5.71 x10^{-3}$		$2.978x10^{-3}$

Table 6.2.8 Effect of ionic strength in the M^{n+} catalysed decomposition of HMTs in ethanol T=37 ^{o}C

4-CH_3COHMT + 0.02MZn^{2+}		3-pyridylHMT + 0.0298MZn^{2+}		3-pyridylHMT + 5.537x10^{-3}M Fe^{3+}	
I/M	kobs/S^{-1}	I/M	kobs/S^{-1}	I/M	kobs/S^{-1}
0.1	0.0158	0.1	5.8x10^{-4}	0.1	3.86x10^{-4}
0.2	0.0156	0.15	6.275x10^{-4}	0.15	3.96x10^{-4}
0.25	0.0134	0.2	6.849x10^{-4}	0.2	4.226x10^{-4}
0.3	0.015	0.25	7.214x10^{-4}	0.25	4.55x10^{-4}
0.15	0.0149	0.3	8.097x10^{-4}		

Table 6.2.9 Pseudo first order rate constants for the N-deuteromethyl derivative of 4-CH_3COHMT by M^{n+} in ethanol I=0.15M T=37 °C

$Zn(ClO_4)_2$		$Fe(ClO_4)_2$		$Fe(ClO_4)_3$	
$[Zn^{2+}]x10^2/M$	$kobsx10^2/S^{-1}$	$[Fe^{2+}]x10^2/M$	$kobsx10^2/S^{-1}$	$[Fe^{3+}]x10^5/M$	$kobsx10^3/S^{-1}$
1.3	1.368	0.433	0.938	1.384	2.631
2.56	2.28	0.573	1.264	2.77	3.58
3.33	2.7	0.86	1.586	4.153	4.341
4.36	3.237	1.196	1.974	5.537	4.978
0.61		1.3		56.3	

$k_{M^{n+}}/M^{-1}S^{-1}$

Table 6.2.10 Pseudo first order rate constants for the decomposition of 4-CH_3COOHMT in EtOD by M^{n+} I=0.15M T=37 °C

$Zn(ClO_4)_2$		$Fe(ClO_4)_2$		$Fe(ClO_4)_3$	
$[Zn^{2+}]x10^2/M$	$kobsx10^2/S^{-1}$	$[Fe^{2+}]x10^3/M$	$kobsx10^2/S^{-1}$	$[Fe^{3+}]x10^4/M$	$kobsx10^2/S^{-1}$
1.12	1.257	2.5	1.137	1.103	0.778
2.9	3.355	5.28	2.198	2.206	1.378
4	4.743	7.86	3.149	3.309	2.036
$k_{M^{n+}}/M^{-1}S^{-1}$	1.2		2.038		57.04

Table 6.2.11 Pseudo first order rate constants for the decomposition of 2-CF_3HMT and the N-ethyl and N-propyl derivatives of 4-CH_3COHMT by Zn^{2+} in ethanol I=0.15M T=37 °C

2-CF_3HMT		4-CH_3COHET		4-CH_3COHPrT	
$[Zn^{2+}]x10^2$/M	$kobsx10^2/S^{-1}$	$[Zn^{2+}]x10^3$/M	$kobsx10^2/S^{-1}$	$[Zn^{2+}]x10^4$/M	$kobsx10^3/S^{-1}$
1.297	0.472	1.89	1.739	2.1	0.631
2.56	0.826	4.22	2.173	4.2	1.15
3.33	1.092	6.08	2.412	6.3	2.052
4.356	1.229	9.73	3.397	8.4	2.698
$k_M^{n+}/M^{-1}S^{-1}$	0.255		2.029		3.382

Table 6.2.12 Ligand effect on the pseudo first order rate constants for the decomposition of 4-CH_3COOHMT by 0.01M $Zn(ClO_4)_2$ in EtOH I=0.15M T=37 °C

a. NaI

$[NaI]\times10^2$/M	$k_{obs}\times10^3/S^{-1}$
0.2	8.162
0.4	7
0.6	6.1
0.75	5.217
2.068	0.754
2.095	0.629
4	0.1
5.27	0.172
5.984	0.162
7.986	0.147
6.7783	0.159

b. NaBr

$[NaBr]\times10^2$/M	$k_{obs}\times10^3/S^{-1}$
2	7.628
4	7.102
6	7.657
8	8.094

c. NaBr $[Zn^{2+}]$ = 0.02M

$[NaBr]\times10^2$/M	$k_{obs}\times10^2/S^{-1}$
1.02	1.604
1.2	1.649
1.88	1.61
1.924	1.652
6.152	1.566
6.28	1.6

d. NaAc

$[NaAc]\times10^2$/M	$k_{obs}\times10^4/S^{-1}$
1	4.92
2	1.815
4	0.455
5	0.329

e. pyridine

[pyridine] x 10^2/M	$k_{obs}\times10^3/S^{-1}$
2.162	1.852
4.159	1.7
6.195	1.487
8	1.338

Table 6.2.12 cont'd.

f. imidazole

$[imid] \times 10^2/M$	$k_{obs} \times 10^3/S^{-1}$
0.2	2.316
0.4	2.474
0.6	2.241
0.7	2.125
1	2.238
2	1.748
3	0.829
3.5	0.335
1.94	1.84
3.76	0.252
6.287	0.0155
8.24	0.0122

g. Job's plot for the decomposition of 4-CH_3COOHMT by Zn^{2+} with NaBr
$[Zn^{2+}]_o$ = 0.01M $[NaBr]_o$ = 0.01M
x = mole ratio of Zn^{2+}

x	$k_{obs} \times 10^3/S^{-1}$
0.2	5.27
0.4	5.74
0.5	6.23
0.6	7.16
0.7	8.134
0.8	8.52
0.9	9.23
1	9.268

Table 6.2.13 Pseudo first order rate constants for the decomposition of MMTs by $Zn(ClO_4)_2$ in ethanol I=0.15M T=37 °C

4-ClMMT		4-H_2NCOMMT		4-CH_3COOMMT		4-CH_3COMMT		4-CF_3MMT		3-pyridylMMT		4-CNMMT		4-NO_2MMT	
$[Zn^{2+}]$ x 10^4/M	kobs x $10^3/S^{-1}$	$[Zn^{2+}]$ x 10^3/M	kobs x $10^3/S^{-1}$	$[Zn^{2+}]$ x 10^3/M	kobs x $10^4/S^{-1}$	$[Zn^{2+}]$ x 10^3/M	kobs x $10^4/S^{-1}$	$[Zn^{2+}]$ x 10^4/M	kobs x $10^4/S^{-1}$	$[Zn^{2+}]$ x 10^3/M	kobs x $10^3/S^{-1}$	$[Zn^{2+}]$ x 10^4/M	kobs x $10^5/S^{-1}$	$[Zn^{2+}]$ x 10^3/M	kobs x $10^2/S^{-1}$
1	0.58	1.177	0.224	1.177	1.866	1.177	2.026	1.177	1.1777	2.514	0.942	1	1.88	2	0.54
2	2.373	2.355	0.542	2.355	5.658	2.94	4.138	2.355	3.558	2.94	1.142	2	2.87	4.01	1.281
3	5.782	3.532	1.122	3.532	9.723	3.532	6.2273	3.532	6.344	3.531	1.626	3	4.9	5.013	1.695
														2.1	0.532
4	9.136	4.71	12.785	4.71	11.026	4.022	7.502	4.71	8.647	4.022	1.118	4	8.21	3.15	0.904
														3.885	1.124
$n^{2+}x10^{-2}$ /$M^{-2}S^{-2}$	568.46		81.3		69.61		37.22		41.08		11.23		4.25		5.59

Table 6.2.14 Effect of ionic strength on the decomposition of 4-CNMMT by 2.17×10^{-3}M $Zn(ClO_4)_2$ in EtOH T=37°C

I/M	$kobs \times 10^2/s^{-1}$
0.082	1.231
0.0157	1.036
0.307	0.639
0.0457	0.453

Table 6.2.15a Pseudo first order rate constants for the decomposition of HMTs by $Zn(ClO_4)_2$ in DMSO

I=0.15M T=37 °C

4-ClHMT		4-H_2NCOHMT		4-CH_3COOHMT		4-CH_3COHMT		4-CF_3HMT		3-pyridylHMT		4-CNHMT		4-NO_2HMT	
$[Zn^{2+}] \times 10^2$/M	$k_{obs} \times 10^5/S^{-1}$	$[Zn^{2+}] \times 10^2$/M	$k_{obs} \times 10^5/S^{-1}$	$[Zn^{2+}] \times 10^2$/M	$k_{obs} \times 10^5/S^{-1}$	$[Zn^{2+}] \times 10^2$/M	$k_{obs} \times 10^5/S^{-1}$	$[Zn^{2+}] \times 10^2$/M	$k_{obs} \times 10^5/S^{-1}$	$[Zn^{2+}] \times 10^2$/M	$k_{obs} \times 10^5/S^{-1}$	$[Zn^{2+}] \times 10^2$/M	$k_{obs} \times 10^5/S^{-1}$	$[Zn^{2+}] \times 10^2$/M	$k_{obs} \times 10^5/S^{-1}$
1.634	5.743	0.994	6.801	1.13	6.036	0.867	6.1	1.313	4.408	1	1.453	1.01	3.814	1.52	3.438
3.053	6.345	1.98	7.477	2.127	6.623	2	6.837	1.955	4.56	1.88	1.378	1.94	4.09	2.03	3.718
4.109	6.966	3.107	8.253	3.615	7.5	3.104	7.45	2.957	5.056	3.24	1.318	2.45	4.251	2.73	4
4.904	7.404	4.83	9.427	4.34	8.07	4.034	8	3.814	5.452	4.29	1.318	4.04	4.79	4.04	4.22
$Zn^{2+} \times 0^4/M^{-1} S^{-1}$	5.063		6.846		6.241		5.923		4.808				3.235		2.997

Table 6.2.15b Pseudo first order rate constants for the decomposition of MMTs in DMSO by $Zn(ClO_4)_2$

I=0.15M T=37 °C

4-Cl		4-H_2NCO		4-CH_3COO		4-CH_3CO		4-CF_3		3-pyridyl		4-CN		4-NO_2	
$[Zn^{2+}]$x 10^2/M	k_{obs} x $10^2/S^{-1}$	$[Zn^{2+}]$x 10^2/M	k_{obs} x $10^2/S^{-1}$	$[Zn^{2+}]$x 10^2/M	k_{obs} x $10^2/S^{-1}$	$[Zn^{2+}]$x 10^2/M	k_{obs} x $10^2/S^{-1}$	$[Zn^{2+}]$x 10^2/M	k_{obs} x $10^2/S^{-1}$	$[Zn^{2+}]$x 10^2/M	k_{obs} x $10^3/S^{-1}$	$[Zn^{2+}]$x 10^2/M	k_{obs} x $10^3/S^{-1}$	$[Zn^{2+}]$x 10^2/M	k_{obs} x $10^3/S^{-1}$
0.986	1.081	0.986	0.521	0.986	0.289	0.986	0.338	0.986	0.215	0.494	2.113	0.986	0.961	0.986	0.403
2.036	2.76	2.036	2.146	2.036	0.674	2.036	0.787	2.02	0.624	1.345	4.688	2.036	2.182	2.036	0.96
3.073	4.9	3.073	3.479	3.073	1.075	3.073	1.377	3.073	0.92	2.02	6.64	3.073	3.555	3.073	1.626
4	6.02	4	4.381	4	1.404	4	1.64	4	1.225	0.986	0.239	4	4.512	4	1.913
$\zeta_{M^{n+}}/M^{-1}S^{-1}$ 1.64		1.141		0.372		0.432		0.335		0.297		0.118		0.05	

Table 6.2.16 Pseudo first order rate constants for the decomposition of deuterated 4-CH_3CO- and 4-CNHMTs in DMSO by $Zn(ClO_4)_2$- I=0.15M T=37 °C

4-CH_3COHMT(OD)		4-CNHMT(OD)	
$[Zn^{2+}]x10^2/M$	$k_{obs}x10^5/S^{-1}$	$[Zn^{2+}]x10^2/M$	$k_{obs}x10^5/S^{-1}$
0.924	6.337	0.991	3.818
1.88	6.905	1.861	4.106
3.188	7.510	2.976	4.483
3.789	8.07	4.22	4.892
$10^4xk_{Zn2+}/M^{-1}S^{-1}$	6.075		3.32

Table 6.2.17 Pseudo first order rate constants for the effect of ionic strength on the decomposition of HMT and MMT by $Zn(ClO_4)_2$- in DMSO T=37°C

4-CH_3COHMT $[Zn^{2+}]$ = 0.031M		4-CNMMT $[Zn^{2+}]$ = 0.03M	
I/M	$k_{obs}x10^5/S^{-1}$	I/M	$k_{obs}x10^3/S^{-1}$
0.1	7.902	0.1	3.378
0.2	8.592	0.2	3.555
0.25	8.931	0.25	3.417
0.3	9.4	0.3	3.621

6.2.5 Product studies

The products were identified by UV spectroscopy and supplemented with GC-MS. The latter was obtained by courtesy of PCMU, Harwell.

Typically after each reaction, the product was scanned. The spectrum obtained was compared with that of the genuine arylamine. Using this method, about 90% of the product in ethanol was found to be the arylamine or its N-methyl and N,N-dimethyl derivatives whereas the reaction in DMSO produced only the arylamine and its derivatives.

The reaction of 4-CH_3COOHMT with Zn^{2+} in EtOH was, however, examined in greater detail. The spectrum obtained at the end of this reaction was compared with that of methyl 4-aminobenzoate, methyl 4-methylaminobenzoate and methyl 4-dimethylaminobenzoate. The extinction coefficients of these compounds at three wavelengths was first calculated. The absorbance of the reaction solution at these three wavelengths were then measured. The concentration of each product at the end of the reaction was obtained by constructing 3 simultaneous linear equation for the above data.

The wavelengths chosen are 291nm (λ_{max} for the aryl-amine), 302 (λ_{max} for the N-methyl derivative), 307 (λ_{max} for the N,N-dimethyl derivative). The absorbances of the reaction solution and the extinction coefficients of the 3 compounds at these wavelengths are tabulated in Table 6.2.18.

Table 6.2.18 UV data for methyl 4-aminobenzoate and the N-methyl and N,N-dimethyl derivatives

λ / nm	extinction coefficient			A (product)
	methyl 4-aminobenzoate	methyl 4-methyl-aminobenzoate	methyl 4-dimethyl-aminobenzoate	
291	20175	22664	18268	0.582
302	16125	26764	28482	0.525
307	11550	25739	32789	0.43

By solving the 3 simultaneous linear equation, the concentration of each product was found to be 2.177×10^{-5}M (68%) for the arylamine, 0.521×10^{-5}M (16%) for the N-methyl derivative and 0.1358×10^{-5}M (4%) for the N,N-dimethyl derivative. Thus 12% of the product remains unaccounted for.

The other products were identified by GC/MS and found to be the arene for the Fe^{2+}, Fe^{3+} and Zn^{2+} reactions. In the case of Cu^{2+} reaction, ethoxyarene, azoarene and biaryl were also found. The mass spectra of these compounds are summarised in Table 6.2.19.

Since methyl benzoate was found to be a product of the reaction of 4-CH_3COOHMT with Zn^{2+} in ethanol, its uv spectrum was obtained. At the λ_{max} of methyl benzoate i.e. 226nm, the absorbance of the reaction solution revealed only 8% of the arene. Comparing this value with that of 12% obtained earlier suggests that the conc. of the arene is ca 10% ± 2%.

Table 6.2.19 Mass spectral data for the products of HMT decomposition by M^{n+}

Substrate	M^{n+}/ solvent	Product	Mass spectral data
2-CF_3HMT	Zn^{2+}/ EtOH	2-CF_3 benzene 2-CF_3 aniline 2-CF_3 N-methylaniline	146(M^+), 127, 96, 77, 51 161(M^+), 141, 114 175(M^+), 154, 135, 127
4-ClHMT	Zn^{2+}/ EtOH	4-Cl benzene 4-Cl aniline 4-Cl N-methylaniline 4-Cl N,N-dimethylaniline	112(M^+), 77, 50, 38 127(M^+), 100, 92, 65 140(M^+), 120, 111, 99, 75 154(M^+), 139, 111, 75
4-CH_3COHMT	Zn^{2+}/ EtOH	4-CH_3CO benzene 4-CH_3CO aniline 4-CH_3CO N-methylaniline	120(M^+), 105, 77, 51 135(M^+), 120, 92, 65, 39 149(M^+), 134, 106, 77
4-CF_3HMT	Fe^{3+}/ EtOH	4-CF_3 benzene 4-CF_3 aniline	146(M^+), 127, 36, 77, 51 161(M^+), 142, 111
4-ClMMT	Zn^{2+}/ EtOH	4-Cl benzene 4-Cl aniline 4-Cl N-methylaniline 4-Cl-N,N-dimethyaniline	112(M^+), 77, 50, 37 127(M^+), 100, 92, 65 140(M^+), 126, 111, 99, 77 155(M^+), 140, 105, 77
4ClHMT	Cu^{2+}/ EtOH	4-Cl azobenzene 4-Cl N,N-dimethylaniline 4-Cl aniline 4-Cl-ethoxybenzene	250(M^+), 139, 111, 75 154(M^+), 139, 111, 73 128(M^+), 100, 73, 65, 39 156(M^+), 128, 111, 99
4-NO_2HMT	Cu^{2+}/ EtOH	4-NO_2 N-methylaniline 4-NO_2 aniline 4-NO_2 benzene	152(M^+), 122, 106, 77, 65 138(M^+), 122, 108, 72, 80, 65 123(M^+), 107, 93, 77, 65

Substrate	M^{n+}/ solvent	Product	Mass spectral data
4-CH_3COOHMT	Cu^{2+}/ EtOH	4-CH_3COO benzene 4-CH_3COO aniline 4-CH_3COO N-methylaniline 4-CH_3COO N,N-dimethylaniline 4-CH_3COO ethoxybenzene	136(M^+), 105, 77, 51 151(M^+), 120, 92, 65 165(M^+), 134, 106, 77 179(M^+), 148, 132, 118, 104, 74 180(M^+), 152, 121, 93, 65
4-CF_3HMT	Cu^{2+}/ EtOH	4-CF_3 azobenzene 4-CF_3 biaryl 4-CF_3 N,N-dimethylaniline 4-CF_3 N-methylaniline 4-CF_3 aniline 4-CF_3 ethoxybenzene	318(M^+), 173, 145, 125, 95 290(M^+), 271, 240, 219, 201, 152, 145 188(M^+), 172, 145, 118, 95 174(M^+), 156, 145, 127 162(M^+), 142, 111, 65 190(M^+), 162, 143, 112
4-CH_3COHMT	Zn^{2+}/ DMSO	4-CH_3CO aniline 4-CH_3CO N-methylaniline 4-CH_3CO N,N-dimethylaniline	135(M^+), 120, 92, 65 149(M^+), 134, 106, 79 163(M^+), 148, 132, 120, 105
3-pyridylHMT	Zn^{2+}/ DMSO	3-aminopyridine	94(M^+), 67, 41, 28
4-CH_3COMMT	Zn^{2+}/ DMSO	4-CH_3CO aniline 4-CH_3CO N-methylaniline	135(M^+), 120, 92, 65 149(M^+), 134, 106, 77

6.3 Use of lanthanide shift reagents in the study of metal ion chelating ability of HMTs

6.3.1 Purification of reagents and solvents

$Pr(thd)_3$ and $Eu(fod)_3$ were commercial samples. They were stored in a desiccator and used without further purification.

$CDCl_3$ was dried over molecular sieves type 4A.

6.3.2 $Pr(thd)_3$

In this study, all the ^{1}Hnmr spectra were recorded on a Perkin Elmer R12B spectrometer. Typically, a known amount of the substrate and ca 0.2 mole equivalent of the shift reagent were weighed into a vessel. $CDCl_3$ (ca 0.5ml) were added to dissolve the solids, sometimes with slight warming. The spectrum of this solution was then taken and the chemical shifts of the protons were compared to those of the unbound substrate. The induced shifts ($\Delta\delta$) of all the substrates used are summarised in Tables 4.2.1 and 4.2.2 in Chapter 4.

6.3.3 $Eu(fod)_3$

The ^{1}Hnmr spectra in this study were obtained using a Jeol FX90Q spectrometer. In a typical experiment, a known amount of HMT was weighed directly into a nmr tube. $CDCl_3$ (ca 0.5ml) was then added to dissolve the sample. A spectrum

of this sample solution was taken, after which a small, weighed-out quantities of $Eu(fod)_3$ was added. A further spectrum was again obtained. Finally, 5 weighed-out quantities of HMT was added successively to the solution, in which a spectrum was obtained after each addition. The results of this study are summarised in Table 6.3.1

G. 3-PyridylHMT $[Eu(fod)_3] = 2.2564 \times 10^{-3} M$

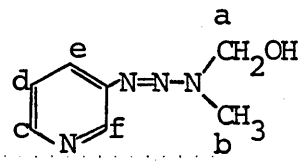

[HMT]/M	a	b	c	d	e	f
0.045	32.32	17.58	93.74	29.86	36.22	97.41
0.065	23.68	12.45	67.37	20.26	24.69	68.36
0.08	19.77	9.76	52.72	15.38	18.84	54.19
0.112	15.13	7.08	36.24	10.56	14.69	38.81
0.163	10.49	3.91	22.33	5.55	7.93	25.14
0.201	9.03	2.68	18.3	4.39	6.02	19.53

Table 6.3.1 Effect of $Eu(fod)_3$ on the chemical shifts ($\Delta\delta$/Hz) of the protons in HMTs.

A. 4-ClHMT $[Eu(fod)_3] = 2.8205 \times 10^{-3}$M

[HMT]/M	$N-CH_2-O$	$N-CH_3$	Ar-N=N	Ar-C
0.04	79.34	28.81	12.45	5.86
0.064	56.64	20.02	8.54	4.15
0.089	42.48	14.4	5.61	2.44
0.116	33.45	10.74	4.39	2.2
0.16	26.12	7.57	2.93	1.22
0.18	21.48	5.73	1.71	0.49

B. $4-COOCH_3HMT$ $[Eu(fod)_3] = 5.641 \times 10^{-3}$M

[HMT]/M	$N-CH_2-O$	$N-CH_3$	Ar-N=N	Ar-X	Others
0.058	36.86	13.43	7.44	14.04	14.16
0.086	30.03	10.5	5.36	10.62	11.23
0.104	26.12	8.55	4.13	8.55	9.28
0.147	21.24	6.35	2.56	5.98	7.08
0.161	18.55	4.89	1.58	4.76	5.86

C. $4-COCH_3HMT$ $[Eu(fod)_3] = 5.641 \times 10^{-3}$M

[HMT]/ M	$N-CH_2-O$	$N-CH_3$	Ar-N=N	Ar-X	Others
0.061	64.45	26.12	20.99	34.18	37.1
0.082	52.25	20.75	15.87	25.39	27.58
0.11	41.26	15.38	11.23	17.82	20.26
0.143	27.34	8.78	5.61	8.55	11.47
0.16	25.15	7.81	4.39	7.33	9.52

D. 4-CF_3HMT $[Eu(fod)_3] = 3.5743 \times 10^{-3}$M

[HMT]/M	N-CH_2-O	N-CH_3	Aromatic
0.043	103.75	39.31	11.23
0.062	81.05	30.52	8.31
0.09	62.74	23.44	6.35
0.108	51.75	18.56	4.64
0.125	44.18	15.38	3.67
0.146	38.57	13.43	2.93

E. 4-CNHMT $[Eu(fod)_3] = 2.0684 \times 10^{-3}$M

[HMT]/M	N-CH_2-O	N-CH_3	Ar-N=N	Ar-X
0.038	41.01	18.55	9.52	5.86
0.058	31	13.91	5.86	3.66
0.089	19.77	9.76	2.93	0.97
0.11	14.16	7.57	1.22	-0.73
0.13	11.72	6.35	0.48	-1.95
0.155	8.3	4.88	-0.28	-2.93

F. 4-NO_2HMT $[Eu(fod)_3] = 2.4444 \times 10^{-3}$M

[HMT]/M	N-CH_2-O	N-CH_3	Ar-N=N	Ar-X
0.035	52.98	20.27	9.28	4.39
0.06	39.55	14.9	6.17	2.44
0.071	35.89	12.94	5.25	1.71
0.089	30.03	11.23	3.53	0.09
0.096	27.1	9.77	2.44	-0.005
0.11	24.17	8.31	1.345	-1.22

6.4 Base promoted decomposition of 1-aryl-3-hydroxymethyl-3-methyltriazenes to 1-aryl-3-methyltriazenes

6.4.1 Qualitative studies

In a typical experiment, a suspension of 0.1g HMT in an aqueous solution of bases (0.036M, 40ml) was stirred overnight at room temperature. The product was filtered, air-dried and identified using ^{1}Hnmr. The results obtained are shown in Table 5.1 in Chapter 5.

6.4.2 Quantitative studies

6.4.2.1 Nmr method

This was performed on a Perkin Elmer R12B spectrometer. The decomposition of HMT was monitored by comparing the integral of the $-CH_2-$ signal of the HMT to that of the total aromatic signals of HMT and MMT. Each signal was integrated three times.

In a typical experiment, 4-CH_3COHMT(0.1g) was dissolved in $(CD_3)_2SO$ (ca 0.5ml) inside a nmr tube. The solution was thermostated at 30 ^{o}C in a water bath for 20 minutes, after which its spectrum was recorded. A known amount of bases was then added into the solution and the spectra of this reaction solution was recorded against time.

6.4.2.2 Hplc method

This was performed on a 25cm x 5mm ID Spherisorb S5ODS2 analytical column. In a typical experiment, an ethanolic solution containing the appropriate amount of bases was prepared and allowed to stand in a water bath set at 37 ^{o}C for 20 minutes. Solid sample of 3-pyridylHMT was then added to initiate the reaction. After the reaction solution was shaken thoroughly, microlitre amounts of the solution were taken up in a syringe and injected into the column through a Rheodyne 7125 injector. The injector volume was set at 1 µl. When the chromatogram has developed, the injector was flushed with the eluent before another sample was injected. This process was repeated until the reaction was ca 95%. A typical run is given in Table 6.4.1.

Table 6.4.1 Decomposition of 3-pyridylHMT in ethanol T=37 °C.

$[HMT]_o = 1.8072 \times 10^{-3} M$

Time/min.	$-\ln \frac{[HMT]_t}{[HMT]_o}$
1	0.028
10	0.2346
17	0.3712
25	0.5321
32	0.6866
40	0.8468
48	1.0234
56	1.2042
64	1.3414
72	1.5314
102	2.001
120	2.2234
118	2.4123
126	2.5282

The rate constants obtained are shown in Tables 5.4 - 5.7 in Chapter 5.

References

1. D.A.Clarke, R.K.Barclay, C.C.Stock and C.S.Rondestvedt Jr., Proc.Soc.Exp.Biol.Med., 1955, 90, 484.

2. C.S.Rondestvedt and S.J.Davis, J.Org.Chem., 1957, 22, 200.

3. C.Hansch, R.N.Smith, R.Engle and H.Woods, Cancer Chemother. Rep., 1972, 56, 443.

4. R.C.S.Andette, T.A.Connors, H.G.Mandel, K.Merai and W.C.J.Ross, Biochem.Pharmacol., 1973, 22, 1855-1864.

5. Y.F.Shealy, J.A.Montgomery and W.R.Laster, Biochem. Pharmacol., 1962, 11, 674.

6. Y.F.Shealy, J.Pharm.Sci., 1970, 59, 1533.

7. S.K.Carter and W.T.Soper, Cancer Treatment Rev., 1974, 1, 1.

8. Y.F.Shealy and C.A.O'Dell, J.Pharm.Sci., 1971, 60, 554.

9. Y.S.Lin, T.L.Loo, S.Vadlamudi and A.Goldin, J.Med.Chem., 1972, 15, 201.

10. P.P.Saunders and G.A.Schultz, Biochem. Pharmacol., 1972, 21, 2065.

11. T.A.Connors, P.M.Goddard, K.Merai, W.C.J.Ross and D.E.V.Wilman, Biochem. Pharmacol., 1976, 25, 241-246.

12. R.Preussman, A.von Hodenberg and H.Hengy, Biochem. Pharmacol., 1969, 18, 1-13.

13. D.H.Hutson, in Foreign Compound Metabolism in Mammals. Vol.2, (D.E.Hathway, ed), The Chemical Society, London, 1972. Ch.4.

14. B.B.Brodie, J.R.Gillette and B.N.La Du, Ann. Rev. Biochem., 1958, 27, 427.

15. B.Testa and P.Jenner, Drug Metabolism, Chemical and Biochemical Aspects p.82, Marcel Dekker, New York, 1976.

16. A.H.Soloway, R.J.Brumbaugh and D.T.Witiak, J.Theor. Biol., 1983, 102, 361-373.

17. J.L.Skibba, D.D.Beal, G.Ramirez and G.T.Bryan, Cancer Research, 1970, 30, 147-150.

18. A.H.Gerulath and T.L.Loo, Biochem. Pharmacol., 1972, 21, 2335-2343.

19. T.L.Loo,in Handbook of experimental pharmacology, NSV38, Springer-Verlag, 1975, Ch.56.

20. J.L.Skibba, G.T.Bryan, Toxicol.Appl.Pharmacol., 1971, 18, 707-719.

21. M.F.G.Stevens and K.Vaughan, Chem.Soc.Rev., 1978, 7(3), 377.

22. T.Ong and F.J. de Serres, Mutation Research, 1971, 13, 276.

23. F.A.Schmid and D.J.Hutchinson, Cancer Research 1974, 34, 1671.

24. N.S.Mizuno and R.W.Decker, Biochem. Pharmacol., 1976, 25, 2643.

25. H.T.Nagasawa, F.N.Shirota and N.S.Mizuno, Chem.Biol. Interactions, 1974, 8, 403.

26. A.Gescher, J.A.Hickman, R.J.Simmonds, M.F.G.Stevens and K Vaughan, Biochem. Pharma. 1981, 30(1), 89-93.

27. A.Gescher, J.A.Hickman, R.J.Simmonds, M.F.G.Stevens and K.Vaughan, Tet. Letts., 1978, 5041.

28. J.A.Hickman, Biochemie., 1978, 60(9) 997-1002.

29. G.F.Kolar, M.Maurer and M,Wildschutte, Cancer Lett., 1980, 10, 235.

30. G.F.Kolar and R.Carubelli, Cancer Lett., 1979, 7, 209.

31. R.L.Petrusek, G.L.Anderson, T.F.Garner, O.L.Fannin, D.J.Kaplan, S.G.Zimmer and L.H.Henley, Biochemistry, 1981, 20, 1111.

32. D.E.Schwartz, G.B.Brubacher and M.Vecchi in 'Radioactive Isotopes in Pharmacology' (P.G.Waser and B.Glasson eds) John Wiley and Sons, New York, 1968, p.63-65.

33. C.Rutty and T.A.Connors, Biochem.Pharma., 1977, 26, 2385.

34. R.J.Weinken and D.A.Shiba, Life Sciences, 1978, 22, 937.

35. G.F.Kolar and R.Preussmann, Z.Naturforsch, 1971, 26b, 950-953.

36. O.Dimroth, Ber. 1903, 36, 909.

37. V.Y.Andakushkin, B.A.Dolgoplosk and I.I.Radchenko, Zhur.Obshchei.Khim., 1956, 26, 2972 (C.A. 1957, 51, 8674a).

38. A.Gescher, J.A.Hickman and M.F.G.Stevens, Biochem. Pharmacol. 1979, 28, 3235.

39. N.Brock, in 'Structure-Activity Relationships of Antitumour Agents' (ed. D.N.Reinhoudt, T.A.Connors, H.M.Pinedo and K.W. Van de Poll) Martinus Mijhoff, B.V.Den Haag, Netherlands, 1983, p.239.

40. P.A.S.Smith in 'Open-Chain Nitrogen Compounds' Benjamin, New York, 1965, Vol.1, 291.

41. G.Zinner and W.Kleigel, Chem.Ber., 1967, 100, 2515.

42. J.M.Z.Gladych and D.Hartley in Comprehensive Organic Chemistry, Vol.2 (ed. I.O.Sutherland), Pergamon Press, 1979, 105.

43. G.Weitzel, F.Schneider, A.M.Fretzdorft, K.Seynsche and H.Finger, Hopper-Seyler's Z. Physical Chem., 1963, 334, 1.

44. T.Wagner, G.Peter, G.Voelcker and H.J.Hohorst, Cancer Research, 1977, 37, 2592.

45. M.M.Sprung, Chem.Rev., 1940, 26, 297

46. P.Ballinger and F.A.Long, J.A.C.S. 1960, 82, 795.

47. R.G.Kallen, R.O.Viale and L.K.Smith, J.A.C.S. 1972, 94, 576.

48. J.Murto in 'The Chemistry of the Hydroxyl Group' ed. S.Patai, Interscience, London, 1971, 1106.

49. R.G.Kallen and W.D.Jencks, J.Biol.Chem., 1966, 241, 5864.

50. W.R.Abrams and R.G.Kallen, J.A.C.S. 1976, 98, 7777.

51. J.Hine and R.D.Weimer Jr. J.A.C.S. 1965, 87, 3387.

52. V.Zverina, M.Remes, J.Divis, J.Marhold and M.Mateka, Coll.Czech. Chem.Commun., 1973, 38, 251.

53. A.N.Lotsova, T.N.Shatkina and O.A.Rentov, Doklady Akad. Nauk. SSSR, 1968, 183, 1091.

54. C.C.Jones, M.A.Kelly, M.L.Sinnott and P.J.Smith, J.C.S. Chem.Commun., 1980, 322.

55. N.S.Isaacs and E.Rannala, J.C.S.Perkins Transactions II, 1974, 899.

56. R.J.LeBlanc and K.Vaughan, Can.J.Chem., 1972, 50, 2544.

57. M.Kawanisi, I.Otani and H.Nozacki, Tetrahedron Letts., 1968, 5575.

58. R.Kreher and K.Goth, Z.Naturforsch. 1976, 31b, 217.

59. W.P.Jencks, J.A.C.S. 1959, 81, 475.

60. E.H.Cordes and W.P.Jencks, J.A.C.S. 1962, 84, 832, 4319.

61. R.Wolfenden and W.P.Jencks, J.A.C.S. 1961, 83, 2763.

62. B.M.Anderson and W.P.Jencks, J.A.C.S. 1960, 82, 1773.

63. J.M.Sayer, M.Peskin and W.P.Jencks, J.A.C.S. 1973, 95, 4277.

64. R.B.Martin, J.Phys.Chem., 1964, 68, 1369.

65. L.S.Levitt and B.W.Levitt, Tetrahedron, 1971, 27, 3777.

66. C.V.McDonnell Jr., M.S.Michailidis and R.B.Martin, J.Phys.Chem., 1970, 74, 26.

67. M.Julliard, G.Vermin and J.Metzger, Synthesis, 1980, 116.

68. R.J.Lafrance, Y.Tang, K.Vaughan and D.L.Hopper, J.C.S Chem. Commun., 1983, 721.

69. A.T.Nielsen, R.L.Atkins, D.W.Moore, R.Scott, D.Mallony and J.M.LaBerge, J.O.C. 1973, 38, 3288.

70. H.W.Manning, C.M.Hemes, R.J.LaFrance, Y.Tang and K.Vaughan, Can.J.Chem., 1984, 62, 749.

71. Y.F.Shealy, R.F.Struck, L.B.Holum and J.A.Montgomery, J.Org.Chem., 1961, 26, 2396.

72. Y.F.Shealy and C.A.Krauther, J.Med.Chem., 1966, 9, 34.

73. Chemical Abstracts, 1962, 56, 6203.

74. D.D.Perrin, B.Dempsey, 'Buffers for pH and metal ion control', Chapman and Hall, London, 1974.

75. IUPAC, Stability Constants of Metal-ion Complexes, Part B, Organic Ligands, Pergamon Press, Oxford, 1979.

76. D.Nicholls, Complexes and First-row Transition Elements, MacMillan, London, 1974, p.31.

77. E.G.Rukhadze, T.V.Ershova, S.A.Fedorova and A.P.Terent'ev Zhur.Obsch.Khim., 1969, 39(2), 283.

78. F.A.Cotton and G.Wilkinson, Advanced Inorganic Chemistry, 4th ed., Wiley Interscience, N.Y., London, 1980, p.14.

79. K.B.Wiberg, Chem.Rev., 1955, 55, 713.

80. W.P.Jencks, Catalysis in Chemistry and Enzymology, McGraw-Hill, New York, 1969, p.490, and references therein.

81. M.L.Bender, Mechanisms of Homogeneous Catalysis from Protons to Proteins, Wiley Interscience, New York, 1971, p.232.

82. Yoe and Jones, Ind.Eng.Chem.Anal.Ed., 1944, 16, 111.

83. R.H.Prince and P.R.Woolley, J.C.S.Dalton, 1972, p.1548.

84. P.R.Woolley, J.C.S. Dalton, 1975, p.1570.

85. P.Woolley, J.C.S.Perkin II, 1977, p.318.

86. A.F.Hegarty in The Chemistry of Diazonium and Diazo Groups, (Saul Patei ed.), Wiley Interscience, 1978, Ch.12, p.555.

87. T.P.Ahren, H.Fong and K.Vaughan, Can.J.Chem., 1977, 55, 1701.

88. J.Hoffmann, J.Klicnar and V.Sterba, Coll.Czech.Chem. Commun., 1971, 36(12), 4057.

89. J.Burgess, Metal Ions in Solution, Ellis Horwood, 1978, p.328.

90. C.C.Hinckley, J.Amer.Chem.Soc., 1969, 91, 5160.

91. C.Reyes-Zamora and C.S.Tsai, J.C.S.Chem.Commun., 1971, p.1047.

92. I.Armitage, G.Dunsmore, L.D.Hall and A.G.Marshall, Can.J.Chem., 1972, 30, 2119.

93. A.F,Cockerill, G.L.O.Davis, R.C.Harden and D.M.Rackham, Chem. Rev., 1973, 73(6), 553.

94. C.Dunboc, Bull.Soc.Chim., Fr. 1970, p.1768.

95. M.L.de S.Fernandes, J.Iley and M.E.N.Rosa, unpublished results.

96. C.C.Jones, M.A.Celly, M.L.Sinnott, P.J.Smith and G.T.Tzotzos, J.Chem.Soc., Perk.II, 1982, p.1655.

97. M.Remes, J.Davis, V.Zverina, J.Marhold and M.Matrka, Cesk.Farm., 1972, 21, 142.

98. D.P.N.Satchell and I.I.Secemski, J.Chem.Soc.(B), 1970, p.1306.